PERMUTATIONAL, TOPOLOGICAL, STEREOCHEMICAL, KINETIC, AND MECHANISTIC STUDIES OF SOME SIX-COORDINATE METAL CHELATE COMPLEXES OF GROUP(IV) ELEMENTS

Douglas George Bickley

A THESIS
in
The Department
of
Chemistry

Presented in Partial Fulfillment of the Requirements for the Degree of Master of Science at Sir George Williams Campus of Concordia University
Montreal, Canada

June, 1975

TO MY MOTHER

Acknowledgements

I want to express my sincere gratitude to Professor N. Serpone for stimulating my interest in inorganic chemistry and developing this interest to the present level. He has devoted much time and scholarship in the course of this endeavor. Dr. Serpone's enthusiastic participation in research and scientific integrity have been truly exemplary.

Thanks are due to Professor J. G. Dick and Dr. R. E. Townshend for serving on my research committee and Dr. L. D. Colebrook for advice on nmr techniques. I would also like to thank the Department of Chemistry of Sir George Williams University and the National Research Council of Canada (1973-74) for providing financial assistance.

Thanks are also due to Roueben Ishayek for advice on experimental techniques, Ken Hersh for the data used in Section III-C-1-c(ii) and for development of computer programs, and John Lawson for preparing some of the figures in this thesis.

I also thank Drs. J. F. Harrod and K. R. Taylor for providing samples of some ~~of the~~ phenoxy complexes and Professor L. H. Pignolet for obtaining carbon-13 nmr spectra.

I wish to express my deep appreciation to Alan Fraser for many chemical and crystallographic discussions, understanding and encouragement, and his continuing friendship. I would also like to thank Alan, John, Dave, George, Derek, and Kathy for their constant encouragement and for their assistance during the "last six months".

I thank Professor M. J. McGlinchey for his incredible patience.

Finally, I am deeply indebted to my mother and brother for their constant encouragement, understanding, patience, and sacrifices during my education.

"What is now proved was once only imagin'd"

"The Marriage of Heaven and Hell"

William Blake

PERMUTATIONAL, TOPOLOGICAL, STEREOCHEMICAL, KINETIC, AND MECHANISTIC STUDIES IN SOME SIX-COORDINATE METAL CHELATE COMPLEXES OF GROUP(IV) ELEMENTS

Douglas George Bickley

ABSTRACT

Several dihalobis(β-diketonato)metal(IV) complexes of the type $M(dik)_2X_2$ [M = Ti(IV); dik = dibm, dpm; X = F, Cl, Br; M = Sn(IV), Ge(IV); dik = dibm; X = Cl; M = Ti(IV); dik = 3-^{i}Pr-acac; X = Cl; M = Ti(IV), Sn(IV); dik = tibm; X = Cl; M = Ti(IV); dik = thd; X = Cl] have been prepared and characterized. Complexes of the type $Ti(acac)_2(phenoxy)_2$ [phenoxy = 2,6-Cl_2-C_6H_3O, 2-ClC_6H_4O, 2-IC_6H_4O, 2-$^iPrC_6H_4O$, 4-ClC_6H_4O, 4-$^iPrC_6H_4O$, 2,6-$^iPr_2C_6H_3O$, 2-$(C_6H_5)C_6H_4O$, 4-$(OCH_2C_6H_5)C_6H_4O$, 3-$CH_3C_6H_4O$] were prepared and investigated. In addition, $Ti(dik)_2X(OR)$ [dik = acac; X = Cl, Br; R = i-C_3H_7; dik = acac; X = Cl; R ≠ 2,6-$^iPr_2C_6H_3$; dik = dibm; X = Cl; R = CH_3] and $Ti(bzac)_2(OR)_2$ [R = i-C_3H_7, 2,6-$^iPr_2C_6H_3$] complexes were also synthesized and characterized.

Variable temperature nmr studies reveal that all complexes exist as the stereochemically nonrigid diastereomer(s) possessing cis monodentate ligands. Diastereotopic probes, incorporated into various positions within complexes of the type cis-$M(AA)_2X_2$, cis-$M(AA)_2XY$, and cis-$M(AB)_2X_2$, reveal that configurational rearrangements in these systems involve inversion of the molecular configuration at the metal center.

A permutational analysis of the stereochemical rearrangements of cis-$M(AA)_2X_2$, cis-$M(AA)_2XY$, and cis-$M(AB)_2X_2$ complexes has been performed, as

well as a complete delineation of feasible physical rearrangement pathways for the same series of complexes. Assignment of various averaging sets to physical processes is also presented.

Total Lineshape analyses on the acetylacetonate methyl group exchange in cis-$Ti(acac)_2(phenoxy)_2$ complexes, and on the isopropyl methyl group exchange in isopropyl-substituted phenoxy $Ti(acac)_2XY$ [X = Y = 2-^{i}PrC_6H_4O, 2,6-$^i Pr_2C_6H_3O$; X = Cl, Y = 2,6-$^i Pr_2C_6H_3O$] complexes have been undertaken, the results of which are presented in this work. Comparison of acetylacetonate methyl group exchange rates with rates of isopropyl methyl group exchange for the $Ti(acac)_2(2,6-^i Pr_2-C_6H_3O)_2$ complex in CH_2Cl_2 solution suggests that rearrangements probably occur via a twist mechanism. Similar comparisons for the $Ti(acac)_2(2-^i PrC_6H_4O)_2$ complex in CH_2Cl_2, and the $Ti(acac)_2(2,6-^i Pr_2C_6H_3O)_2$ complex in m-$Cl_2C_6H_4$ are not unequivocal.

A Total Lineshape analysis of isopropyl methyl group exchange in the series of complexes $Ti(chelate)_2(2,6-^i Pr_2C_6H_3O)_2$ [chelate = acac, ox, quin] in m-dichlorobenzene is also presented. The activation energy (kcal/mole) and activation entropy (eu) are, respectively, 6.3 ± 1.7 and -36.5 ± 5.7 (acac), 14.7 ± 0.8 and -9.7 ± 2.2 (quin), and 21.2 ± 1.3 and 2.2 ± 3.3 (ox). Environmental averaging of isopropyl methyl groups in the oxinate (ox) and quinaldinate (quin) complexes probably proceeds by a Ti-N bond rupture via TBP-axial intermediates.

Activation parameters for configurational rearrangement phenomena in the six-coordinate $Ti(acac)_2(2-IC_6H_4O)_2$, $Ti(acac)_2(4-ClC_6H_4O)_2$, $(C_6H_5)ClGe(acac)_2$, $(CH_3)ClSn(acac)_2$, $(C_6H_5)_2Sn(acac)_2$, and $(C_6H_5)ClSi(acac)_2$ complexes obtained from calculating nmr total lineshapes are compared with those calculated using approximate equations. The complexes were chosen with regard to the magnitude of the chemical shift in the uncoupled AB system. It is shown that, in general, activation parameters extracted from using a particular approximate expression

may lead to serious deviations from those calculated using the total lineshape method. However, an averaging of all exchange rates from the various approximate methods leads to closer agreement. The assumption that $\delta\upsilon$ is temperature independent yields severe discrepancies in the activation parameters.

A preliminary investigation on the apparent five-coordinate titanium(IV) complexes $Ti(dik)X_3$ [dik = acac, bzac, dpm, dibm; X = F, Cl, Br] is reported. Reaction between $Ti(acac)_2F_2$ and $TiCl_4$ in a 1:1 molar ratio produces a substance which possesses the $Ti(acac)FCl_2$ stoichiometry. From the absence of terminal Ti-F stretching bands in this complex, it is suggested that the complex is dimeric in the solid state, and contains bridging fluorine groups:

TABLE OF CONTENTS

LIST OF TABLES

LIST OF FIGURES

I. INTRODUCTION

Most discrete ensembles of atoms possess a single well-defined configuration representing an energy minimum. Despite intrinsic motion due to vibrational modes about an equilibrium position, the lifetime of a particular configuration of nuclei may be considered to be large. However, in many cases, more than one energetically similar configuration may exist and molecular vibrations or an "intramolecular"* rearrangement may interconvert a molecule between these configurations. If such a process occurs at a rate which is detectable by at least some physical method, the molecule is designated as stereochemically nonrigid (1,2)

Stereochemical nonrigidity is thus a convenient, broad term applied to molecules which undergo rapid intramolecular rearrangements. It is, however, rather vague as to the relationship between interconverting configurations. For example, the configurations may be related in the sense that they are diastereomers or enantiomers (3). Several descriptive terms which further specify the relationships between interconverting configurations may be found in the literature, e. g., fluxional (5) molecules in organometallic chemistry. The more general term configurational rearrangements is encountered in transition metal chelate chemistry (6,7).

Perhaps the most important point concerning nonrigid molecules is the time scale (8) of the physical method used to determine molecular

---

*A popular synonym for "intramolecular" is non-bond-breaking, which is rather imprecise and frequently requires an operational definition (4). The adjective "intramolecular" is used here in the sense that no portion of the molecule is at any time completely dissociated and recombines to form a different configuration, thus requiring that the process under study exhibit first order kinetic behaviour.

structure. Although time scales are sensitive to the particular system under study, the extremes are found in the actual physical separation of diastereomers or enantiomers (very slow) and diffraction methods (very fast). In general, diffraction methods reveal the "instantaneous" structure of the molecule due to the very small time scale inherent to the technique based on the wavelength of the radiation used. Nuclear magnetic resonance (nmr) techniques cover a wide middle range of lifetimes, into which many rearrangement rates conveniently fall. In many cases, application of nmr methods to detect nonrigidity and diffraction methods to determine the instantaneous structure provides enhanced information concerning dynamics and rearrangement mechanisms. Such a combination has proven eminently successful in the study of fluxional organometallic molecules (5,9,10).

The ability of magnetic resonance methods to detect and measure the rates of dynamic processes is well-documented in the disciplines of organic (11,12), organometallic (5,9,10), and transition metal chelate (6,7) chemistry. NMR techniques allow for the investigation of intramolecular movement with activation energies of ca. 5-25 kcal/mole via the observation of line broadening and coalescence phenomena. General discussions of experimental procedures, theories, and errors involved in extracting kinetic data from lineshape parameters have appeared (13-16) in a continuously broadening stream of publications since the early work of Gutowsky and Holm (17). Factors relevant to the work presented in this thesis are discussed in Sections II-B and II-C.

Within the realm of inorganic chelate chemistry, the elucidation of mechanisms of intramolecular rearrangements of six-coordinate complexes has received considerable attention (6,7). While the vast majority of work

has centered on complexes containing at least one bidentate chelate ring, some complexes containing six monodentate ligands have recently been found to be stereochemically nonrigid (1,2,18-20). Possible rearrangements for six-coordinate chelate complexes involve, in general, diastereomerization and/or enantiomerization. Stereoisomeric possibilities can vary widely depending on the relative numbers of mono- and bidentate ligands and the nature of the chelating ligand(s) (symmetrical, unsymmetrical, or asymmetric).

Rearrangement rates frequently exhibit a marked dependence on the nature of the ligands and on the size and electronic features of the coordinated metal ion. A classification of chelates in terms of their rearrangement rates has introduced the designations "slow" and "fast" (21). Slow complexes allow for the separation of diastereomers and resolution of enantiomers under ordinary conditions, thus permitting rearrangement kinetics to be determined by the rate of approach to equilibrium. "Fast" or stereochemically nonrigid complexes have rearrangement rates that are too large to permit isolation of diastereomers and enantiomers but do allow isomer detection and, in most cases, kinetic studies by nmr line shape analysis. As an example of the dependence of rearrangement rates on the nature of the ligands, consider the tris(β-diketonato) and tris-(tropolonato)* complexes of cobalt(III). The former are slow complexes (21-24) while the latter complexes are stereochemically nonrigid (25,26).

While diastereomers and enantiomers may be readily isolated for slow complexes, until recently, enantiomers could not be detected for fast complexes in the nmr experiment. It is now well known (11) that when a $-CXY_2$ group is bound to some dissymmetric group, the two Y groups neither

*A complete list of abbreviations and structures for bidentate chelating ligands used in this thesis may be found in Appendix A.

achieve equivalence in any rotational conformation nor as a result of internal rotation, however rapid. To achieve equivalence, inversion of the dissymmetric moiety must occur. The simplest alkyl $-CXY_2$ system would be the ethyl group ($X = CH_3$; $Y = H$), but the geminal H-H coupling superimposed on the quartet splitting due to the CH_3 group generally leads to a complex broad resonance for diamagnetic complexes, rendering this group a poor choice for interpretation and kinetic analysis. A more useful probe is the isopropyl group ($X = H$; $Y = CH_3$) since CH_3-CH_3' coupling is negligible and each methyl group will be split only into doublets by the unique proton. Another useful probe is the benzyl group ($X = C_6H_5$; $Y = H$) which will result in a relatively simple AB resonance pattern.

Ethyl, benzyl, and isopropyl groups have all been used to detect enantiomerization processes in chelate complexes. Optical inversion has been detected (27-29) in nonrigid paramagnetic iron complexes of the type $M(AA)_2(BB)$ using an ethyl group as the diastereotopic probe. The benzyl group (30-33) has also recently proven successful in probing enantiomerization processes in $M(AB)_3$ complexes. The isopropyl group has proven to be the most useful and extremely successful in detecting enantiomerization processes in nonrigid tris chelates of the type $M(AA)_3$ (34), $M(AB)_3$ (25, 26,35-37), and $M(AA)_2(BB)$ (34).

The ability to detect enantiomerization processes in nonrigid chelate complexes has enabled significant progress in the elucidation of the mechanism(s) of rearrangement. It is generally considered that these processes may occur <u>via</u> two limiting types of pathways which are distinguishable by the effective coordination number of the transition state (6,7).

In the bond-rupture mechanism originally proposed by Werner (38) a five-coordinate intermediate is initially formed *via* rupture of a metal-ligand bond. The resulting "unidentate" or dangling ligand then reattaches so as to form the rearranged product.

The alternative to the formation of a lower coordination polyhedron during rearrangement is the formation of a polytopal isomer of the six-atom family (39); that is, the ligating nuclei approximate the vertex positions of a trigonal prism (TP). Although various modifications of twisting processes have been advanced (40,41), the Bailar (42) twist motion is the most general process. In this mechanism, one triangular face of the octahedron is rotated by 60° while keeping the opposite face fixed. The resulting transition state resembles a trigonal prism which can then either decay back to the original diastereomer or by continued rotation in the same sense form the rearranged octahedral polytope.

These two distinct types of mechanisms are physically reasonable because all of the various postulated intermediates have been found to occur as stable entities in other transition metal complexes. Five-coordinate complexes in both polytopal forms are plentiful (43), and the number of trigonal prismatic chelate complexes is constantly increasing (44), or at least distortions towards TP geometries have been recognized (45-47).

A more detailed description and discussion of the above mentioned mechanisms may be found in Section III-A-4a.

Although the postulated mechanisms are certainly reasonable, there is no assurance that every feasible mechanism has been considered. Since the nmr experiment can only define a particular permutation of nonequivalent sites, the observed set of interchanges must be compared

with all possible permutations of nuclei for the system under study. Thus once the exact permutation of nuclei is known, the most reasonable physical process which produces that particular permutation may be deduced. Since more than one physical process may be envisioned, the final deduction is, of course, not unique and requires some degree of chemical intuition.

A more thorough discussion of some of the basic concepts of permutational analysis may be found in Section III-A-2.

Depending on the number and nature of the bidentate chelating rings, a wide variety of stereoisomeric possibilities exist. The simplest procedure for delineating the stereoisomeric interconversions allowed for a particular mechanism operating on a specific type of complex is through the use of a topological figure. Stereoisomers are represented at the vertices of a three dimensional geometric figure and specific operations that interconvert two stereoisomers are represented by a line joining the two vertices, with the intermediate located midway along this line. If these operations are performed on all possible isomers for the particular system of interest, a complete description of the stereochemical consequences of a single mechanism is produced. Then by simple reference to the topological figure, one may determine whether a particular mechanism gives the desired stereochemical interconversions.

Despite the interest in nonrigid six-coordinate chelate complexes (6,7), the number of systems for which unique rearrangement mechanisms have been proven have not as yet been commensurately rewarding. Operation of a particular mechanism has only been demonstrated in a few cases: $M(\alpha\text{-}C_3H_5T)_3$ and $M(\alpha\text{-}C_3H_7T)_3$ where M = Al(III) (26), Ga(III) (37), and Co(III) (26), $[Fe(Me,Bz\text{-}dtc)_3]BF_4$ (30,32), $Fe(Me,Bz\text{-}dtc)_3$ (32,48),

and $Ru(Me,Bz\text{-}dtc)_3$ (31). Less definitive but analagous results have recently been obtained for a series of tris(N,N-disubstituted dithiocarbamato)metal(III) complexes (33), where M = V(III), Mn(III), Ga(III), In(III), and Cr(III). For all these complexes the most reasonable physical process has been identified as a trigonal twist motion about a pseudo-C_3 axis of the trans isomer and the real-C_3 axis of the cis isomer. A similar process most likely operates in the mixed complexes $Fe(R_1,R_2\text{-}dtc)_2(BB)$ where BB = tfd and mnt, although the evidence is less definitive.

Basically two techniques have been employed in the assignment of this particular mechanism: (1) complex coalescence patterns are computer simulated for a variety of mechanisms and visual comparison with experimental spectra yields the most probable rearrangement mechanism (26,37); (2) coalescence patterns of well separated resonances are observed and the rearrangement mechanism is determined directly from the observed permutation of nuclei (27-32,48). The second technique invariably requires the use of paramagnetic complexes manifesting large isotropic shifts which magnify small chemical shift differences (49).

To explain the operation of a twist mechanism, relationships between structure and kinetics and mechanism have been sought. Extensive discussion (26,28,32,33,37,45-47,50,51) has centered on the distortions toward TP geometry induced by those ligands with a short "bite" distance. Such distortions should facilitate rearrangement via a twist mechanism. However, structural data alone cannot account for the relative rates of operation of a twist mechanism (32,33) and any explanation for the various barriers must be based on electronic configuration (50,51) arguments. Pignolet and co-workers (32,33) have found that the difference in Ligand

Field Stabilization Energy (LFSE) for the octahedral and trigonal prismatic geometries, Δ(LFSE) = Oh(LFSE) - TP(LFSE), correlates well with the $\Delta H^{\neq}$ for optical inversion in a series of tris(N,N-disubstituted-dithiocarbamato)metal complexes, where the metal varies from low spin Fe(II) to low-spin Rh(III), which cover possible orbital occupancies for the d^4 - d^6 systems.

While intensive efforts have focused on tris chelate complexes, relatively little attention has been centered on the important class of bis chelates containing two monodentate ligands (6,7). The most thoroughly studied examples of this class of complexes are the dihalobis(β-diketonato)metal(IV) complexes, where M(IV) = Ti, Zr, Hf, Ge, and Sn (52-60). Most of these complexes are stereochemically nonrigid, existing in solution as the cis-dihalo isomer which undergoes rapid intramolecular configurational rearrangements. Analagous results have been obtained for a series of dialkoxy- (61) and diphenoxybis(β-diketonato)titanium(IV) (62) complexes. Dialkoxybis(β-diketonato)zirconium(IV) complexes behave similarly (63). Despite the significant synthetic and stereochemical studies which have been made on complexes of the type $M(chelate)_2X_2$ (where M is a group IV metal, chelate = β-diketonate, etc., and X = uninegative, unidentate ligand), there is a paucity of kinetic data surrounding the rearrangement processes occurring in these complexes. There is even a scarcity of detailed knowledge as to the actual configurational changes taking place during the rearrangement. For example, does the rearrangement involve the enantiomerization of the optically active cis-X_2 species? Thus, despite the vigorous study of rearrangements of chelate complexes, the $M(chelate)_2X_2$ systems remain somewhat ignored.

This thesis reports an investigation into the kinetics and

mechanisms of configurational rearrangements of group IV metal complexes of the type $M(AA)_2X_2$, $M(AA)_2XY$, and $M(AB)_2X_2$, in which the chelating groups are β-diketones and 8-hydroxyquinoline-type ligands. Of particular interest was the use of diastereotopic groups to probe the importance of enantiomerization processes during the rearrangement. The isopropyl group was chosen as the probe and was placed in all conceivable positions within the $M(chelate)_2X_2$ framework.

It was evident early in the investigation that a thorough and complete delineation of the stereoisomeric interconversions allowed for these systems had not been undertaken. Consequently, a complete permutational and mechanistic analysis was performed on the cis-$M(AA)_2X_2$, cis-$M(AA)_2XY$, and cis-$M(AB)_2X_2$ systems in the hopes that such an analysis would facilitate the interpretation of experimental observations.

The kinetics of configurational rearrangements were measured using a Total Line Shape (TLS) method for a series of $Ti(acac)_2(phenoxy)_2$ complexes, where the size and electronic features of the phenoxy ligand were varied. Since kinetic data for similar alkoxy (61) and some identical phenoxy (62) complexes had previously been obtained by the use of approximate equations, an experimental comparison was made between kinetic data obtained using TLS and approximate methods. This serves as a guide to the accuracy and reliability of approximate methods in extracting kinetic data from variable temperature nmr experiments.

Since a five-coordinate intermediate could possibly be involved in the rearrangement of these complexes, it was of interest to attempt to determine the veracity of reports of stable five-coordinate titanium(IV) complexes (64-68). Although a thorough investigation was

not made, some evidence is presented which suggests that these species are not five-coordinate in the solid state, but rather dimeric species containing halogen or alkoxy bridging groups.

II. EXPERIMENTAL SECTION

A. Preparation of Compounds

1. Reagents and Solvents

The following metal-containing reagents were procured from commercial sources and used without further purification: titanium (IV) fluoride (Research Organic/Inorganic), titanium(IV) chloride (Fisher), titanium(IV) bromide (Alpha Inorganics), titanium(IV) isopropoxide (Research Organic/Inorganic), anhydrous tin(IV) chloride (Fisher), germanium(IV) chloride (Research Organic/Inorganic), silicon(IV) chloride (Alpha Inorganics), and antimony(V) chloride (Allied Chemicals).

β-diketones were obtained from commercial suppliers and were employed without further purification: reagent grade 2,4-pentanedione (Fisher), 1-phenyl-1,3-butanedione (Aldrich), 2,6-dimethyl-3,5-heptanedione (Eastman), 2,2,6,6-tetramethyl-3,5-heptanedione (Eastman), 1,1,1-trifluoro-5,5-dimethyl-2,4-pentanedione (Eastman), 1,1,1-trifluoro-5,5-dimethyl-2,4-hexanedione (Eastman), and 3-isopropyl-2,4-pentanedione (K & K Laboratories).

8-quinolinol and 2-methyl-8-quinolinol were used as received from Eastman and Aldrich Chemical Cos., respectively.

Phenols were used as received from the indicated suppliers: phenol (Eastman), 4-isopropylphenol (Aldrich), 2-phenylphenol (Eastman), and 2,6-di-t-butylphenol (Aldrich). 2-isopropylphenol and 2,6-di-isopropylphenol were kindly supplied by Drs. J. F. Harrod and K. R. Taylor of McGill University.

Diols were used as received from commercial sources: 1,2-dihydroxybenzene (catechol), Eastman, and 3,5-diisopropyl-1,2-dihydroxybenzene (3,5-diisopropylcatechol), Pfaltz and Bauer. 3,6-diisopropyl-1,2-dihydroxybenzene (3,6-diisopropylcatechol), Aldrich, was obtained from Dr. K. R. Taylor.

All organic solvents used in the preparation and purification of compounds were reagent grade and were dried by refluxing over calcium hydride for at least 12 hr and distilled therefrom immediately before use; the only exception to this procedure was diethyl ether, which was dried by standing over sodium metal. Glacial acetic acid was used as received, from a freshly opened bottle.

2. General Techniques

Since most of the complexes reported in this thesis are subject to some degree of hydrolysis, especially in solution, all syntheses and subsequent handling of compounds were conducted under anhydrous conditions in a nitrogen atmosphere. All reactions and recrystallizations were carried out under nitrogen in a glass-stoppered erlenmeyer flask equipped with a side-arm nitrogen inlet. To reflux solutions, the erlenmeyer flask was fitted with a reflux condenser which had a Drierite drying tube connected at the exit. The assembly was purged with nitrogen before applying heat and, occasionally, during reflux to help remove any evolved gases. In the case of very soluble compounds, solutions were routinely cooled to -78° by immersing the flask in an acetone/dry ice bath to initiate crystallization. Filtrations were performed using a modified fritted glass funnel similar to that described by Pinnavaia and Fay (69). Solutions were concentrated either by passing a stream of nitrogen over the surface or

applying a partial vacuum produced by an efficient water aspirator. Transfers of solids, solutions, and hydrolytically unstable reagents were done in a nitrogen-filled glove bag containing a dish of phosphorous(V) oxide. All glassware used was with standard-taper joints which were generally lubricated with Dow-Corning High Vacuum grease when drying a material in vacuo. Glassware was routinely cleaned in a saturated KOH/C_2H_5OH solution and glass frits were further cleaned by allowing a concentrated HCl/HNO_3 mixture to slowly drip through the pores. Finally, all glassware was dried at temperatures greater than 120^{o} for several hours and cooled in a nitrogen atmosphere prior to use.

Samples were stored in screw-top vials sealed with electrical vinyl tape and stored in a dessicator containing Drierite.

3. Melting Points

Melting points were measured in capillaries, sealed with modeling clay, with a Gallenkamp Melting Point Apparatus Model No. MF-370. Reported melting points are uncorrected.

4. Elemental Analyses

All analyses were performed by Galbraith Laboratories, Inc., Knoxville, Tennessee, U.S.A. Samples were sent in screw-top vials sealed with vinyl tape.

5. Difluorobis(2,6-dimethyl-3,5-heptanedionato)titanium(IV).-

A solution of 10.25 g (65.6 mmols) of diisobutyrylmethane in 25 ml of dichloromethane was added to a suspension of 4.00 g (32.3 mmols) of titanium(IV) fluoride in 75 ml of dichloromethane. The mixture was refluxed

under nitrogen for 5.5 hr and filtered to remove a small amount of insoluble white material. Removal of solvent under a stream of nitrogen gave a yellow-orange residue, which was dissolved in 250 ml of boiling hexane to give, on concentrating and cooling, a pale yellow solid; 7.80 g (60% theoretical). The crude product was recrystallized twice from hot hexane and dried in vacuo; mp 73-75° (dec).

Anal. Calcd. for $TiC_{18}H_{30}O_4F_2$: C, 54.55; H, 7.63. Found: C, 54.94; H, 7.60.

6. Dichlorobis(2,6-dimethyl-3,5-heptanedionato)titanium(IV).-

To a solution of 8.03 g (51.4 mmols) of diisobutyrylmethane in 50 ml of dichloromethane was added dropwise, from a syringe, 2.70 ml (4.66 g; 24.6 mmols) of titanium(IV) chloride. A deep red solution was formed and copious amounts of hydrogen chloride were evolved. The solution was purged with a gentle stream of nitrogen for 0.5 hr to aid in the removal of hydrogen chloride. Removal of some dichloromethane and addition of hexane gave an orange-red solid; yield 8.87 g (84% theoretical). The crude product was recrystallized from dichloromethane-hexane solutions and dried in vacuo; mp 135-136° (dec).

Anal. Calcd. for $TiC_{18}H_{30}O_4Cl_2$: C, 50.37; H, 7.05; Ti, 11.16; Cl, 16.52. Found: C, 50.73; H, 7.01; Ti, 11.41; Cl, 16.75.

7. Dibromobis(2,6-dimethyl-3,5-heptanedionato)titanium(IV).-

A solution of 8.40 g (53.8 mmols) of diisobutyrylmethane in 50 ml of dichloromethane was added to 9.63 g (26.2 mmols) of solid titanium(IV) bromide. A blood red solution formed instantly. The solution was purged with a gentle stream of nitrogen for 1 hr to

dissipate evolved hydrogen bromide. Addition of hexane and evaporation of dichloromethane led to the formation of a bright red solid, which was recrystallized twice from dichloromethane-hexane solutions and dried *in vacuo*; mp 122-124° (dec).

Anal. Calcd. for $TiC_{18}H_{30}O_4Br_2$: C, 41.73; H, 5.84. Found: C, 41.85; H, 5.81.

8. Dichlorobis(2,6-dimethyl-3,5-heptanedionato)tin(IV).-

A solution of 2.12 ml (4.73 g; 18.2 mmols) of anhydrous tin(IV) chloride and 5.68 g (36.4 mmols) of diisobutyrylmethane in 50 ml of dichloromethane was refluxed for 3.5 hr under a nitrogen atmosphere. The pale yellow solution was concentrated to *ca.* 25 ml; addition of hexane gave an off-white solid, which was collected, washed with 10 ml of hexane, and dried *in vacuo*; yield 7.30 g (80% theoretical). The crude product was recrystallized from dichloromethane-hexane, chloroform-ether, and finally from a dichloromethane-hexane mixture to give colorless crystals, which were dried *in vacuo*; mp 129-131°.

Anal. Calcd. for $SnC_{18}H_{30}O_4Cl_2$: C, 43.24; H, 6.05. Found: C, 43.39; H, 5.95.

9. Dichlorobis(2,6-dimethyl-3,5-heptanedionato)germanium(IV).-

A mixture of 10.12 g (64.8 mmols) of diisobutyrylmethane and 3.40 ml (6.39 g; 29.8 mmols) of germanium(IV) chloride, dissolved in *ca.* 70 ml of hexane, was refluxed for 12 hr under a nitrogen atmosphere. The pale yellow solution was filtered and concentrated to a volume of *ca.* 20 ml. Cooling to -78° resulted in the deposition of a bright white powder, which was collected, washed with three 15 ml portions of hexane (pre-

cooled to -78°), and dried *in vacuo*; yield 9.26 g (65% theoretical). The crude product was recrystallized from a dichloromethane-hexane mixture at -78°; mp 116-118°.

Anal. Calcd. for $GeC_{18}H_{30}O_4Cl_2$: C, 47.63; H, 6.66. Found: C, 47.93; H, 6.57.

10. Chloromethoxybis(2,6-dimethyl-3,5-heptanedionato)titanium(IV).-

To an orange-red solution of 4.39 g (10.2 mmols) of $Ti(dibm)_2Cl_2$ in *ca.* 40 ml of dichloromethane was added 0.85 ml (0.84 g;10.6 mmols) of pyridine to give a green-yellow solution. Addition of 0.45 ml (0.36 g; 11.1 mmols) of methanol resulted in an orange-yellow solution, which on stirring deposited a white solid. The solution was concentrated to one-half its original volume and 20 ml of hexane added. The white solid was collected, washed with hexane, and dried *in vacuo*. The filtrate was further concentrated and *ca.* 80 ml of hexane added and the solution stored in a freezer for several hours. A small amount of white solid was filtered off and the solvent stripped from the filtrate to give a viscous orange liquid, which was dissolved in 20 ml of hexane and stored in a freezer. The resulting yellow-orange solid was collected and dried *in vacuo*; yield 2.70 g (62% theoretical). The crude product was recrystallized from hexane at low temperature (*ca.* -10°); mp 43-45°. The purity of the product was verified by infrared and proton nmr spectroscopy.

The white solid initially isolated was washed exhaustively with hexane containing a small amount of dichloromethane and dried *in vacuo*. It melted at 142-146°. Thompson and co-workers (70) report a melting point of 139-145° for the pyridinium chloride produced in the reaction of $Ti(acac)_2Cl_2$ with allyl alcohol in the presence of pyridine.

11. Tris(2,6-dimethyl-3,5-heptanedionato)titanium(IV) Hexachloroantimonate(V).-

A suspension of 4.00 g (9.32 mmols) of $Ti(dibm)_2Cl_2$ in ca. 50 ml of glacial acetic acid was heated until a clear red solution was obtained. To this hot solution was added dropwise a solution of 0.87 ml (2.03 g; 6.79 mmols) of antimony(V) chloride in 15 ml of glacial acetic acid. After the addition was complete, the solution was stirred vigorously for 2 hr while cooling to room temperature. Scratching the inside of the flask resulted in the formation of a fluffy orange solid, which was collected and dried in vacuo. A second crop of product was obtained on concentrating the filtrate. The combined yield of crude product was 3.73 g (71% theoretical).

Attempted recrystallization from dichloromethane-hexane solutions resulted in the formation of an oil. Successful purification was achieved by recrystallization from chloroform-ether solutions; mp 152-154° (dec).

Anal. Calcd. for $TiC_{27}H_{45}O_6SbCl_6$: C, 38.24; H, 5.35; Ti, 5.65; Cl, 25.08; Sb, 14.36. Found: C, 38.13; H, 5.30; Ti, 5.48; Cl, 25.28; Sb, 14.17.

12. Tris(2,6-dimethyl-3,5-heptanedionato)silicon(IV) Chloride.-

A mixture of 1.92 ml (2.84 g; 16.7 mmols) of silicon(IV) chloride and 7.83 g (50.1 mmols) of diisobutyrylmethane was refluxed for 2 hr in 60 ml of benzene. A pale yellow solution was formed and a yellow oil was formed while hydrogen chloride was evolved. On cooling to room temperature the oil did not solidify. After removing the benzene in a stream of nitrogen, the addition of a large excess of ether gave a fluffy white product, which was collected, washed with ether, and dried in vacuo; yield 7.00 g (70%

theoretical).

The crude product was recrystallized from chloroform-ether solutions. This compound was characterized only by its unique proton nmr spectrum and infrared spectroscopy. The product is formulated as the chloride salt of the $[Si(dibm)_3]^+$ cation on the basis of the failure to observe a resonance from the HCl_2^- anion, which is the other possible counterion.

13. Tris(2,6-dimethyl-3,5-heptanedionato)germanium(IV) Hexachloroantimonate(V).-

To a solution of 4.86 g (10.7 mmols) of $Ge(dibm)_2Cl_2$ in 20 ml of chloroform was added 1.38 ml (3.23 g; 10.8 mmols) of antimony(V) chloride. The pale yellow solution was stirred at room temperature for 2 hr, after which a white solid began to precipitate from the solution. After adding ca. 150 ml of ether, the fluffy white solid was collected, washed with ether, and dried in vacuo; yield 4.31 g (69% theoretical).

The crude product was recrystallized from chloroform-ether solutions. This product was characterized only by its proton nmr and infrared spectra.

14. Difluorobis(2,2,6,6-tetramethyl-3,5-heptanedionato)titanium(IV).-

A solution of 9.30 g (50.4 mmols) of dipivaloylmethane in 25 ml of dichloromethane was added to a suspension of 5.05 g (25.1 mmols) of titanium(IV) fluoride in 75 ml of dichloromethane. The mixture was refluxed under nitrogen for 6 hr and filtered to remove a small amount of insoluble white material. Removal of solvent under a stream of nitrogen gave a yellow residue, which was extracted with 150 ml of boiling hexane

to give, on concentrating and cooling, a pale yellow solid; 9.5 g; 84% theoretical). The crude material was recrystallized twice from hot hexane and dried *in vacuo*; mp 138-140°. Lit: (58,71) mp 144-146°.

Anal. Calcd. for $TiC_{22}H_{38}O_4F_2$: C, 58.40; H, 8.47. Found: C, 59.48; H, 7.90. The material was further sublimed at *ca.* 95° (*ca.* 0.01 torr) and was judged pure by proton nmr and infrared spectroscopy; mp 139-141°.

15. Dichlorobis(2,2,6,6-tetramethyl-3,5-heptanedionato)titanium(IV).-

To a solution of 5.90 g (32.0 mmols) of dipivaloylmethane in 50 ml of dichloromethane was added, dropwise from a syringe, 1.70 ml (2.93 (2.93 g; 15.5 mmols) of titanium(IV) chloride. An orange solution formed. The solution was purged for 30 min with a gentle stream of nitrogen to dispell evolved hydrogen chloride. Evaporation of some dichloromethane and addition of hexane yielded an orange-yellow [redacted]. The crude product was recrystallized twice from dichloromethane-he[redacted]lutions and dried *in vacuo* to give a bright yellow powder; mp 124-[redacted]ec).

Anal. Calcd. for $TiC_{22}H_{38}O_4Cl_2$: C, 54.44; H, 7.89; Ti, 9.87; Cl, 14.61. Found: C, 54.60; H, 7.82; Ti, 9.62; Cl, 14.88.

16. Dibromobis(2,2,6,6-tetramethyl-3,5-heptanedionato)titanium(IV).-

A solution of 6.05 g (32.8 mmols) of dipivaloylmethane in 50 ml of dichloromethane was added to a slurry of 5.82 g (15.8 mmols) of titanium(IV) bromide in 25 ml of dichloromethane. A blood-red solution formed with vigorous evolution of hydrogen bromide. The solution was purged with a gentle stream of nitrogen for 1 hr to aid in the removal of hydrogen bromide and subsequently filtered to remove traces of an

insoluble material. Concentrating the solution to a volume of ca. 10 ml and adding excess hexane gave a red-orange powder; yield 8.64 g (95% theoretical). The crude product was recrystallized twice from boiling hexane; mp 133-135° (dec).

Anal. Calcd. for $TiC_{22}H_{38}O_4Br_2$: C, 46.02, H, 6.67. Found: C, 46.26; H, 6.59.

17. Dichlorobis(1,1,1-trifluoro-5-methyl-2,4-hexanedionato)-titanium(IV).

To a solution of 5.40 g (29.7 mmols) of 1,1,1-trifluoro-5-methyl-2,4-hexanedione in 50 ml of benzene was added, dropwise from a syringe, 1.50 ml (2.58 g; 13.7 mmols) of titanium(IV) chloride. A red-orange solution formed immediately with concomitant hydrogen chloride evolution. The solution was purged with a gentle stream of nitrogen for 30 min, followed by evaporation of some benzene. Addition of hexane resulted in the formation of a yellow-green solid, which was collected, washed with hexane, and dried in vacuo; yield 6.50 g (78% theoretical). Two recrystallizations from dichloromethane-hexane solutions yielded a bright yellow-green solid; mp 90-92° (dec).

Anal. Calcd. for $TiC_{14}H_{16}O_4F_6Cl_2$: C, 34.95; H, 3.35; Ti, 9.96; F, 23.70; Cl, 14.56. Found: C, 34.99; H, 3.59; Ti, 10.03; F, 23.54; Cl, 14.56.

18. Dichlorobis(1,1,1-trifluoro-5-methyl-2,4-hexanedionato)tin(IV).

A mixture of 1.10 ml (2.46 g; 9.42 mmols) of anhydrous tin(IV) chloride and 5.30 g (29.1 mmols) of 1,1,1-trifluoro-5-methyl-2,4-hexanedione in 50 ml of dichloromethane was refluxed for 3.5 hr. The resulting

pale yellow solution was filtered and the solvent was removed with a nitrogen sweep to yield an off-white solid, which was slurried in -78° hexane, filtered, and dried in vacuo; yield 4.16 g (80% theoretical). Several recrystallizations from dichloromethane-hexane solutions gave a bright white solid; mp 72-74°.

The purity of this complex was verified from infrared and proton nmr spectra.

19. Dichlorobis(1,1,1-trifluoro-5,5-dimethyl-2,4-hexanedionato)-titanium(IV).-

To a solution of 5.00 g (25.5 mmols) of 1,1,1-trifluoro-5,5-dimethyl-2,4-hexanedione in 50 ml of dichloromethane was added, dropwise from a syringe, 1.30 ml (2.25 g; 11.3 mmols) of titanium(IV) chloride. An orange solution was formed and hydrogen chloride was evolved. The solution was purged with nitrogen for ca. 30 min and the solution concentrated to a volume of ca. 10 ml. Addition of excess hexane led to the formation of an orange solid. Two recrystallizations from dichloromethane-hexane solutions yielded an orange solid; mp 119-121° (dec).

The purity of this complex was verified by infrared and proton nmr spectroscopy.

20. Dichlorobis(3-isopropyl-2,4-pentanedionato)titanium(IV).-

To a solution of 3.00 g (21.1 mmols) of 3-isopropyl-2,4-pentanedione in 50 ml of dichloromethane was added, dropwise from a syringe syringe, 1.04 ml (1.80 g; 9.46 mmols) of titanium(IV) chloride. A blood red solution was formed immediately and some hydrogen chloride was evolved evolved. The solution was refluxed under nitrogen until evolution of

hydrogen chloride has ceased (3.5 hr). The solution was then filtered and concentrated to a volume of ca. 10 ml. Addition of hexane yielded a red solid, which was stored under nitrogen overnight in a freezer (ca. 0°). The crude product was collected, washed with cold hexane, and dried in vacuo; yield 2.75 g (73% theoretical). The crude product was recrystallized twice from dichloromethane-hexane solutions; mp 170-172° (dec).

Anal. Calcd. for $TiC_{16}H_{26}O_4Cl_2$: C, 47.90; H, 6.53. Found: C, 47.69; H, 6.58.

In another preparation of this complex, titanium(IV) chloride and 3-isopropylacetylacetone (1:2 mole ratio) were mixed in dichloromethane. Some hydrogen chloride was evolved. After standing at room temperature for 2 hr, hexane was added and the solution placed in a freezer (ca. 0°) for 3 hr. An orange solid was collected, washed with hexane, and dried in vacuo; mp 102-104° (dec). The infrared spectrum (nujol mull) of the solid exhibited a strong band at ca. 1670 cm^{-1} and a medium-weak band at ca. 800 cm^{-1}, which would not be expected for a complex containing a β-diketonate anion. This orange product appears to be the titanium tetrachloride adduct of the keto tautomer of 3-isopropyl-2,4-pentanedione; similar adducts have been isolated with 2,4-pentanedione and 3-methyl-2,4-pentanedione with titanium(IV) chloride (72). As with previously isolated adducts, the 3-isopropylacetylacetone adduct apparently evolved hydrogen chloride at elevated temperature to form the titanium(IV) enolate anion complex.

21. Reaction of Anhydrous Tin(IV) Chloride with 3-isopropyl-2,4-pentanedione.-

To a solution of 2.00 g (14.1 mmols) of 3-isopropylacetylacetone in 50 ml of hexane was added, dropwise from a syringe, 0.80 ml (1.79 g; 6.85 mmols) of anhydrous tin(IV) chloride. A bright white solid formed immediately. The suspension was refluxed under nitrogen for 14 hr. Some decomposition occurred as the solution developed a slight brown color. The solid was filtered, washed thoroughly with four 20 ml portions of hexane, and dried in vacuo to yield a chalky, sticky white solid. Evaporation of the brown filtrate gave a brown sticky mass and was not investigated further.

An infrared spectrum (nujol mull) of the white solid showed the following bands which were not expected from a complex containing an enolate anion: ca. 3400 (s,br), ca. 1660 (s), and ca. 800 cm^{-1}. The similarity between this spectrum and that of the titanium(IV) adduct with 3-isopropylacetylacetone indicates that an analagous adduct with tin(IV) chloride was formed. Stable adducts of the keto tautomer of β-diketones with tin tetrachloride have also been isolated (72). Interestingly, on prolonged heating the tin adduct with 3-isopropylacetylacetone did not expel hydrogen chloride to form an enolate anion complex, as was the case with the titanium(IV) adduct and the tin tetrachloride-acetylacetone adduct (72).

22. Bis(isopropoxy)bis(2,4-pentanedionato)titanium(IV).-

This complex was prepared by the direct reaction of titanium(IV) isopropoxide with acetylacetone (1:2 mole ratio) in benzene. After stirring at room temperature for several hours, benzene and isopropyl alcohol were removed under reduced pressure to give a viscous orange liquid. This product, $Ti(acac)_2(OC_3H_7^i)_2$, was used without

further purification in subsequent syntheses.

23. Bis(phenoxy)bis(2,4-pentanedionato)titanium(IV).-

A solution of 6.02 g (16.5 mmols) of $Ti(acac)_2(OC_3H_7^i)_2$ and 3.16 g (33.6 mmols) of phenol in 50 ml of benzene was refluxed for ca. 16 hr. Removal of solvent under reduced pressure and cooling under nitrogen gave a cake of orange crystals. Addition of excess hexane, filtration, and drying in vacuo yielded 6.45 g (90% theoretical) of crude product. The orange solid was recrystallized twice from dichloromethane-hexane solutions; mp 128-130° (dec). Lit. (73) mp 127-128°.

The purity of this compound was verified by infrared and proton nmr spectroscopy.

24. Bis(2-chlorophenoxy)bis(2,4-pentanedionato)titanium(IV).-

A sample of this complex was kindly provided by Dr. K. R. Taylor. Recrystallization from a dichloromethane-hexane solution gave a yellow solid; mp 166-168° (dec).

Anal. Calcd. for $TiC_{22}H_{22}O_6Cl_2$: C, 52.72; H, 4.42. Found: C, 52.39; H, 4.40.

25. Bis(2-iodophenoxy)bis(2,4-pentanedionato)titanium(IV).-

A generous sample of this compound was kindly supplied by Dr. K. R. Taylor. Recrystallization from a dichloromethane-hexane solution gave a yellow-orange solid; mp 141-143° (dec). Lit. (73) mp 145-146°.

Anal. Calcd. for $TiC_{22}H_{22}O_6I_2$: C, 38.63; H, 3.24. Found: C, 38.47; H, 3.16.

26. Bis(2,6-dichlorophenoxy)bis(2,4-pentanedionato)-titanium(IV).-

A generous sample of this complex was kindly provided by Dr. K. R. Taylor. Recrystallization from a dichloromethane-hexane solution gave a yellow-orange solid; mp 112-114° (dec).

Anal. Calcd. for $TiC_{22}H_{20}O_6Cl_4$: C, 46.35; H, 3.54. Found: C, 46.23; H, 3.73.

27. Bis(4-chlorophenoxy)bis(2,4-pentanedionato)titanium(IV).-

A sample of this complex was kindly supplied by Dr. K. R. Taylor. Recrystallization from a dichloromethane-hexane solution gave a yellow solid; mp 114-116° (dec). Lit. (73) mp 124-125°.

Anal. Calcd. for $TiC_{22}H_{22}O_6Cl_2$: C, 52.72; H, 4.42. Found: C, 52.64; H, 4.42.

28. Bis(2,6-diisopropylphenoxy)bis(2,4-pentanedionato)-titanium(IV).-

This compound was obtained from Dr. K. R. Taylor. Recrystallization from dichloromethane-hexane and finally benzene-hexane solutions gave a red solid; mp 136-138° (dec). Lit. (73) mp 139-140°.

The purity of this complex was verified by infrared and proton nmr spectroscopy.

29. Bis(2-isopropylphenoxy)bis(2,4-pentanedionato)titanium(IV).-

A solution of 6.30 g (46.3 mmols) of 2-isopropylphenol in 50 ml of benzene was added to a solution of 8.05 g (22.1 mmols) of $Ti(acac)_2(OC_3H_7^i)_2$ in 10 ml of benzene; the resulting red solution was

stirred at room temperature for 4 hr. Removal of solvent under reduced pressure gave a viscous red liquid. This liquid was dissolved in ca. 50 ml of hexane and upon concentrating and cooling the solution, a red-orange solid formed, which was collected, washed with hexane, and dried in vacuo. The crude product was purified by recrystallization from dichloromethane-hexane solutions to give an orange solid; mp 102-103° (dec). Lit. (73) mp 106-107°.

Anal. Calcd. for $TiC_{28}H_{36}O_6$: C, 65.11; H, 7.03. Found: C, 65.11; H, 7.07.

30. Bis(4-isopropylphenoxy)bis(2,4-pentanedionato)titanium(IV).- To a solution of 5.53 g (15.2 mmols) of $Ti(acac)_2(OC_3H_7^i)_2$ in 10 ml of benzene was added a solution of 4.30 g (31.6 mmols) of 4-isopropylphenol in 40 ml of benzene. The red-orange solution was stirred at room temperature for 2 hr and filtered. Concentrating the solution to a volume of ca. 20 ml under reduced pressure and adding hexane produced a cake of orange crystals. The mother liquor was decanted under nitrogen and the solid slurried in 20 ml of hexane, filtered, washed with another 20 ml of hexane, and dried in vacuo; yield 3.74 g (48% theoretical). The orange solid was recrystallized from a benzene-hexane solution; mp 147-149° (dec).

Anal. Calcd. for $TiC_{28}H_{36}O_6$: C, 65.11; H, 7.03; Ti, 9.27. Found: C, 64.91; H, 7.04; Ti, 9.05.

31. Bis(2-phenylphenoxy)bis(2,4-pentanedionato)titanium(IV).- A slurry of 4.63 g (27.2 mmols) of 2-phenylphenol in 50 ml of benzene was added to a solution of 4.81 g (13.2 mmols) of $Ti(acac)_2$-

$(OC_3H_7^i)_2$ in 20 ml of benzene. The solution turned a deep red color and the solid phenol gradually dissolved as the reaction proceeded. After stirring at room temperature for 3 hr, the solution was filtered and then concentrated under reduced pressure to yield a viscous red liquid. This liquid was taken up in a minimum amount of dichloromethane and addition of hexane resulted in the formation of an orange solid in 67% yield. Two recrystallizations from dichloromethane-hexane solutions gave an orange powder; mp 123-125° (dec).

Anal. Calcd. for $TiC_{34}H_{32}O_6$: C, 69.87; H, 5.52. Found: C, 69.97; H, 5.60.

32. Bis(3-methylphenoxy)bis(2,4-pentanedionato)titanium(IV).-

To a solution of 9.70 g (26.6 mmols) of $Ti(acac)_2(OC_3H_7^i)_2$ in ca. 10 ml of benzene was added a solution of 5.91 g (54.7 mmols) of 3-methylphenol in 50 ml of benzene. The red solution that formed immediately was stirred overnight at room temperature under nitrogen. Removal of solvent under reduced pressure gave a dark red viscous liquid, which on cooling yielded red-orange crystals. The crude product was slurried in excess hexane, filtered, and dried in vacuo; yield 11.12 g (91% theoretical). The crude product was recrystallized twice from dichloromethane-hexane solutions and once from a benzene-hexane solution to give an orange solid; mp 103-105° (dec).

Anal. Calcd. for $TiC_{24}H_{28}O_6$: C, 62.61; H, 6.13. Found: C, 62.64; H, 6.08.

33. Bis(4-benzyloxyphenoxy)bis(2,4-pentanedionato)titanium(IV).-

To a solution of 5.40 g (14.8 mmols) of $Ti(acac)_2(OC_3H_7^i)_2$

in 10 ml of benzene was added a suspension of 6.11 g (30.5 mmols) of 4-benzyloxyphenol in 50 ml of benzene. The resulting deep red solution was stirred overnight at room temperature, filtered, and concentrated to a volume of ca. 10 ml under reduced pressure. Addition of hexane gave a red-orange solid; yield 8.76 g (92% theoretical). The crude product was recrystallized twice from dichloromethane-hexane solutions; mp 121-123° (dec).

Anal. Calcd. for $TiC_{36}H_{36}O_8$: C, 67.08; H, 5.63. Found: C, 67.33; H, 5.53.

34. Chloroisopropoxybis(2,4-pentanedionato)titanium(IV).- A red-orange solution of 6.95 g (21.9 mmols) of $Ti(acac)_2Cl_2$* in 30 ml of dichloromethane was added to 6.88 g (24.2 mmols) of pure liquid titanium(IV) isopropoxide. The solution gradually changed to a bright yellow color and was stirred overnight at room temperature. Removal of solvent under reduced pressure gave a yellow oil which was taken up in a minimum amount of hexane. Cooling overnight in a freezer (ca. 0°) yielded a yellow powder. The mixture was cooled to -78°, filtered, the solid washed with pre-cooled hexane (-78°), and dried in vacuo; yield 4.16 g (56% based on $Ti(acac)_2Cl_2$). The crude product was recrystallized from a benzene-hexane solution; mp 106-108°. Lit. (70) mp 110-114° (dec).

The purity of this product was verified by infrared and proton nmr spectroscopy.

35. Bromoisopropoxybis(2,4-pentanedionato)titanium(IV).- A slurry of dark red $Ti(acac)_2Br_2$* (5.44 g; 13.4 mmols) in

*Prepared according to literature methods (54).

50 ml of dichloromethane was added to 4.21 g (14.8 mmols) of pure liquid titanium(IV) isopropoxide. A green-yellow solution formed; stirring was continued overnight at room temperature. Removal of solvent under reduced pressure gave a viscous yellow liquid which was taken up in hexane. Cooling overnight in a freezer (ca. 0^{o}) gave a yellow powder. The suspension was cooled to -78^{o}, filtered, and the solid washed with pre-cooled hexane (-78^{o}) and dried in vacuo; yield 1.60 g (36% based on $Ti(acac)_2Br_2$). The crude product was recrystallized from a benzene-hexane solution; mp 105-107°.

The purity of this complex was verified by infrared and proton nmr spectroscopy.

36. Chloro(2,6-diisopropylphenoxy)bis(2,4-pentanedionato)-titanium(IV).-

To a yellow solution of 1.50 g (4.40 mmols) of $Ti(acac)_2Cl(OC_3H_7^i)$ in 20 ml of benzene was added 1.02 g (5.72 mmols) of 2,6-diisopropylphenol. The resulting blood red solution was stirred at room temperature overnight. The solvent was removed under reduced pressure; the viscous red residue was dissolved in hexane and cooled to yield a red solid. The product was collected, washed with hexane, and dried in vacuo; yield 1.63 g (81% theoretical). The crude product was purified by recrystallization from a benzene-hexane solution; mp 125-127° (dec). Before analysis, the sample was dried at 80° for 4.5 hr in vacuo.

Anal. Calcd. for $TiC_{22}H_{31}O_5Cl$: C, 57.59; H, 6.81. Found: C, 57.81; H, 7.13.

37. Bis(isopropoxy)bis(1-phenyl-1,3-butanedionato)titanium(IV).-

A solution of 6.35 g (39.2 mmols) of benzoylacetone in

50 ml of dichloromethane was added to a solution of 5.46 g (19.2 mmols) of pure titanium(IV) isopropoxide. The pale yellow solution was stirred overnight at room temperature. Concentrating the solution to a volume of 20 ml and addition of 50 ml of hexane yielded a cream colored solid, which was collected, washed with hexane, and dried in vacuo; yield 8.00 g (85% theoretical). The crude product was recrystallized from a dichloromethane-hexane solution; mp 102-104°.

The purity of this compound was further verified by infrared and proton nmr spectroscopy.

If this product is exposed to light for several days, it undergoes photochemical decomposition to a greenish-blue solid. This complex was stored in a vial wrapped with aluminum foil. Similar behaviour was observed (74) for the $Ti(bzac)_2(OC_2H_5)_2$ and $Ti(bzbz)_2(OC_2H_5)_2$ complexes.

38. Bis(2,6-diisopropylphenoxy)bis(1-phenyl-1,3-butanedionato)-titanium(IV).-

To a solution of 3.21 g (6.57 mmols) of $Ti(bzac)_2(OC_3H_7^i)_2$ in 20 ml of benzene was added 2.93 g (16.4 mmols) of 2,6-diisopropylphenol. The resulting dark-red solution was stirred overnight at room temperature. Concentrating the solution under reduced pressure gave a viscous red liquid, which was dissolved in the minimum amount of dichloromethane. After adding hexane, the solution was frozen in liquid nitrogen. On warming to room temperature, a red-orange solid remained, which was collected, washed with hexane, and dried in vacuo. A second crop of product was obtained from the above filtrate; combined yield 3.47 g (73% theoretical). The crude product was recrystallized from a dichloromethane-hexane solution; mp 89-92° (dec).

The purity of this complex was verified by infrared and proton nmr spectroscopy.

39. Bis(isopropoxy)bis(8-quinolinolato)titanium(IV).-

A warm solution of 22.35 g (154 mmols) of 8-quinolinol in ca. 100 ml of benzene was added dropwise to 21.16 g (74 mmols) of titanium(IV) titanium(IV) isopropoxide. The yellow solution was stirred for 2 hr while cooling to room temperature. This process led to the deposition of a bright yellow solid, which was collected, washed with 30 ml of hexane, and dried in vacuo. Concentration of the filtrate and addition of hexane yielded a second crop of product; combined yield 28.63 g (85% theoretical). The first crop was recrystallized from a hot 1:1 benzene-hexane solution and dried in vacuo; mp 184-185°. Lit. (73) mp 182-183°.

Anal. Calcd. for $TiC_{24}H_{26}N_2O_4$: C, 63.44; H, 5.77. Found: C, 63.69; H, 5.91.

40. Bis(2,6-diisopropylphenoxy)bis(8-quinolinolato)titanium(IV).-

This complex was kindly provided by Dr. K. R. Taylor. The sample was recrystallized twice from hot benzene-hexane solutions; mp 270-271° (dec). Lit. (73) mp 259-260°.

The purity of this complex was further checked by infrared and proton nmr spectroscopy.

41. Reaction of Bis(isopropoxy)bis(8-quinolinolato)titanium(IV) with 2,6-di-t-butylphenol.-

A solution of 2.60 g (5.72 mmols) of $Ti(ox)_2(OC_3H_7^i)_2$ and 2.57 g (12.5 mmols) of 2,6-di-t-butylphenol in ca. 75 ml of benzene was

refluxed for 43.5 hr under nitrogen. The solution was filtered while hot and concentrated to a volume of ca. 10 ml. Addition of hexane yielded a bright yellow solid, which was collected, washed with hexane, and dried in vacuo. On the basis of melting point, infrared and proton nmr spectra the product was identified as unreacted $Ti(ox)_2(OC_3H_7^i)_2$.

42. Bis(isopropoxy)bis(2-methyl-8-quinolinolato)titanium(IV).-

To 7.79 g (27.4 mmols) of titanium(IV) isopropoxide was added a warm solution of 8.95 g (55.9 mmols) of 2-methyl-8-quinolinol in 75 ml of benzene. The yellow-green solution was stirred at room temperature for 2 hr and filtered. The solution was concentrated under reduced pressure until a yellow solid began to form. An excess of hexane was added and the bright yellow solid was collected, washed with hexane, and dried in vacuo; yield 11.04 g (84% theoretical). This product, $Ti(quin)_2(OC_3H_7^i)_2$, was used in subsequent syntheses without further purification.

43. Bis(2,6-diisopropylphenoxy)bis(2-methyl-8-quinolinolato)-titanium(IV).-

A solution of 5.42 g (30.4 mmols) of 2,6-diisopropylphenol in 25 ml of benzene was added to a slurry of 6.76 g (14.0 mmols) of $Ti(quin)_2$-$Ti(quin)_2(OC_3H_7^i)_2$ in 50 ml of the same solvent. The mixture was refluxed for 2 hr until a clear red solution was formed, which was filtered and cooled to give an orange solid. After adding hexane to ensure complete crystallization, the solid was collected, washed with hexane, and dried in vacuo; yield 7.66 g (76% theoretical). The crude product was dissolved in the minimum amount of hot benzene, filtered, hexane added, and the solution allowed to stand at room temperature overnight. The orange solid was collected and dried in vacuo; mp 268-270° (dec). Lit. (73) mp 258-259°.

was collected and dried *in vacuo*; mp 268-270° (dec). Lit. (73) mp 258-259°.

The purity of this complex was checked by infrared and proton nmr spectroscopy.

44. (1,2-Benzenediolato)bis(2,4-pentanedionato)titanium(IV).- To a solution of 5.35 g (14.7 mmols) of $Ti(acac)_2(OC_3H_7^i)_2$ in 25 ml of benzene was added 1.76 g (16.0 mmols) of solid 1,2-dihydroxybenzene (catechol). The solution immediately turned a very dark red-brown color and the solid catechol dissolved as the reaction progressed. After stirring at room temperature for 2 hr the solution was concentrated to one-half its original volume and hexane was added to yield 4.16 g (82% theoretical) of a very dark red-brown solid, after filtering and drying *in vacuo*. The crude product was recrystallized twice from dichloromethane-hexane solutions; mp 227-229°. Lit. (75) mp 222-223°.

The purity of this complex was verified by infrared and proton nmr spectroscopy.

A complex of this constitution has been reported (75) *via* a different preparative route. The reaction of $Ti(cat)(OC_3H_7^i)_2$ with 2,4-pentanedione gave a brown solid, mp 222-223°, shown to be the monomeric nonelectrolyte $Ti(cat)(acac)_2$ by elemental analysis, molecular weight and conductance measurements. However, no spectroscopic properties were reported. The similarity in physical properties and the observation of expected infrared and proton nmr spectra for the material reported here indicates that the $Ti(cat)(acac)_2$ complex is accessible *via* two preparative routes.

45. (1,2-Benzenediolato)bis(1-phenyl-1,3-butanedionato)-titanium(IV).-

A suspension of 1.03 g (9.35 mmols) of 1,2-dihydroxybenzene in ca. 60 ml of benzene was added to a solution of 4.00 g (8.19 mmols) of $Ti(bzac)_2(OC_3H_7^i)_2$ in 20 ml of benzene. An immediate reaction occurred to give a dark red-brown solution. After stirring at room temperature for 1 hr the solution was concentrated to one-half its original volume and 50 ml of hexane was added. After standing at room temperature for 24 hr, a cake of black crystals formed. The solid was collected, washed with 20 ml of hexane, and dried in vacuo; yield 3.26 g (82% theoretical). The dark red-brown solid was recrystallized from a dichloromethane-hexane solution; mp 241.5-242.5°.

Anal. Calcd. for $TiC_{26}H_{22}O_6$: C, 65.28; H, 4.64. Found: C, 61.46; H, 4.88.

The sample on which the above analysis was obtained was recrystallized again from a dichloromethane-hexane solution; mp 244-246°.

Anal. Calcd. for $TiC_{26}H_{22}O_6$: C, 65.28; H, 4.64. Found: C, 61.70; H, 4.42.

Although a satisfactory analysis consistent with the $Ti(cat)(bzac)_2$ formulation could not be obtained, the product appeared to be pure from infrared and proton nmr spectra.

46. (3,6-Diisopropyl-1,2-benzenediolato)bis(2,4-pentanedionato)-titanium(IV).-

To a solution of 5.55 g (15.2 mmols) of $Ti(acac)_2(OC_3H_7^i)_2$ in 50 ml of benzene was added a solution of 3.15 g (16.2 mmols) of 3,6-diisopropyl-1,2-dihydroxybenzene in 50 ml of benzene. The solution turned

a very dark red-brown color. The solution was stirred at room temperature for 1.5 hr and all solvent was removed under reduced pressure to yield a viscous black liquid. Addition of hexane and vigorous stirring resulted in the formation of a dark red-brown solid, which was collected, washed with 10 ml of hexane, and dried in vacuo; yield 6.00 g (90% theoretical). The crude product was recrystallized twice from dichloromethane-hexane solutions; mp 143-146°.

Anal. Calcd. for $TiC_{22}H_{30}O_6$: C, 60.28; H, 6.90. Found: C, 60.93; H, 6.88.

47. (3,6-Diisopropyl-1,2-benzenediolato)bis(1-phenyl-1,3-butanedionato)titanium(IV).

A solution of 1.75 g (9.00 mmols) of 3,6-diisopropyl-1,2-dihydroxybenzene in 25 ml of chloroform was added to a solution of 4.30 g (8.80 mmols) of $Ti(bzac)_2(OC_3H_7^i)_2$ in 50 ml of chloroform. The resulting black solution was stirred at room temperature for 2 hr and filtered. Solvent was removed under reduced pressure until a viscous black liquid remained. An excess of hexane was added and the solution was stored in a freezer (ca. 0°) overnight. The resulting cake of black solid was collected, washed with 20 ml of hexane and dried in vacuo; yield 3.73 g (75% theoretical).

48. (3,6-Diisopropyl-1,2-benzenediolato)bis(2-methyl-8-quinolinolato)titanium(IV).-

To a suspension of 5.53 g (11.5 mmols) of $Ti(quin)_2(OC_3H_7^i)_2$ in 50 ml of benzene was added a solution of 2.48 g (12.8 mmols) of 3,6-diisopropyl-1,2-dihydroxybenzene in 50 ml of benzene. A dark red-brown

solution formed. After stirring at room temperature for 30 min, a dark brown solid began to appear. The mixture was stirred for another hour and the solid collected and dried in vacuo. Concentration of the filtrate and addition of hexane gave a second crop of product. The combined yield of crude product was 5.75 g (90% theoretical). The first crop was recrystallized from a dichloromethane-hexane solution; mp 234-236°.

Anal. Calcd. for $TiC_{32}H_{34}N_2O_4$: C, 68.82; H, 6.14. Found: C, 69.11; H, 5.51.

49. (3,5-Diisopropyl-1,2-benzenediolato)bis(2-methyl-8-quinolinolato)titanium(IV).-

To a slurry of 3.07 g (6.36 mmols) of $Ti(quin)_2(OC_3H_7^i)_2$ in 50 ml of benzene was added 1.43 g (7.35 mmols) of solid 3,5-diisopropylcatechol. A dark red-brown solution formed immediately and was stirred at room temperature for 2 hr. Addition of 20 ml of hexane yielded a red-brown solid, which was collected, washed with hexane, and dried in vacuo. Concentration of the filtrate and addition of hexane yielded a second crop of product. The combined yield of crude product was 3.58 g (100% theoretical). The first crop was recrystallized from a dichloromethane-hexane solution; mp 240-243°.

The purity of this product was checked by infrared and proton nmr spectroscopy.

B. Physical Measurements

1. Solvents and Preparation of Solutions

a. Solvents

Deuteriochloroform was prepared according to a modified version of Paulsen and Cooke's method (76). Hexachloro-2-propanone was reacted with deuterium oxide in the presence of pyridine at ca. 0^{0}. Further details are available elsewhere (77). The purity of the deuterated product was ascertained from its proton nmr spectrum.

Benzene, dichloromethane, 1,1,2,2-tetrachloroethane, carbon tetrachloride, chlorobenzene, and 1,3-dichlorobenzene were reagent grade and used as received.

All solvents were dried by refluxing over calcium hydride for at least 24 hr and distilling therefrom into an amber bottle containing molecular sieves (Linde Type 4A) which was then sealed with a septum cap. Subsequently, enough tetramethylsilane (TMS) was added to give a 1% v/v TMS-solvent mixture.

b. Preparation of Solutions

Because of the hydrolytic instability of most of the complexes studied, all handling of solids and preparations of solutions were conducted entirely under anhydrous conditions in a dry nitrogen-filled glove bag. Solids were either weighed directly into a dry 9-in precision nmr tube or into a 1.00-ml volumetric flask (previously dried in an oven and cooled under nitrogen in a glove bag). Then, a calculated amount of solvent-TMS mixture was measured into a 1.00-ml precision glass syringe (previously dried in an oven and cooled under nitrogen in a glove bag) and added to the solid to give a solution of the desired concentration. When a volumetric flask was used, the solution was then transferred to a dry 9-in precision nmr tube. The tube was then flame-sealed *in vacuo* after several freeze-thaw cycles to degass the solution.

All compounds, except for the $Ti(chel)_2(2,6\text{-diisopropylphenoxy})_2$ (chel = ox, quin) complexes in 1,3-dichlorobenzene, gave completely homogeneous solutions at room temperature. The latter complexes were insufficiently soluble at room temperature; however, once sealed in vacuo, clear solutions were obtained at elevated temperatures.

2. Infrared Spectra

Infrared spectra were recorded as nujol mulls between KBr plates on a Perkin-Elmer 457 (or 225) infrared spectrometer. Nujol mulls were prepared in a nitrogen-filled glove bag. No special precautions were taken to dry the nujol used for obtaining spectra. Most spectra were recorded to insure the purity of the complexes and were recorded on the Perkin-Elmer 457 instrument. When expanded spectra and accurate band positions were desired, the Perkin-Elmer 225 Grating spectrometer was employed. The expansion chart paper was calibrated versus the cm^{-1} dial, which was subsequently calibrated with polystyrene and indene. Band positions so obtained are believed to be accurate to within $\pm$ 3 cm^{-1}.

3. Nuclear Magnetic Resonance Spectra

a. Proton NMR Spectra

Room temperature and variable temperature proton nmr spectra were recorded with a Varian A-60A spectrometer operating at 60.00 MHz. The spectrometer was equipped with a variable temperature probe accessory, Model V-4343, and a temperature controller accessory, Model V-6040. The spectrometer sweep widths (50, 100, and 250 Hz) were calibrated at room temperature using the standard audiofrequency sideband technique. Before each run, the 500 Hz sweep width of the spectro-

meter was calibrated at room temperature with a standard chloroform-TMS reference sample, a method in agreement with the sideband technique (78).

Room temperature chemical shifts were measured at a 500 Hz sweep width and represent the average of a triplicate determination; room temperature chemical shifts are believed accurate to ± 0.01 ppm. Variable temperature chemical shifts are believed accurate to ± 0.02 ppm.

Reported coupling constants were recorded at a sweep width of 50 Hz with a scan rate of 0.2 Hz/sec. In the case of the $Ti(chel)_2$-(2,6-diisopropylphenoxy)$_2$ (chel = ox, quin) complexes, the 100 Hz sweep width had to be used at some temperatures owing to the large chemical shift differences involved.

Temperatures below room temperature were measured from the chemical shift differences between the CH_3 and OH proton resonances of methanol, $\Delta\upsilon(CH_3OH)$. Sample temperatures were calculated from $\Delta\upsilon(CH_3OH)$ using the equation given by Van Geet (79)

$$T\ (^{o}K) = 435.5 - 1.193\left|\Delta\upsilon(CH_3OH)\right| - 29.3[10^{-2}\left|\Delta\upsilon(CH_3OH)\right|^{2}] \quad [1]$$

Temperatures above room temperature were determined from the chemical shift difference between the OH and CH_2 resonances of 1,2-ethanediol (ethylene glycol), $\Delta\upsilon$(E.G.). Sample temperatures were calculated from the appropriate Van Geet (79) expression

$$T\ (^{o}K) = 466.0 - 1.694\left|\Delta\upsilon(E.G.)\right| \quad [2]$$

The value of $\Delta\upsilon$ to be used in the calculation of the sample temperature from equations [1] or [2] represented the average of five determinations.

The temperature calibration charts supplied with Varian Associates Instruction Manuals are in error (79-82). Use of the Varian

methanol calibration curve can introduce a temperature error of as much as 4^{o} (82). The error decreases as room temperature is approached using the methanol "thermometer". Fortunately, the error in the ethylene glycol calibration chart is not very large. The use of the Varian methanol calibration chart may lead to substantial errors in derived kinetic parameters, as may be seen in Section III-C-1-c(i).

b. ^{13}Carbon NMR Spectra

Variable temperature carbon-13 nmr spectra were kindly run by Professor L. H. Pignolet of the University of Minnesota. Spectra were recorded on a Varian Associates XL-100-15 spectrometer in the Pulse Fourier Transform Mode with ^{1}H decoupling. Deuterated acetone was employed as the internal ^{2}H lock and dichloromethane was used as solvent. Chemical shifts are reported relative to TMS after calculating the shift from the internal $^{13}CH_2Cl_2$. $^{13}CH_2Cl_2$ has a chemical shift of 54.0 ppm downfield from tetramethylsilane (83).

C. Kinetics of Configurational Rearrangements

1. Sources of Error in the Variable Temperature NMR Method

a. Solvents

The temperature range at which the nmr spectrometer is physically capable of operating is effectively further limited only by the freezing and boiling points of the particular solvent system used. The low temperature region is fixed by the solvent's freezing point because (i) crystallization of the compound under study from solution precludes any reasonable level of resolution and/or (ii) increases in

the viscosity of the solvent renders lineshape parameters unreliable. The upper limit at which spectra can be obtained is fixed by the solvent's boiling point because: (i) convection currents and bubbles reduce the homogeneity of the spectrometer as they pass through the liquid and, (ii) bumping in the solution can cause the nmr tube to move in the teflon spinner because the fit is no longer tight due to unequal rates of thermal expansion. Such changes in the position of the sample relative to the heater of the probe in turn causes temperature fluctuations.

A desirable solvent would be one which encompassed a long liquid range which conveniently included the slow- and fast-exchange limits of the system under study. If the solvent possesses a single sharp resonance, this signal may also be used as a means of "peaking-up" the resolution of the spectrometer.

In this investigation, all variable temperature nmr spectra were recorded in either dichloromethane (titanium complexes) or 1,1,2,2-tetrachloroethane (tin and germanium complexes). Unfortunately, the higher coalescence temperatures of the tin and germanium complexes precluded the use of dichloromethane as solvent. The choice of 1,1,2,2-tetrachloroethane as solvent for these complexes was based on the fact that kinetic data for configurational rearrangements in $Sn(acac)_2X_2$ (X = F, Cl, Br, I) complexes (59) were obtained in this solvent, which bears a homologous relationship to dichloromethane. The latter solvent was used to obtain kinetic data for the corresponding $Ti(acac)_2X_2$ (X = F, Cl, Br) complexes (54). Only in the case of the $Ti(chel)_2(2,6\text{-diisopropylphenoxy})_2$ (chel = acac, ox, quin) complexes was a different solvent (1,3-dichlorobenzene) used. This choice was necessitated by the limited solubility of the $Ti(ox)_2(2,6\text{-}^iPr_2C_6H_3O)_2$ and $Ti(quin)_2(2,6\text{-}^iPr_2C_6H_3O)_2$ complexes in

most potential solvents.

b. Temperature Control

In variable temperature nmr studies it is essential to insure a minimum of temperature fluctuations at any one setting. Temperature fluctuations arise from variations in heater current and flow rate of gas; the magnitude of the error depends on both the heat capacity and amount of sample present (15). Variations in the sample temperature affect the resolution which in turn affects the line shapes. Allerhand and co-workers (15) observed a 1^{0} difference in temperature between a spinning and a non-spinning sample. For these reasons care was taken to maintain as stable a temperature as possible. This was achieved by maintaining a constant flow of nitrogen, by maintainjng the pressure cap screw in approximately the same position, and by maintaining a constant coolant level in the dewar when spectra were recorded at low temperatures.

An additional problem when operating at very low temperatures was the formation of an ice ring at the bottom of the teflon spinner; this tends to affect the spinning rate. The problem was minimized by placing silica gel drying tubes in the spinner air supply line and in the nitrogen supply line.

At each new temperature setting at least seven minutes were allowed for the system to reach thermal equilibrium.

c. Magnetic Field Inhomogeneities

One of the major problems of the variable temperature nmr experiment is the maintainence of maximum instrument resolution. Probably the most important effect of temperature changes is the loss of resolution.

This may be due to several factors (15): these include (i) changes in sample position as a result of thermal expansion or contraction, and (ii) perturbations in field distribution produced by changes in bulk magnetic susceptibility. Loss of resolution will alter the lineshapes of the resonances. Before each run, the resolution of the instrument was maximized with a standard sample of acetaldehyde. A line width at one-half of the maximum amplitude of < 0.4 Hz for the inner two peaks of the acetaldehyde quartet was deemed satisfactory. At each new temperature, the resolution of the spectrometer was "peaked-up" using either an intense, sharp solvent resonance or the resonance of the internal TMS standard.

Instrument instabilities commonly occur in the sweep rate, in the frequency, and in the static magnetic field. Their effects were minimized by averaging five scans of the spectrum at each temperature.

Spectral distortions can arise from several sources (15): these include (i) inhomogeneities in the applied magnetic field H_o, (ii) improper matching of sweep rate and instrumental response times, and (iii) saturation effects of too large a radiofrequency (rf) level. The first source may be minimized by averaging several scans. To minimize the possibility of a dampened response leading to spectral distortions, a scan rate of 0.2 Hz/sec was used with a maximum filter-band-width setting of 4. This was varied by the smallest possible amount when reasonable peak heights became difficult at the above filter-band-width setting. Some spectra for the $Ti(chel)_2(2,6\text{-}^{i}Pr_2C_6H_3O)_2$ (chel = ox, quin) complexes were recorded at a scan rate of 0.4 Hz/sec with a filter-band-width setting of 2. Saturation of the resonances will affect the transverse relaxation

time, T_2, as well as lineshapes. Care was taken to keep rf magnitudes below saturation levels.

d. Mathematical Approximations

Solution of the lineshape function corresponding to the Bloch equations as modified for exchange is a tedious and time-consuming process. Approximate solutions have been developed (15) in order to simplify calculations. However, these methods of calculation can lead to serious errors in rate constants and activation parameters (15). The TLS analysis has been found to be the most satisfactory of all the available methods (15,84,85) provided that potential sources of error in the TLS method are appreciated (82). A more thorough discussion and comparison of approximate methods and TLS procedures, as applied to configurational rearrangements within six-coordinate metal β-diketonate complexes may be found in Section III-C-1-c(ii).

2. Calculation of Kinetic Parameters

a. General Calculation Methods

The rate of exchange of chemically equivalent nuclei between two nonequivalent, uncoupled sites A and B may be calculated by determining τ_A (or τ_B), the mean lifetime of a nucleus on site A (or B). The nmr experiment provides access to the quantity τ_A (or τ_B). For the simple system above, Gutowsky and Holm (17) provided the solution to the Bloch equations modified to include the effects of chemical exchange. The resulting lineshape function expresses transverse magnetization as a function of the frequency and of the three parameters: (i) the chemical shift or frequency separation between the two absorption maxima in the absence of

exchange, $\delta\upsilon = \upsilon_A - \upsilon_B$ (in Hz); (ii) T_{2A} and T_{2B}, the transverse relaxation time for nuclei in site A and B, respectively, in the absence of exchange; and (iii) the first order rate constant, $k = 1/2\tau$, where $\tau = \tau_A\tau_B/(\tau_A + \tau_B)$. Once $\delta\upsilon$ and T_{2A} and T_{2B} have been measured experimentally, these values may be substituted into the Gutowsky-Holm equation and a solution obtained for τ.

Before this equation can be applied, however, certain assumptions must be made and experimental problems taken into account. It is assumed that the number of protons in each environment are equal; that is, the fractional populations of sites A and B are equal, $P_A = P_B = 0.5$. Also, the T_2 values for both sites are assumed equal; that is, $T_{2A} = T_{2B}$ (long range coupling is thus ignored). Finally, the dependence of both $\delta\upsilon$ and T_{2A} (and T_{2B}) on temperature must be known in the slow exchange region (82).

In the complexes studied in this thesis, T_2 values are temperature dependent as evidenced from viscosity broadening in the region of slow exchange. Also, the chemical shift separation between the sites A and B in the absence of exchange is temperature dependent. This dependence of T_2 and $\delta\upsilon$ on temperature probably arises from changes in the degree of molecular association (82). For $Ti(acac)_2(subsituted\text{-}phenoxy)_2$ complexes studied in dichloromethane solution, T_2 values for the acetylacetonate methyl groups were obtained from the closely related complex cis-$Zr(acac)_2Cl_2$; this complex is not affected by exchange broadening because at all accessible temperatures the rate of exchange is fast on the nmr time scale (52). The dependence of the linewidth at one-half maximum amplitude ($= 1/\pi T_2$) of the acetylacetonate methyl resonance of cis-$Zr(acac)_2Cl_2$ in dichloromethane solution on temperature has been reported

by Fay and Lowry (54). Their data was used to determine the appropriate T_2 value to be used for lineshape calculations at each temperature for all complexes studied in dichloromethane solution.

For the complexes $Ti(chel)_2(2,6\text{-}^iPr_2C_6H_3O)_2$ [chel = acac, ox, and quin] studied in 1,3-dichlorobenzene solution, a constant value for T_2 was used in lineshape calculations. That T_2 was temperature independent was determined from a temperature dependence study of the methyl resonance of the 2-methyl-8-quinolinolate ligand in the $Ti(quin)_2(2,6\text{-}^iPr_2C_6H_3O)_2$ complex in the slow exchange region; a constant linewidth was observed.

At the outset of this study, no complexes of the type $Zr(acac)_2(phenoxy)_2$ were known. Thus their suitability as T_2 reference compounds was unknown. Since their preparation and properties would form a separate project, the choice of the $Zr(acac)_2Cl_2$ complex to serve as the T_2 reference compound was made. It is only recently that bis(alkoxy)bis(acetylacetonato)zirconium(IV) complexes have been prepared and have been found to exist as the cis isomer; two acetylacetonate methyl resonances are observed in the low temperature nmr spectrum (63,86). The bis(phenoxy) complexes would be expected to behave similarly and thus would be unsuitable as T_2 reference compounds.

It has been shown (59) that failure to correct for the temperature dependence of T_2 during lineshape calculations will result in curvature of the Arrhenius plots of log k vs. 1/T in the slow exchange region, with a consequent increase in the "random" errors in E_a and $\Delta S^{\neq}$ obtained by linear least-squares analysis.

The appropriate value of $\delta\upsilon$ to be used in the calculations was determined from the measurement of $\delta\upsilon$ at a series of temperatures

in the slow exchange region. From the plot of $\delta\upsilon$ vs. temperature, the straight line portion in the slow exchange region was extrapolated (87) into the intermediate and fast exchange regions. Values of $\delta\upsilon$ appropriate to the particular temperature were then read directly from this plot. A problem arises if the linear portion of the $\delta\upsilon$ vs. temperature plot does not fall within an accessible temperature range. Two calculation techniques were used depending on whether this linear portion was observed. These are presently described.

b. Known Dependence of $\delta\upsilon$ on Temperature

If the linear portion of the $\delta\upsilon$ vs. temperature plot was obtained, the following procedure was employed. Values of the mean residence times were obtained by comparing the experimental spectra with theoretical spectra computed using the Gutowsky-Holm TLS equation. A modified version (88) of Brown's (89) Fortran program was used to calculate theoretical spectra at intervals of 0.005 Hz for an appropriate range of ca. 240 values of τ. In the case of the $Ti(ox)_2(2,6\text{-}^{i}Pr_2C_6H_3O)_2$ and $Ti(quin)_2(2,6\text{-}^{i}PrC_6H_3O)_2$ complexes, spectra were calculated at intervals of 0.01 Hz because of the large chemical shift differences involved. Input parameters for this program consist of a value for $\pi\delta\upsilon$, T_{2A} and T_{2B}, and P_A and P_B at each temperature. In general, the following characteristic lineshape parameters were used to numerically compare theoretical and experimental spectra: line widths at one-quarter ($W_{1/4}$), one-half ($W_{1/2}$), and three-quarters ($W_{3/4}$) maximum amplitude, and, below coalescence, $\delta\upsilon_e$, the experimental frequency separation during exchange between the two absorptions, and R, the ratio of the maximum amplitude to the central minimum. The τ values giving the best agreement between

theoretical and experimental spectra for each lineshape parameter were then averaged (each lineshape parameter was given equal weight). It should be noted that not every lineshape parameter was used for all compounds studied. For example, a poor balancing of the detector zero and phasing controls on the spectrometer will affect the $W_{1/4}$ values, rendering this parameter unreliable. There also exists certain regions where certain lineshape parameters are no longer very sensitive to changes in τ values. For example, near the slow exchange region, the R value increases and the experimental uncertainty attached to it becomes large, rendering this parameter unreliable. For each particular complex studied, characteristic lineshape parameters used to evaluate τ values are tabulated in the appropriate division of Section III.

c. Dependence of $\delta\upsilon$ on Temperature Unknown

In the case where the temperature dependence of $\delta\upsilon$ is not known, a different procedure for analyzing spectra had to be employed. This method involved the complete point by point comparison of the experimental nmr spectra with a calculated lineshape.

Before nmr spectra could be subjected to computer fitting, they had to be converted into digital form and transferred to magnetic tape. Digitization of the spectra was achieved with the aid of a Hewlett-Packard 2114A computer, an Analog/Digital converter, a Moseley Autograph Model 7001AM X-Y recorder, a Hewlett-Packard G-2B Null Detector, and a Hewlett-Packard Type F-3B Line Follower. A description of the functions of these various components may be found elsewhere (77). A description of the detailed procedure* for synchronizing and coordinating

*We thank Professor L. D. Colebrook for the HP-2114A computer program package which controlled these operations.

the whole operation of digitization of spectra and transfer to magnetic tape is also available (77).

Once on magnetic tape, the spectra are ready for computer fitting. The computer fitting program NLINGH (90) was used for this operation. Input parameters for NLINGH are: an initial trial value of τ_A and τ_B, the chemical shift, with respect to some arbitrary zero, of the two absorptions, the linewidth in the absence of exchange ($= 1/\pi T_2$), and finally a scaling factor (given the value of 1500). An option exists for keeping any combination of these parameters fixed for each spectrum. Program NLINGH then searches for the best combination of the variable parameters such that the corresponding lineshape plot deviates by the sum of the least squares of its points from that of the experimental plot. After a best fit has been determined, the computer prints out the resulting calculated lineshape together with the experimental spectrum. If the initial trial values of τ_A and τ_B are not within a reasonable range of the "true" values, either a bad fit is obtained or the iteration limit is exceeded and the program terminated, thus requiring a new set of trial values and the process repeated.

As found previously (77), problems were encountered when NLINGH attempted to fit spectra above coalescence where only one resonance line exists. Solutions for this problem have also been discussed (77). For the $Ti(acac)_2(2,6\text{-}Cl_2C_6H_3O)_2$ complex (the only compound for which this procedure was used), the characteristic lineshape parameters which were fixed and those which were allowed to vary are specifically indicated in Table XXXIII.

d. Activation Parameters

Activation parameters, with their associated error limits at the 95% confidence level (based only on the scatter of points on the Arrhenius plot) were calculated with program ACTPAR, whose input consisted of the most reliable τ_A or 2τ values at their respective temperatures.

III. RESULTS AND DISCUSSION

A. Permutational and Mechanistic Analysis of Rearrangements in the cis-$M(AA)_2X_2$, cis-$M(AA)_2XY$, and cis-$M(AB)_2X_2$ Systems

1. Introduction

With the ever increasing application of dynamic nmr techniques to the study of intramolecular rearrangements in molecular systems (91,92), attention has recently been focused on an inherent problem with this technique. For stereochemically nonrigid molecules it is impossible to physically separate diastereomers and/or enantiomers; thus the problem is to decide what configurational changes are occurring to cause the observed nmr site interchanges. In the absence of information concerning the stereochemistry of the rearrangement, any comments regarding the mechanism of the rearrangement are inoperative.

In order to overcome this problem and also to insure that every feasible mechanism has been considered, permutational analyses have recently been applied (93-104) to six-coordinate molecules to enumerate all theoretically possible, physically distinguishable, intramolecular rearrangements. This type of analysis yields a mathematical description of all the possible permutations of ligating nuclei about a particular polytopal form without specifying how atoms move from an initial configuration to a final configuration. From such a description, nmr observable site interchanges and actual configurational changes (diastereomerization and/or enantiomerization) may be deduced from the allowed permutations.

It should be noted, that in molecules possessing some degree

of symmetry, not every allowed permutation will be physically distinguishable by nmr methods. An averaging set (104) is comprised of all allowed permutations which generate the same net nmr site interchange pattern. A rearrangement mode (99,100) refers to a class of stereoisomerizations in which the relative orientation of a certain subset of all ligands changes. In some molecules, the presence of mirror image symmetry renders various modes indistinguishable and the rearrangements are classified in terms of "Observable Processes" (OP's) (100,101). In an octahedron, for example, an averaging set can be defined as a class of permutations in which x ligands retain their relative configuration, while 6-x ligands rearrange according to some well-specified procedure. It should be emphasized here that averaging sets (rearrangement modes or observable processes) are concerned only with the difference between an initial and final configuration, and contain no connotations concerning the actual physical motions of ligating nuclei. There are numerous physical rearrangement mechanisms possible for a given molecule but there are only a finite number of averaging sets possible.

The nmr experiment can only determine the site interchange pattern and hence the averaging set or rearrangement mode. Once the averaging set is known, the most probable physical pathway which generates that particular averaging set may be deduced. This final deduction is not unique and chemical intuition must play a significant role. Thus, a rearrangement mechanism can only be demonstrated as operating in the sense that it is the most reasonable physical motion which yields the observed averaging set.

The determination of the allowed permutations (and hence averaging sets) of nuclei surrounding a particular polytopal form may

be achieved by several methods, which include the mathematical structure of combinatorial analysis and double cosets (95-103) and symmetry groups for nonrigid molecules developed by Longuet-Higgins (105).

Section III-A-3 of this thesis describes the application of Longuet-Higgins' procedure to determine the allowed averaging sets for nonrigid six-coordinate bis-chelate complexes of the type cis-$M(AA)_2X_2$, cis-$M(AA)_2XY$, and cis-$M(AB)_2X_2$. A recent report by Eaton and Eaton (104) describes the application of this procedure to nonrigid tris-chelates of the type $M(AB)_3$ and $M(AB)_2(CC)$. Musher and Agosta (101) have also recently published an analysis of rearrangement modes in cis-$M(AA)_2X_2$ complexes.

Section III-A-4 then analyzes the most physically reasonable mechanisms for rearrangements within these bis-chelate complexes. Detailed discussion of experimental results for these various types of complexes is presented in the appropriate divisions of Section III-B.

Before plunging directly into the analysis, some basic concepts and definitions of permutational analysis are presented in the next section.

2. Basic Concepts

Permutational isomers (or permutamers (106)) are defined (107) as "chemical compounds which have in common the same molecular skeleton and set of ligands, differing only by the distribution of the ligands on the skeletal positions". Assigning a set of indexed labels to the ligands*,

---

*It is generally assumed that all permutational isomers of a molecule have the same molecular point group which means that all ligands must be identical and distinguishable only by their labels. If all the ligands are not identical but similar so that the different isomers generated deviate only slightly from an idealized skeletal framework, then the point group of the idealized skeletal framework may be used. If the skeletal framework of two isomers are significantly different, then the isomers are polytopal isomers (108), and a modified treatment is necessary (109).

$L = \{\ell_1, \ell_2, \ldots, \ell_n\}$ and a set of indexed labels $S = \{s_1, s_2, \ldots, s_n\}$ to the skeletal positions of the molecule allows a permutamer to be defined by a 2 x n matrix

$$\begin{pmatrix} \ell \\ s \end{pmatrix}_a = \begin{pmatrix} 1 & 2 & 3 & \ldots & n \\ i & j & k & \ldots & \ell \end{pmatrix}$$

where the top row lists the indices of the ligand labels and below each ligand is placed the index of the skeletal position which that ligand occupies. The description of molecules by a double numbering and mapping process has the advantage that one may carry out ligand permutations and skeletal operations separately. This is necessary (110) if skeletal symmetries and permutational equivalence of some of the ligands must be considered simultaneously.

If one permutamer rearranges into a different permutational isomer, a permutational isomerization reaction has taken place. Suppose, for example, that

$$\begin{pmatrix} \ell \\ s \end{pmatrix}_a \quad \text{rearranges to form} \quad \begin{pmatrix} \ell \\ s \end{pmatrix}_b$$

This reaction is defined by the permutation p_i, which when operating on the skeletal positions in

$$\begin{pmatrix} \ell \\ s \end{pmatrix}_a \quad \text{generates} \quad \begin{pmatrix} \ell \\ s \end{pmatrix}_b$$

A standard permutation notation is used, that is, $p_i = (12)(345)(6)$, which means: "replace 1 with 2, replace 2 with 1, replace 3 with 4, replace 4 with 5, replace 5 with 3, and leave 6 fixed", according to the scheme

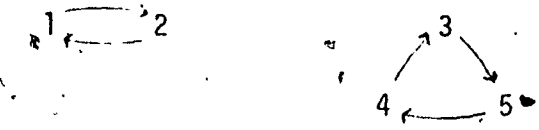

Permutational isomerization reactions are conveniently described using arrows, which simply express the mathematical result of the permutation p_i = (12)(345)(6) and does not describe rearrangement mechanisms.

For n identical objects there exists n! distinct permutations. Then for a molecule with n identical unidentate ligands distributed over n skeletal positions, it would at first appear that there exists n! different permutational isomerization reactions. However, if the molecule possesses point group symmetry, two factors (95) make the number of different permutational isomerization reactions less than n!.

First, certain permutations do not generate new isomers, but merely represent proper rotations of the molecular point group. Figure 1(b) demonstrates that the permutation p_i = (1)(4)(2356) is equivalent to a four-fold rotation about the 1-4 axis. This particular permutation does not define a permutational isomerization reaction. For a molecule containing n ligands distributed over n skeletal positions, the number of different permutamers (and hence permutational isomerization reactions) is reduced (93) from n! to $n!/h_r$, where h_r is the order of the rotational subgroup of the molecular point group.

Second, if all ligands are assumed to be identical and distinguishable only by labels, certain permutational isomerization reactions are rendered indistinguishable by the point group of the molecule (95). In Figure 1(c), the permutations p_m and p_n are both simple axial-equatorial interchanges and are indistinguishable if the ligands are indistinguishable. This is intuitively reasonable as a molecular point group operation

Figure 1.- (a) Defines the indexing of skeletal positions. (b) The equivalence of p_i = (1)(4)(2356) and a C_4 rotation operation about the 1-4 axis. (c) Two indistinguishable permutational isomerization reactions, p_m and p_n.

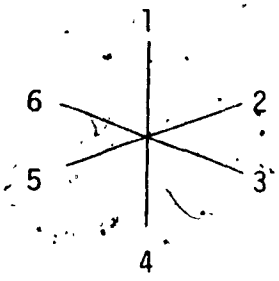
1
6
2
5
3
4

(a)

(b)

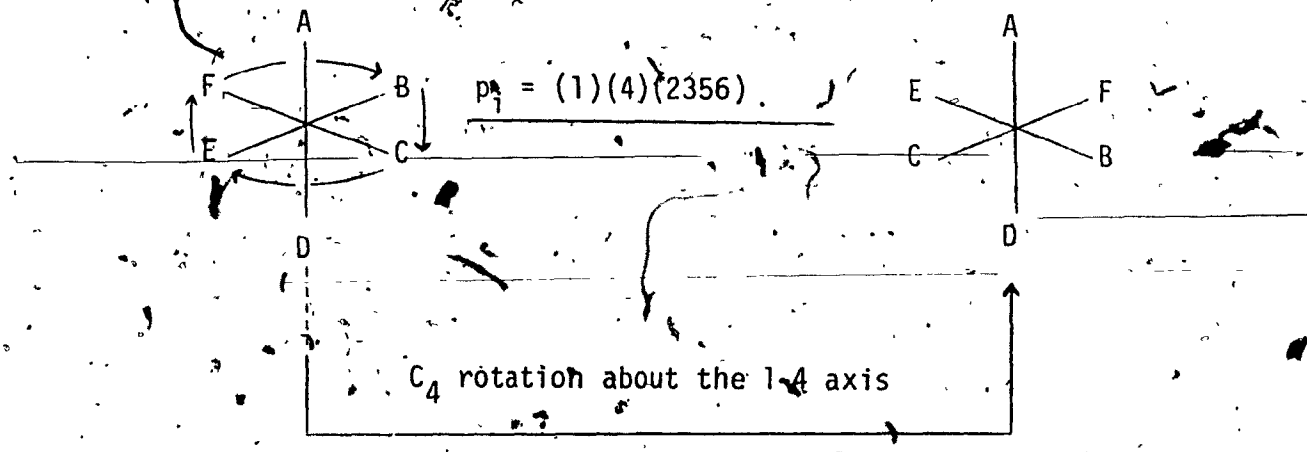
A
F
B
E
C
D
p_l = (1)(4)(2356)
A
E
F
C
B
D
C_4 rotation about the 1-4 axis

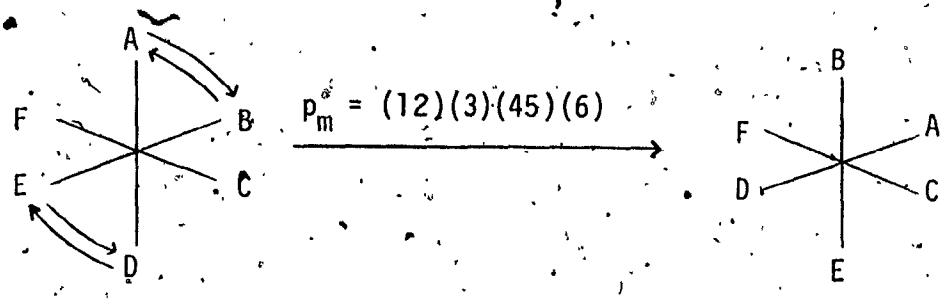
A
F
B
E
C
D
p_m = (12)(3)(45)(6)
B
F
A
D
C
E

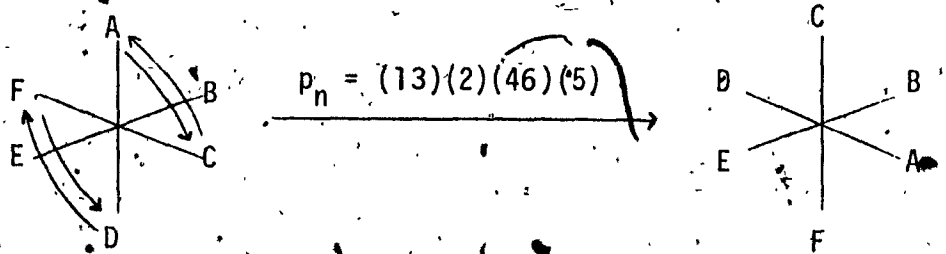
A
F
B
E
C
D
p_n = (13)(2)(46)(5)
C
D
B
E
A
F

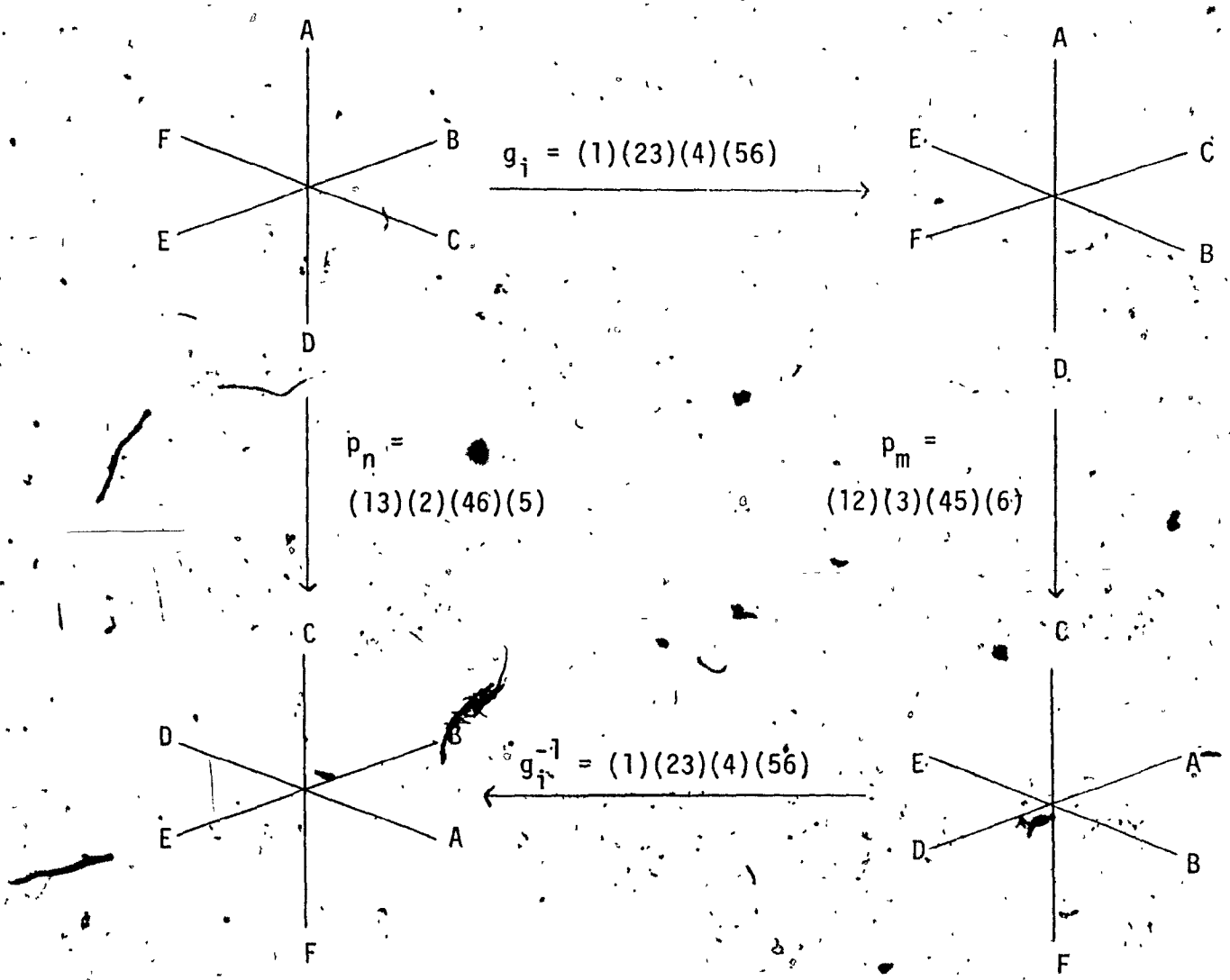

Figure 2.- The relationship between the two indistinguishable permutational isomerization reactions p_m and p_n, introduced in Figure 1. This diagram illustrates the mathematical relationship $p_n = g_i^{-1} \cdot p_m \cdot g_i$, where g_i^{-1} is the inverse of g_i and $p_m \cdot g_i$ means operation g_i followed by operation p_m. The physical process associated with g_i is a σ_d reflection across the plane containing the 1 and 4 vertices and bisecting the 2-3 and 5-6 axes. Skeletal positions are indexed as in Figure 1(a).

transforms the arrows describing p_n into those describing p_m. This indistinguishability of p_m and p_n can be expressed mathematically as shown in Figure 2, namely $p_n = g_i^{-1} \cdot p_m \cdot g_i$ or $p_m = g_i \cdot p_n \cdot g_i^{-1}$. The operation g_i = (1)(23)(4)(56) is the permutation generated by the σ_d plane containing the 1 and 4 vertices and bisecting the 2-3 and 5-6 axes.

These two factors which reduce the number of allowed permutational isomerization reactions may be briefly summarized as rotational and symmetry equivalencies, respectively.

3. Application of Longuet-Higgins' Molecular Symmetry Groups for Nonrigid Molecules to Rearrangements in the cis-$M(AA)_2X_2$, cis-$M(AA)_2XY$, and cis-$M(AB)_2X_2$ Systems.

a. Method

By definition, a nonrigid molecule undergoes rearrangement within the time scale of the physical technique being used to establish structure. Suppose a tris-chelate rearranges from 1 to 2 during the measurement time. Should the symmetry of the complex be considered to be D_3 or D_{3h} for the purpose of analyzing the data? As another example, consider that a bis-chelate complex exists as a mixture of cis (3) and trans (4) isomers in rapid equilibrium. Is such a system to be analyzed in terms of C_2 or D_{2h} symmetry?

As an answer to this seemingly paradoxical question, Longuet-Higgins (105) suggested that the system should not be analyzed in terms of the rigid molecular point group. Instead, Longuet-Higgins (105) proposed that nonrigid molecules should be interpreted using a molecular symmetry

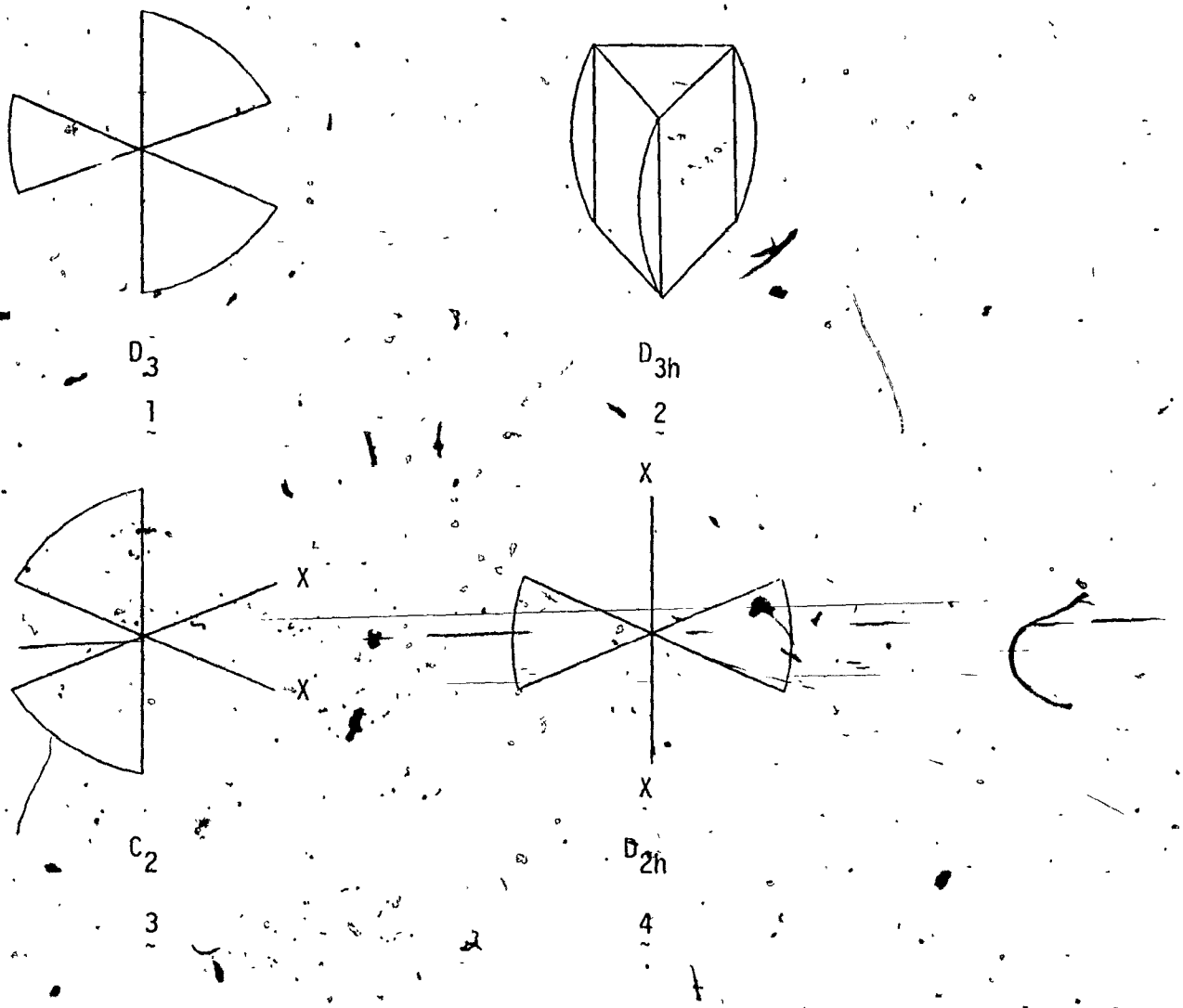

group which is the set of (a) all feasible permutations, P, of the positions and spins of the identical nuclei (including the identity E) and (b) all feasible permutation-inversions, P^*, which simultaneously permute and invert the relative coordinates of all atoms in the center of mass of the molecule. P^* is the product $PE^* = E^*P$, where E^* is the inversion of the positions of all atoms and may not always be among the feasible operations (105).

The problem thus becomes one of determining the number of distinguishable permutational isomers and the corresponding P and P^* operations which interconvert these permutamers.

b. The cis-$M(AA)_2X_2$ System

The analysis of the cis-$M(AA)_2X_2$ system will be presented in detail since the basic set of distinguishable permutamers and allowed P and P^* operations is identical to those for the cis-$M(AA)_2XY$ and cis-$M(AB)_2X_2$ systems, with the appropriate inclusion of different substituents in these latter systems.

Consider the skeletal framework of a cis-$M(AA)_2X_2$ complex as represented by 5, for which the X^5 and X^6 ligands are required to remain in a mutually cis configuration. The number of permutamers of 5 is (94)

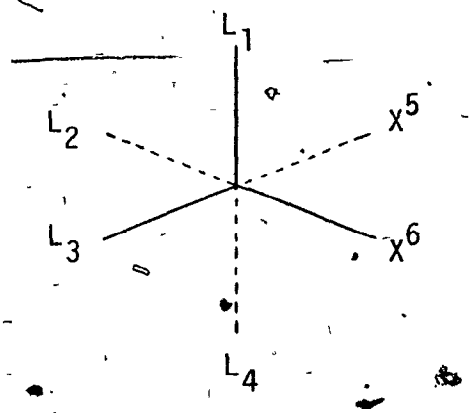

5

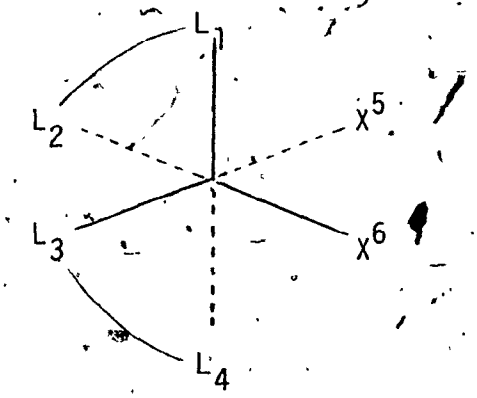

6

simply the product of the number of permutations of L_1, L_2, L_3, and L_4 among themselves and all possible permutations of the two X groups among themselves; that is, there are 4! x 2! = 48 possible permutations of the groups in configuration 5. With the additional constraints that L_1L_2 and L_3L_4 represent the ligating nuclei of bidentate ligands and that these ligands cannot span trans positions, 16 of the above 48 permutamers are no longer allowed, thus there remains 32 permutations of the groups in configuration 6. The C_2 rotation axis produces pairwise equivalencies

within the 32 permutamers; thus the number of distinguishable permutational isomers for configuration 6 is 16. While configuration 6 possesses only one real proper rotation axis, its skeletal framework can be considered sufficiently close to octahedral symmetry to consider the effects of the 24 proper rotation axes of an octahedron. One permutamer of 6 may be converted into 15 other permutational isomers, which cannot be superimposed on 6 by proper rotations of the molecule, only by P and P^* operations. The same permutamer of 6 may be converted to 23 rearranged forms by the proper rotation axes of the octahedron. These 23 rearranged forms, of course, can be superimposed on the original permutamer by proper rotations and thus do not constitute permutational isomers. The 24 proper rotation operations have group properties and are referred to as rigid body rotations of the molecule. Thus the set of all permutamers of a complex of configuration 6 is a group of order 384, which factors into a unique Abelian group of 16 consisting of distinguishable permutational isomers and a group of order 24 consisting of rearranged forms resulting from rigid body rotations.

The set of all permutations and permutation-inversions of the ligating nuclei for a complex having configuration 6 may be derived in a slightly more formal fashion as follows. For a general octahedral complex $ML_1L_2L_3L_4L_5L_6$ there are $6! = 720$ permutations of the six identical, indexed monodentate ligands L_i. Since the order of the rotational subgroup in octahedral symmetry is 24, the original set of permutations is factored into a group of 24 regarded as rigid body rotations of the molecular skeleton and a group of $720/24 = 30$ consisting of the number of distinguishable permutamers. If ligands L_5 and L_6 are restricted to

positions cis to each other, the number of permutamers is reduced from 30 to 24. With the additional constraint that L_1L_2 and L_3L_4 represent ligating nuclei of a bidentate ligand, and that such a ligand cannot span trans positions, the unique set of permutational isomers is further reduced to 16. Thus the complete set of all permutations and permutation-inversions of the ligating nuclei of a complex of configuration 6 is 16 x 24 = 384.

The notation used to describe the 16 permutamers and an illustration of P and P^* operations may be found in Figure 3. As the complex is viewed down an imaginary threefold (i-C_3) axis with the triangular face including position 1 upward, the ligating nuclei are labelled clockwise for this face starting with 1, followed by the labels for the lower triangular face starting with the vertex to the right of 1. Square brackets denote permutational isomers and parentheses represent P and P^* operations. The 16 permutational isomers for a complex of general configuration 6 are listed in Table I. The 16 allowed P and P^* operations may be determined by selecting one of the sixteen permutamers and ascertaining what interchanges of nuclei generate the other 15 isomers. The 16 P and P^* operations which interconvert the isomers within the set of 16 isomers are listed in Table III. Permutations other than those in Table III either correspond to rigid body rotations or generate configurations in which one of the bidentate ligands must span the trans positions. The effect of each of the 16 allowed operations on the [163-542] isomer is given in Table III. The complete 16 x 16 group multiplication table for the group of 16 P and P^* operations may be found elsewhere (104).

Rearrangements within the cis-$M(AA)_2X_2$ system are analyzed in terms of the four A A pairs shown in Figure 4. The prime is used to indicate that an A end of the ligand is one of the nonequivalent terminal

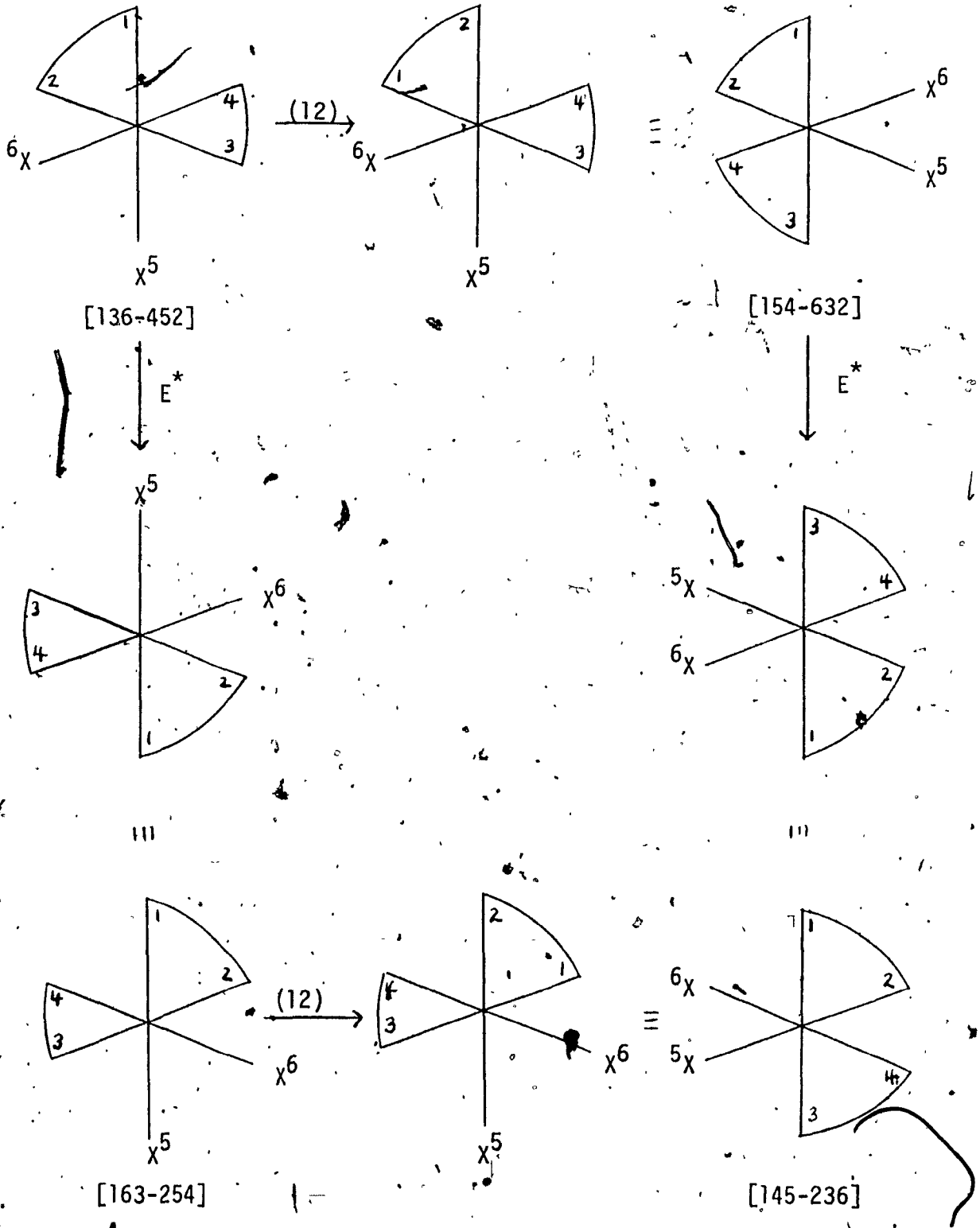

Figure 3.- Illustration of notation and P and P* operations for a cis-$M(AA)_2X_2$ complex. This diagram also illustrates the equivalence relation $PE^* = E^*P$.

Table I

The Sixteen Permutational Isomers for a cis-$M(AA)_2X_2$ System

[135-462] [a]	[153-264]
[136-452]	[163-254]
[135-246]	[153-642]
[136-245]	[163-542]
[145-362]	[154-263]
[145-236]	[154-632]
[146-235]	[164-532]
[146-352]	[164-253]

[a] For a definition of notation used, see text and Figure 3.

group environments which is trans to an X group. The other terminal group environment is unprimed. Each configuration is then labelled according to its absolute configuration with subscripts referring to which A groups are primed. The possible scrambling patterns for the nonequivalent terminal groups on the bidentate ligands are summarized in Table II. The analysis of physical rearrangement pathways, presented in Section III-A-4b is based on the same notation of four Δ-Λ pairs as shown in Figure 4.

When all sixteen operations are performed on the sixteen permutational isomers, it is found that certain permutations produce equi equivalent configurational changes and site interchanges. Permutations that give rise to the same net averaging pattern for the nonequivalent sites are placed together in averaging sets, A_i, although the permutations within each set may have different effects on a particular isomer. This

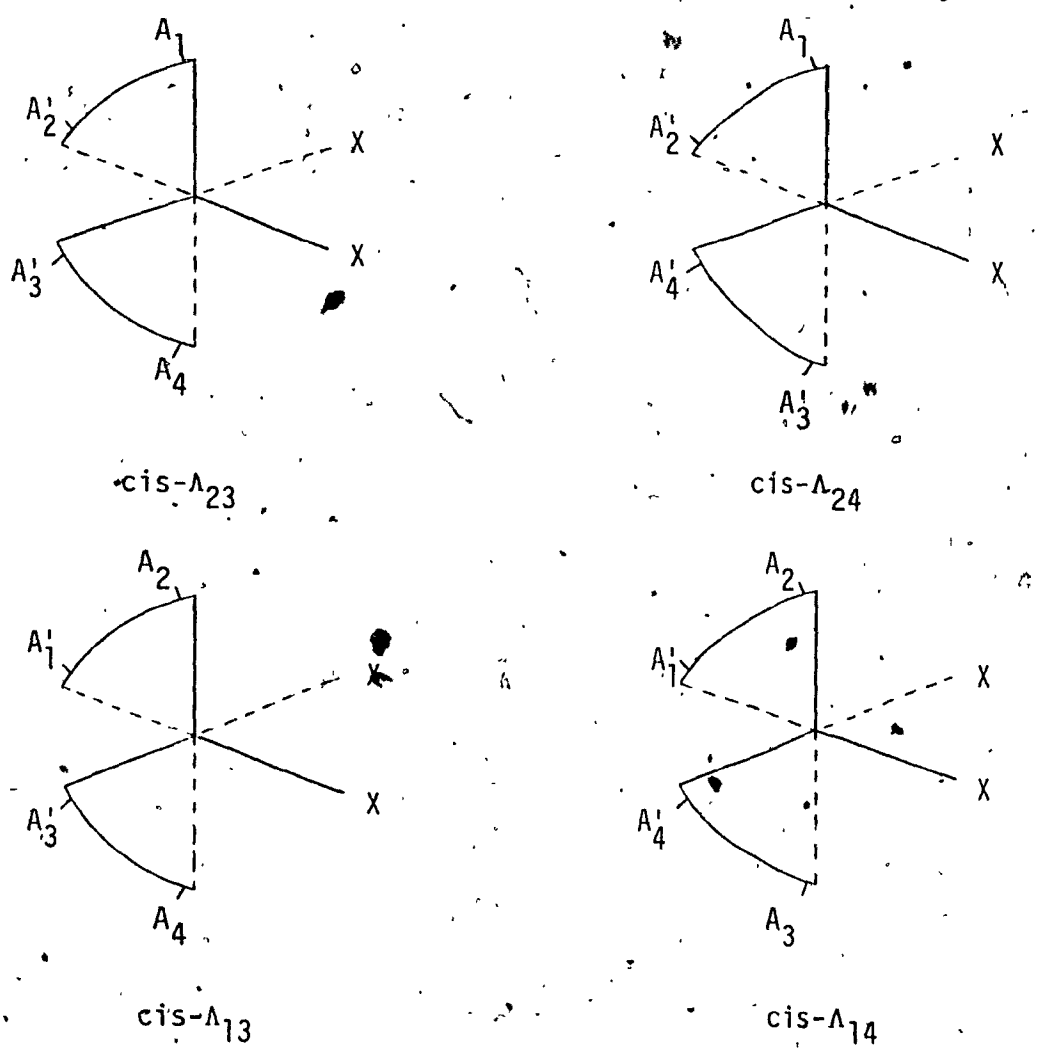

Figure 4.- Illustration of the notation used in the analysis of the cis-$M(AA)_2X_2$ system in terms of four Δ-Λ pairs. See text for the significance of the primes and subscripts.

condition arises from the fact that the nmr experiment can detect only the net effect on all isomers. The configurational changes, site interchanges, and averaging sets that individual permutations belong to are summarized in Table III for the cis-$M(AA)_2X_2$ system.

For the cis-$M(AA)_2X_2$ system the sixteen P and P^* operations

Table II

Scrambling Patterns for Nonequivalent Terminal Groups in Rearrangements of a cis-$M(AA)_2X_2$ Complex[a]

1. NO EXCHANGE

   e.g.- $(\Delta,\Lambda)_{23} \leftrightarrow (\Delta,\Lambda)_{23}$

2. $(\Delta,\Lambda)_{23} \leftrightarrow (\Delta,\Lambda)_{13}$
   $(\Delta,\Lambda)_{14} \leftrightarrow (\Delta,\Lambda)_{24}$

3. $(\Delta,\Lambda)_{23} \leftrightarrow (\Delta,\Lambda)_{24}$
   $(\Delta,\Lambda)_{14} \leftrightarrow (\Delta,\Lambda)_{13}$

4. $(\Delta,\Lambda)_{23} \leftrightarrow (\Delta,\Lambda)_{14}$
   $(\Delta,\Lambda)_{13} \leftrightarrow (\Delta,\Lambda)_{24}$

[a] Scrambling patterns contain no connotation concerning whether inversion does or does not occur during exchange of the terminal groups.

may be classified into eight averaging sets, A_i. The changes in signal multiplicities for nondiastereotopic and diastereotopic substituents on either the AA or X ligands which result from the averaging sets A_i are shown in Table IV. In the absence of diastereotopic substituents the site exchange patterns do not indicate whether a rearrangement occurs with inversion or retention of configuration at the metal center. Thus, the following averaging sets are pairwise indistinguishable: (A_1,A_5), (A_2,A_6), (A_3,A_7), and (A_4,A_8).

Consider now the distinctions between the averaging sets A_1, A_2, A_3, and A_4* when all substituents within the complex are nondiastereotopic. Averaging sets A_1 and A_4 are obviously distinct; the differences between A_2, A_3, and A_4 are subtle. Individually, A_2 and A_3 are distinct from A_4 as both A_2 and A_3 would predict a fast exchange limit of three

* An exactly analagous situation arises in distinguishing between averaging sets A_5, A_6, A_7, and A_8.

Table III

Permutational Analysis of the cis-$M(AA)_2X_2$ System

Operation[a]	Product Permutamer	Exchange Pattern[b]	Inversion	Averaging Set
E	[163-542]	1	-	A_1
(56)	[153-642]			
(12)	[145-362]	2	-	A_2
(12)(56)	[146-352]			
(34)	[164-532]	3	-	A_3
(34)(56)	[154-632]			
(12)(34)	[135-462]	4	-	A_4
(12)(34)(56)	[136-452]			
E*	[136-245]	1	$\Delta \leftrightarrow \Lambda$	A_5
(56)*	[135-246]			
(12)*	[154-263]	2	$\Delta \leftrightarrow \Lambda$	A_6
(12)(56)*	[164-253]			
(34)*	[146-235]	3	$\Delta \leftrightarrow \Lambda$	A_7
(34)(56)*	[145-236]			
(12)(34)*	[153-264]	4	$\Delta \leftrightarrow \Lambda$	A_8
(12)(34)(56)*	[163-254]			

[a] Operations performed on the [163-542] permutamer.

[b] Exchange patterns are defined in Table II.

Table IV.

Changes in Signal Multiplicities Resulting from the Averaging Sets A_i Operating on a cis-$M(AA)_2X_2$ Complex Containing Diastereotopic and/or Nondiastereotopic Ligands[a]

Averaging Set	A-A Nondiastereotopic (Diastereotopic)	-CR= Nondiastereotopic (Diastereotopic)	X Nondiastereotopic (Diastereotopic)
A_1	2 (4) → 2 (4)	1 (2) → 1 (2)	1 (2) → 1 (2)
A_2	2 (4) → 3 (6)	1 (2) → 1 (2)	1 (2) → 1 (2)
A_3	2 (4) → 3 (6)	1 (2) → 1 (2)	1 (2) → 1 (2)
A_4	2 (4) → 1 (2)	1 (2) → 1 (2)	1 (2) → 1 (2)
A_5	2 (4) → 2 (2)	1 (2) → 1 (1)	1 (2) → 1 (1)
A_6	2 (4) → 3 (4)	1 (2) → 1 (1)	1 (2) → 1 (1)
A_7	2 (4) → 3 (4)	1 (2) → 1 (1)	1 (2) → 1 (1)
A_8	2 (4) → 1 (2)	1 (2) → 1 (1)	1 (2) → 1 (1)
$(A_2 + A_3)$	2 (4) → 1 (2)	1 (2) → 1 (2)	1 (2) → 1 (2)
$(A_6 + A_7)$	2 (4) → 1 (2)	1 (2) → 1 (1)	1 (2) → 1 (1)

[a] The number of predicted resonances refer to groups which are not coupled either to each other or to another group. For example, if the substituent on the ligand(s) was an isopropyl group, the multiplicities given in this table would refer to the number of spin coupled doublets for the isopropyl methyl groups due to coupling with the geminal methyl proton.

A-A terminal group resonances in the nmr spectrum of a labile cis-$M(AA)_2X_2$ complex while A_4 predicts a single resonance in the fast exchange region. However, both A_2 and A_3 predict the identical fast exchange spectrum and one might suggest that A_2 and A_3 should be combined to give a single averaging set, $(A_2 + A_3)$. However, this new averaging set, $(A_2 + A_3)$ would then be identical with A_4 and one could then argue that really

only two averaging sets, A_1 and A_4, exist. The analagous problem with averaging sets A_5 to A_8 suggests that $(A_6 + A_7)$ would be identical to A_8. This is, however, not the case. While A_8 would predict a ratio of the rate of terminal group exchange to the rate of enantiomerization to be unity, $(A_6 + A_7)$ would predict a ratio of rates of 2. For this reason, while including the combined $(A_2 + A_3)$ and $(A_6 + A_7)$ sets in Table IV, all eight averaging sets are considered separate.

The above problem arises because of the double degeneracy of the two terminal group resonances in the slow exchange spectrum of a cis-$M(AA)_2X_2$ complex. While A_2 (or A_6) averages only the nonequivalent groups on one chelate ring, A_3 (or A_7) averages only the nonequivalent terminal groups on the other chelate ring. When this terminal group degeneracy is removed on progressing to a cis-$M(AA)_2XY$ complex, the problem is removed as the macroscopic degeneracy of the operations within A_2 and A_3 (and A_6 and A_7) are lifted.

c. The cis-$M(AA)_2XY$ System

In a cis-$M(AA)_2XY$ complex, all four terminal groups are nonequivalent and in the specific case where AA represents a β-diketonate ligand, the two -CH= protons (or -CR= groups) are also in nonequivalent environments. An illustration of the geometry and labelling of nonequivalent sites within the [163-542] permutamer is provided in Figure 5. The letters in parentheses specify the sites occupied by the various groups in the following order: (R_1, R_2, R_3, R_4; $-CH_1=$). The nonequivalent sites are defined as follows. The site trans to the ligand Y is always b, the one trans to the ligand X is labelled c. Sites c and d are always connected with the same ring; similarly for sites a and b. Thus, if R_1 is in site c, then R_2 is in site d. Site m for the ring proton (or group) is the site

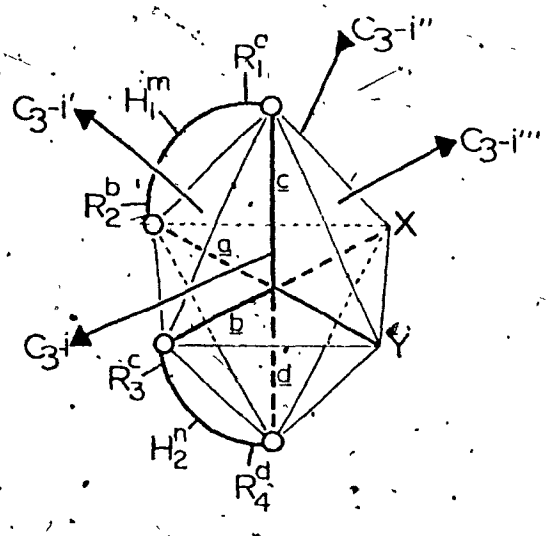

cis-Λ(abcd;m)

Figure 5.- A general view of a cis-$M(AA)_2XY$ complex in the Λ configuration along the threefold axis C_3-i. Numerical subscripts label the terminal and ring proton groups; letter superscripts label the nonequivalent environments. It also illustrates the [163-542] permutamer for the cis-$M(AA)_2XY$ system where Y is number 6 and X is number 5. The letters a, b, c, and d define the four nonequivalent metal-chelate bonds. The four imaginary threefold rotation axes of the octahedron are also illustrated.

cis to the ligand X; site n is cis to the ligand Y.

The same basic set of 16 permutational isomers found for the cis-$M(AA)_2X_2$ system apply to the cis-$M(AA)_2XY$ system (where Y is number 6 and X is number 5). The effect of performing the 16 P and P^* operations on the [163-542] ≡ c-Λ(abcd;m) isomer is summarized in Table V. Those permutations that result in the same net exchange pattern after all 16 operations are performed on the 16 permutational isomers are placed in the same averaging set A_i; these averaging sets for a cis-$M(AA)_2XY$ complex

Table V

Permutational Analysis of the cis-$M(AA)_2XY$ System

Operation[a]	Net Site Interchange: Terminal Groups (abcd)[b]	-CR= (m)	Inversion	Averaging Set
E	(abcd)	m	-	A_1
(12)	(bacd)	m	-	A_2
(34)	(abdc)	m	-	A_3
(56)	(dcba)	n	-	A_4
(12)(34)	(badc)	m	-	A_5
(12)(56)	(cdba)	n	-	A_6
(34)(56)	(dcab)	n	-	
(12)(34)(56)	(cdab)	n	-	A_7
E*	(abcd)	m	$\Delta \leftrightarrow \Lambda$	A_8
(12)*	(bacd)	m	$\Delta \leftrightarrow \Lambda$	A_9
(34)*	(abdc)	m	$\Delta \leftrightarrow \Lambda$	A_{10}
(56)*	(dcba)	n	$\Delta \leftrightarrow \Lambda$	A_{11}
(12)(34)*	(badc)	m	$\Delta \leftrightarrow \Lambda$	A_{12}
(12)(56)*	(cdba)	n	$\Delta \leftrightarrow \Lambda$	A_{13}
(34)(56)*	(dcab)	n	$\Delta \leftrightarrow \Lambda$	
(12)(34)(56)*	(cdab)	n	$\Delta \leftrightarrow \Lambda$	A_{14}

[a] Operations performed on the [163-542] $\equiv$ c-Λ(abcd;m) permutamer.

[b] Sites of groups within product permutamer in the order (R_1,R_2,R_3,R_4); sites are defined in text and an example is given in Figure 5.

are listed in Table V.

It is found that fourteen averaging sets exist for the cis-$M(AA)_2XY$ system. Changes in signal multiplicities for diastereotopic and nondiastereotopic substituents on the AA and X (or Y) ligands predicted by the A_i averaging sets are summarized in Table VI. The distinctions which can be made between averaging sets A_i on the basis of changes in signal multiplicities for the eight possible combinations of diastereotopic and nondiastereotopic ligands are given in Table VII. If the ligands do not contain a diastereotopic substituent it is not known whether a rearrangement occurs with or without inversion at the metal center and the averaging sets A_i are pairwise indistinguishable (Table VIIa): (A_1,A_8), (A_2,A_9), (A_3,A_{10}), (A_4,A_{11}), (A_5,A_{12}), (A_6,A_{13}), and (A_7,A_{14}). The maximum number of distinguishable averaging sets is obtained for case b of Table VII.

In this table, distinctions between averaging sets are based only on the predicted signal multiplicities for various substituents in the fast exchange limit. This also assumes that all resonances are well resolved in the slow exchange region and no chemical shift degeneracies occur, either in the fast or slow exchange regions. For example, for case a of Table VII, averaging sets A_6 and A_7 could generate identical spectra in the fast exchange limit for a particular complex with a unique set of chemical shifts and thus be indistinguishable, even though according to Table VIIa they are distinguishable. This particular case has been observed for the cis-$Sn(acac)_2(CH_3)Cl$ complex (111).

Another feature of Table VII, which emphasizes the need for caution in its use, is that although averaging sets are listed as being indistinguishable, they may not be so if resonance lines can be assigned to specific nuclei. For example, consider A_2 and A_3 of case a in Table VII.

Table VI

Changes in Signal Multiplicities Resulting from the Averaging Sets A_i Operating on a cis-$M(AA)_2XY$ Complex Containing Diastereotopic and/or Nondiastereotopic Ligands[a]

Averaging Set	A-A Nondiastereotopic (Diastereotopic)	-CR= Nondiastereotopic (Diastereotopic)	X (or Y) Nondiastereotopic (Diastereotopic)
A_1	4 (8) → 4 (8)	2 (4) → 2 (4)	1 (2) → 1 (2)
A_2	4 (8) → 3 (6)	2 (4) → 2 (4)	1 (2) → 1 (2)
A_3	4 (8) → 3 (6)	2 (4) → 2 (4)	1 (2) → 1 (2)
A_4	4 (8) → 2 (4)	2 (4) → 1 (2)	1 (2) → 1 (2)
A_5	4 (8) → 2 (4)	2 (4) → 2 (4)	1 (2) → 1 (2)
A_6	4 (8) → 1 (2)	2 (4) → 1 (2)	1 (2) → 1 (2)
A_7	4 (8) → 2 (4)	2 (4) → 1 (2)	1 (2) → 1 (2)
A_8	4 (8) → 4 (4)	2 (4) → 2 (2)	1 (2) → 1 (1)
A_9	4 (8) → 3 (4)	2 (4) → 2 (2)	1 (2) → 1 (1)
A_{10}	4 (8) → 3 (4)	2 (4) → 2 (2)	1 (2) → 1 (1)
A_{11}	4 (8) → 2 (4)	2 (4) → 1 (2)	1 (2) → 1 (1)
A_{12}	4 (8) → 2 (4)	2 (4) → 2 (2)	1 (2) → 1 (1)
A_{13}	4 (8) → 1 (2)	2 (4) → 1 (2)	1 (2) → 1 (1)
A_{14}	4 (8) → 2 (4)	2 (4) → 1 (2)	1 (2) → 1 (1)

*See footnote a in Table IV.

Although both predict a multiplicity change of 4 → 3 for AA terminal groups, if reasonable specific assignments of resonances can be made, averaging sets A_2 and A_3 may be distinguished. This, of course, depends on the assignments and the relative chemical shifts.

Table VII

Distinctions Between Averaging Sets A_i for a cis-$M(AA)_2XY$ Complex on the Basis of Changes in Signal Multiplicities

(a)		(b)		(c)	
A-A	Nondiastereotopic	A-A	Nondiastereotopic	A-A	Nondiastereotopic
-CR=	Nondiastereotopic	-CR=	Nondiastereotopic	-CR=	Diastereotopic
X (or Y)	Nondiastereotopic	X (or Y)	Diastereotopic	X (or Y)	Nondiastereotopic
(A_1, A_8)		A_1		A_1	
(A_2, A_3, A_9, A_{10})		(A_2, A_3)		(A_2, A_3)	
$(A_4, A_7, A_{11}, A_{14})$		(A_4, A_7)		$(A_4, A_7, A_{11}, A_{12}, A_{14})$	
(A_5, A_{12})		A_5		A_5	
(A_6, A_{13})		A_6		(A_6, A_{13})	
		A_8		A_8	
		(A_9, A_{10})		(A_9, A_{10})	
		(A_{11}, A_{14})			
		A_{12}			
		A_{13}			

Table VII (continued)

(d)	(e)	(f)
A-A -CR= X (or Y) Nondiastereotopic Diastereotopic	A-A -CR= X (or Y) Diastereotopic Nondiastereotopic	A-A -CR= X (or Y) Diastereotopic Nondiastereotopic
A'_1	A'_1	A'_1
(A'_2, A'_3)	(A'_2, A'_3)	(A'_2, A'_3)
(A'_4, A'_7)	$(A'_4, A'_7, A'_{11}, A'_{14})$	(A'_4, A'_7)
A'_5	$(A'_5, A'_8, A'_9, A'_{10}, A'_{12})$	A'_5
A'_6	(A'_6, A'_{13})	A'_6
A'_8		$(A'_8, A'_9, A'_{10}, A'_{12})$
(A'_9, A'_{10})		(A'_{11}, A'_{14})
$(A'_{11}, A'_{12}, A'_{14})$		A'_{13}
A'_{13}		

Table VII (continued)

(g)

A-A	Diastereotopic
-CR=	Diastereotopic
X (or Y)	Nondiastereotopic

A_1'

(A_2', A_3')

$(A_4', A_7', A_8', A_9', A_{10}', A_{11}', A_{12}', A_{14}')$

A_5'

(A_6', A_{13}')

(h)

A-A	Diastereotopic
-CR=	Diastereotopic
X (or Y)	Diastereotopic

A_1'

(A_2', A_3')

(A_4', A_7')

A_5'

A_6'

$(A_8', A_9', A_{10}', A_{11}', A_{12}', A_{14}')$

A_{13}'

d. The cis-$M(AB)_2X_2$ System

Complexes of the type cis-$M(AB)_2X_2$ may exist in three diastereomeric forms in which the X groups are mutually cis.* As shown in Figure 6, the cis,cis,cis** isomer has no symmetry and consequently possesses four nonequivalent terminal R groups, two nonequivalent -CH= (or -CR= groups), and two nonequivalent X groups. The nonequivalent sites are defined as follows. Sites a and b refer to the X groups, site a being trans to R_1 and site b trans to R_2. Sites c, d, e, and f refer to the terminal R groups. The site trans to a is always e, the one trans to site b is labelled f. Sites c and e are always connected with the same ring; similarly for d and f. Thus, if R_1^1 is in site d, then R_2^2 is in site f. Site m for the $-CH_1^1=$ ring proton (or group) on the R_1^1-R_2^2 ring is surrounded by terminal groups in the f and d sites; if the terminal groups on the ring associated with the ring proton (or group) are in sites c and e, the ring proton (or group) is then in site n.

Both the cis,cis,trans and cis,trans,cis diastereomers possess a twofold symmetry axis and thus both isomers have only one environment for each of the R_1, R_2, -CH= (or -CR=), and X groups.

Scrambling patterns for the various nonequivalent environments within the cis,cis,cis isomer are listed in Table VIII.

The same basic set of 16 permutational isomers found for the cis-$M(AA)_2X_2$ system apply in the cis-$M(AB)_2X_2$ case (where X^1 is

---

*Two other diastereomers exist which possess mutually trans X groups. These are not considered here but are included in the mechanistic analysis of Section III-4-d.

**Diastereomers are referred to by three cis or trans prefixes which specify the relative orientations of the X, R_1, and R_2 groups in that particular sequence.

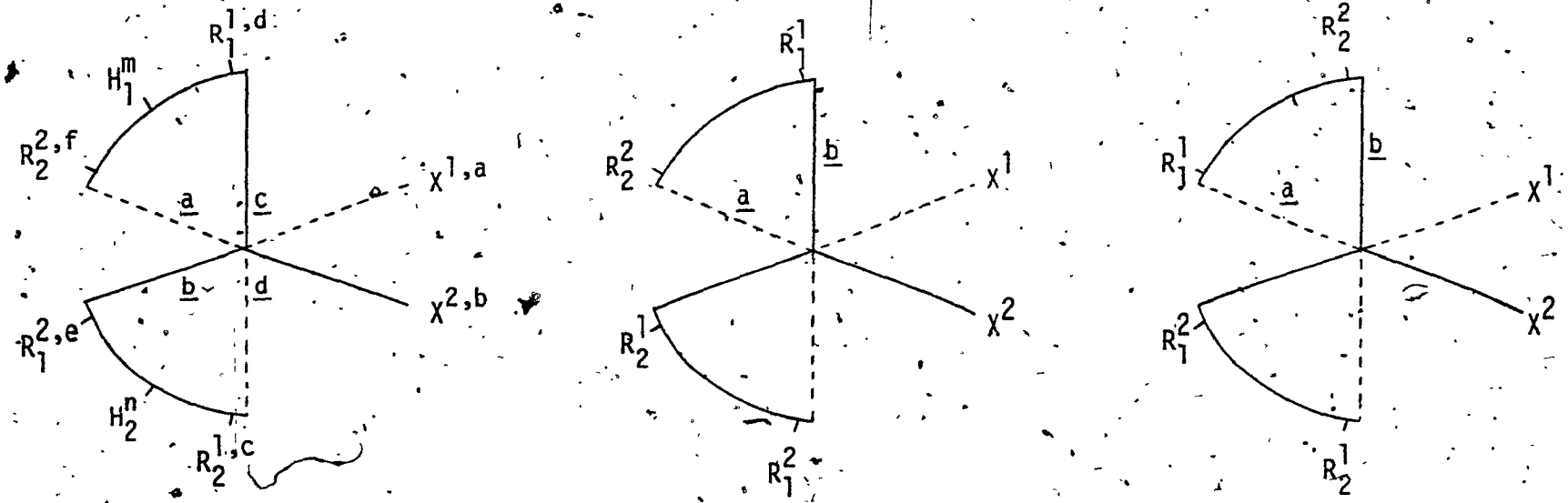

cis,cis,cis - Λ cis,trans,cis - Λ cis,cis,trans - Λ

Figure 6.- The three diastereomers containing mutually cis X groups for a cis-$M(AB)_2X_2$ complex. The numerical superscripts label the terminal, ring proton, and X groups; letter superscripts label the nonequivalent environments. Letter subscripts label the two types of R groups on the A-B ligand. The letters a, b, c, and d define the four nonequivalent metal-chelate bonds in the three diastereomers.

Table VIII

Scrambling Patterns for Nonequivalent Environments in the cis,cis,cis-Δ → cis,cis,cis-Δ(Λ) Rearrangements of a cis-$M(AB)_2X_2$ Complex

1.	[ijkl;a;m] [a]	↔ [ijkl;a;m]	no exchange
2.	[ijkl;a;m]	↔ [jilk;a;n]	R_1, R_2, and -CH= exchange
3.	[ijkl;a;m]	↔ [ijkl;b;m]	X exchange
4.	[ijkl;a;m]	↔ [jilk;b;n]	R_1, R_2, -CH=, and X exchange

*The sites in brackets refer to the various nonequivalent groups within the cis,cis,cis isomer in the following order:

R_1^1, R_1^2, R_2^1, R_2^2; X^2; $-CH_1=$

and are defined in Figure 6 and the text. The letters used in the above table simply define a general case for each type of scrambling pattern.

number 5 and X^2 is number 6).

Those permutations that result in the same net exchange pattern after all 16 operations are performed on the 16 permutational isomers are placed in the same averaging set A_i''; these averaging sets for a cis-$M(AB)_2X_2$ complex are listed in Table IX.

It is found that ten averaging sets exist for the cis-$M(AB)_2X_2$ system. Changes in signal multiplicities for diastereotopic and nondiastereotopic AB and X ligands predicted by the A_i'' averaging sets are summarized in Table X. The distinctions which can be made between averaging sets A_i'' on the basis of changes in signal multiplicities for the various combinations of diastereotopic and nondiastereotopic ligands are given in Table XI. In the absence of a diastereotopic probe to detect inversion at the metal center, the averaging sets A_i'' are pairwise indistinguishable (Table XIa): (A_1'',A_6''), (A_2'',A_7''), (A_3'',A_8''), (A_4'',A_9''), and

Table IX

Permutational Analysis of the cis-$M(AB)_2X_2$ System

Permutation [a]	Isomerization	Inversion	Scrambling Pattern in cis,cis,cis Isomer [b]	Averaging Set
E	-	-	1	A_1''
(12)(34)(56)	c,c,t ↔ c,t,c	-	2	A_2''
(56)	-	-	3	A_3''
(12) (34) (12)(56) (34)(56)	c,c,t ↔ c,c,c ↔ c,t,c	-	-	A_4''
(12)(34)	c,c,t ↔ c,t,c	-	4	A_5''
E*	-	Δ ↔ Λ	1	A_6''
(12)(34)(56)*	c,c,t ↔ c,t,c	Δ ↔ Λ	2	A_7''
(56)*	-	Δ ↔ Λ	3	A_8''
(12)* (34)* (12)(56)* (34)(56)*	c,c,t ↔ c,c,c ↔ c,t,c	Δ ↔ Λ	-	A_9''
(12)(34)*	c,c,t ↔ c,t,c	Δ ↔ Λ	4	A_{10}''

[a] See footnote a, Table III; [b] Scrambling patterns defined in Table VIII.

Table X.

Changes in Signal Multiplicities Resulting from the Averaging Sets A_i'' Operating on a cis-$M(AB)_2X_2$ Complex Containing Diastereotopic and/or Nondiastereotopic Ligands[a]

Averaging Set	A-B Nondiastereotopic (Diastereotopic)	-CR= Nondiastereotopic (Diastereotopic)	X Nondiastereotopic (Diastereotopic)
A_1''	4 (8) → 4 (8)	4 (8) → 4 (8)	4 (8) → 4 (8)
A_2''	4 (8) → 2 (4)	4 (8) → 2 (4)	4 (8) → 3 (6)
A_3''	4 (8) → 4 (8)	4 (8) → 4 (8)	4 (8) → 3 (6)
A_4''	4 (8) → 1 (2)	4 (8) → 1 (2)	4 (8) → 1 (2)
A_5''	4 (8) → 2 (4)	4 (8) → 2 (4)	4 (8) → 2 (4)
A_6''	4 (8) → 4 (4)	4 (8) → 4 (4)	4 (8) → 4 (4)
A_7''	4 (8) → 2 (4)	4 (8) → 2 (4)	4 (8) → 3 (4)
A_8''	4 (8) → 4 (4)	4 (8) → 4 (4)	4 (8) → 3 (4)
A_9''	4 (8) → 1 (2)	4 (8) → 1 (2)	4 (8) → 1 (2)
A_{10}''	4 (8) → 2 (4)	4 (8) → 2 (4)	4 (8) → 2 (4)

[a] See footnote a in Table IV.

(A_5'',A_{10}''). The maximum number of distinguishable averaging sets is obtained in cases c, e, and g of Table XI.

In the event that the X ligands contain nuclei which are incapable of serving as nmr probes, the permutational analysis is simplified but at the expense of mechanistic information. When the two X groups are indistinguishable, only eight distinct permutational isomers are found and eight operations, which form an Abelian group, interconvert the isomers. This is a subset of the group in Table IX, obtained by eliminating all

Table XI

Distinctions Between Averaging Sets A_i'' for a cis-$M(AB)_2X_2$ Complex on the Basis of Changes in Signal Multiplicities

(a)		(b)		(c)	
A-B	Nondiastereotopic	A-B	Nondiastereotopic	A-B	Diastereotopic
-CR=	Nondiastereotopic	-CR=	Nondiastereotopic	-CR=	Nondiastereotopic
X	Nondiastereotopic	X	Diastereotopic	X	Nondiastereotopic
(A_1'', A_6'')		A_1''		A_1''	
(A_2'', A_7'')		A_2''		(A_2'', A_7'')	
(A_3'', A_8'')		A_3''		A_3''	
(A_4'', A_9'')		(A_4'', A_9'')		(A_4'', A_9'')	
(A_5'', A_{10}'')		(A_5'', A_7'', A_{10}'')		(A_5'', A_{10}'')	
		(A_6'', A_8'')		A_6''	
				A_8''	

Table XI (continued)

(d)

A-B	Diastereotopic
-CR=	Nondiastereotopic
X	Diastereotopic

A_1''
A_2''
A_3''
(A_4'', A_9'')
(A_5'', A_7'', A_{10}'')
(A_6'', A_8'')

(e)

A-B	Nondiastereotopic
-CR=	Diastereotopic
X	Nondiastereotopic

A_1''
(A_2'', A_7'')
A_3''
(A_4'', A_9'')
(A_5'', A_{10}'')
A_6''
A_8''

(f)

A-B	Nondiastereotopic
-CR=	Diastereotopic
X	Diastereotopic

A_1''
A_2''
A_3''
(A_4'', A_9'')
(A_5'', A_7'', A_{10}'')
(A_6'', A_8'')

Table XI (continued)

(g)

A-B	Diastereotopic
-CR=	Diastereotopic
X	Nondiastereotopic

A_1''

A_2''

A_3''

(A_4'', A_9'')

(A_5'', A_{10}'')

A_6''

(A_7'', A_8'')

(h)

A-B	Diastereotopic
-CR=	Diastereotopic
X	Diastereotopic

A_1''

A_2''

A_3''

(A_4'', A_9'')

$(A_5'', A_6'', A_7'', A_8'', A_{10}'')$

operations which involve the (56) permutation. The nmr averaging sets A_i''' for this case are listed in Table XII. Changes in signal multiplicities that may be deduced from Table XII for cases in which the AB ligand contains diastereotopic and nondiastereotopic groups lead to the distinctions between averaging sets A_i'''. These are listed in Table XIII. The maximum information would be obtained from a complex possessing both diastereotopic and nondiastereotopic groups on the AB ligands. The study of complexes of the type cis-$M(AB)_2X_2$ in which the X groups do not serve as nmr probes severely restricts the conclusions that can be made from the nmr experiment.

As was mentioned in Section III-A-3c, distinctions between averaging sets are based only on the predicted signal multiplicities for various substituents in the fast exchange limit. The identical cautions mentioned for the cis-$M(AA)_2XY$ system apply in the cis-$M(AB)_2X_2$ case.

e. Correlations Amongst Averaging Sets

Since the averaging sets for the various molecular systems, derived in the preceding three sections, are all based on the same 16 permutation and permutation-inversion operations of an Abelian molecular symmetry group, it is to be expected that there will be an interrelation between the A_i, A_i', A_i'', and A_i''' averaging sets.

On changing the nature of the bidentate and monodentate ligands the symmetry of the molecule will be altered and degeneracies within averaging sets may be removed. Correlation of the constituent P and P^* operations with the various averaging sets of the cis-$M(AA)_2X_2$, cis-$M(AA)_2XY$, and cis-$M(AB)_2X_2$ systems leads to the correlation of averaging sets presented in Table XIV. Thus, once a unique averaging set

Table XII

Permutational Analysis of the cis-$M(AB)_2X_2$ System when the X Ligand does not Function as a Nuclear Magnetic Resonance Probe

Permutation[a]	Isomerization	Inversion	Scrambling Pattern in cis,cis,cis Isomer[b]	Averaging Set
E	-	-	1	A_1'''
(12)(34)	c,c,t ↔ c,t,c	-	2 (or 4)	A_2'''
(12) (34)	c,c,t ↔ c,c,c ↔ c,t,c	-	1 -	A_3'''
E^*	-	Δ ↔ Λ	1	A_4''
$(12)(34)^*$	c,c,t ↔ c,t,c	Δ ↔ Λ	2 (or 4)	A_5'''
$(12)^*$ $(34)^*$	c,c,t ↔ c,c,c, ↔ c,t,c	Δ ↔ Λ	-	A_6'''

[a] See footnote a of Table III; [b] Scrambling patterns are defined in Table VIII with the added restriction that exchange of X groups can no longer be detected.

Table XIII

Distinctions Between Averaging Sets A_i''' for a cis-$M(AB)_2X_2$ complex (in which the X group is not a NMR Probe) on the Basis of Changes in Signal Multiplicities

(a)	(b)	(c)
A-B Nondiastereotopic -CR= Nondiastereotopic	A-B Nondiastereotopic -CR= Diastereotopic	A-B Diastereotopic -CR= Diastereotopic
(A_1''', A_4''')	A_1'''	A_1'''
(A_2''', A_5''')	(A_2''', A_5''')	(A_2''', A_4''', A_5''')
(A_3''', A_6''')	(A_3''', A_6''')	(A_3''', A_6''')
	A_4'''	
	A-B Diastereotopic -CR= Nondiastereotopic	

has been determined for one of the systems in Table XIV, this same averag-ing set can be correlated with those for another system for which a unique choice is not possible. The correlation may lend support for the preference of one averaging set over another, despite the fact that they may be nmr indistinguishable.

A tacit assumption involved in this argument is that differences in the nature of the various combinations of ligands are not sufficiently great so as to sterically or electronically force a particular complex of the series in Table XIV to undergo a radically different physical rearrangement process from other members of the series.

Table XIV

Correlations Between the Averaging Sets for the cis-$M(AA)_2X_2$, cis-$M(AA)_2XY$, and cis-$M(AB)_2X_2$ Systems

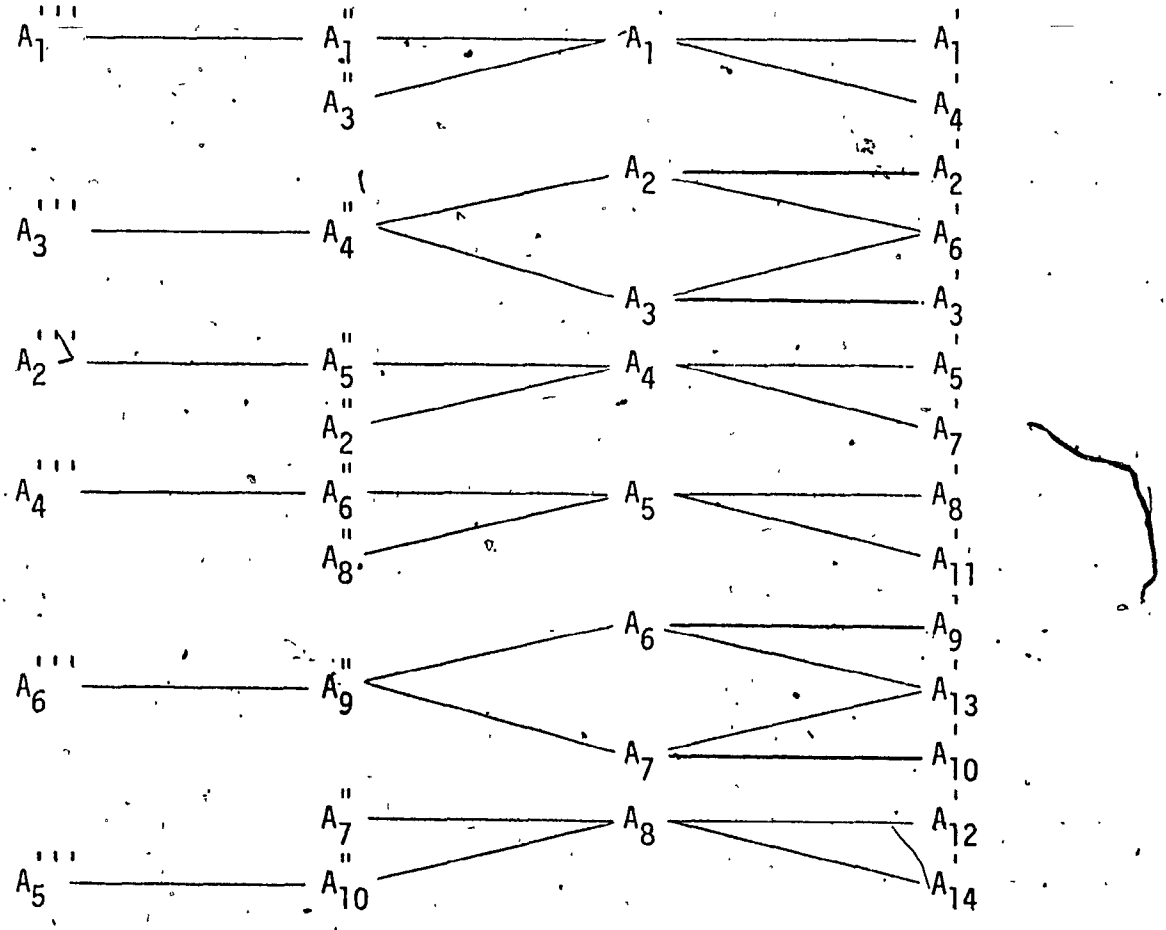

4. Mechanisms of Configurational Rearrangements in cis-$M(AA)_2X_2$, cis-$M(AA)_2XY$, and cis-$M(AB)_2X_2$ Complexes.

a. Introduction

There has been considerable discussion of possible intramolecular rearrangement mechanisms for six-coordinate metal chelate complexes (6,7,112,113). It is generally considered that rearrangement processes can proceed by two limiting types of pathways which are distinguished by the effective coordination number of the transition state. These pathways may also be distinguished as occurring with or without metal-ligand bond rupture.

A bond rupture mechanism was originally proposed by Werner (38) to account for the enantiomerization of the optically active tris(oxalato)-cobalt(III) cation. This intramolecular mechanism was visualized as resulting from the momentary rupture of one end of the bidentate ligand from the central metal ion; before it can rejoin, a rearrangement of the remaining groups in the five-coordinate intermediate can take place such that reattachment of the "unidentate" or "dangling" ligand results in the formation of the enantiomer. The geometry of the intermediate (transition state) is based on polyhedra actually found for five-coordinate complexes (43); it may have either an idealized square-pyramidal (SP) or trigonal-bipyramidal (TBP) geometry with the dangling ligand in an axial (ax) or equatorial (eq) position. It is generally assumed that energy differences between SP and TBP geometries are small (114) and an excellent example is afforded by the chlorobis[1,2-bis(diphenylphosphino)ethane]cobalt (III) trichlorostannate(II) complex, which exists as a mixture of SP and TBP forms (115). Indeed, a SP geometry is postulated as the intermediate in the Berry pseudorotation mechanism, the favoured process for stereo-

chemically nonrigid five-coordinate TBP complexes (10,116,117).

The alternative to the formation of a lower coordination polyhedron during rearrangement is the formation of a polytopal isomer of the six-atom family (39); the ligating nuclei approximate the vertex positions of a trigonal prism (TP). The first such non-bond rupture mechanism was described by Ray and Dutt (40) and is illustrated in Figure 7 for the cis-Δ isomer of a $M(AB)_3$ complex. The formation of the transition state may be visualized as follows. One ring is kept fixed while the other two rings rotate in their planes in different directions, through an angle of 45^0 about axes perpendicular to their respective planes. Continuing the motion past the transition state reforms the trigonal antiprismatic (TAP) or octahedral polyhedron. This process is commonly referred to as the Ray and Dutt or "rhombic" twist.

Another non-bond rupture process was envisioned by Bailar (42) (and also proposed independently by Gehman (118) and by Seiden (119)) as occuring by rotation of one triangular face of the octahedron by 120^0 while keeping the opposite face fixed. The process is illustrated for the cis-Δ isomer of a $M(AB)_3$ complex in Figure 8. The triangular face contained by solid lines is considered fixed while the opposite face is rotated clockwise through an angle of 60^0 about the threefold molecular axis of the octahedral framework to form the idealized TP transition state. Continued rotation in the same sense reforms the TAP polyhedron. This type of molecular motion is commonly referred to as the Bailar or "trigonal" twist.

An alternative to the Bailar and Ray and Dutt twists has more recently been proposed by Springer and Sievers (41). In this process, illustrated in Figure 9 for the cis-Δ isomer of a $M(AB)_3$ complex, one ring is kept fixed, while the other two rings revolve past each other while

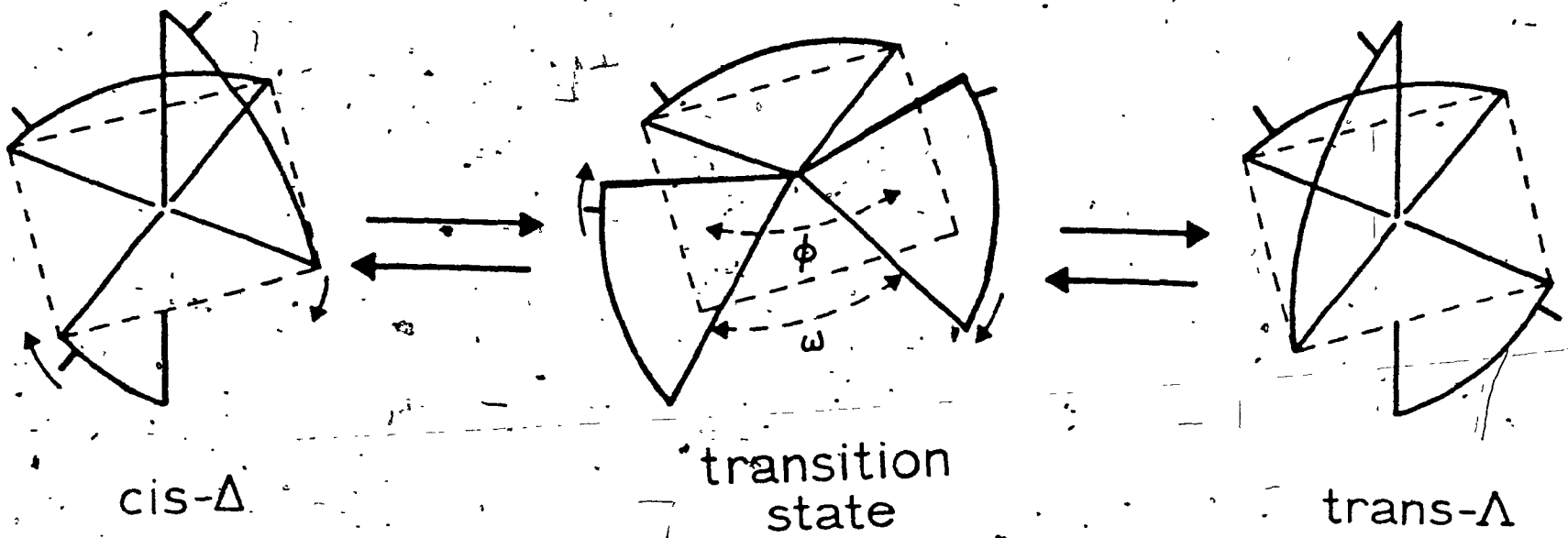

Figure 7.- The Ray and Dutt (rhombic) twist for the cis-Δ isomer of an $M(AB)_3$ complex. The dihedral angle between planes, ϕ, is assumed to remain constant at 90^{o}. The angle between adjacent metal-ligand bonds is denoted ω.

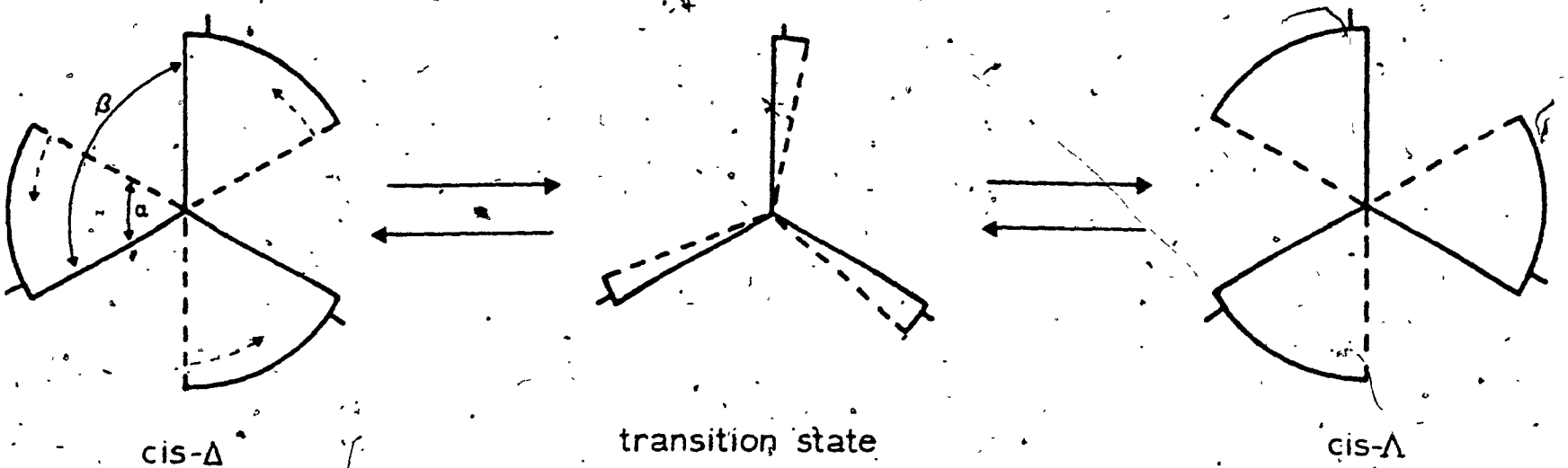

Figure 8.- The Bailar (trigonal) twist about the r-C_3 axis of the cis-Δ isomer of an $M(AB)_3$ complex viewed along the r-C_3 axis. The internal chelate ring angle is denoted α while β represents adjacent metal-ligand bond angles.

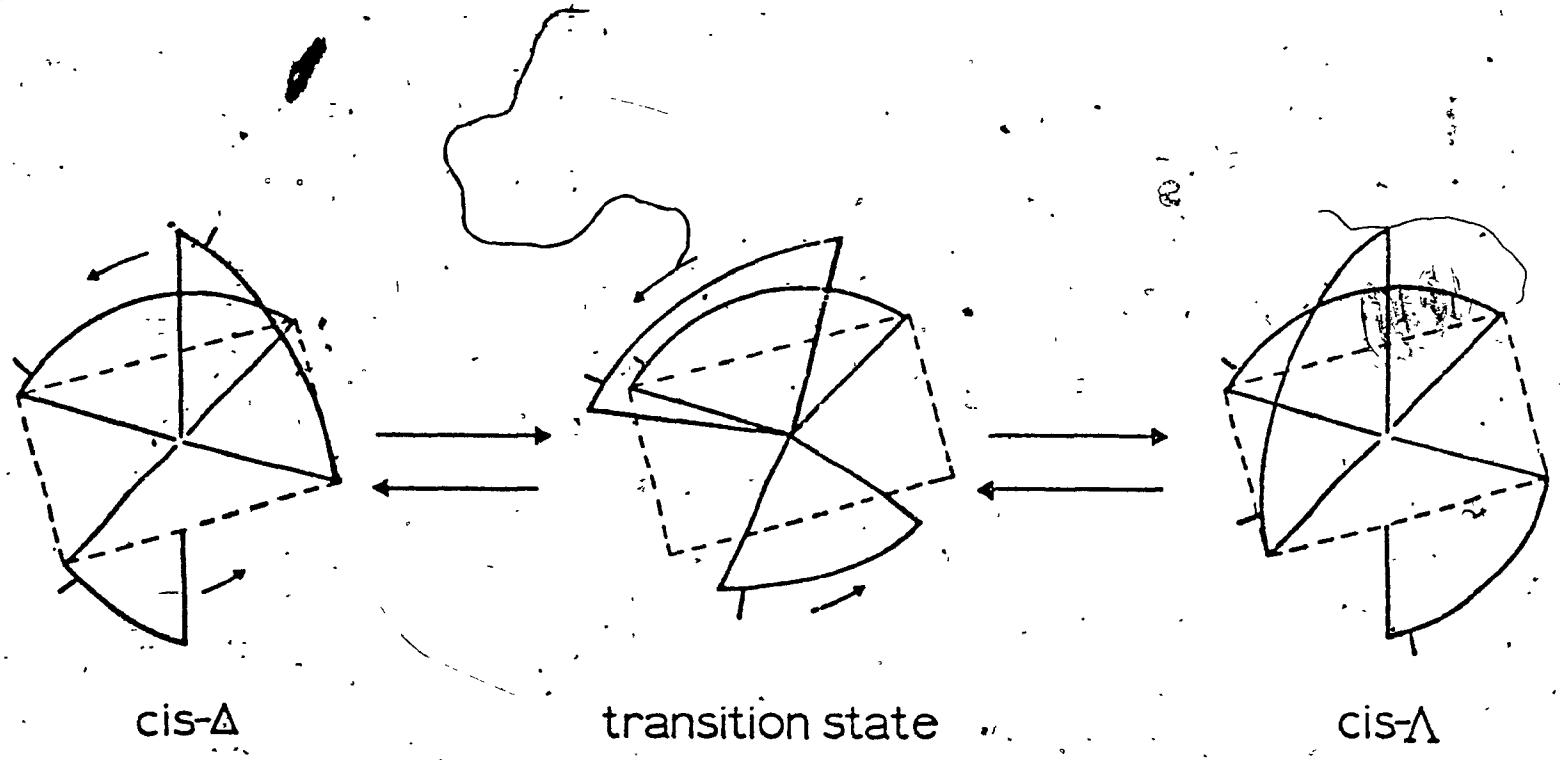

Figure 9.- The Springer and Sievers twist mechanism for the cis-Δ isomer of an $M(AB)_3$ complex.

continuously changing planes. Consequently, one may imagine that the two front faces of the octahedron rotate 120° counterclockwise, simultaneously but independently, about axes passing perpendicularly through their respective face centers.

The differences between the three twist mechanisms mentioned above appear to arise from differences in chelate ring bond angles during ring motion. It has been shown that the Ray and Dutt twist is completely identical to a Bailar twist about an imaginary-C_3 axis* (41,120); the Springer and Sievers twist is identical to a Bailar twist about a real-C_3 axis (39). Considering these mechanisms as the concerted twist motion of the ligating nuclei around a reference axis allows the Bailar twist to be performed about any of the real-, pseudo-, or imaginary-C_3 axes of an octahedral complex. These equivalent relationships are illustrated in Figure 10 for the cis-Δ isomer of a $M(AB)_3$ complex.

Figure 10a shows that a Bailar twist about an i-C_3 axis and the Ray and Dutt twist produce the identical idealized TP intermediate (7) which must decay to identical products, Similarly, Figure 10b illustrates the equivalence of a Bailar twist about a real-C_3 axis and the Springer and Sievers twist via TP intermediate (8). As a result of these equivalent relationships, twist mechanisms are generally considered to arise from a Bailar-type twist motion about the four molecular face axes of the octahedral framework.

*The octahedral geometry possesses four threefold axes passing through the centers of opposite triangular faces. These axes are real-C_3 (r-C_3) axes considering only the MA_6 octahedral core. In a chelate complex containing no r-C_3 axes, these axes are labeled pseudo-C_3 (p-C_3) axes if removal of chelate asymmetry would make them r-C_3 axes. Otherwise, they are labeled imaginary-C_3 (i-C_3) axes.

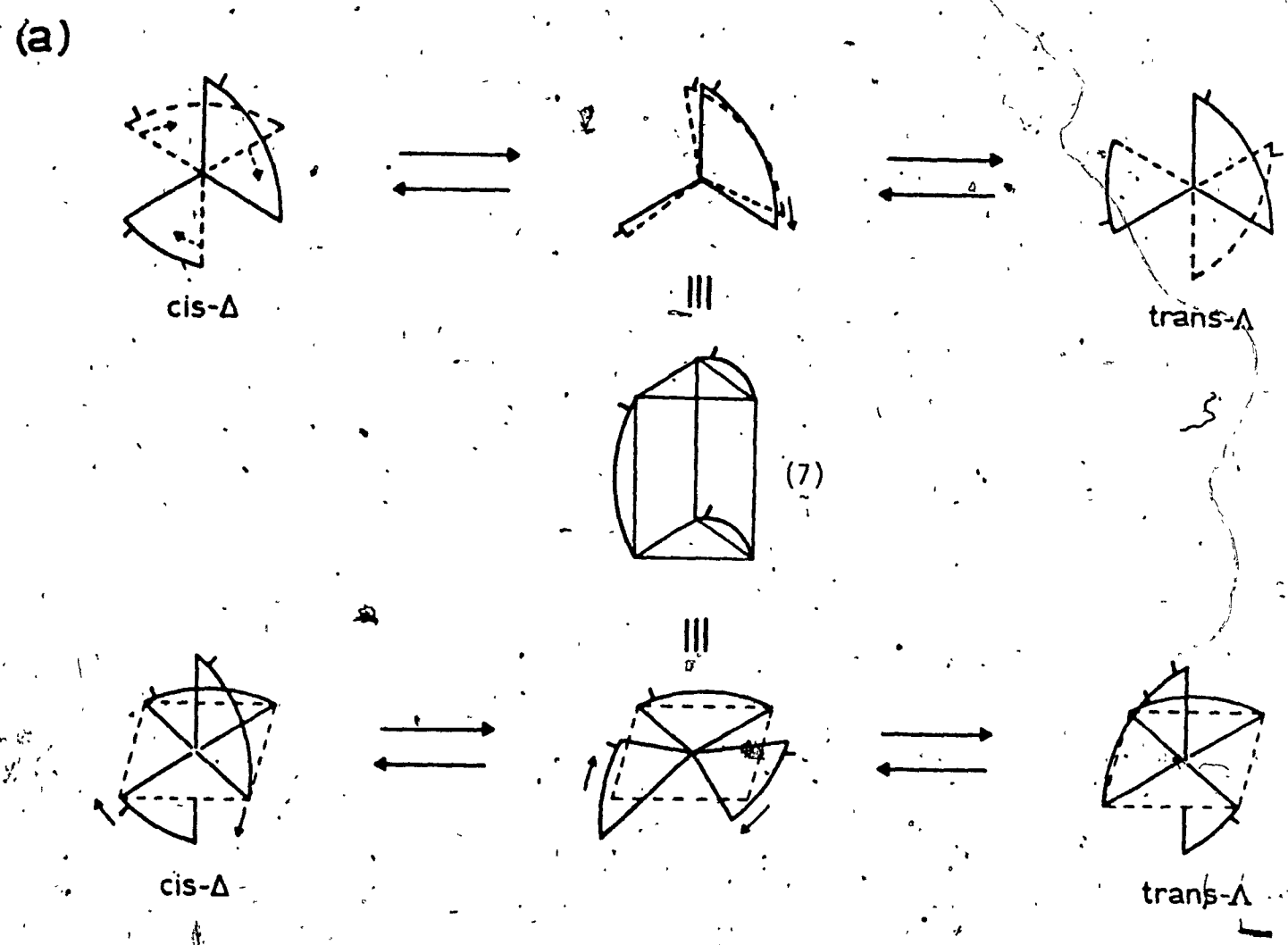

Figure 10.- (a) The equivalence of a Bailar twist about an imaginary-C_3 axis and the Ray and Dutt twist, through the nearly trigonal prismatic intermediate (7), illustrated for the cis-Δ isomer of an $M(AB)_3$ complex.

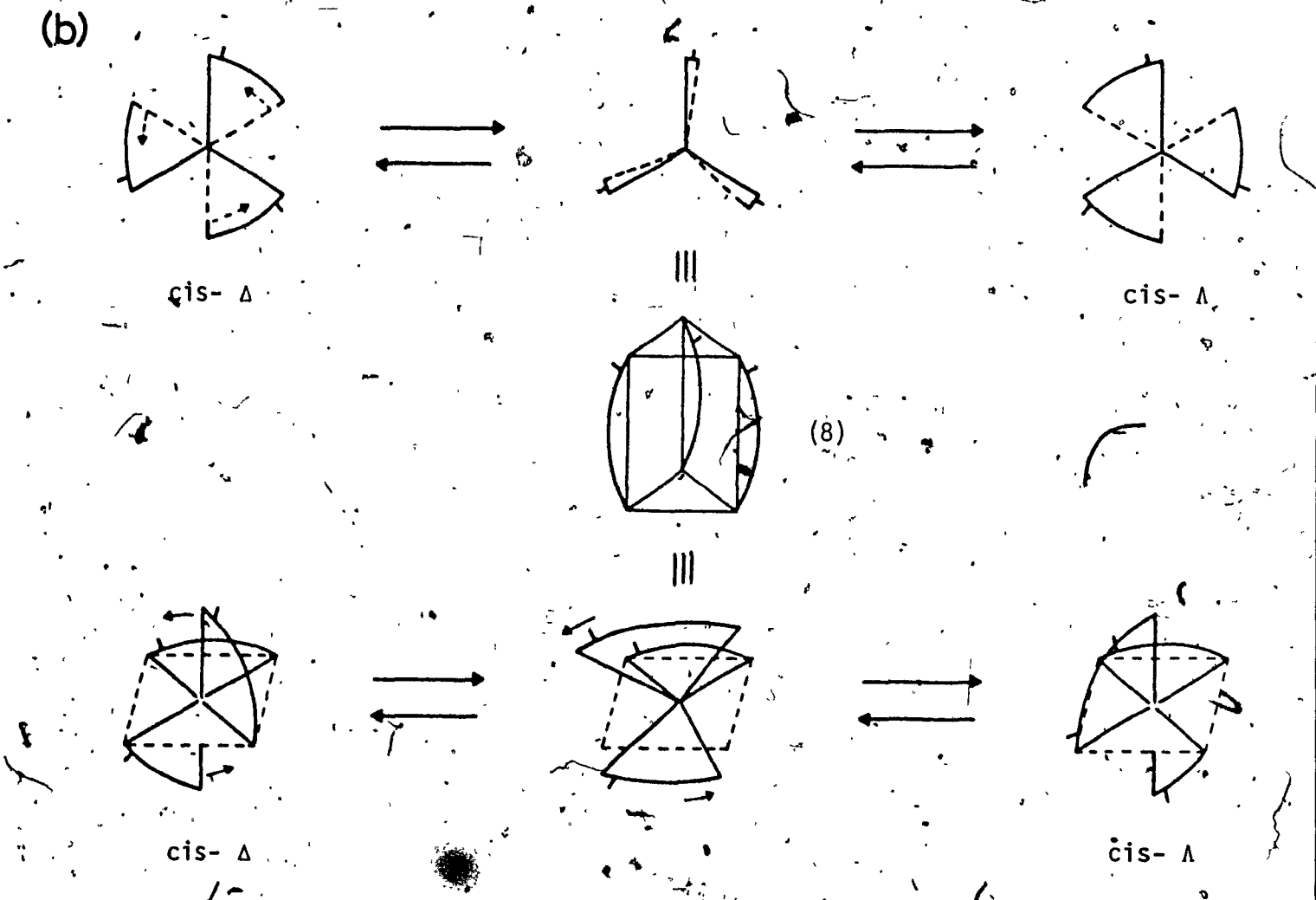

Figure 10.- (b) The equivalence of a Bailar twist about a real-C_3 axis and the Springer and Sievers twist, through the nearly trigonal prismatic intermediate (8), illustrated for the cis-Δ isomer of an $M(AB)_3$ complex.

The two distinct types of mechanisms (bond rupture versus twist motions) are quite physically reasonable because all of the postulated intermediates have been found to occur as stable entities in other transition metal complexes. Five-coordinate complexes in both polytopal forms (SP and TBP) are plentiful (43) and the number of trigonal prismatic chelate complexes is constantly increasing (44) or distortions toward TP geometry realized (45,46,121). As mentioned in Section III-A-1, any physical motion which produces the experimentally observed rearrangement is plausible. An example of a topologically equivalent mechanism for the twist mechanism in tris chelates was described by Stiefel and Brown (45). This process is best described as a simultaneous rotation of the three chelate rings 180^{o} about their C_2 axes via an approximate hexagonal-planar transition state and was suggested for highly compressed (45) tris chelates; however, the energetics of the process would appear to be formidable.

The simplest procedure for enumerating allowed rearrangements for a particular complex via a single physical process is through the use of graph theory (topology) (39,108). The various isomers for a particular coordination polyhedron may be represented as corners of a three-dimensional geometric figure. Specific operations that interconvert two isomers are represented by the line joining the two corners representing these isomers, with the intermediate located midway along this line. If the process is repeated for all possible stereoisomers, a complete description of the stereochemical consequences of a particular mechanism is produced. Then, by simple reference to the topological figure one may determine whether a particular mechanism gives the desired stereochemical interconversions.

The isomers represented by the vertices of the topological

figure may be either real, physically distinguishable diastereomers and/or enantiomers or permutational isomers. The former case obtains for the cis-$M(AB)_2X_2$ system while the latter situation prevails for the cis-$M(AA)_2X_2$ system.

The remainder of this section is devoted to the tabulation of the consequences of the various physical mechanisms discussed above on the cis-$M(AA)_2X_2$, cis-$M(AA)_2XY$, and cis-$M(AB)_2X_2$ systems. Correlations between physical processes and averaging sets are also put forth.

b. The cis-$M(AA)_2X_2$ System

This system is analyzed using the same four Δ-Λ pairs that were used in the permutational analysis of Section III-A-3b and illustrated in Figure 4. These isomers correspond to the 16 permutational isomers of Section III-A-3b after the removal of those permutamers generated by the distinguishability of the two X groups. Hence, this analysis could be described as a permutational mechanistic analysis. A similar procedure has been developed by Springer (122,123) for the $M(AA)_2(BB)$ system.

Figure 11a* illustrates the labeling of the four imaginary-C_3 axes for a cis-$M(AA)_2X_2$ complex while Figure 11b illustrates the twist mechanism about the four i-C_3 axes of the cis-Δ_{23} form of a cis-$M(AA)_2X_2$ complex. Twists about the $C_3(i)$ and $C_3(i'')$ axes give exchange of both terminal groups with inversion of the molecular configuration (corresponding to averaging set A_8); in addition, rotations about the latter axis also provide a path for the conversion of the cis enantiomers to the trans diastereomer, since the bidentate ligands do not span the upper and

*In Figure 11 the bidentate ligand is identified as BB while in other figures and text pertaining to this system the designation AA is used.

Figure 11.- (a) Labeling of the four imaginary C_3 axes for a cis-$M(AA)_2X_2$ complex; (b) twist mechanisms for a cis-$M(AA)_2X_2$ complex about the four i-C_3 axes of (a). Note that the twist motion about the C_3(i) axis may continue past the initial products to provide a path for cis-trans isomerization. This axis is unique in that the twist motion can be carried through a full cycle, since no chelate ring spans the upper and lower faces of the octahedron. This is the only twist process that accomodates cis-trans isomerization. Nomenclature is defined in Figure 4.

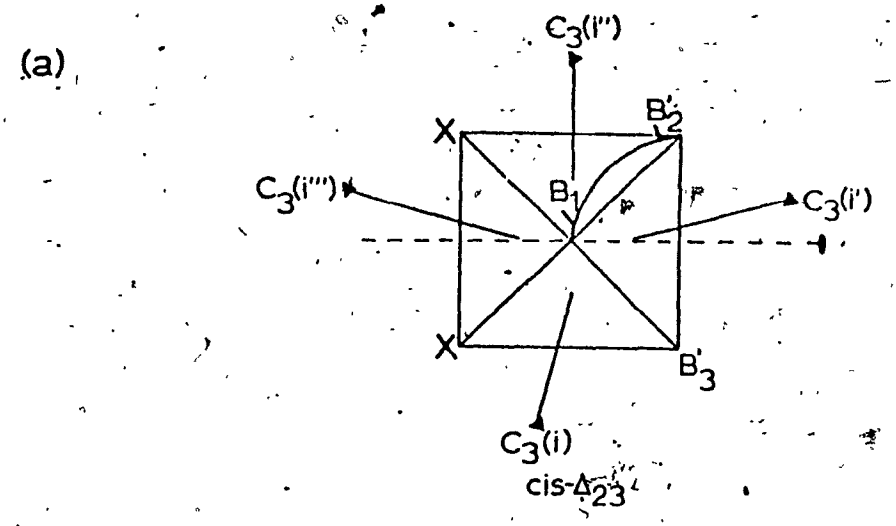
(a)
$C_3(i'')$
B'_2
X
$C_3(i''')$
B_1
$C_3(i')$
X
B'_3
$C_3(i)$
cis-Δ_{23}

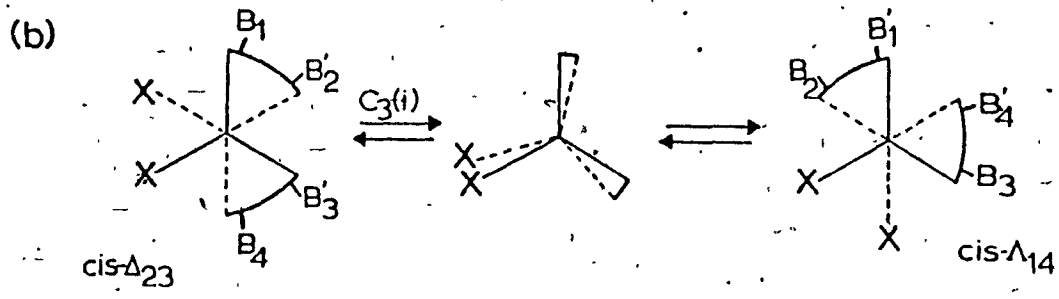
(b)
B_1
B'_2
X
$C_3(i)$
X
B'_3
B_4
cis-Δ_{23}
B'_1
B_2
B'_4
X
B_3
X
cis-Λ_{14}

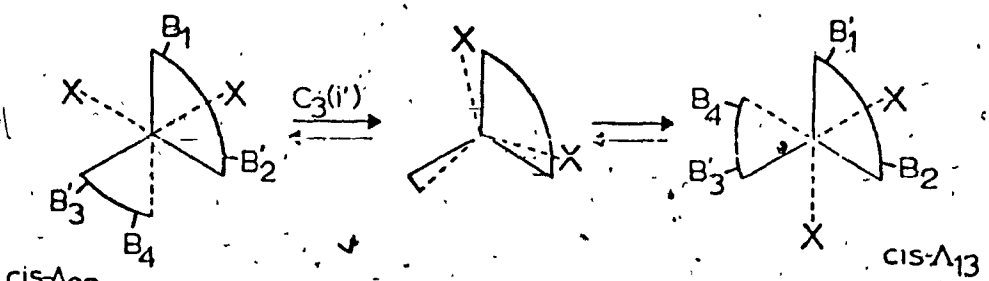
B_1
X
X
$C_3(i')$
B'_2
B'_3
B_4
cis-Δ_{23}
X
B'_1
B_4
X
B'_3
B_2
X
cis-Λ_{13}

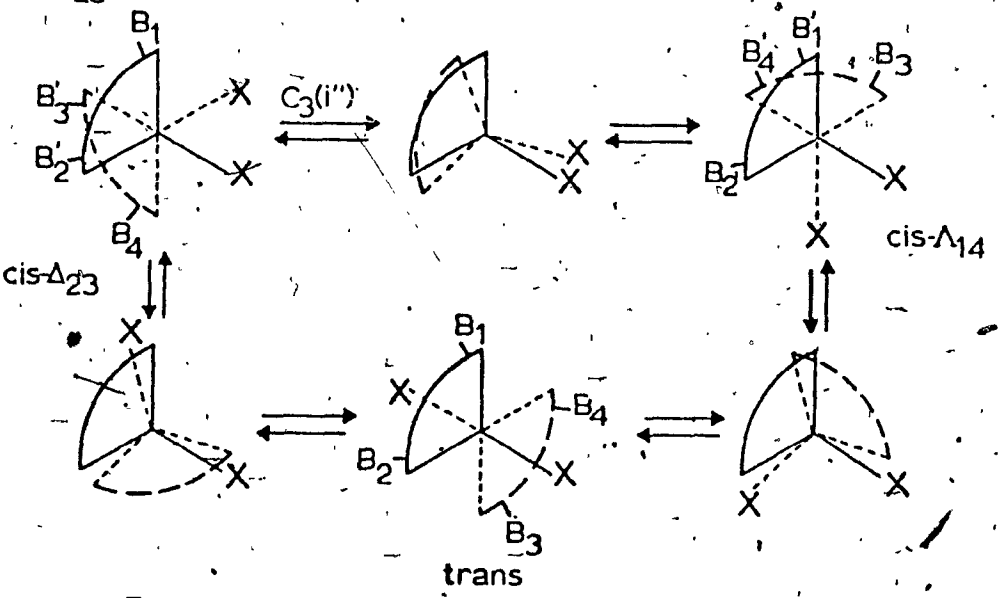
B_1
B'_3
X
$C_3(i'')$
B'_2
X
B_4
cis-Δ_{23}
B'_1
B'_4
B_3
B_2
X
cis-Λ_{14}
X
B_1
X
B_4
B_2
X
B_3
trans

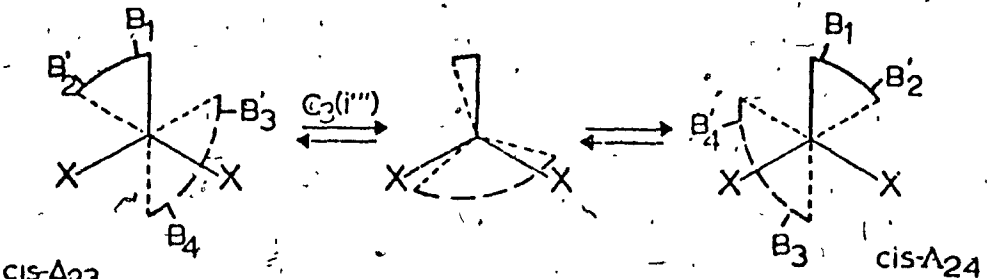
B_1
B'_2
B'_3
$C_3(i''')$
X
X
B_4
cis-Δ_{23}
B_1
B'_2
B'_4
X
X
B_3
cis-Λ_{24}

lower octahedral faces. Twists about the $C_3(i')$ and $C_3(i''')$ axes provide for exchange of only one (but different) set of nonequivalent terminal groups along with optical inversion and correspond to averaging sets A_6 and A_7, respectively.

Once the twist mechanism has been applied to the four Δ-Λ pairs of Figure 4, the stereochemical consequences of the twist mechanism on all isomers may be summarized in the topological diagram shown in Figure 12. Three types of trigonal-prismatic-like transition states are formed and are represented by squares, open circles, and triangles with a permutational degeneracy of four, four, and eight, respectively.

Transition states represented as squares and circles always correspond to averaging set A_8 and predict a ratio of rates of terminal group exchange to enantiomerization of unity, that is, a $\Delta_{23} \rightarrow \Lambda_{14}$ process. Transition states represented by triangles correspond to either averaging set A_6 or A_7 and any <u>one</u> step produces a ratio of rates of terminal group exchange to enantiomerization of 1/2. In order to explain exchange of both sets of terminal groups <u>via</u> triangle-type intermediates, twists must occur about the $C_3(i')$ and $C_3(i''')$ axes with equal probability to produce the reaction

$$\Delta_{23} \rightarrow \begin{cases} \Lambda_{13} \\ \Lambda_{24} \end{cases}$$

and since the Δ form is converted to the Λ form twice as fast as terminal groups are exchanged, the ratio of rates of terminal group exchange to enantiomerization is 1/2.

The topological diagram summarizing the interconversions amongst the four Δ-Λ pairs of a <u>cis</u>-$M(AA)_2X_2$ system is shown in Figure 13 for a bond rupture mechanism proceeding <u>via</u> TBP intermediates. The two

Figure 12.- Topological correlation diagram for the stereochemical rearrangements of the four Δ-Λ pairs (solid circles) of a cis-$M(AA)_2X_2$ complex via a twist mechanism. The three different types of intermediates are represented as open circles, squares, and triangles, with the permutational degeneracy of each indicated below the transition state. See Figure 4 for the nomenclature used.

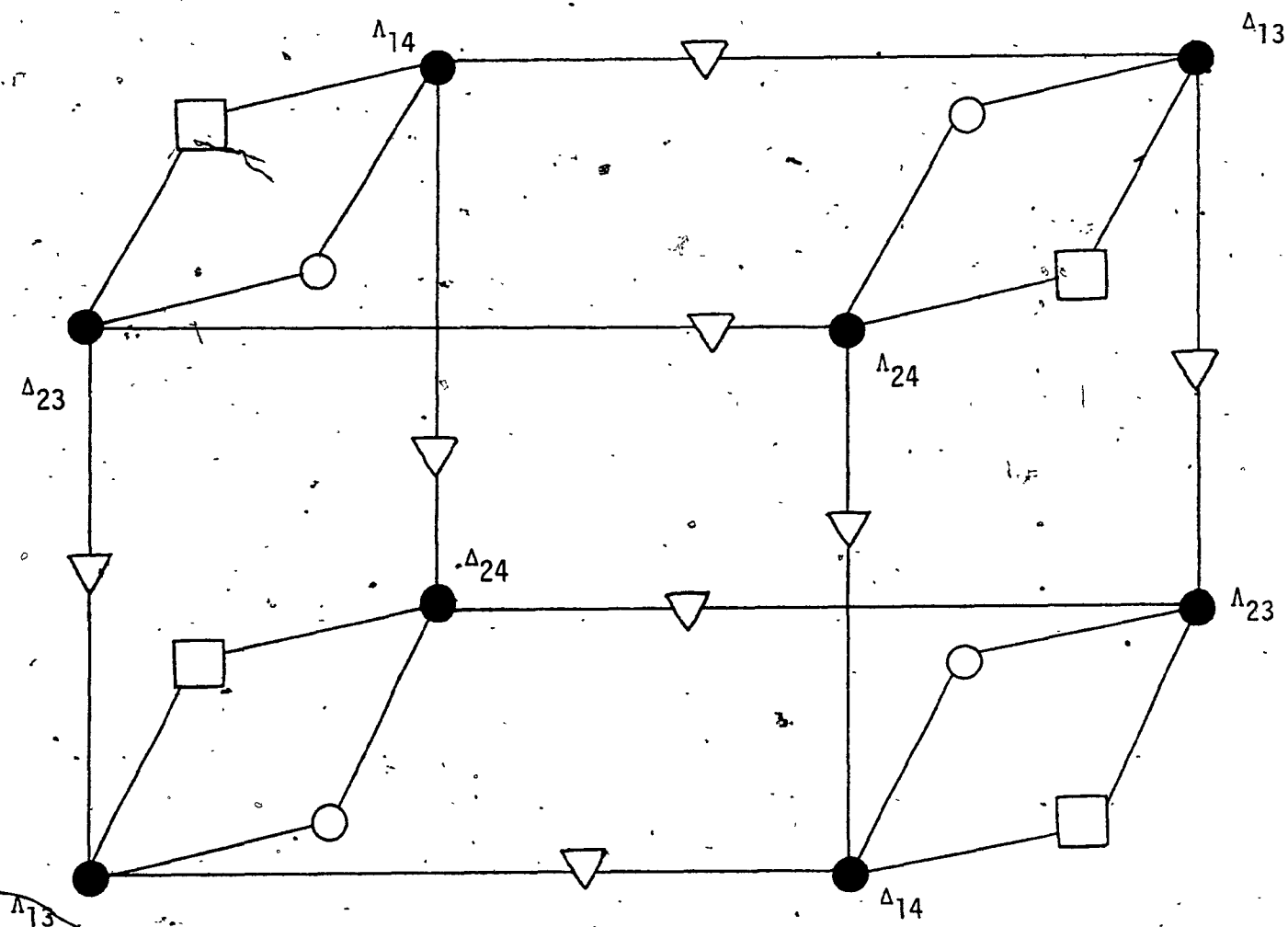
Λ_{14}
Δ_{13}
Δ_{23}
Λ_{24}
Δ_{24}
Λ_{23}
Λ_{13}
Δ_{14}

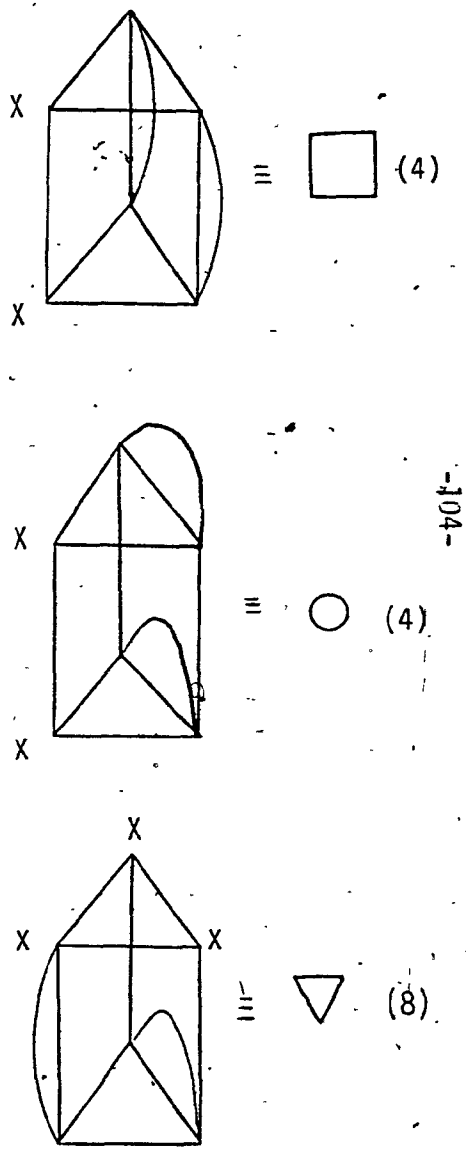
X
X
≡ (4)
X
X
≡ (4)
X
X
X
≡ (8)

Figure 13.- Topological correlation diagram for the interconversions of the four Δ-Λ pairs (solid circles) of a cis-$M(AA)_2X_2$ complex through trigonal bipyramidal-axial and -equatorial intermediates. The two types of TBP-axial intermediates are designated α and β, while TBP-equatorial intermediates are labeled γ. Indicated beside each type of intermediate is its permutational degeneracy. See Figure 4 for the nomenclature used.

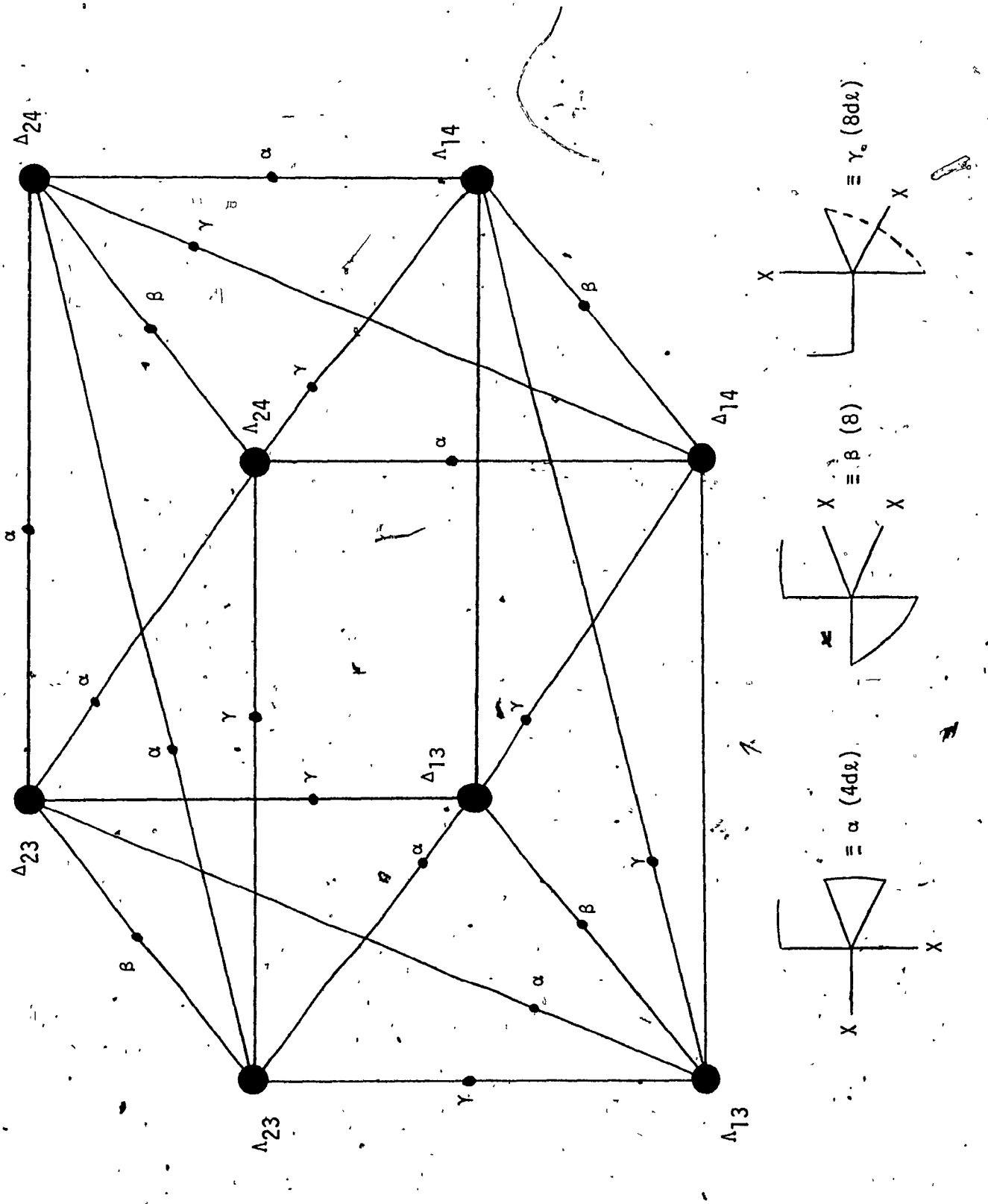
Δ24
Λ14
Λ24
Δ14
Δ23
Δ13
Λ23
Λ13
α
β
γ
≡ γ₀ (8dℓ)
≡ β (8)
≡ α (4dℓ)
X

types of TBP-axial intermediates are designated by α and β. There are eight permutational forms for each type of intermediate and in the case of α intermediates, they may be broken down into four enantiomeric pairs. TBP-equatorial intermediates, represented by γ, comprise eight enantiomeric pairs.

The most important aspect of Figure 13 is that, on inspection, there is no process which will result in simultaneous exchange of both sets of nonequivalent terminal groups in addition to enantiomerization, that is, a $\Delta_{23} \rightarrow \Lambda_{14}$ process. Therefore, this mechanism will not produce a ratio of rates of terminal group exchange to enantiomerization of unity. Intermediates α and β always correspond to either averaging set A_6 or A_7, while γ-type intermediates will correspond to either averaging set A_2 or A_3, since a TBP-equatorial transition state never results in inversion of the molecular configuration.

The topological diagram summarizing the interconversions between the four Δ-Λ pairs for the cis-$M(AA)_2X_2$ system is shown in Figure 14 for a bond rupture mechanism proceeding via SP-axial intermediates. The four enantiomeric SP-axial intermediates a, b, c, and d are illustrated in Figure 15. In Figure 14, the mirror images of the intermediates shown in Figure 15 are designated as $\bar{a}$, $\bar{b}$, $\bar{c}$, and $\bar{d}$. Two microscopically reversible pathways exist for the formation of SP-axial intermediates after the initial bond rupture; they are denoted as primary (p) and secondary (s) processes (21). After the initial rupture of a metal-ligand bond, the ligating nuclei trans to the dangling ligand may migrate directly to the vacant coordination site to form the SP-axial transition state; this is the primary process. During this migration, rotation of the ring may occur such that the ligand end cis to the dangling ligand fills the empty coordination site; this is the secondary

Figure 14.- Topological correlation diagram for the interconversions of the four Δ-Λ pairs (solid circles) of a cis-$M(AA)_2X_2$ complex proceeding via square pyramidal-axial transition states which are formed and decay to products by the primary process alone. There are four enantiomeric pairs of SP-axial intermediates, denoted a, b, c, and d (their mirror images correspond to $\bar{a}$, $\bar{b}$, $\bar{c}$, and $\bar{d}$). These intermediates are illustrated in Figure 15. See Figure 4 for the nomenclature used.

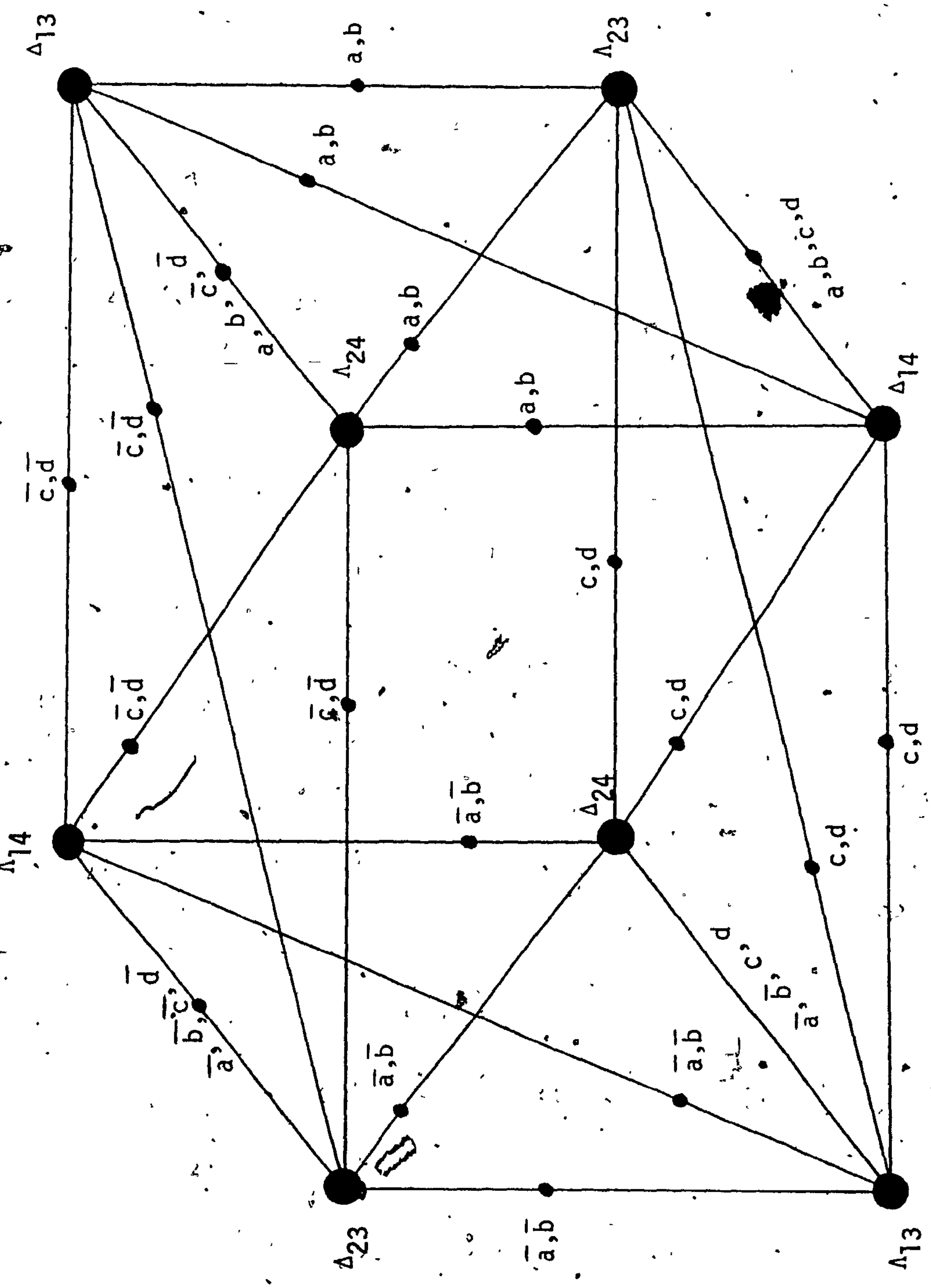
Λ13
Λ23
Λ24
Λ14
Λ14
Λ24
Λ23
Λ13

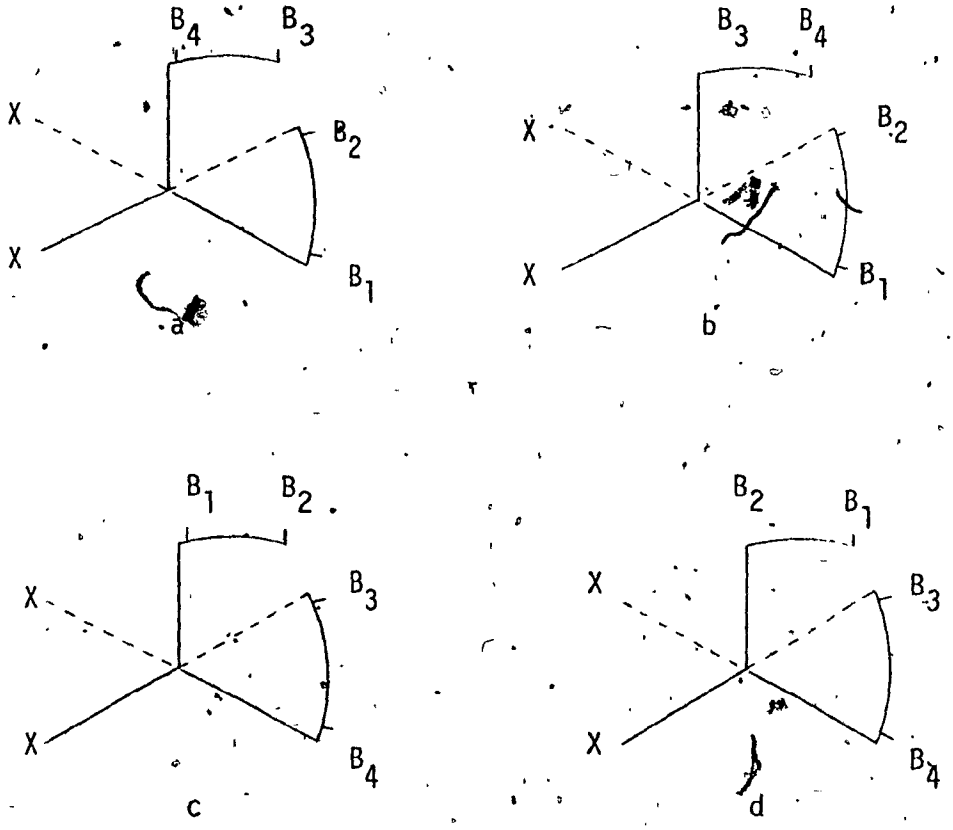

Figure 15.- Illustration of four square pyramidal-axial transition states for rearrangements of the four Δ-Λ pairs of a cis-$M(AA)_2X_2$ complex. A mirror image exists for each of these intermediates and is represented as $\bar{a}$, $\bar{b}$, $\bar{c}$, and $\bar{d}$.

process. The formation of products results from the attack of the dangling ligand end at any one of the four basal positions of the square pyramid and the displacement of the appropriate end of the basal ligand to the vacant coordination site below the plane without (primary) or with (secondary) rotation of the entire ligand.

Attention is here directed to the primary process alone, which on an a priori basis is much more probable than the secondary process because of the lesser degree of ligand motion involved both in

the formation of transition states and in their decay to products.

Transition states and products were obtained exclusively from primary processes in the construction of Figure 14. All feasible interconversions are possible except for those corresponding to averaging sets A_1, A_4, and A_5.

c. The cis-$M(AA)_2XY$ System

Identical nomenclature to that used and described in the permutational analysis of Section III-A-3c is employed here. The cis-Λ isomer is shown in Figure 5 which illustrates the various nonequivalent sites and rupturable metal-ligand bonds.

Twist motions about the four imaginary-C_3 axes (as defined in Figure 5) are illustrated in Figure 16 and summarized in Table XVa, which assigns averaging sets to various operations. There are a total of six trigonal-prismatic-like transition states, including two enantiomeric dℓ pairs and two which are achiral. Again, all twist motions result in inversion of the molecular configuration but generate only the A'_{12}, A'_{13}, and A'_{14} averaging sets.

Metal-ligand bond rupture can result in the formation of TBP or SP intermediates. The possible intermediates are shown in Figure 17. There are a total of four TBP-axial intermediates including one enantiomeric dℓ pair. Allowed TBP-equatorial intermediates consist of two enantiomeric pairs. A single enantiomeric dℓ pair of SP-axial intermediates exists. An illustration of the bond rupture mechanism via TBP-axial, TBP-equatorial, and SP-axial intermediates is provided by Figure 18. Stereochemical consequences of bond rupture mechanisms involving these three types of intermediates are summarized in Table XV, which also assigns averaging sets to the various physical operations.

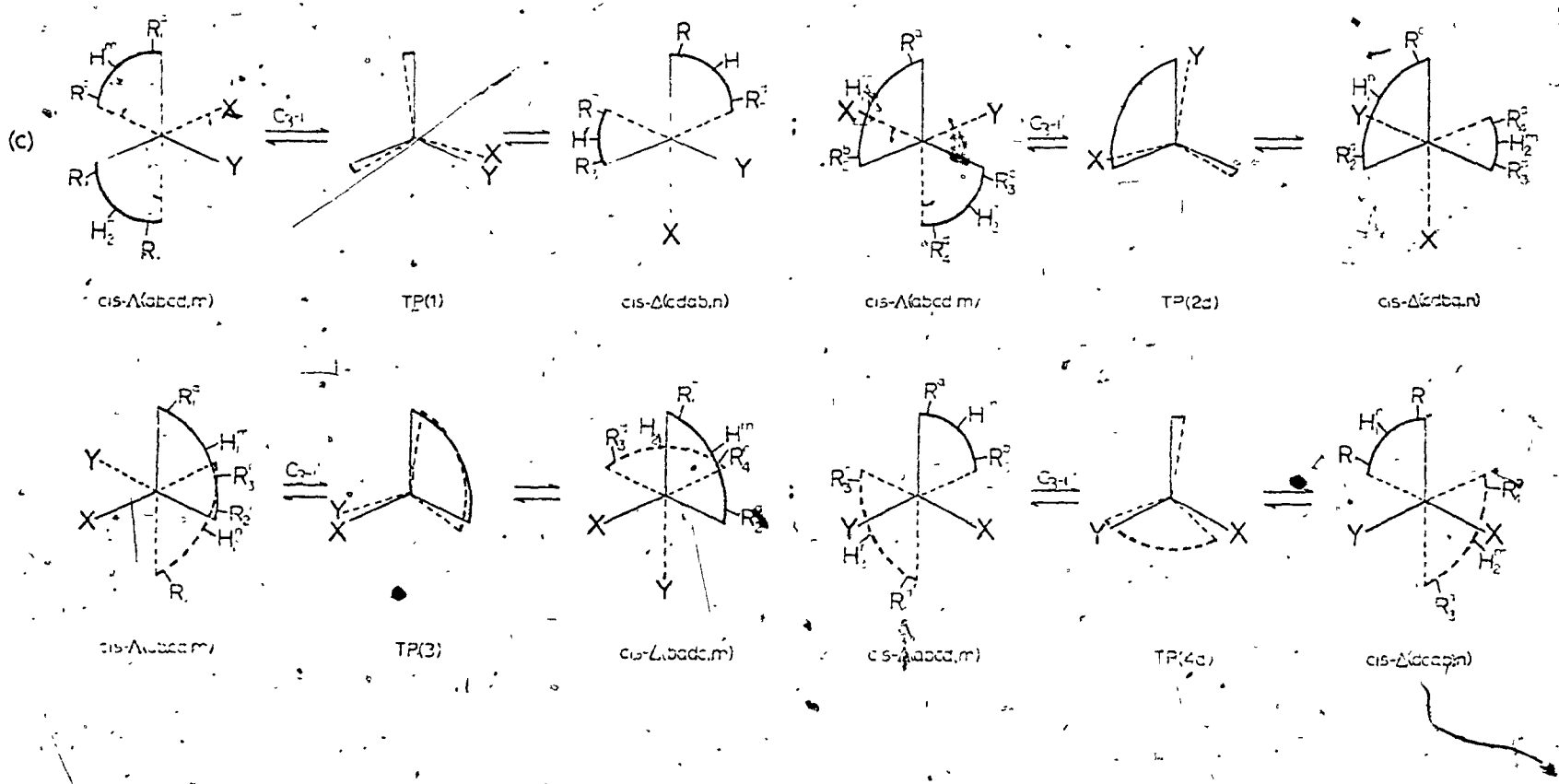

Figure 16.- Configurational rearrangements of a cis-Λ(abcd;m) isomer of a cis-$M(AA)_2XY$ complex via twist motions about octahedral face axes. Axes and complex nomenclature are defined in Figure 5. Note that rotation about the $C_3(i")$ axis may also provide a path for formation of the trans isomer.

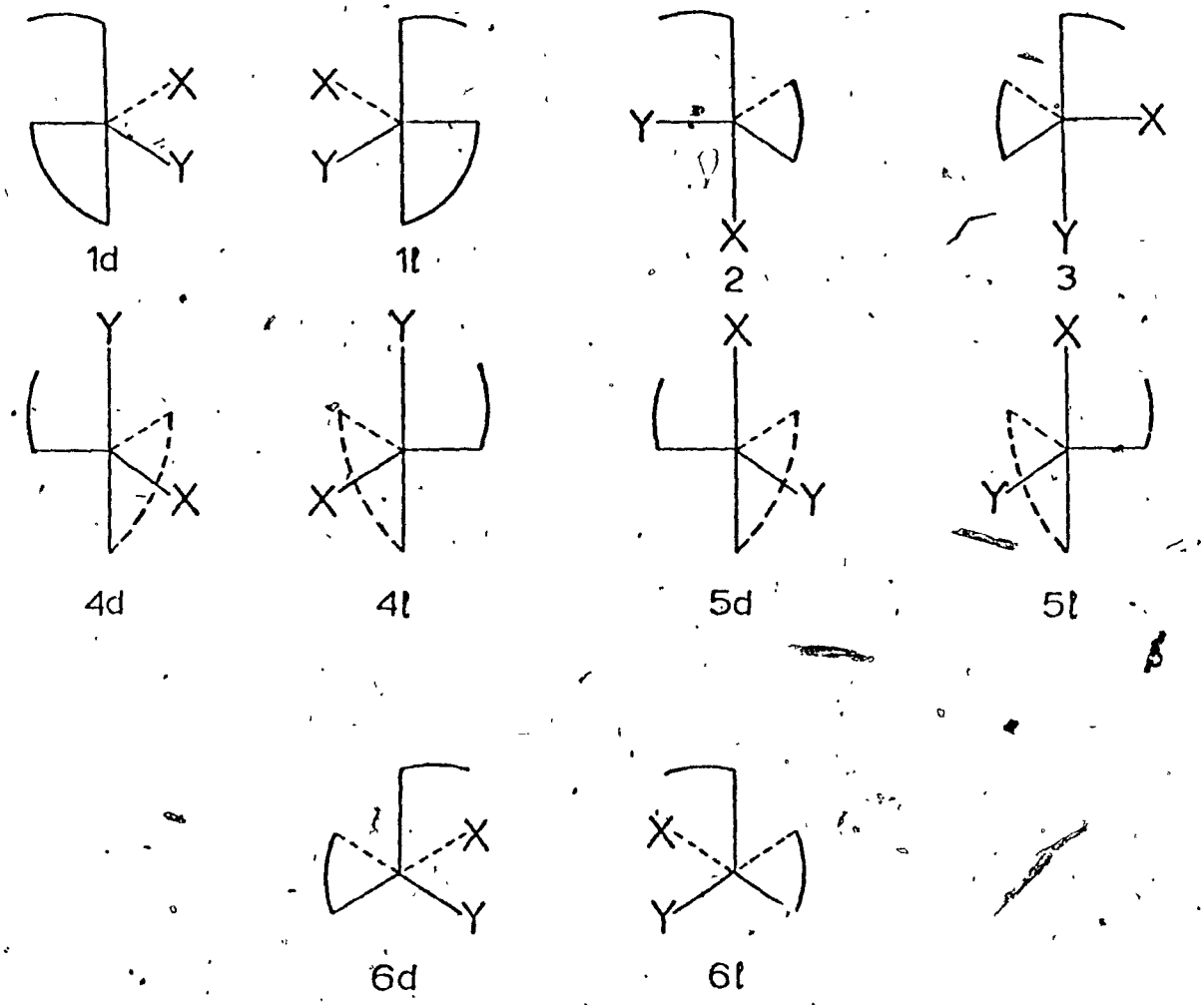

Figure 17. Possible TBP-axial, TBP-equatorial, and SP-axial intermediates arising from metal-chelate bond rupture in a cis-$M(AA)_2XY$ complex.

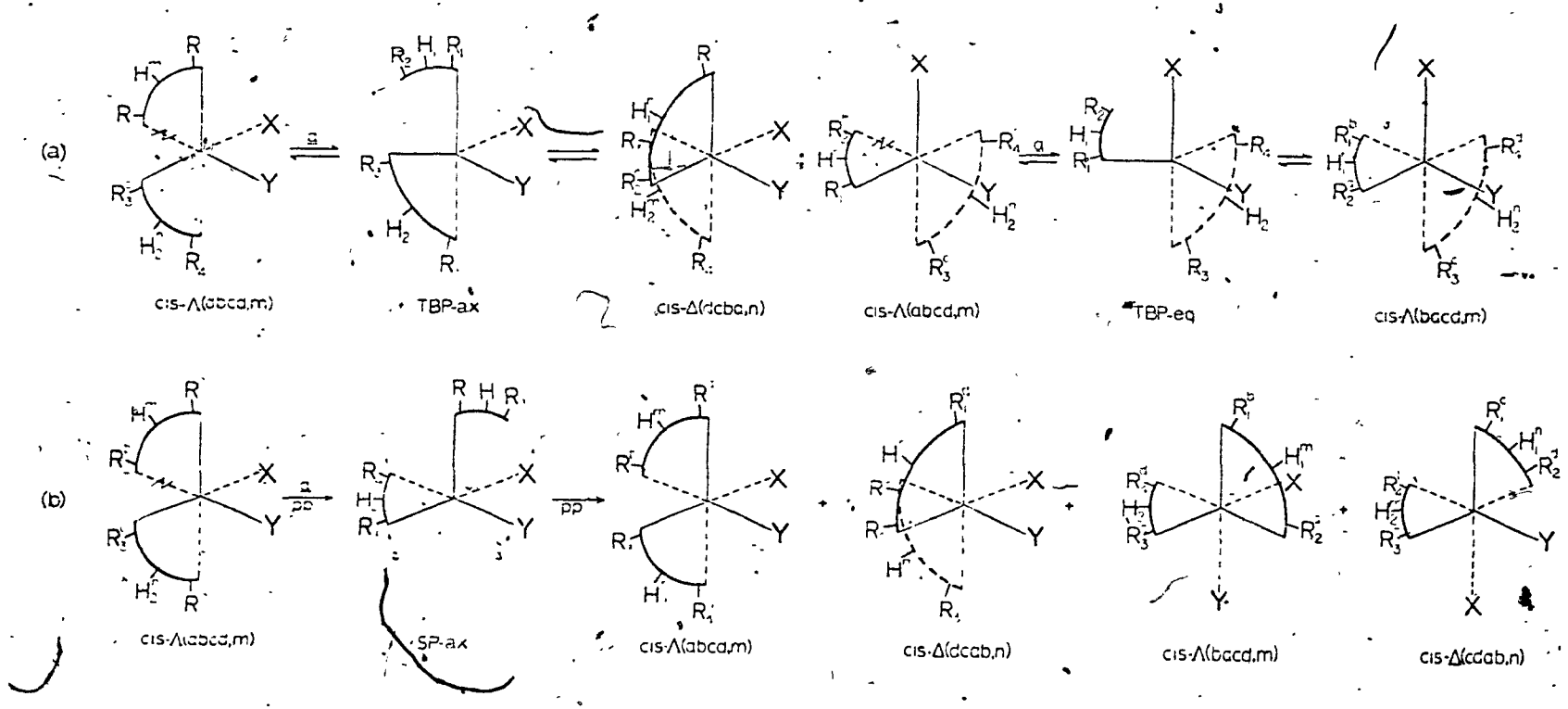

Figure 18.- Illustrations of configurational rearrangements of a cis-$M(AA)_2XY$ complex proceeding through metal-chelate bond rupture processes. (a) Rearrangements proceeding via TBP-axial and -equatorial intermediates derived from rupture of bond a. (b) Rearrangements occurring via an SP-axial intermediate derived from rupture of the metal-chelate bond a and decaying to products through the primary process. Intermediates are labeled according to Figure 17. See 5 for the nomenclature used.

Table XV

Intermediates and the Fate of the cis-Λ(Δ)(abcd;m) Permutamer of a cis-$M(AA)_2XY$ Complex on Application of Various Physical Rearrangement Mechanisms and Assignment of Averaging Sets to Physical Processes

(A) Twist Mechanism[a]

Initial Permutamer[b]	Rotation Axis[c]	TP Intermediate	Product Permutamer	Averaging Set[g]
c-Λ(Δ)(abcd;m)	i	1 (1)	c-Δ(Λ)(cdab;n)	A_{14}
	i'	2d((2ℓ)	c-Δ(Λ)(cdba;n)	A_{13}
	i''	3 (3)	c-Δ(Λ)(badc;m)	A_{12}
	i'''	4d (4ℓ)	c-Δ(Λ)(dcab;n)	A_{13}

(B) Bond Rupture- TBP Intermediate Mechanism[d]

Initial Permutamer	Bond Broken[b]	TBP-axial Intermediate[e]	Product Permutamer	Averaging Set
c-Λ(Δ)(abcd;m)	a	1d(1ℓ)	c-Δ(Λ)(dcba;n)	A_{11}
	b	1ℓ(1d)	c-Δ(Λ)(dcba;n)	A_{11}
	c	3(3)	c-Δ(Λ)(abdc;m)	A_{10}
	d	2(2)	c-Δ(Λ)(bacd;m)	A_9
		TBP-equatorial Intermediate[e]		
	a	5d(5ℓ)	c-Λ(Δ)(bacd;m)	A_2
	b	4d(4ℓ)	c-Λ(Δ)(abdc;m)	A_3
	c	5d(5ℓ)	c-Λ(Δ)(bacd;m)	A_2
	d	4d(4ℓ)	c-Λ(Δ)(abdc;m)	A_3

Table XV (continued)

(C) Bond Rupture- SP-axial Intermediate-Mechanism (Primary Process)[d].

Initial Permutamer	Bond Broken[b]	SP-axial Intermediate[f]	Product Permutamer	Averaging Set[g]
c-Λ(Δ)(abcd;m)	a	6d(6ℓ)	c-Λ(Δ)(abcd;m)	A_1
			c-Δ(Λ)(dcab;n)	A_{13}
			c-Λ(Δ)(bacd;m)	A_2
			c-Δ(Λ)(cdab;n)	A_{14}
	b	6ℓ(6d)	c-Λ(Δ)(abcd;m)	A_1
			c-Δ(Λ)(cdba;n)	A_{13}
			c-Λ(Δ)(abdc;m)	A_3
			c-Δ(Λ)(cdab;n)	A_{14}
	c	6d(6ℓ)	c-Λ(Δ)(bacd;m)	A_2
			c-Δ(Λ)(cdab;n)	A_{14}
			c-Λ(Δ)(abcd;m)	A_1
			c-Δ(Λ)(dcab;n)	A_{13}
	d	6ℓ(6d)	c-Λ(Δ)(abdc;m)	A_3
			c-Δ(Λ)(cdab;n)	A_{14}
			c-Λ(Δ)(abcd;m)	A_1
			c-Δ(Λ)(cdba;n)	A_{13}

[a]For specification of intermediates and illustration of the mechanism, see Figure 16; [b]Defined in Figure 5; [c]For definition of rotation axes, see Figure 5; [d]Intermediates are illustrated in Figure 17; [e]This mechanism is illustrated in Figure 18; [f]Intermediates are illustrated in Figure 17; [g]Averaging sets A_i are defined in Table V.

Considering TBP-axial intermediates first, inspection of Table XV reveals that this process always causes optical inversion to occur and may generate averaging sets A'_9, A'_{10}, or A'_{11}.

On the other hand, TBP-equatorial intermediates will not produce enantiomerization while generating averaging sets A'_2 or A'_3. Thus, if enantiomerization can be demonstrated as occurring, this mechanism may be unequivocally ruled out as the primary physical pathway for rearrangement.

SP-axial intermediates formed by and decaying via primary processes result in an equal balance of enantiomerization and retention of configuration, while generating averaging sets A'_1, A'_2, A'_3, A'_{13}, and A'_{14}.

For one final comment on this system, Table XV reveals that there are five averaging sets which do not correspond to the physical processes considered in Table XV; these are A'_4, A'_5, A'_6, A'_7, and A'_8. Should one of these averaging sets be indicated from the nmr experiment, considerable thought would have to be given to determining new, alternative mechanistic pathways.

d. The cis-$M(AB)_2X_2$ System

This system is analyzed in terms of the three diastereomers having cis-X_2 groups illustrated in Figure 6. In addition, two diastereomers having trans-X_2 groups are possible and are shown below. The nomenclature for the diastereomers is defined in Section III-A-3d. Mechanisms which can potentially cause cis-X_2 ↔ trans-X_2 isomerization are noted in Tables XVI and XVII; however, attention is focused on cis-X_2 ↔ cis-X_2 rearrangements.

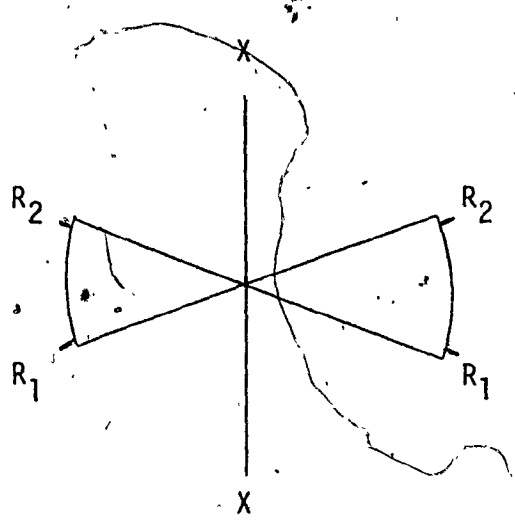

trans,cis,cis (C_{2v})

$1R_1$, $1R_2$; 1 ring H, 1X

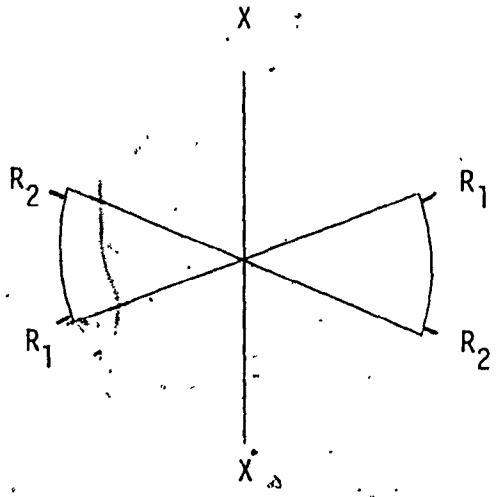

trans,trans,trans (C_{2h})

$1R_1$, $1R_2$, 1 ring H, 1X

Throughout this section, subscripts attached to the label of the rearranged complex refer to scrambling patterns for cis,cis,cis-Δ(Λ) ↔ cis,cis,cis-Δ(Λ) rearrangements defined in Table VIII. The labeling of nonequivalent sites is defined in Section III-A-3d while nonequivalent metal-ligand bonds are labeled in Figure 6.

Figure 19a defines the four i-C_3 axes for a cis-$M(AB)_2X_2$ complex while Figure 19b illustrates the twist mechanism operating on the cis,cis,cis-Δ diastereomer. A total of ten transition states are produced, which include four enantiomeric dℓ pairs. These intermediates are shown in Figure 20 and are labeled according to the notation of Pignolet and co-workers (28). The consequences of the twist mechanism operating on the three cis-X_2 diastereomers are summarized in Table XVI and the topological correlation diagram in Figure 21. For each cis-X_2 isomer, rotation about the $C_3(i'')$ axis after the initial product is formed provides a path for formation of trans-X_2 diastereomers. This axis is unique in this regard.

Figure 19.- (a) Labeling of the four imaginary C_3 axes of the cis,cis,cis-Δ isomer of a cis-$M(AB)_2X_2$ complex. (b) Twist mechanisms for the cis,cis,cis-Δ isomer about the four axes of (a). Note that rotations about the $C_3(i')$ axis provides a path for formation of the trans-X_2 isomers. Nomenclature is defined in Figure 6. The numerical subscripts attached to the products are the scrambling patterns for the cis,cis,cis isomers, as defined in Table VIII. Intermediates are labeled and illustrated in Figure 20.

(a)

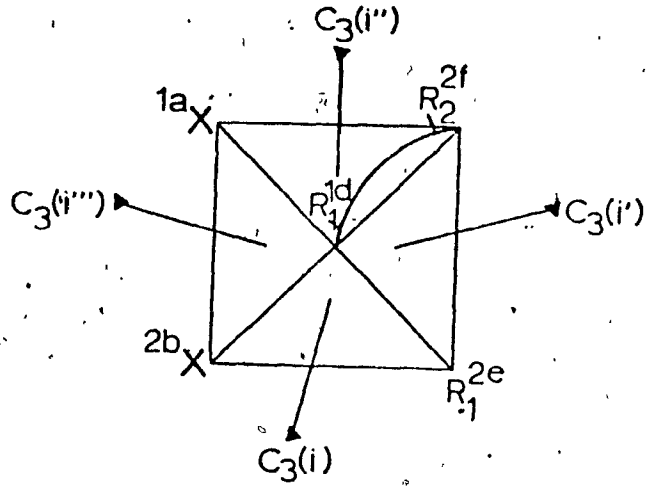

cis,cis,cis-Δ

(b)

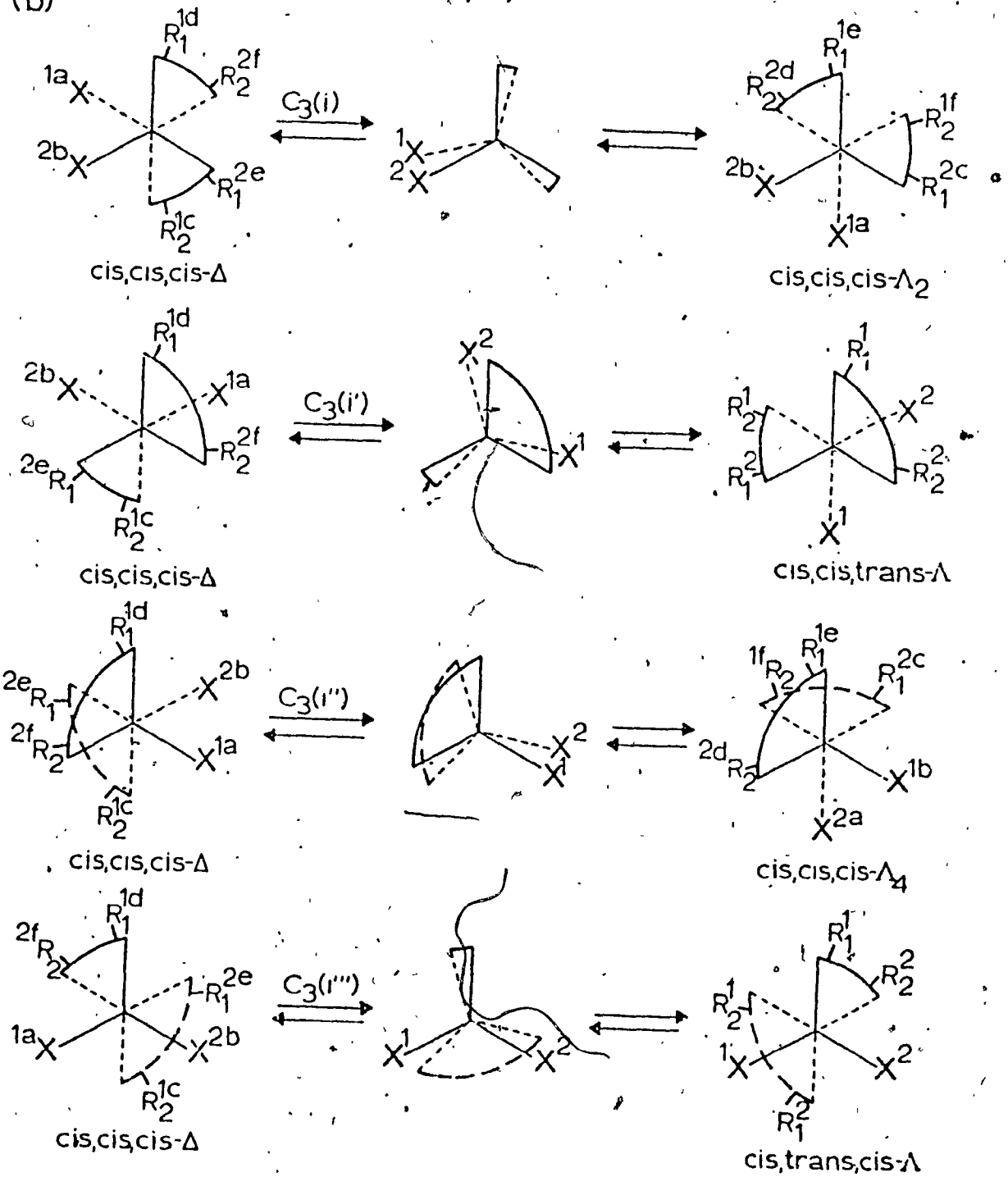

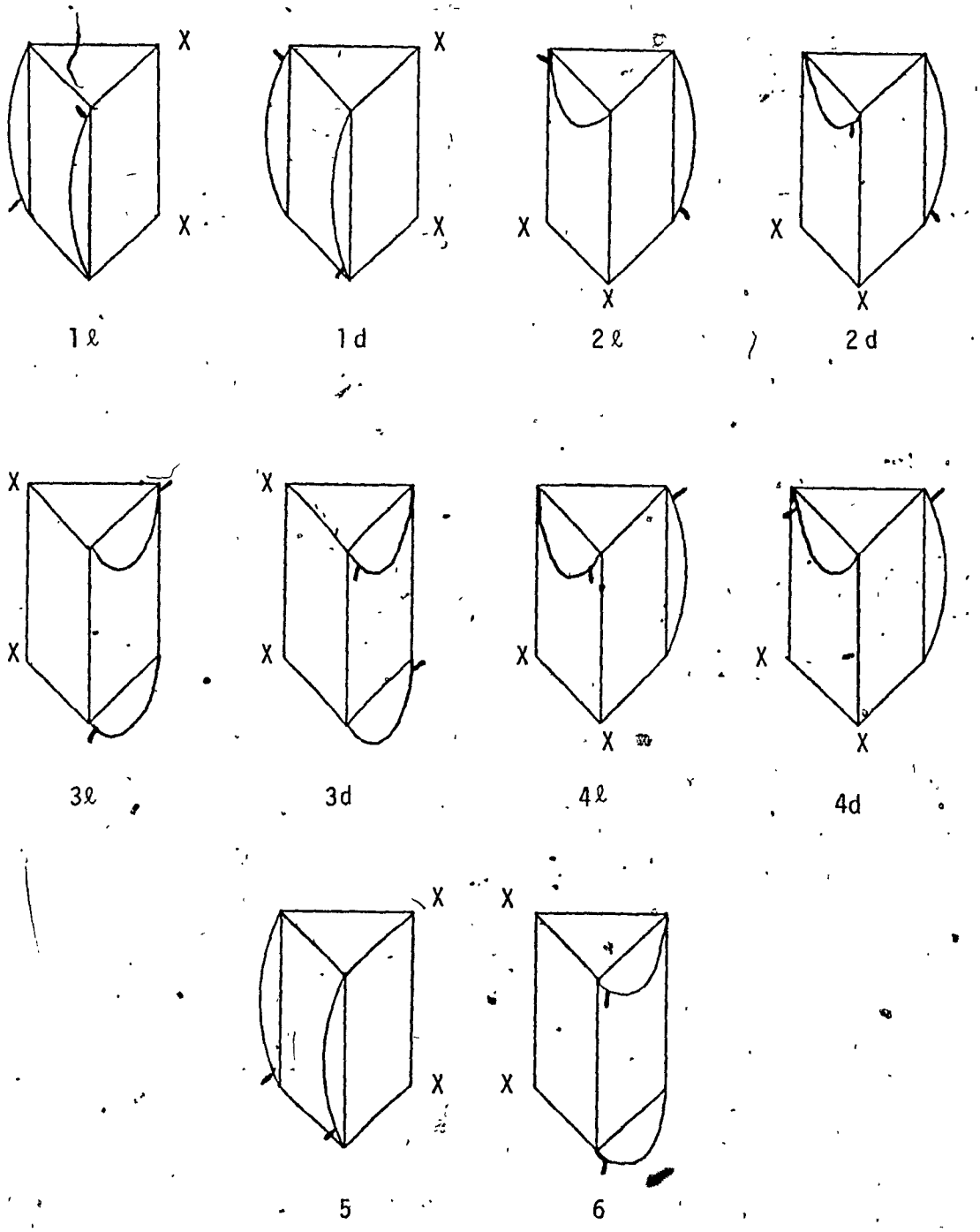

Figure 20.- Labeling and illustration of all possible trigonal prismatic transition states obtained through a twist mechanism about the four imaginary C_3 axes of the three cis-X_2 diastereomers of a cis-$M(AB)_2X_2$ complex.

Table XVI

Transition States and Diastereomer Distributions Obtained by a Twist-Mechanism for a cis-$M(AB)_2X_2$ Complex and Assignment of Averaging Sets to Physical Processes

Initial Isomer[a]	Rotation Axis[b]	Transition State[c]	Product	Averaging Set[e]
c,c,c-Λ(Δ)	i	5 (5)	c,c,c-$\Delta_2(\Lambda_2)$[d]	A_7''
	i'	4d(4ℓ)	c,c,t-Δ(Λ)	A_9''
	i"[f]	6 (6)	c,c,c-$\Delta_4(\Lambda_4)$	A_{10}''
	i'''	2d(2ℓ)	c,t,c-Δ(Λ)	A_9''
c,c,t-Λ(Δ)	i	1ℓ(1d)	c,t,c-Δ(Λ)	A_7''
	i'	4ℓ(4d)	c,c,c-Δ(Λ)	A_9''
	i"[g]	3d(3ℓ)	c,t,c-Δ(Λ)	A_{10}''
	i'''	4ℓ(4d)	c,c,c-Δ(Λ)	A_9''
c,t,c-Λ(Δ)	i	1d(1ℓ)	c,c,t-Δ(Λ)	A_7''
	i'	2ℓ(2d)	c,c,c-Δ(Λ)	A_9''
	i"[g]	3ℓ(3d)	c,c,t-Δ(Λ)	A_{10}''
	i'''	2ℓ(2d)	c,c,c-Δ(Λ)	A_9''

[a]The symbols c and t refer to cis and trans, respectively; [b]For definition of rotation axes, see Figure 19a; [c]For specification of transition states, see Figure 20; [d]For scrambling patterns for c,c,c-Δ(Λ) ↔ c,c,c-Δ(Λ) rearrangements, see Table VIII; [e]Averaging sets A_i'' are defined in Table IX; [f]Rotation about this axis only provides a path for the formation of the trans,trans,trans diastereomer; [g]Rotation about this axis only provides a path for the formation of the trans,cis,cis diastereomer.

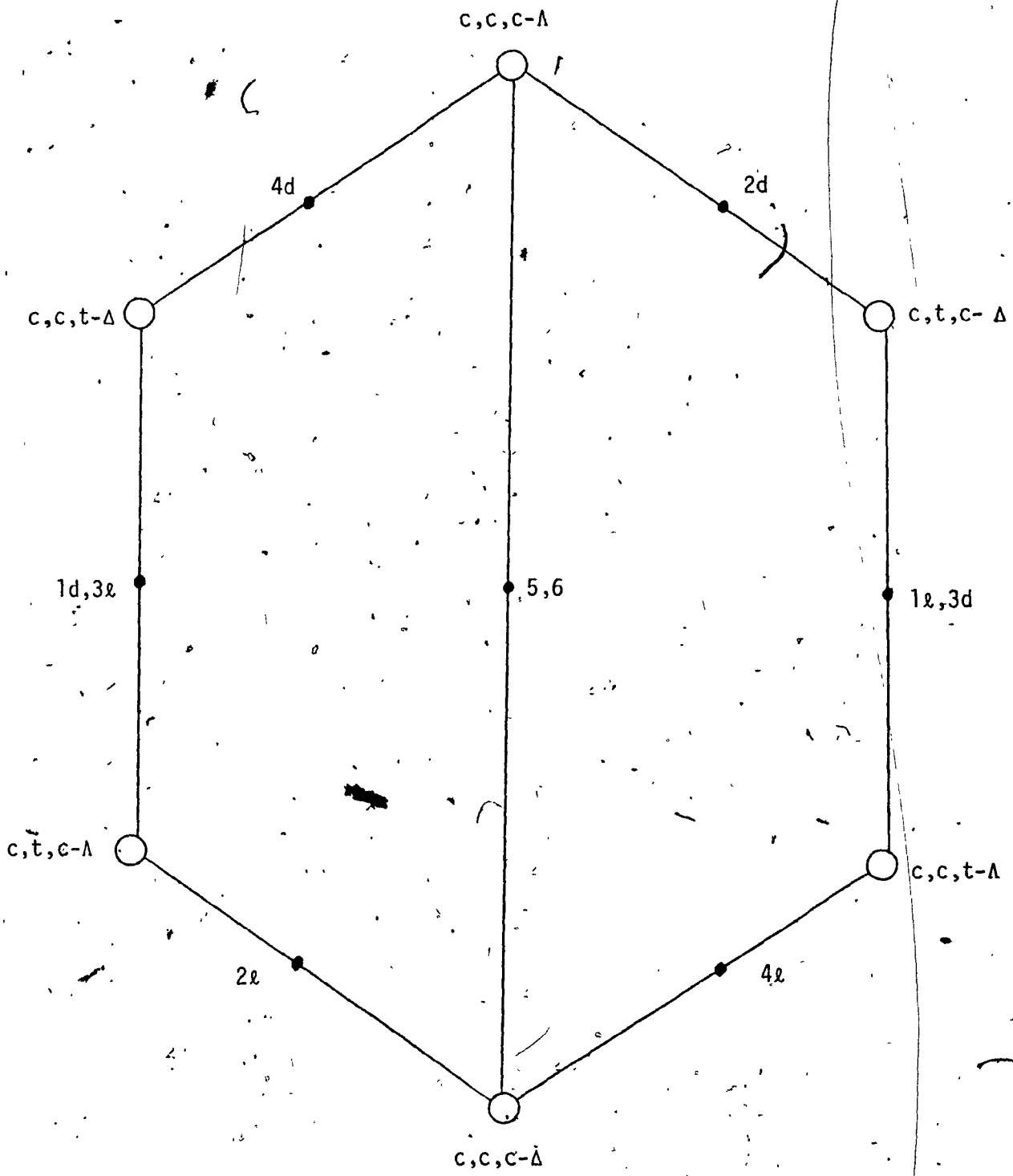

Figure 21.- Topological correlation diagram for interconversions amongst the three cis-X_2 diastereomers of a cis-$M(AB)_2X_2$ complex proceeding via twist motions about the four octahedral face axes of each isomer. Intermediates are defined in Figure 20.

Rupture of a metal-ligand bond may result in the formation of idealized five-coordinate TBP and SP intermediates, with the dangling ligand in an axial or equatorial position. As before, metal-X bond rupture is not permitted. The TBP intermediates are considered first.

Rupture of one metal-ligand bond will give rise to a TBP-axial and TBP-equatorial intermediate. All possible TBP intermediates may be generated by rupture of the nonequivalent bonds in the three cis-X_2 diastereomers (cf. Figure 6 for labeling of nonequivalent bonds). There are a total of sixteen TBP intermediates (8 axial, 8 equatorial) including four achiral and six enantiomeric dℓ pairs. Transition states are illustrated in Figure 22 and labeled according to the designations used by Pignolet and co-workers (28). Four pairs (12dℓ, 13dℓ, 14dℓ, and 15dℓ) are nonfunctional with respect to inversion of the parent diastereomer but do result in diastereomerization, while four other transition states (4, 5, 7, 8) are active in enantiomerization but inactive in diastereomerization. Products obtained by reattachment of the dangling ligand in the equatorial plane are set out in Table XVII. All possible interconversions between cis-X_2 isomers via TBP intermediates are summarized in the topological correlation diagram presented in Figure 23. The only interconversions not allowed by the TBP mechanism are:

$$\text{cis,cis,trans-}\Delta(\Lambda) \leftrightarrow \text{cis,trans,cis-}\Lambda(\Delta)$$

The TBP-axial intermediates 4, 5, 7, and 8 are also capable of forming trans-X_2 diastereomers on reattachment of the dangling ligand.

Square pyramidal intermediates obtained from the rupture of nonequivalent bonds in the three cis-X_2 isomers are given in Figure 24 and

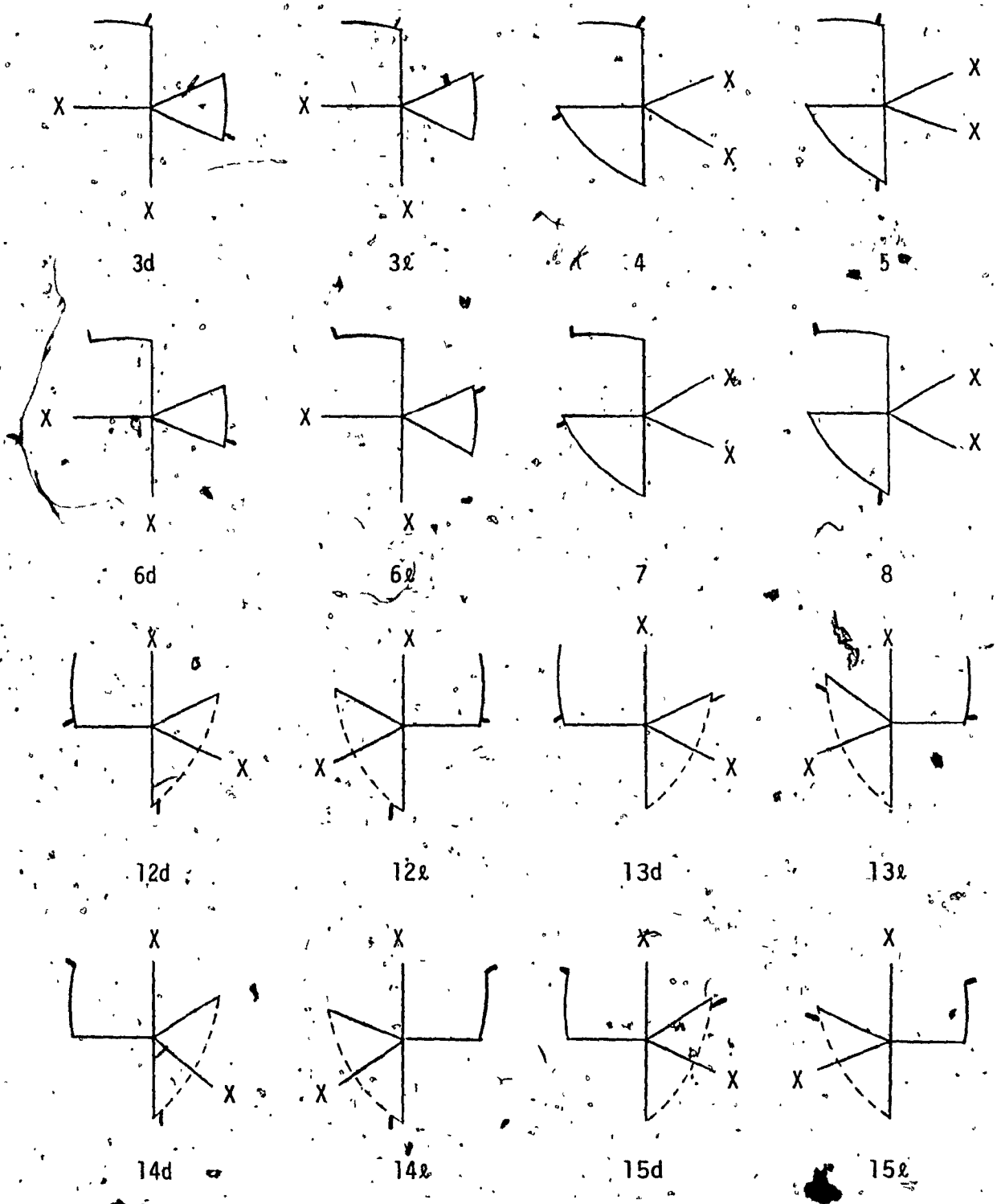

Figure 22.- Possible TBP-axial and -equatorial intermediates arising from rupture of nonequivalent metal-chelate bonds within the three cis-X_2 isomers of a cis-$M(AB)_2X_2$ complex.

Table XVII

Intermediates and Fates of the Diastereomers of a cis-$M(AB)_2X_2$ Complex Undergoing Rearrangement via a Bond Rupture Mechanism through Trigonal Bipyramidal-Axial and -equatorial Intermediates and Assignment of Averaging Sets to Physical Processes

Initial Isomer[a]	Rupture of Bond[b]	Intermediate[c]	Product	Averaging Set[e,f,g]
(A) TBP-axial				
c,c,c-Λ(Δ)	a	4 (4)	c,c,c-$\Delta_3(\Lambda_3)$[d]	A_8''
	b	8 (8)	c,c,c-$\Delta_3(\Lambda_3)$	A_8''
	c	6ℓ (6d)	c,t,c-Δ(Λ)	A_9''
	d	3d (3ℓ)	c,c,t-Δ(Λ)	A_9''
c,t,c-Λ(Δ)	a	5 (5)	c,t,c-Δ(Λ)	A_7''
	b	6d (6ℓ)	c,c,c-Δ(Λ)	A_9''
c,c,t-Λ(Δ)	a	7 (7)	c,c,t-Δ(Λ)	A_7''
	b	3ℓ (3d)	c,c,c-Δ(Λ)	A_9''
(B) TBP-equatorial				
c,c,c-Λ(Δ)	a	12d (12ℓ)	c,c,t-Λ(Δ)	A_4''
	b	15d (15ℓ)	c,t,c-Λ(Δ)	A_4''
	c	14d (14ℓ)	c,c,t-Λ(Δ)	A_4''
	d	13d (13ℓ)	c,t,c-Λ(Δ)	A_4''
c,t,c-Λ(Δ)	a	13d (13ℓ)	c,c,c-Λ(Δ)	A_4''
	b	15d (15ℓ)	c,c,c-Λ(Δ)	A_4''
c,c,t-Λ(Δ)	a	14d (14ℓ)	c,c,c-Λ(Δ)	A_4''
	b	12d (12ℓ)	c,c,c-Λ(Δ)	A_4''

[a] The symbols c and t refer to cis and trans, respectively; [b] Nonequivalent metal-ligand bonds defined in Figure 6; [c] Intermediates shown in Figure 22; [d] Scrambling patterns defined in Table VIII; [e] Averaging sets defined in Table IX; [f] This intermediate may generate the t,c,c diastereomer as product; [g] This intermediate may generate the t,t,t diastereomer as product.

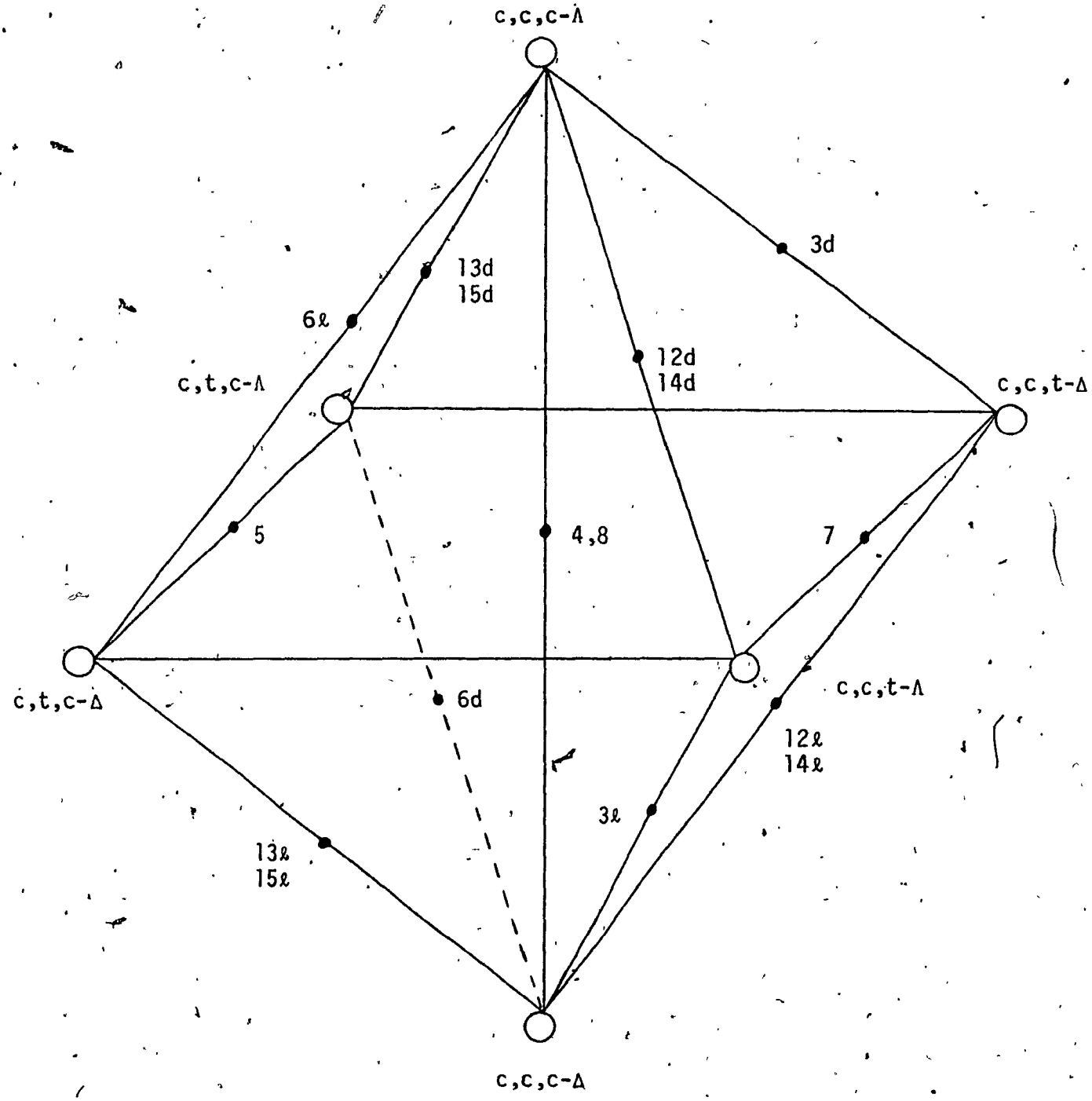

Figure 23.- Topological correlation diagram for interconversions amongst the three cis-X_2 diastereomers of a cis-$M(AB)_2X_2$ complex proceeding via a bond rupture mechanism utilizing trigonal bipyramidal intermediates, which are defined in Figure 22.

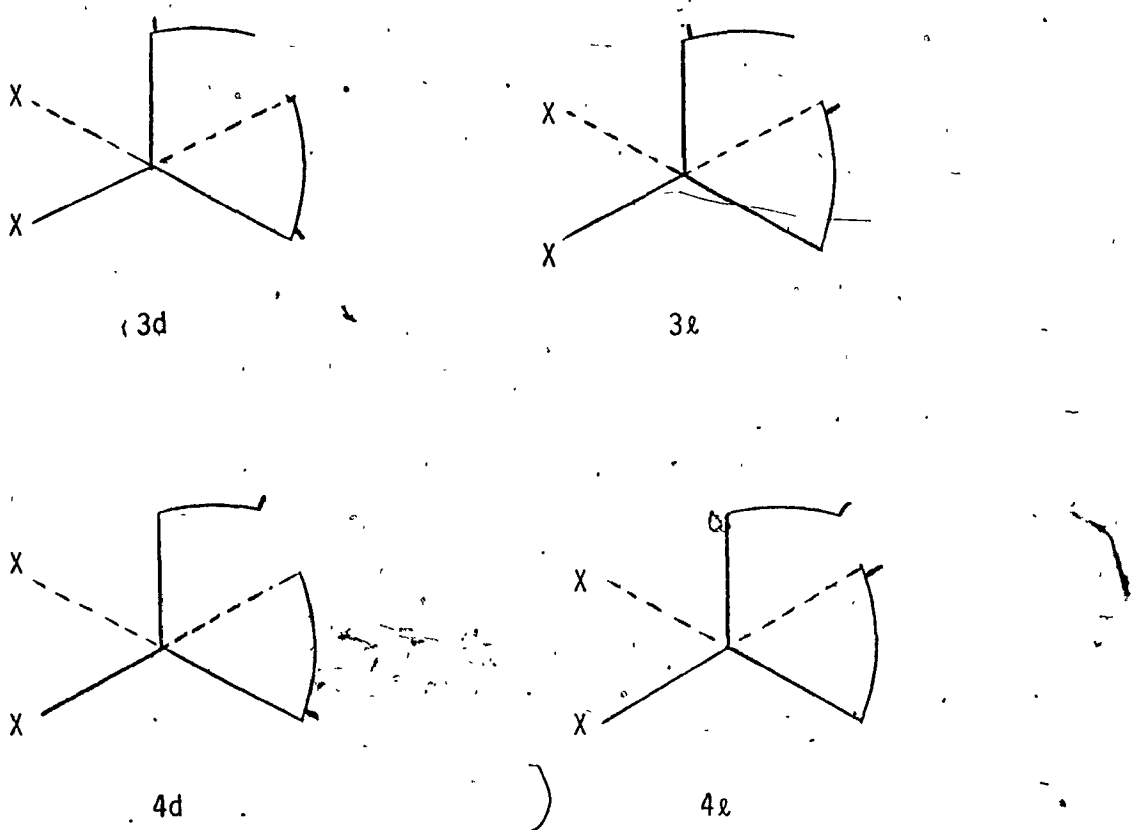

Figure 24.- The four SP-axial transition states formed by the primary process after rupture of the nonequivalent bonds in the three cis-X_2 diastereomers of a cis-$M(AB)_2X_2$ complex.

and consist of two enantiomeric pairs. Only SP-axial intermediates are shown as SP-basal transition states are kinetically equivalent to those of the TBP-equatorial type (21), previously considered. SP-intermediates are formed and decay to products via the primary process. Table XVIII lists product distributions for SP-axial transition states resulting from rupture of nonequivalent bonds in the three cis-X_2 diastereomers. All possible interconversions between these cis-X_2 diastereomers via SP-axial intermediates are summarized in the topological correlation diagram of Figure 25. The only interconversions not allowed by this mechanism are:

Table XVIII

Intermediates and Fates of the Diastereomers of a cis-$M(AB)_2X_2$ Complex Undergoing Rearrangement via a Bond Rupture Mechanism through Square Pyramidal-Axial Intermediates (Primary Process) and Assignment of Averaging Sets to Physical Processes

Initial Isomer[a]	Rupture of Bond[b]	Intermediate[c]	Product	Averaging Set[e]
c,c,c-$\Lambda(\Delta)$	a	3ℓ (3d)	c,c,c-$\Lambda_1(\Delta_1)$[d]	A_1''
			c,c,t-$\Lambda(\Delta)$	A_4''
			c,c,c-$\Delta_2(\Lambda_2)$	A_7''
			c,t,c-$\Delta(\Lambda)$	A_9''
	b	4d (4ℓ)	c,c,c-$\Lambda_1(\Delta_1)$	A_1''
			c,t,c-$\Lambda(\Delta)$	A_4''
			c,c,c-$\Delta_2(\Lambda_2)$	A_7''
			c,c,t-$\Delta(\Lambda)$	A_9''
	c	4ℓ (4d)	c,c,c-$\Lambda_1(\Delta_1)$	A_1''
			c,c,t-$\Lambda(\Delta)$	A_4''
			c,c,c-$\Delta_2(\Lambda_2)$	A_7''
			c,t,c-$\Delta(\Lambda)$	A_9''
	d	3d (3ℓ)	c,c,c-$\Lambda_1(\Delta_1)$	A_1''
			c,t,c-$\Lambda(\Delta)$	A_4''
			c,c,c-$\Delta_2(\Lambda_2)$	A_7''
			c,c,t-$\Delta(\Lambda)$	A_9''
c,c,t-$\Lambda(\Delta)$	a	4ℓ (4d)	c,c,t-$\Lambda(\Delta)$	A_1''
			c,c,c-$\Lambda(\Delta)$	A_4''
			c,t,c-$\Delta(\Lambda)$	A_7''
			c,c,c-$\Delta(\Lambda)$	A_9''
	b	3ℓ (3d)	c,c,t-$\Lambda(\Delta)$	A_1''
			c,c,c-$\Lambda(\Delta)$	A_4''

Table XVIII (continued)

			c,t,c-Δ(Λ)	A_7''
			c,c,c-Δ(Λ)	A_9''
c,t,c-Λ(Δ)	a	3d (3ℓ)	c,t,c-Λ(Δ)	A_1''
			c,c,c-Λ(Δ)	A_4''
			c,c,t-Δ(Λ)	A_7''
			c,c,c-Δ(Λ)	A_9''
	b	4d (4ℓ)	c,t,c-Λ(Δ)	A_1''
			c,c,c-Λ(Δ)	A_4''
			c,c,t-Δ(Λ)	A_7''
			c,c,c-Δ(Λ)	A_9''

[a]The symbols c and t refer to cis and trans, respectively; [b]Nonequivalent bonds are defined in Figure 6; [c]For specification of intermediates, see Figure 24; [d]For scrambling patterns for c,c,c-Δ(Λ)↔c,c,c-Δ(Λ) rearrangements, see Table VIII; [e]Averaging sets are defined in Table IX.

mechanism are:

cis,trans,cis-Δ(Λ) ↔ cis,trans,cis-Λ(Δ)

cis,cis,trans-Λ(Δ) ↔ cis,cis,trans-Δ(Λ)

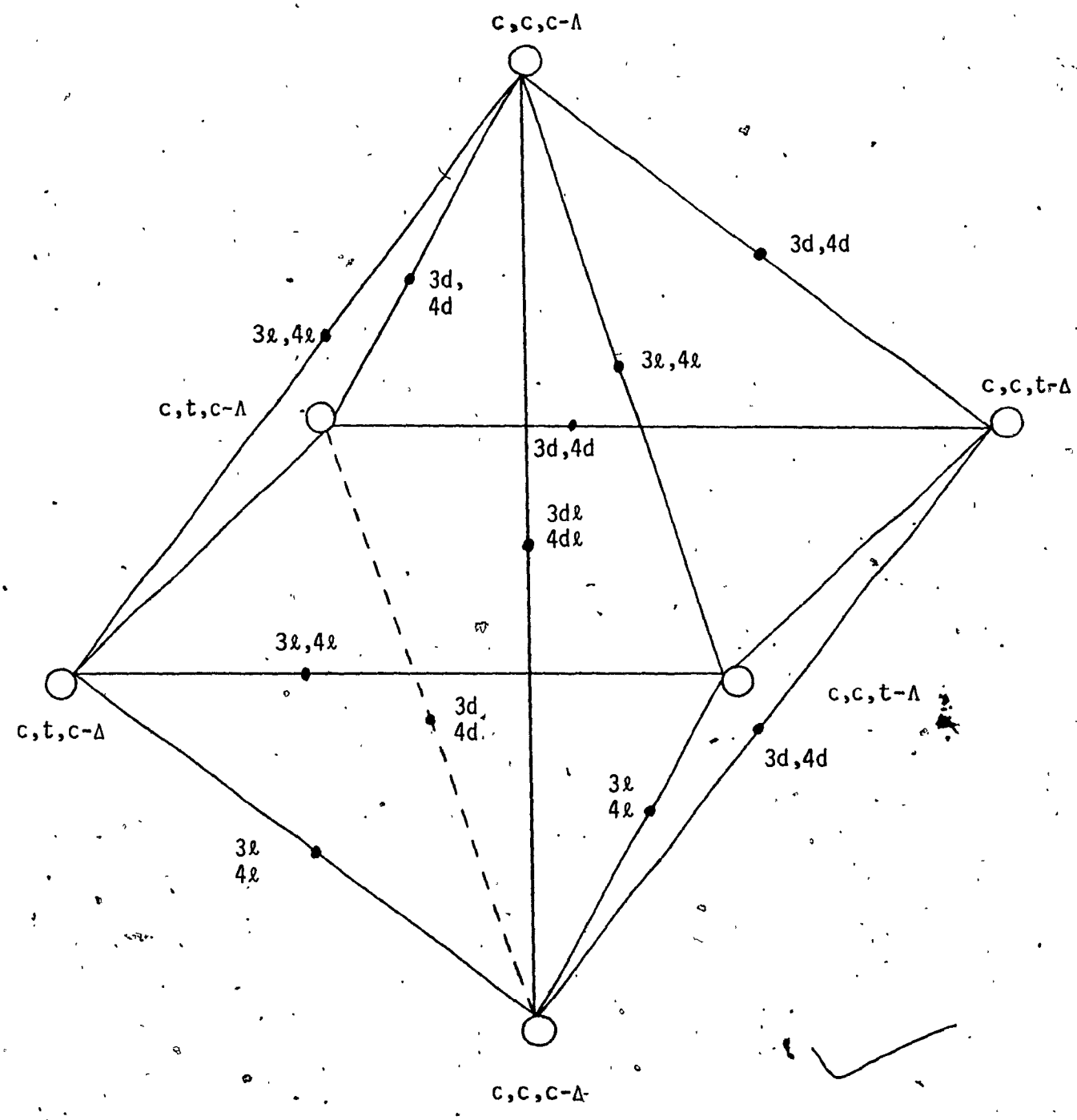

Figure 25.- Topological correlation diagram for interconversions amongst the three cis-X_2 diastereomers of a cis-$M(AB)_2X_2$ complex proceeding via a bond rupture mechanism utilizing square pyramidal intermediates, which are defined in Figure 24.

B. Synthesis and Characterization of Group IV Chelate Complexes

1. Dihalobis(β-diketonato)metal(IV) Complexes

The reaction of a free β-diketone (Hdik) with anhydrous group IV metal halides has proven to be a useful general synthetic route to dihalobis(β-diketonato)metal(IV) complexes, $M(dik)_2X_2$, according to equation [3]. Such reactions have been used to prepare numerous complexes

$$TiX_4 + 2Hdik \longrightarrow M(dik)_2X_2 + 2HX \qquad [3]$$

of the type $M(acac)_2X_2$ [M = Zr(IV),Hf(IV); X = Cl,Br] (52,53), $Ti(dik)_2X_2$ [dik = acac,bzac,bzbz,3-CH_3-acac,dpm; X = Cl,Br] (54-56,114), $Ti(acac)_2I_2$ (57), $Ti(dik)_2F_2$ [dik = acac,bzac,bzbz,3-CH_3-acac,dpm,tfac,hfac,bztf,thtf] (54-56, 58), $Si(acac)_2Cl_2$ (115), $Sn(dik)_2Cl_2$ [dik = acac,bzac,dpm] (59,60), and $Ge(dik)_2Cl_2$ [dik = acac,bzac,dpm,dhd] (60,116,117). Not limited to group IV metal halides, this synthetic route has also been used to prepare $M(dik)_2X_2$ complexes of V(IV) (118,119), Mo(IV) (120), and W(IV) (120).

The following complexes reported in this thesis were prepared by the direct reaction of the β-diketone with the appropriate metal halide: $Ti(dibm)_2X_2$ [X = F,Cl,br], $M(dibm)_2Cl_2$ [M = Sn(IV),Ge(IV)], $Ti(dpm)_2X_2$ [X = F,Cl,Br], $M(tibm)_2Cl_2$ [M = Ti(IV),Sn(IV)], $Ti(tdh)_2Cl_2$, and $Ti(3\text{-}^{i}Pr\text{-}acac)_2Cl_2$. The $Ti(dpm)_2F_2$ (58,71) and $Ti(dpm)_2Cl_2$ (114,119) complexes have been reported previously.

These new compounds were characterized by elemental analysis (except for $Ti(tdh)_2Cl_2$ and $Sn(tibm)_2Cl_2$), melting point, and proton nmr and infrared spectroscopy. In all cases, satisfactory agreement was obtained between experimental analyses and theoretical values for the $M(dik)_2X_2$ formulation.

Infrared spectra of these complexes (as nujol mulls) showed no bands in the 1800 - 1600 cm^{-1} region and in the 4000 - 3000 cm^{-1} region, thus assuring, respectively, that all diketonate carbonyl groups are coordinated to the metal (121,122) and that no contamination of the samples had occurred. Proton nmr spectra also confirmed that all chelating ligands were coordinated. Addition of free ligand to a solution of the complex resulted in separate resonances for free and complexed ligands.

The titanium(IV) complexes reported in this section are subject to hydrolysis, especially in solution. The relative ease of hydrolysis for complexes having the same diketonate ligand appears to increase in the order X = F < Cl < Br. The Sn(IV) and Ge(IV) complexes appear to be air and moisture sensitive; however, they were nevertheless prepared and handled under anhydrous, inert atmospheric conditions.

Previous work (60,71,74) on $M(dik)_2X_2$ [M = Ti(IV), Sn(IV), Ge(IV); X = halogen] complexes has established that these complexes exist as monomeric, six-coordinate nonelectrolytes in slightly polar organic solvents. The complexes reported in this section are expected to have an analagous formulation.

2. Bis(alkoxy)- and Bis(phenoxy)bis(chelate)titanium(IV) Complexes

The reaction of acetylacetone with titanium(IV) alkoxides results in the formation of bis(alkoxy)bis(acetylacetonato)titanium(IV) complexes (57,61,86,123-125), according to equation [4]. This reaction

$$Ti(OR)_4 + 2\ Hacac \longrightarrow Ti(acac)_2(OR)_2 + 2\ ROH \qquad [4]$$

has proven successful in cases where R = CH_3 (61,64,124), C_2H_5 (57,61,64,

123,124), i-C_3H_7 (61,64,123,124), n-C_4H_9 (61,124), t-C_4H_9 (61,124), and CH_2CF_3 (61,124). Several of these complexes may also be synthesized by replacement of the methoxy groups in $Ti(acac)_2(OCH_3)_2$ with the appropriate free alcohol (64,123). Complexes of the type $Ti(dik)_2(OC_2H_5)_2$ are known for cases where dik = tfac (57,71), hfac (57,71), bzac (74), and bzbz (74). Harrod and Taylor (62,126) recently reported the preparation of $Ti(chelate)_2(OR)_2$ [chelate = ox,quin; R = i-C_3H_7,n-C_4H_9] complexes in a reaction analagous to equation [4].

Recently, it has been reported (62,126) that alkoxy groups in $Ti(chelate)_2(OR)_2$ complexes are easily replaced with phenols, according to equation [5]. Taylor (126) reports the preparation and characterization

$$Ti(chelate)_2(OR)_2 + 2\ phenol \longrightarrow Ti(chelate)_2(phenoxy)_2 + 2\ ROH \qquad [5]$$

of an extensive series of substituted phenoxy complexes of the type $Ti(chelate)_2(OR)_2$ [R = aryl] in which chelate = acac, ox, and quin.

Some complexes studied in this thesis containing phenoxy groups were kindly provided by Drs. J. F. Harrod and K. R. Taylor of McGill University.

The following complexes were either prepared following Taylor's procedure (126) or provided by Drs. Harrod and Taylor but many had not been completely characterized (126): $Ti(ox)_2(O^iC_3H_7)_2$, $Ti(acac)_2(2\text{-}ClC_6H_4O)_2$, $Ti(acac)_2(2\text{-}IC_6H_4O)_2$, $Ti(acac)_2(4\text{-}ClC_6H_4O)_2$, $Ti(acac)_2(2,6\text{-}Cl_2C_6H_3O)_2$, and $Ti(acac)_2(2\text{-}^iPrC_6H_4O)_2$. Satisfactory carbon and hydrogen analyses were obtained for these complexes.

The following complexes, prepared according to equation [5], are new compounds and not previously reported: $Ti(acac)_2(3\text{-}CH_3C_6H_4O)_2$, $Ti(acac)_2(4\text{-}^iPrC_6H_4O)_2$, $Ti(acac)_2(2\text{-}(C_6H_5)C_6H_4O)_2$, and $Ti(acac)_2$-

$(2\text{-}(OCH_2C_6H_5)C_6H_4O)_2$. Carbon and hydrogen elemental analyses are in excellent agreement with the proposed formulation.

The $Ti(bzac)_2(O^iC_3H_7)_2$ and $Ti(bzac)_2(2,6\text{-}^iPr_2C_6H_3O)_2$ complexes, prepared according to equations [4] and [5], respectively, are new compounds and were characterized only by spectroscopic techniques and not by elemental analysis.

Before investigating the bis(alkoxy) and bis(phenoxy) complexes, their purity was verified by melting point, infrared and proton nmr spectroscopy, and elemental analysis (where appropriate). Infrared spectra were carefully checked in the 1800 - 1600 cm^{-1} and 4000 - 3000 cm^{-1} regions to verify that all diketonate carbonyl groups were coordinated, that no free ligand or phenol was occluded, and that no water and/or hydrolysis product was present. For a number of the bis(acac) complexes, acac methyl resonances in the pmr spectra were broad at room temperature and could easily mask any resonances from impurities. Also, the chemical shifts of the free and complexed acac ligands in most bis(phenoxy) complexes were so similar that proton nmr spectroscopy could not detect the presence of any free ligand as an impurity.

In general, the bis(phenoxy) complexes are less air- and moisture-sensitive than corresponding bis(alkoxy) complexes, and for the same monodentate ligand, stability appears to decrease in the order quin ~ ox > acac. All complexes are subject to some degree of hydrolysis and therefore were prepared and handled under anhydrous conditions. The acac complexes are very soluble in common organic solvents; the ox and quin complexes are quite insoluble. As has been previously noted (74) for the $Ti(dik)_2(OC_2H_5)_2$ [dik = bzac,bzbz] complexes, the $Ti(bzac)_2(O^iC_3H_7)_2$ complex underwent photochemical decomposition to form a dark green solid,

which has a pmr spectrum identical to that of the pure complex.

Molecular weight and conductance data for a number of $Ti(chelate)_2(OR)_2$ [chelate = acac,ox,quin; R = alkyl, aryl] complexes demonstrates that these complexes are monomeric, six-coordinate non-electrolytes in slightly polar organic solvents (126).

3. Mixed Haloalkoxy- and Halophenoxybis(β-diketonato)-titanium(IV) Complexes.

Although mixed haloalkoxybis(acetylacetonato)titanium(IV) complexes have been generated in solution by ligand exchange reactions and detected by proton nmr spectroscopy (57,71), it is only recently that such mixed complexes have been isolated (70). These complexes may be prepared by the reaction of the $[Ti(acac)Cl_3]_2$ dimer (127) or the $Ti(acac)_2Cl_2$ complex with a 1:1 mixture of the appropriate alcohol and pyridine, according to equations [6] and [7], respectively.

$$[Ti(acac)Cl_3]_2 + 2\,ROH + 2\,C_5H_5N \longrightarrow Ti(acac)_2Cl(OR) + [C_5H_5NH]_2[Ti(OR)Cl_5] \qquad [6]$$

$$Ti(acac)_2Cl_2 + ROH + C_5H_5N \longrightarrow [C_5H_5NHCl] + Ti(acac)_2Cl(OR) \qquad [7]$$

While attempting to form dimeric complexes via the reaction of $Ti(acac)_2X_2$ [X = F,Cl,Br] complexes with $Ti(O^iC_3H_7)_4$, it was found that the main product isolated was the mixed haloisopropoxy complex, $Ti(acac)_2X(O^iC_3H_7)$. When X = F, a pale white solid was isolated but proved to be so unstable that it decomposed within minutes of isolation and was not characterized. The $Ti(acac)_2Cl(O^iC_3H_7)$ complex was identified

by comparison with its literature properties (70). Similar physical properties, including variable temperature nmr spectra, for the product of the reaction of $Ti(acac)_2Br_2$ with $Ti(O^iC_3H_7)_4$, demonstrates that the $Ti(acac)_2Br(O^iC_3H_7)$ complex was isolated (cf. Section III-C-2(c)). This synthetic route appears to be simpler than the use of reactions [6] and [7], although its generality was not investigated. These $Ti(acac)_2Cl(OR)$ complexes have recently been found to act as efficient catalysts for the alkylation of alkenols (128).

The mixed chloromethoxy complex, $Ti(dibm)_2Cl(OCH_3)$, was prepared from the reaction of $Ti(dibm)_2Cl_2$ with a methanol/pyridine mixture according to equation [7]. A low melting orange solid was isolated from this reaction. The product was characterized by melting point and infrared and proton nmr spectroscopy.

The isopropoxy group in the $Ti(acac)_2Cl(O^iC_3H_7)$ complex proved to be labile and was readily replaced on addition of 2,6-di-isopropylphenol to form the $Ti(acac)_2Cl(2,6\text{-}^iPr_2C_6H_3O)$ complex via a reaction analagous to equation [5]. This complex was completely characterized by melting point, infrared and proton nmr spectroscopy, and elemental analysis.

4. Cationic Tris(β-diketonate)metal(IV) Complexes

A variety of cationic tris(β-diketonato)metal(IV) complexes, $[M(dik)_3]^+X^-$ [$X = SbCl_6^-, FeCl_4^-$, etc.] of titanium(IV) (30,56, 129), germanium(IV) (129-131), silicon(IV) (129,130,132,133), and vanadium(IV) (118,119) have been reported in recent years. The most convenient synthetic route involves the reaction of the $M(dik)_2Cl_2$ complex with a suitable Lewis acid, according to equation [8]. A different

$$3\ M(dik)_2Cl_2 + 2\ M'Cl_x \longrightarrow 2\ [M(dik)_3]M'Cl_{x+1} + MCl_2 \qquad [8]$$

e.g.; M = Ti(IV); dik = acac; M' = Sb(V); x = 5; ref. (129)

synthetic route is necessary to prepare $[Si(acac)_3]X$ complexes. The direct reaction of acetylacetone with silicon(IV) chloride yields (130) $[Si(acac)_3]HCl_2$ (and small amounts of the unstable $Si(acac)_2Cl_2$ (115) complex) which readily loses one molecule of hydrogen chloride to form the $[Si(acac)_3]Cl$ complex (130), according to equation [9].

$$SiCl_4 + 3\ Hacac \longrightarrow [Si(acac)_3]HCl_2 + 2\ HCl$$
$$\Big\downarrow -HCl \qquad [9]$$
$$[Si(acac)_3]Cl$$

The $[Ti(dibm)_3]SbCl_6$, $[Ge(dibm)_3]SbCl_6$, and $[Si(dibm)_3]Cl$ complexes were prepared according to the appropriate reaction outlined in equations [8] and [9]. Only the titanium(IV) complex was completely characterized by elemental analysis, melting point, and infrared and proton nmr spectroscopy. The Si(IV) and Ge(IV) complexes were identified by their characteristic proton nmr spectra and were not further characterized. The relative order of stability appears to be Si(IV) > Ti(IV) > Ge(IV), with the germanium(IV) complex exhibiting extensive decomposition after one day at room temperature under anhydrous conditions.

5. Titanium(IV) Complexes with 1,2-Benzenediols

Titanium(IV) complexes with chelating diols appear to be relatively scarce. Bradley and Holloway (61) reported the preparation of the neopentyl glycollate derivative $Ti(acac)_2(OCH_2C(CH_3)_2CH_2O)$ from the reaction of the glycol with $Ti(acac)_2(OCH_3)_2$.

1,2-Benzenediols present an opportunity to prepare chelated $M(AA)_2(BB)$-type complexes of titanium(IV) analagous to the bis(phenoxy) complexes of Section III-B2. The reaction of catechol with titanium(IV) chloride (134) and alkoxides (75) have been reported. A dicyclopentadienyltitanium(IV) derivative of catechol is also known (135). Recently, tris(1,2-benzenedithiolato)titanium(IV) anions have been reported (136).

Potentially chelating aromatic diols reacted rapidly and cleanly with $Ti(acac)_2(O^iC_3H_7)_2$ to yield the desired $Ti(acac)_2$(1,2-benzenediolato) complexes, according to equation [10]. Benzenediols studied were

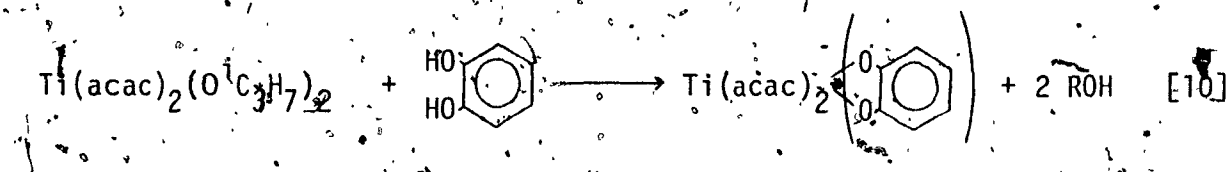

$$Ti(acac)_2(O^iC_3H_7)_2 + \text{(HO)}_2\text{C}_6\text{H}_4 \longrightarrow Ti(acac)_2(\text{O}_2\text{C}_6\text{H}_4) + 2\ ROH \qquad [10]$$

catechol, 3,6-diisopropylcatechol, and 3,5-diisopropylcatechol with acac, bzac, and quin bidentate ligands completing the coordination sphere.

The parent member of the series, $Ti(acac)_2(cat)$, was found to be identical with the material reported by Dahl and Block (75), which they found to be monomeric and a nonelectrolyte, thereby supporting the above formulation.

These complexes were not subjected to an intensive investigation; however, characterization was achieved by melting point and infrared and proton nmr spectra. Satisfactory carbon and hydrogen analyses were obtained for $Ti(acac)_2(3,6\text{-}{}^i Pr_2cat)$ and $Ti(bzac)_2(cat)$ but not for the product believed to be $Ti(quin)_2(3,6\text{-}{}^i Pr_2cat)$.

C. Stereochemistry and Lability of Group IV Chelate Complexes

1. The $M(AA)_2X_2$ System

a. Introduction

Complexes of the type $M(AA)_2X_2$, where AA and X represent, respectively, symmetrical bidentate and monodentate ligands, may exist in two diastereomeric forms having either cis or trans X groups, as shown in Figure 26. The cis form is enantiomeric. In the cis isomer, the terminal R

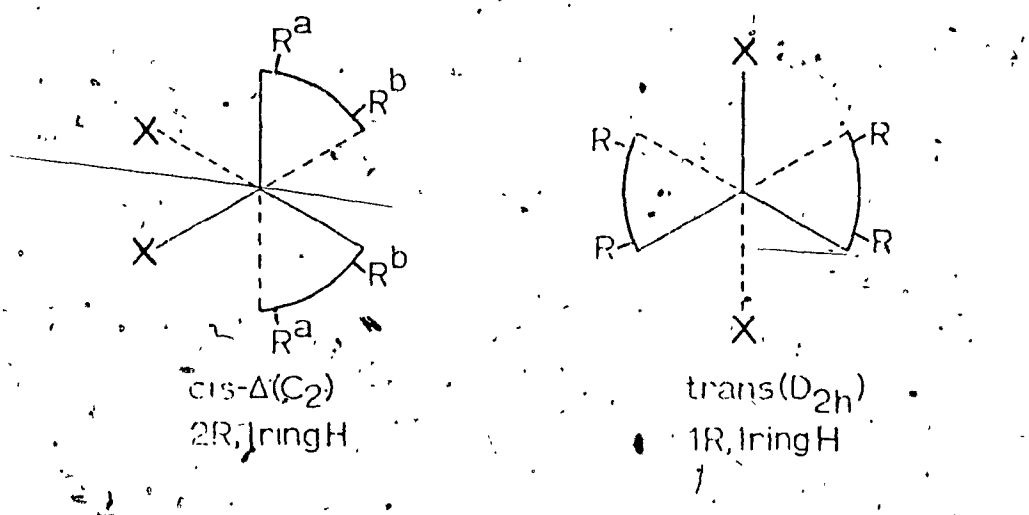

Figure 26.- Possible isomers for a $M(AA)_2X_2$ complex, Letter superscripts label nonequivalent environments. Expected signal multiplicities are indicated below each diastereomer.

groups of the bidentate ligands are symmetry nonequivalent, so that two R group resonances should be observed in the nmr spectrum of this isomer; a single R group resonance is expected for the trans diastereomer. This difference in signal multiplicity may be used as a method of distinguishing between cis and trans diastereomers.

However, caution must be exercised when using this criterion

since the failure to resolve two terminal group resonances for a $M(AA)_2X_2$ complex does not preclude a cis structure. Several reasons, such as rapid intra- or intermolecular exchange processes and/or accidental chemical shift degeneracy might cause the nonequivalent terminal groups to give rise to a single resonance in the nmr spectrum.

A single acac methyl resonance is observed (52,53) for $M(acac)_2X_2$ [M = Zr(IV),Hf(IV); X = halogen] complexes even at temperatures as low as -108°; however, infrared spectroscopic evidence (52,53) and dipole moment studies (137) support the polar cis structure. The corresponding $Zr(acac)_2(OR)_2$ [R = $t\text{-}C_4H_9$,$i\text{-}C_3H_7$,C_2H_5] complexes reveal two acac methyl resonances at low temperature, indicating that these complexes possess the cis structure in solution.

With the exception of the $Ti(acac)_2I_2$ complex (57), which exists in solution as a mixture of cis and trans diastereomers, all $Ti(chelate)_2X_2$ [chelate = acac; X = F,Cl,Br,OR,OC_6H_5,NCO,NCS; chelate = dpm; X = NCO,NCS,Cl; chelate = 3-CH_3-acac; X = F,Cl,Br; chelate = dmm, tmm; X = OCH_3,$N(CH_3)_2$] complexes (54,56,61,62,114,124,126,138) that have been thoroughly studied in solution adopt the cis geometry, as shown by infrared spectra (61,71,114), variable temperature nmr spectroscopy (54, 56,61,62,114,126,138), and dipole moment measurements (126,137). In the solid state, $Ti(acac)_2(2,6\text{-}{}^{i}Pr_2C_6H_3O)_2$ adopts the cis geometry (139) while $Ti(acac)_2Br_2$ and $Ti(acac)_2I_2$ may be exclusively trans in the solid state (119).

A recent study of $V(dpm)_2X_2$ [X = Cl,Br,NCO,NCS] complexes (118,119) illustrates the subtle factors affecting population of cis and trans geometries. When X = NCO,NCS, the complexes are cis in the solid state, but both complexes exhibit a cis-trans equilibrium in solution. For $V(dpm)_2Cl_2$, the concentration of the polar cis isomer increases with

increasing polarity of the solvent.

All known $Sn(dik)_2X_2$ [dik = acac,dpm; X = halogen] complexes have been shown to adopt the cis geometry in solution and in the solid state by a combination of infrared (59,60) and proton nmr (59,60) spectroscopy, dipole moment studies (137), and X-ray diffraction studies (140). However, when X is an alkyl or aryl group, the choice of stereochemistry appears to vary. Thus, $Sn(acac)_2(C_6H_5)_2$ is cis in solution (141,142) and in the solid state (143) while $Sn(acac)_2(CH_3)_2$ is trans in the solid state (144) and appears to be trans in solution (145) also; however, the solution structure is not unequivocal (142).

A number of dihalobis(β-diketonato)germanium(IV) complexes [dik = acac; X = Cl; dik = dpm; X = Cl,Br] are known (60,116) to exist in solution as an equilibrium mixture of cis and trans diastereomers. The $Ge(dik)_2Cl_2$ [dik = acac,dpm] complexes appear to be trans in the solid state; a fresh solution of these complexes contains only the trans isomer, which slowly isomerizes to an equilibrium mixture of cis and trans diastereomers (60,116). The $Ge(dpm)_2I_2$ complex appears to exist exclusively in the cis geometry (60).

To complete the group IVb complexes, $Si(acac)_2Cl_2$ appears to adopt only the trans configuration (115). $Si(acac)_2(CH_3COO)_2$ exists predominantly in the trans form in the solid state and freshly prepared solutions but isomerizes in solution to an equilibrium mixture of cis and trans diastereomers (146).

For every complex of Zr(IV), Hf(IV), Ti(IV), Sn(IV), and Ge(IV) which falls under the heading of this section, it has been found that the cis isomer is stereochemically nonrigid on the nmr time scale as a result of a rapid intramolecular rearrangement process which exchanges terminal groups on the bidentate ligands between the two symmetry

nonequivalent sites of the cis diastereomer (52-54,56-63,114,124-126, 138,142). This rearrangement process constitutes a two-site nmr exchange problem, for which a Total Line Shape (TLS) analysis, based on the solutions to the Bloch equations as provided by Gutowsky and Holm (17), yields kinetic parameters. A complete TLS analysis has yielded accurate kinetic data for a number of $M(dik)_2X_2$ [M = Ti(IV), dik = acac, X = F,Cl, Br,NCO; dik = dpm, X = Cl,NCO; M = Sn(IV), dik = acac,dpm, X = F,Cl,Br,I, dik = acac, X = C_6H_5; M = Ge(IV), dik = dpm, X = Cl,Br,I] complexes (54, 59,60,114,142). The $Ti(chelate)_2X_2$ [chelate = dmm,tmm; X = OCH_3,$N(CH_3)_2$] complexes have also been found to be stereochemically nonrigid and kinetic parameters have been reported (138). A less accurate approximate method has been used to gather kinetic data for $Ti(acac)_2(OR)_2$ [R = alkyl, aryl] complexes (61,62,124,126). A detailed comparison of the relative merits of TLS and approximate methods for extracting kinetic data from variable temperature nmr spectra is presented in Section III-C-1-c(ii).

Several groups have speculated on the mechanism for the configurational rearrangement processes occurring in cis-$M(AA)_2X_2$ complexes. Fay and Lowry (54) preferred a metal-oxygen bond rupture process via a five-coordinate intermediate for the rearrangement of $Ti(acac)_2X_2$ [X = F,Cl,Br] complexes. However, for the $Ti(acac)_2(OR)_2$ [R = alkyl] complexes, Bradley and Holloway (61) suggested a twist mechanism proceeding via idealized trigonal prismatic transition states. Harrod and Taylor (62) proposed that rearrangements of $Ti(acac)_2(OR)_2$ [R = aryl] complexes involves formation of a tightly bound ion-pair and that rearrangement occurs via migration of a phenoxide ion across the surface of the resulting five-coordinate cationic complex, followed by collapse of the ion-pair to a neutral six-coordinate species. Following

the rigorous analysis of rearrangements of $M(dik)_2X_2$ [M = Sn(IV),Ge(IV); dik = acac,dpm; X = halogen] complexes, Jones (60) concluded that the probable mechanism involves a metal-oxygen bond rupture process via a five-coordinate intermediate.

It is generally assumed that equilibration of terminal R groups in cis-$M(AA)_2X_2$ complexes occurs during the interconversions of enantiomers, although this has not been demonstrated experimentally. In fact, no such $\Delta \leftrightarrow \Lambda$ interconversion is necessary to explain terminal group exchange (vide infra, Section III-A-4b). While these stereochemically nonrigid molecules cannot be resolved into enantiomers, some of these complexes exhibit the Pfeiffer effect (147,148), which tends to substantiate the above assumption.

This section presents the results of an attempt to detect and measure the rate of enantiomerization for a number of labile cis-$M(AA)_2X_2$ complexes of titanium(IV) and a tin(IV) complex. Any $-CXY_2$ group attached to a center of dissymmetry will possess diastereotopic Y groups (11),which may be anisochronous. That is, the Y groups are able to sense the relative configurations about the dissymmetric center; the isopropyl group was chosen as the diastereotopic probe. Positioning the probe on the AA bidentate ligand is considered first; subsequently, positioning the probe on the X group is considered.

b. Diastereotopic Probe on the Bidentate Ligand

The isopropyl group may be substituted onto the β-diketonate framework at two positions: as terminal groups on the carbonyl carbon or in the 3-position of the ring. The former case is considered first.

(i). $M(dibm)_2X_2$ and $Ti(dpm)_2X_2$ Complexes

The stereochemistry of these complexes will be inferred from nmr spectra. Referring to Figure 26, with R = i-C_3H_7, the cis isomer may give rise to four spin coupled doublets for the isopropyl methyl groups. This results from the gross terminal group nonequivalence together with the diastereotopic relationship of the methyl groups within each isopropyl moiety as a result of the dissymmetry centered on the metal ion in the cis diastereomer. Each nonequivalent isopropyl methyl group will appear as a doublet owing to coupling with the geminal methine proton. For the trans diastereomer, a single doublet is expected for the isopropyl methyl groups.

Proton nmr spectra of the isopropyl methyl groups of the $Ti(dibm)_2Cl_2$ complex at selected temperatures between room temperature and -62° are reproduced in Figure 27. At room temperature, a single spin coupled doublet is observed. As the temperature is lowered, this doublet broadens until, at ca. -23°, a broad, featureless resonance is observed, which on further cooling to ca. -60° resharpens to form three doublets in a 2:1:1 intensity ratio. The isopropyl methine resonance appears as as septet at room temperature and on lowering the temperature, the fine structure of the multiplet is lost and a broad, featureless resonance is observed. A single -CH= resonance is observed at all temperatures. Analagous spectra were obtained for the $Ti(dibm)_2F_2$ and $Ti(dibm)_2Br_2$ complexes, with small changes in chemical shift separations at low temperature.

At ambient temperatures, a 1,1,2,2-tetrachloroethane solution of $Sn(dibm)_2Cl_2$ reveals five resonances in the isopropyl methyl region of the proton nmr spectrum, which may be resolved into three

partially overlapping doublets with intensity ratios of 2:1:1. As the temperature is raised, these resonances coalesce into a broad, featureless resonance signal which sharpens to a single time-averaged doublet above ca. 85°. This temperature dependence is shown in Figure 28(b). No coupling between the tin nucleus and the isopropyl methyl protons is observed. The isopropyl methine protons appear as a septet at room temperature. As the temperature is raised, some fine structure is lost and then regained to reveal a septet at ca. 110°. The -CH= resonance is masked by the solvent absorption but appears as a single resonance in a dichloromethane solution. Solutions in dichloromethane were investigated down to -60°; no further splitting of the isopropyl methyl resonance pattern was observed.

The $Ge(dibm)_2Cl_2$ complex possesses a room-temperature spectrum analagous to that of the tin(IV) complex with the exception of a shoulder on the lowerfield side of the most intense component of the isopropyl methyl resonance pattern. On warming a 1,1,2,2-tetrachloroethane solution to ca. 100°, no change in the isopropyl methyl resonance pattern is observed. For example, $W_{1/2}$ for the lowest field component is 1.60 Hz at 39° and 1.68 Hz at 100°. This indicates that no exchange processes occur at temperatures less than ca. 120°, which is not unexpected since the t-butyl methyl resonances in the $Ge(dpm)_2Cl_2$ complex coalesce at ca. 200° (60). The same comments on the methine and -CH= resonances made for the tin complex apply to the germanium complex. A dichloromethane solution of $Ge(dibm)_2Cl_2$ exhibits a single -CH= resonance and an identical isopropyl methyl resonance pattern, indicating that in solution the complex adopts the cis geometry, with no evidence of a cis-trans equilibrium being established.

Figure 27.- Temperature dependence of the isopropyl methyl resonances in the proton nmr spectrum of $Ti(dibm)_2Cl_2$ in dichloromethane solution, 0.300 M.

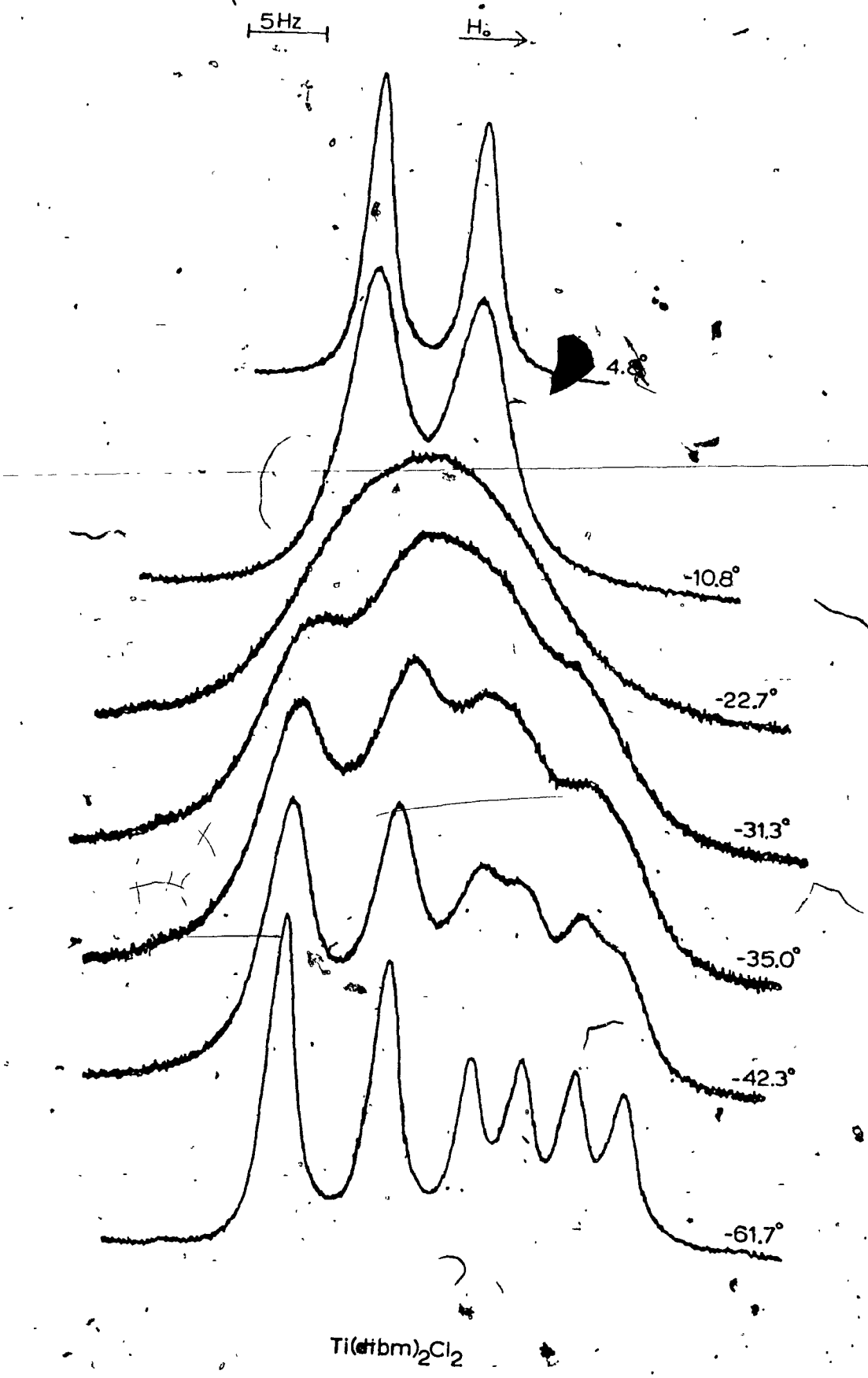

$Ti(dtbm)_2Cl_2$

Figure 28.- Temperature dependence of the isopropyl methyl resonances in the proton nmr spectrum of (a) $Sn(tibm)_2Cl_2$ and (b) $Sn(dibm)_2Cl_2$ in 1,1,2,2-tetrachloroethane solutions, 0.300 M.

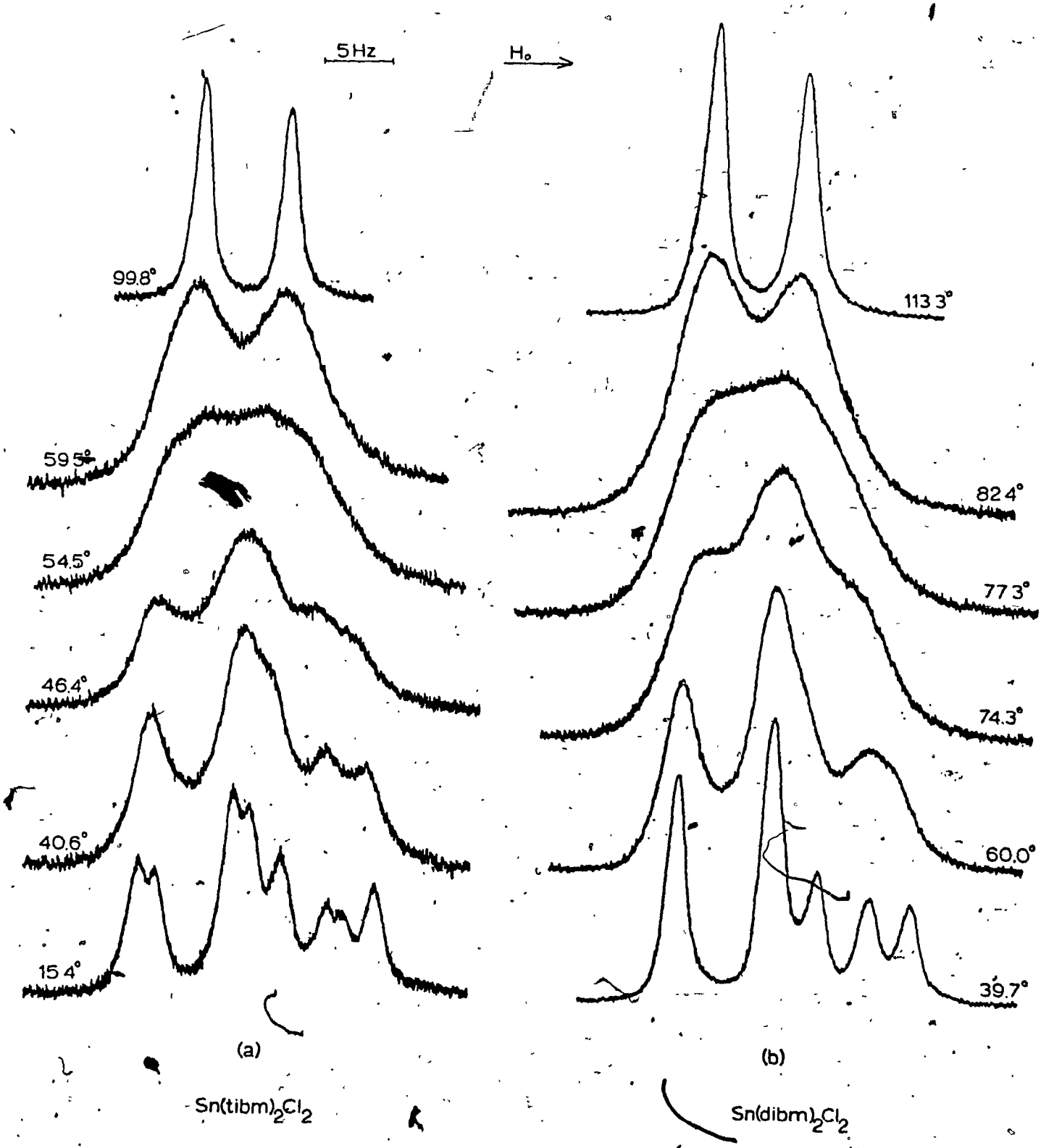
5Hz
H_o
99.8°
59.5°
54.5°
46.4°
40.6°
15.4°
(a)
$Sn(tibm)_2Cl_2$
113.3°
82.4°
77.3°
74.3°
60.0°
39.7°
(b)
$Sn(dibm)_2Cl_2$

Since the proton nmr spectra of the $M(dibm)_2X_2$ complexes failed to reveal the expected four spin coupled doublets for the isopropyl methyl groups, carbon-13 nmr spectra were recorded at -80° for $Ti(dibm)_2Cl_2$ and at room temperature for the $Sn(dibm)_2Cl_2$ complex in dichloromethane solutions by Professor L. H. Pignolet of the University of Minnesota. Since the chemical shifts of carbon nuclei cover a much greater spread than proton chemical shifts (149), so it was hoped that the expected four isopropyl methyl carbon resonances could be detected. Unfortunately, for both $Ti(dibm)_2Cl_2$ and $Sn(dibm)_2Cl_2$, only two isopropyl methyl carbon resonances, in a 3:1 intensity ratio, were observed (150) in the proton-decoupled carbon-13 nmr spectrum in the slow exchange regions. For the titanium(IV) complex at -80° in dichloromethane, two carbonyl carbon and two $-CH(CH_3)_2$ carbon resonances are observed, confirming the cis geometry. Chemical shift data for the $Ti(dibm)_2Cl_2$ complex at -80° is collected in Table XLX. Apparently, the less dominant diamagnetic term for chemical shifts of carbon nuclei compared to proton chemical shifts, and the greater distance of the carbon nuclei from the chlorine atoms combine to generate less resolution in the carbon-13 spectra than in the proton spectra.

Observation of diastereotopic isopropyl methyl groups is undoubtedly due to the dissymmetry centered on the metal ion. However, it is possible -though not probable- that, owing to hindered rotation about the $-C-CH(CH_3)_2$ bond, the isopropyl methyl groups may be locked in a conformation which results in nonequivalent methyl groups. Rotation about this bond would then generate equivalent methyl groups. In order to distinguish between these sources the t-butyl analogues $Ti(dpm)_2X_2$ complexes were investigated. Hindered rotation should be more predominant

TABLE XIX

Carbon-13 Shieldings[a] for $Ti(dibm)_2Cl_2$ at -80°

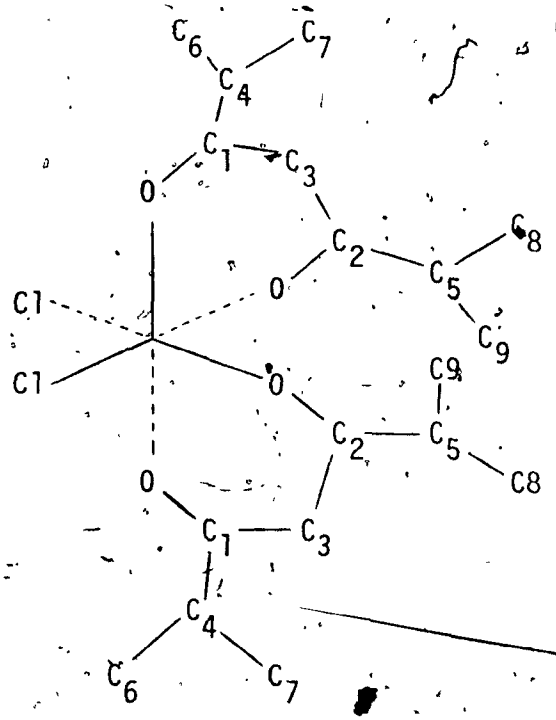

Carbon	δ
C_1, C_2	-165.7, -161.6
C_3	-105.6
C_4, C_5	-38.8, -37.7
C_6, C_7, C_8, C_9	-20.3, -19.6

[a] In dichloromethane solution and shifts reported in ppm (±0.1) from TMS (upfield positive).

in these complexes as a result of the greater bulk of the t-butyl groups.

The $Ti(dpm)_2X_2$ [X = F,Cl,Br] complexes reveal a single t-butyl methyl resonance at room temperature which broadens on cooling and splits into two equally intense resonances by -60^o. This is simply a result of the exchange of nonequivalent t-butyl groups within the cis isomer. This process has been observed and measured in several $Ti(dpm)_2X_2$ [X = Cl,NCO] (114), $Sn(dpm)_2X_2$ [X = F,Cl,Br,I] (60), and $Ge(dpm)_2X_2$ [X = Cl,Br,I] (60,116) complexes. Should hindered rotation be a viable process, extra resonances should appear. Also, in the proton spectrum of 1,3,5-trimethyl-2-isopropylbenzene, in which the rotation of the isopropyl group about the sp^3-sp^2 bond is restricted, no splitting of the isopropyl methyl doublet is observed even at -60^o (151). Thus, the only plausible source remaining for the splitting observed in the $M(dibm)_2X_2$ complexes is the dissymmetry centered on the metal ion.

No complete lineshape analysis of the temperature dependent nmr spectra of the $M(dibm)_2X_2$ complexes was attempted. Since these complexes present a four-site exchange problem, six first-order rate constants are necessary to completely describe the exchange process. In addition, coupling to the methine protons must be considered and, to make matters worse, the relaxation times T_2 appear to be temperature dependent.

It is possible, however, to make estimates of approximate rate constants at the temperatures of coalescence of the isopropyl methyl resonances. Such estimates are useful indications of the relative labilities of $M(dik)_2X_2$ complexes and of the dependence of lability on the nature of the halogen.

Figures 27 and 28(b) suggest that the four nonequivalent methyl groups may be classified into two sets: a set of two forming the low field doublet (which may be assigned to the equatorial groups trans to the X groups (142)) and a set of two which form the two doublets at higher field. In order to estimate rate constants, the four-site exchange problem is approximated by a two-site process; the chemical shift between the two sites, $\delta\upsilon$ (in Hz), being the chemical shift between the centers of the low field doublet and the higher field quartet in the low temperature spectra, as illustrated below for $Ti(dibm)_2Cl_2$. Since the two sites are equally populated, the first-

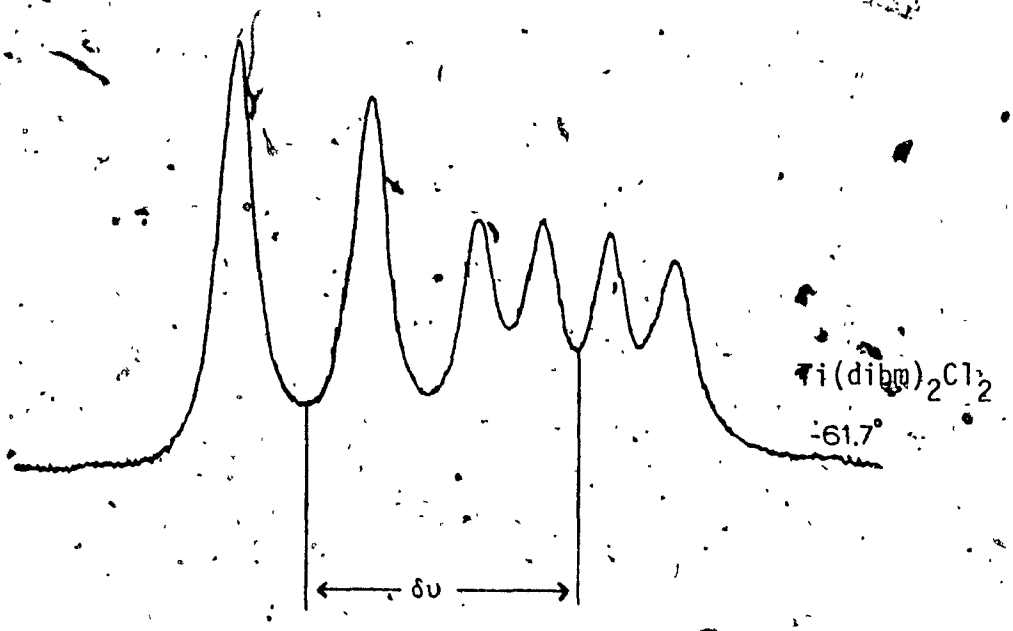

order rate constant, k_{Tc}, at the coalescence temperature, T_c, for exchange of isopropyl methyl groups between the two sites is given by $\pi\delta\upsilon/\sqrt{2}$ (13). The coalescence temperature is taken as the temperature at which the entire spectrum collapses into a single, broad resonance.

Approximate rate constants obtained by this procedure for the $Ti(dibm)_2X_2$ complexes are listed in Table XX, along with values

Table XX

Approximate Rate Constants for Exchange of Isopropyl Groups in $Ti(dibm)_2X_2$ Complexes

X	$\delta\upsilon$ (Hz)	T_c (^oC)	k at T_c $Ti(dibm)_2X_2$	k at T_c $Ti(acac)_2X_2$[a]	k at T_c $Ti(dpm)_2Cl_2$[b]	k[c] at -36^o
F	11.5	-39	26	75	-	36
Cl	13.5	-23	30	18	89	8.7
Br	15.5	-36	34	14	-	34

[a]Calculated from data in ref. (54); [b]Calculated from data in ref. (114); [c]For $Ti(dibm)_2X_2$ (see text).

for $\delta\upsilon$ and T_c. The fifth column of Table XX gives rate constants for exchange of methyl groups in $Ti(acac)_2X_2$ complexes (54) at temperatures corresponding to T_c for the related $Ti(dibm)_2X_2$ complex. Column six gives the rate constant for exchange of t-butyl groups in the $Ti(dpm)_2Cl_2$ complex at T_c for the $Ti(dibm)_2Cl_2$ complex. In the last column of Table XX are listed the values of k for $Ti(dibm)_2X_2$ extrapolated to a common temperature, -36^o, T_c for $Ti(dibm)_2Br_2$. These values were calculated assuming that the activation energies for the $Ti(dibm)_2X_2$ complexes are the same as those found for the corresponding acetylacetonates [11.6 kcal/mole (X = F); 11.2 kcal/mole (X = Cl)] (54). Comparison of the fourth and fifth columns indicates that the lability of the $Ti(dibm)_2X_2$ and the $Ti(acac)_2X_2$ complexes is quite comparable, at least for X = Cl and Br, although $Ti(dibm)_2F_2$ appears to be less labile than the corresponding acetylacetonate, a feature noted previously concerning the $Ti(bzac)_2F_2$ complex (74). Comparison of columns four, five, and six for X = Cl establishes a lability order for $Ti(dik)_2Cl_2$ complexes; the exchange rates increase in the order acac < dibm < dpm. The last column establishes the dependence of the exchange rate on the nature of the halogen, lability increasing in the order Cl < Br ~ F. For the acetylacetonates, exchange rates were found to increase in the order Cl < Br < F (54) while the $Ti(bzac)_2X_2$ complexes possessed a halogen dependence (74) similar to that found above for the $Ti(dibm)_2X_2$ complexes.

Approximate rate constants obtained by this procedure for the $Sn(dibm)_2Cl_2$ complex are presented in Table XXI. Calculation of the exchange rate for the $Sn(acac)_2Cl_2$ and $Sn(dpm)_2Cl_2$ complexes at the T_c for the $Sn(dibm)_2Cl_2$ complex allows the dependence of the lability on the nature of the bidentate ligand to be established. Exchange rates in

Table XXI

Approximate Rate Constants for Exchange in $Sn(dik)_2Cl_2$ Complexes

	$Sn(acac)_2Cl_2$[a]	$Sn(dibm)_2Cl_2$	$Sn(dpm)_2Cl_2$[b]
$\delta\upsilon$ (Hz)	5.41	8.5	8.82
T_c (°C)	82	79	65
k at T_c for $Sn(dibm)_2Cl_2$	10	19	54

[a]Calculated from data in ref. (59); [b]Calculated from data in ref. (60).

$Sn(dik)_2Cl_2$ complexes increase in the order acac < dibm < dpm, the same order as found above for the $Ti(dik)_2Cl_2$ series.

Permutational and mechanistic analyses of allowed rearrangements within the cis-$M(AA)_2X_2$ system have been presented in Sections III-A-3b and III-A-4b, respectively. Consulting Table IV, which lists the expected changes in signal multiplicities for the various averaging sets, one finds that no averaging set will predict the collapse of the diastereotopic terminal groups of the A-A ligand to a single doublet. The minimum number of doublets predicted is two, generated by sets A_4, A_5, and A_8 and the linear combinations $(A_2 + A_3)$ and $(A_6 + A_7)$. It is quite reasonable to expect the collapse of the low temperature spectra (which already encompasses groups with degenerate shifts) for these $M(dibm)_2X_2$ complexes to a single doublet to be the result of an accidental shift degeneracy of the expected two doublets. Averaging sets predict that the number of doublets is a multiple of two, i.e., two, four, six, or eight. It is unlikely that four (or more) doublets would overlap in the fast exchange region. It is then necessary to distinguish between averaging sets A_4, A_5, and A_8, as well as

the $(A_2 + A_3)$ and $(A_6 + A_7)$ combinations.

The following arguments may lead to the elimination of some of these averaging sets. Since exchange of nonequivalent methyl and t-butyl groups occur in the $Ti(dik)_2X_2$ and $Sn(dik)_2X_2$ complexes [dik = acac,dpm; X = halogen] (54,59,60,114), it is reasonable to suppose that exchange of axially and equatorially nonequivalent isopropyl groups must occur in the rearrangement of $M(dibm)_2X_2$ complexes; A_5 may then be eliminated. Since diastereotopic splitting is observed in the slow exchange region and is removed on warming, and the Pfeiffer effect is observed for related $Ti(acac)_2X_2$ and $Sn(acac)_2X_2$ complexes (147,148), inversion processes are probably occurring during the rearrangement. On the basis of this assumption, averaging set A_4 and the linear combination $(A_2 + A_3)$ may be eliminated since they do not provide a path for optical inversion. Note that the $M(dibm)_2X_2$ spectra can be explained using averaging set A_4 or $(A_2 + A_3)$ without invoking enantiomerization processes; however, attachment of diastereotopic isopropyl probes in other chelate systems has shown that these systems rearrange *via* a process which involves enantiomerization processes (26,35,37,152). Thus exclusion of averaging sets A_4 and $(A_2 + A_3)$ is reasonable.

This leaves us to distinguish between averaging sets A_8 and $(A_6 + A_7)$. The most obvious difference between these two possible averaging sets is that they predict different ratios of rate of enantiomerization to rate of terminal group exchange. A_8 predicts a ratio of unity; $(A_6 + A_7)$ predicts a ratio of 2:1. Figures 27 and 28(b) show that the diastereotopic splitting observed in the slow exchange region for the $M(dibm)_2X_2$ complexes is removed first and then complete collapse to a single doublet occurs. This may simply be a result of the smaller diastereotopic splitting (*ca.* 3-6 Hz) *versus* overall group nonequivalence (*ca.* 9-16 Hz) causing the

diastereotopic splitting to possess a lower coalescence temperature with the operation of the A_8 averaging set. On the other hand, it may reflect a greater rate for enantiomerization than for terminal group exchange, as $(A_6 + A_7)$ would necessitate. A detailed total lineshape computer simulation could possibly distinguish between these two alternatives; however, owing to the difficulties mentioned earlier, viz. the six first-order rate constants and the temperature dependence of T_2's, a detailed kinetic analysis of the problem was not attempted.

Some evidence does exist for support of the $(A_6 + A_7)$ combination as the averaging set responsible for the observed permutation of nuclei in the $M(dibm)_2X_2$ complexes. The averaging set A'_{13} appears to explain the rearrangement processes in the $Ti(dibm)_2Cl(OCH_3$ complex (cf. Section III-C-2b). Using the correlations listed in Table XIV, with the tacit assumption of similar physical mechanisms, on going from the cis-$M(AA)_2XY$ to the cis-$M(AA)_2X_2$ system, A'_{13} correlates with A_6 and A_7.

On the basis of these arguments, the linear combination $(A_6 + A_7)$ is favoured over the A_8 averaging set.

Appendix C contains chemical shift data for the complexes described in this section.

In order to simplify the system to obtain a more direct measure of the relative rates of enantiomerization and terminal group exchange, the isopropyl probe was positioned in the 3-position of the acetylacetonate ring. The next section presents the results of this investigation.

(ii). Stereochemistry and Lability of $Ti(3-^{i}Pr\text{-}acac)_2Cl_2$

Placement of an isopropyl group in the γ- (or 3-) position of the acetylacetonate ring in a $M(AA)_2X_2$ complex provides an opportunity to study the averaging of terminal R groups and the inversion of the molecular configuration independently. Should such a complex adopt the cis configuration, the proton nmr spectrum should reveal two terminal methyl group resonances and two isopropyl methyl doublets resulting from the dissymmetry centered on the metal ion. For a trans geometry, a single terminal methyl resonance and a single isopropyl methyl doublet would be expected in the nmr spectrum.

Figure 29 shows the temperature dependence of the terminal and isopropyl methyl resonances of the $Ti(3-^{i}Pr\text{-}acac)_2Cl_2$ complex in a dichloromethane solution. At room temperature a single terminal methyl resonance is observed, which on cooling broadens and splits into two equally-intense resonances below ca. -40^{o}. At all accessible temperatures on a 60 MHz instrument and at -80^{o} on a 100 MHz instrument a single isopropyl methyl doublet is observed. This resonance is considerably broadened at low temperatures: $W_{1/2}$ is 0.8 Hz at room temperature and 3.0 Hz at -69.6^{o}.

Observation of two terminal methyl group resonances indicates that this complex adopts the cis geometry and is stereochemically nonrigid. Analagous observations were made by Thompson and co-workers in a study of $Ti(3\text{-}CH_3\text{-}acac)_2X_2$ [X = F,Cl,Br] complexes (56). Failure to observe two isopropyl methyl doublets could be a result of chemical shift degeneracy or a very rapid exchange process still occurring at -70^{o}. This point will be considered later.

A TLS analysis was carried out on the exchange of terminal

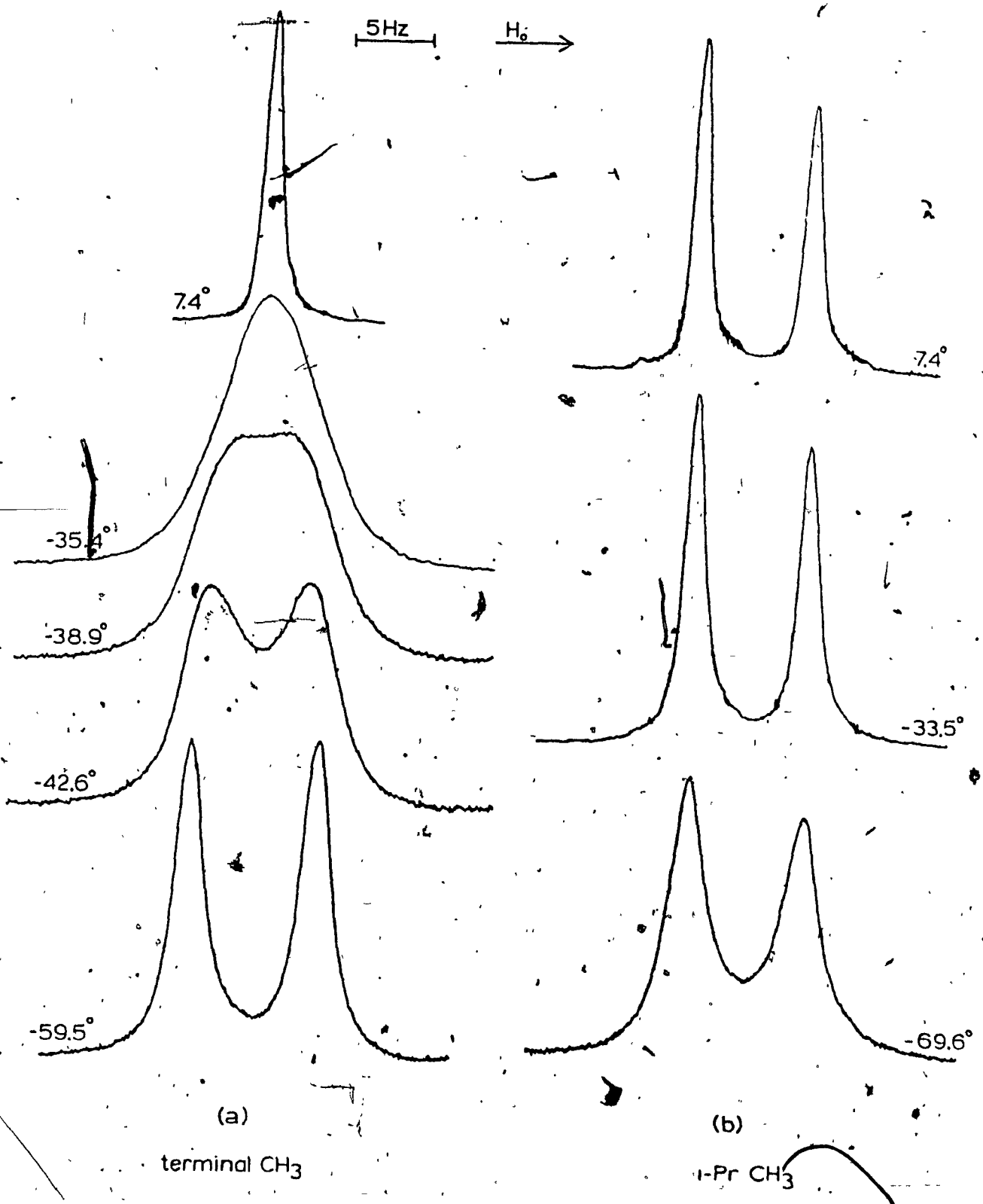

Figure 29.- Temperature dependence of the (a) terminal methyl and (b) isopropyl methyl resonances in the proton nmr spectrum of the $Ti(3\text{-}^{i}Pr\text{-}acac)_2Cl_2$ complex in dichloromethane solution, 0.300 M.

methyl groups in the Ti(3-^{i}Pr-acac)$_2$Cl$_2$ complex in order to assess the effect of γ-substitution on the rate of terminal group exchange in Ti(dik)$_2$Cl$_2$ complexes. Table XXII lists the characteristic lineshape parameters used to extract mean lifetimes, $\tau = \tau_A\tau_B/(\tau_A + \tau_B)$, for the two-site exchange process. Mean lifetimes were obtained by comparing experimental lineshape parameters (Table XXII) with those from calculated spectra using the Gutowsky-Holm total lineshape equation (17), as described in Section II-C. The temperature dependence of δυ is shown in Figure 30 and listed in Appendix B; a constant value was observed in the low temperature limit. The cis-Zr(acac)$_2$Cl$_2$ complex was employed as the T_2 reference compound. The concentration dependence of the mean residence times, presented in Table XXIII, demonstrates that the environmental averaging process is independent of concentration and is a first-order process.

Arrhenius activation parameters were obtained in the usual fashion from the least-squares straight line plot of log k versus 1/T, shown in Figure 31, where $k = 1/2\tau$ is the first-order rate constant for exchange. The entropy of activation, $\Delta S^{\neq}$, was obtained from the expression $\Delta S^{\neq} = R[\ln A - \ln RT/Nh] - R$.

Arrhenius and Eyring activation parameters are collected in Table XXIV, along with the corresponding values for the exchange process in Ti(dik)$_2$X$_2$ [dik = acac,dpm; X = halogen or pseudo-halogen] complexes (54, 114). The errors in the activation parameters for Ti(3-^{i}Pr-acac)$_2$Cl$_2$ represent the random scatter of the data points in Figure 31. Since T_2 is temperature dependent, a reasonable uncertainty for this parameter may lead to systematic errors of the order of ± 1 kcal/mole in the activation energy and ± 4 eu in the activation entropy (59,60).

Comparison of the kinetic data for terminal methyl group

Table XXII

Terminal Methyl PMR Lineshape Parameters and Values of τ for $Ti(3\text{-}^{i}Pr\text{-}acac)_2Cl_2$[a]

Temp., [b] °C	R[c] LF	R[c] HF	$\delta\upsilon_e$, [d] Hz	Linewidths, [e] Hz $W_{1/4}$ LF	$W_{1/4}$ HF	$W_{1/2}$ LF	$W_{1/2}$ HF	$W_{3/4}$ LF	$W_{3/4}$ HF	$\tau \times 10^2$, sec
-52.2	4.60	4.71	7.82	4.88	4.69	2.58	2.56	1.50	1.50	12
-49.8	3.51	3.65	7.65	-	-	2.92	2.86	1.68	1.67	9.7
-46.2	2.14	2.22	7.22	-	-	4.46	4.20	2.22	2.17	6.6
-42.6	1.41	1.43	6.33	-	-	-	-	3.68	3.33	4.7
-40.0	1.09	1.09	4.64	-	-	-	-	-	-	3.6
-38.9	1.01	1.02	2.94	-	-	-	-	-	-	3.2
-35.4	-		-	10.60		7.37		4.84		2.4
-33.5	-		-	8.79		5.39		3.27		1.9
-31.3	-		-	7.23		4.27		2.52		1.5
-27.3	-		-	5.32		3.09		1.82		1.1

[a] 0.300 M in dichloromethane; [b] Calculated using the Van Geet equation for methanol; [c] Ratio of the maximum amplitude to the central minimum; [d] Observed frequency separation; [e] Full line width at designated fraction of maximum amplitude.

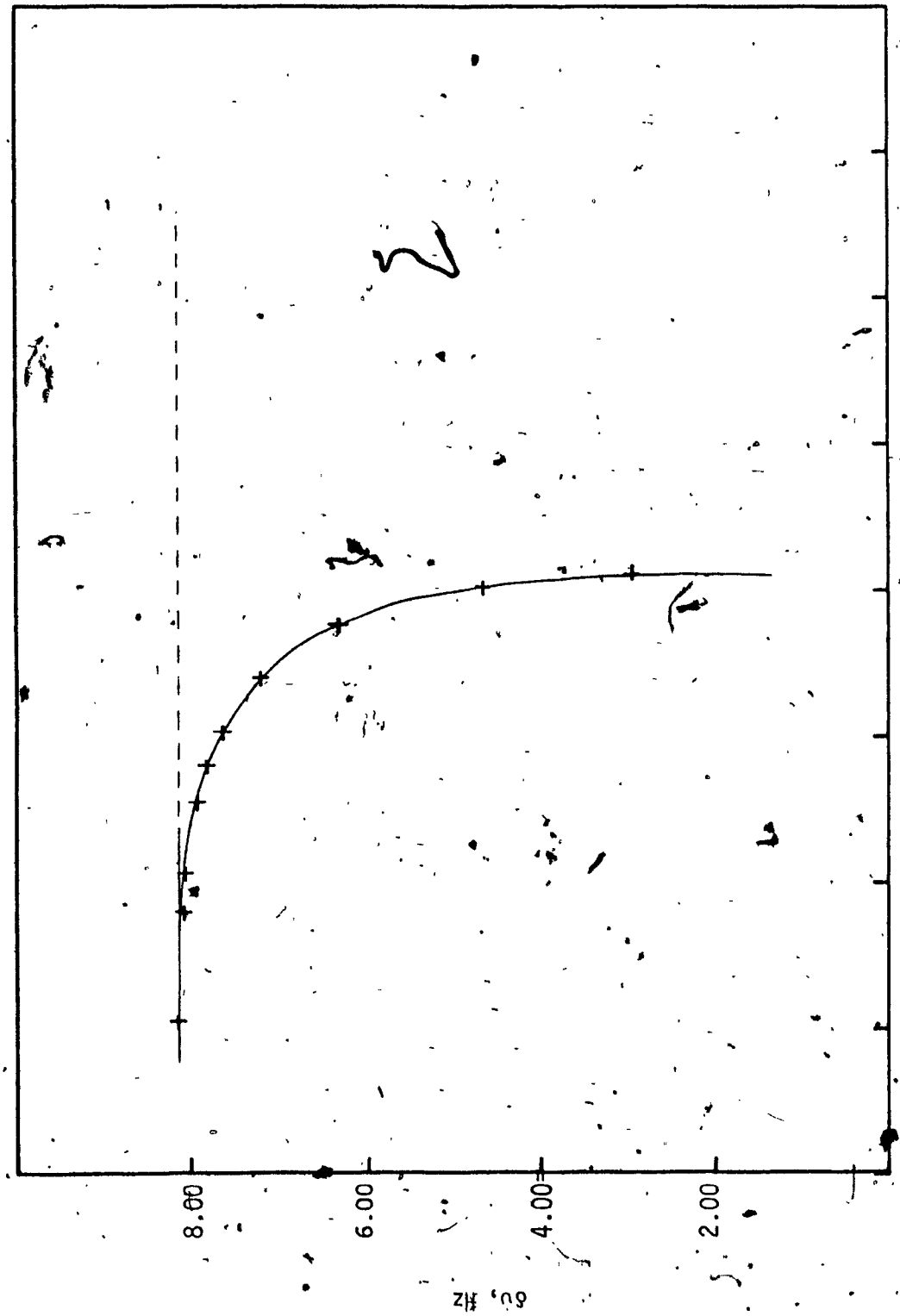

Figure 30.- Temperature dependence of the chemical shift separation, $\delta\upsilon$, of the terminal methyl resonances of the $Ti(3\text{-}^{i}Pr\text{-}acac)_2Cl_2$ complex in dichloromethane solution.

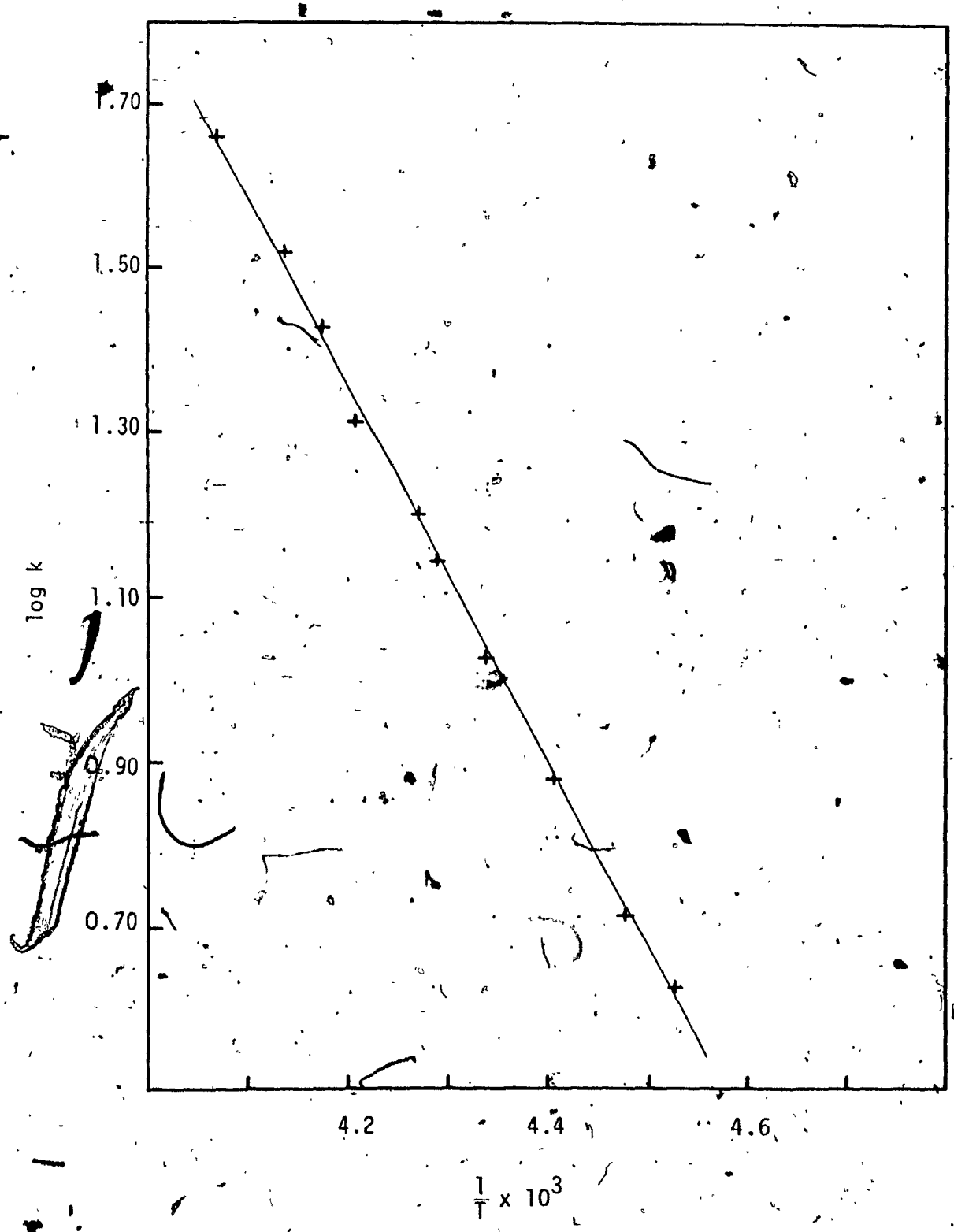

Figure 31.- Arrhenius (log k versus 1/T) least-squares plot for terminal methyl group exchange in the $Ti(3\text{-}^{i}Pr\text{-}acac)_2Cl_2$ complex in dichloromethane solution.

Table XXIII

Concentration Dependence of Mean Residence Times for Terminal Group Exchange in $Ti(3\text{-}^{i}Pr\text{-}acac)_2Cl_2$ at Selected Temperatures[a]

Temp., °C	τ_t, sec	
	0.300 M	0.150 M
-33.5	0.019	0.018
-35.4	0.024	0.024
-42.6	0.047	0.048
-46.2	0.066	0.067

[a]In dichloromethane solution.

exchange in $Ti(3\text{-}^{i}Pr\text{-}acac)_2Cl_2$ with data for other $Ti(dik)_2X_2$ complexes reveals no startling differences. The largest differences appear to be in the entropies of activation; however, since this parameter has the largest determinate error and probably contains more indeterminate errors, the differences are of little validity. The most interesting comparisons are amongst the $Ti(acac)_2Cl_2$, $Ti(3\text{-}^{i}Pr\text{-}acac)_2Cl_2$, and $Ti(dpm)_2Cl_2$ complexes, lability increasing in this order. Since the same solvent was employed for the study of these three complexes, solvation differences are expected to be small. Placement of an inductive electron-donating alkyl group on the acetylacetonate ring would be expected to increase the electron density within the ring and hence result in stronger Ti-O bonds. Should a bond-rupture mechanism be operative, the $Ti(dpm)_2Cl_2$ complex would be expected to be less labile (higher E_a) than the acetylacetonate analogue; similar arguments prevail for the $Ti(3\text{-}^{i}Pr\text{-}acac)_2Cl_2$ complex. However, the $Ti(3\text{-}^{i}Pr\text{-}acac)_2Cl_2$ complex reveals a slightly lower E_a relative to that for $Ti(acac)_2Cl_2$ and the $Ti(dpm)_2Cl_2$ complex shows no change in activation energy from that of the acetylacetonate analogue.

Table XXIV

Kinetic Data for Terminal Group Exchange in $Ti(dik)_2X_2$ Complexes [a]

Compound	k_{298} (sec^{-1})	$\Delta H^{\neq}_{298}$ (kcal/mole)	$\Delta S^{\neq}_{298}$ (eu)	E_a (kcal/mole)	log A	Ref.
$Ti(acac)_2Cl_2$	6.7×10^2	10.7 ± 0.6	-9.7 ± 2.3	11.2 ± 0.6	11.03 ± 0.51	54
$Ti(acac)_2(NCO)_2$	1.1×10^3	10.5 ± 0.6	-9.3 ± 2.4	11.0 ± 0.6	11.08 ± 0.52	114
$Ti(3\text{-}^{i}Pr\text{-}acac)_2Cl_2$	1.9×10^3	9.8 ± 0.3	-10.4 ± 1.5	10.4 ± 0.3	10.94 ± 0.33	This work
$Ti(acac)_2Br_2$	2.3×10^3	11.0 ± 0.5	-6.2 ± 2.0	11.6 ± 0.4	11.85 ± 0.36	54
$Ti(dpm)_2Cl_2$	3.5×10^3	10.9 ± 0.4	-5.6 ± 1.5	11.4 ± 0.4	11.91 ± 0.33	114
$Ti(dpm)_2(NCO)_2$	6.7×10^3	9.4 ± 0.3	-9.5 ± 1.5	9.8 ± 0.3	11.04 ± 0.32	114
$Ti(acac)_2F_2$	1.6×10^4	11.1 ± 0.4	-2.2 ± 2.0	11.6 ± 0.5	12.70 ± 0.49	54

[a] In dichloromethane solution; [b] All errors are random errors estimated at the 95% confidence level.

Similarly enigmatic is the expected slight increase in steric hindrance to the operation of a twist mechanism when the more bulky isopropyl or t-butyl groups are substituted onto the acetylacetonate framework. The experimental results for the $Ti(dik)_2Cl_2$ series indicates that the rate and energetics of the rearrangement process is not dependent to any significant degree on the nature of the β-diketonate ring. Even the cis-$Ti(hfac)_2Cl_2$ complex (71,114) does not exhibit the usual rate enhancement of ca. 10^4 observed for tris-chelates of Al(III) and Ga(III) on introduction of hexafluoroacetylacetonate ligands (153).

Referring to the expected changes in signal multiplicities generated for the allowed averaging sets of a cis-$M(AA)_2X_2$ complex, listed in Table IV, again a distinction between averaging sets A_8 and the linear combination $(A_6 + A_7)$ is necessary. On the basis of arguments presented in the previous section, the combination $(A_6 + A_7)$ is favoured. This set predicts a ratio of rates of inversion to terminal group exchange of two. For the $Ti(3\text{-}^iPr\text{-}acac)_2Cl_2$ complex, no splitting of the isopropyl methyl doublet is observed for a dichloromethane solution at -80^o on a 100 MHz instrument (150). It is reasonable to expect smaller diastereotopic splittings for the $Ti(3\text{-}^iPr\text{-}acac)_2Cl_2$ complex than in the $Ti(dibm)_2Cl_2$ complex as the isopropyl methyl groups are further away from the metal and the chlorine atoms in the former case. This would result in a lower temperature being necessary to observe any splitting in the $Ti(3\text{-}^iPr\text{-}acac)_2Cl_2$ complex relative to the $Ti(dibm)_2Cl_2$ complex. As mentioned above, the isopropyl methyl doublet for $Ti(3\text{-}^iPr\text{-}acac)_2Cl_2$ broadens from a $W_{1/2}$ of 0.8 Hz at ambient temperature to ca. 3.0 Hz at -69.6^o, in a dichloromethane solution. The acac methyl resonance of the $Zr(acac)_2Cl_2$ complex in a dichloromethane solution broadens from a $W_{1/2}$ of 0.5 Hz at room temperature

to ca. 1.2 Hz at -65° (54). Thus the broadening observed for the isopropyl methyl resonance of the $Ti(3\text{-}^{i}Pr\text{-}acac)_2Cl_2$ complex appears to be greater than that expected for viscosity broadening in dichloromethane solutions. This may be explained by assuming that the rate of inversion is simply greater than the rate of terminal group exchange; thus favouring the linear combination $(A_6 + A_7)$ over the A_8 averaging set.

The attachment of diastereotopic groups to the bidentate chelating rings of cis-$M(AA)_2X_2$ complexes has resulted in some evidence for the operation of a linear combination of averaging sets in these complexes, viz. $(A_6 + A_7)$ of Table IV. Physical processes which generate this combined averaging set are numerous and may be found by consulting Figures 12, 13, and 14 of Section III-A-4b. Such evidence and implications are by no means conclusive. An implicit assumption is that site interchanges in cis-$M(AA)_2X_2$ complexes probably result from a single averaging set. A mixture of physical processes can generate a mixture of averaging sets, that cannot be distinguished from averaging sets operating individually.

Chemical shift data for the $Ti(3\text{-}^{i}Pr\text{-}acac)_2Cl_2$ complex is summarized in Appendix C.

In an attempt to further delineate the cis-$M(AA)_2X_2$ system, studies were conducted on complexes in which diastereotopic probes were incorporated onto the monodentate X ligand. The results of these studies are reported in the following section.

c. Diastereotopic Probe on the Monodentate Ligand

An alternative placement of the diastereotopic probe for $M(AA)_2X_2$ complexes is on the monodentate ligand, X. The simplest possibility is the direct attachment of an isopropyl group to the metal ion; however, titanium carbon σ-bonds are notoriously unstable (154). An isopropoxy group constitutes a good choice and such complexes have been studied. However, it is not possible to vary bonding and steric factors for such a group. Isopropyl-substituted phenoxy groups satisfy the latter two factors as well as providing for the diastereotopic probe. Another possible advantage of the phenoxy group is the larger chemical shift differences for exchanging groups which may result from the magnetic anisotropic effect of the aromatic ring.

Harrod and Taylor (62,126) have prepared and studied a number of $Ti(chelate)_2(phenoxy)_2$ [chelate = acac,ox,quin] complexes with a variety of substituents on the phenoxy ligand. However, kinetic data for their complexes was obtained using an approximate lineshape method of analysis (126) and thus subject to severe systematic errors. In part (i) of this section, a TLS analysis of terminal group exchange in a series of cis-$Ti(acac)_2(phenoxy)_2$ complexes, with a variety of substituents on the phenoxy ligands, is presented. All complexes exhibited acac methyl group exchange and in the case of some isopropyl-substituted phenoxy complexes, isopropyl methyl group exchange is also observed. The study of the former process was conducted in an attempt to delineate the effect of the X ligand on the rate of exchange of acetylacetonate methyl groups. In comparing kinetic data for isopropyl methyl group exchange, data for the exchange process in the $Ti(acac)_2Cl(2,6\text{-}^iPr_2C_6H_3O)$ complex is also included. This complex is also discussed in Section III-C-2c.

Part (ii) then compares the TLS and approximate methods of extracting kinetic data from variable temperature nmr spectra for a variety of cis-$M(acac)_2X_2$ and cis-$M(acac)_2XY$ complexes. Severe errors introduced by the use of approximate methods are analyzed and discussed.

Finally, the dependence of the rate of isopropyl methyl group exchange on the 2,6-diisopropylphenoxy ligand on the nature of the bidentate ligand was investigated in a study of the series of complexes $Ti(chelate)_2(2,6\text{-}^iPr_2C_6H_3O)_2$ [chelate = acac,ox,quin]. These results are presented in part (iii). This particular series of complexes was chosen since their solid state structures are known (139).

(i) Rearrangement Processes in Bis(phenoxy)bis(acetylacetonato)-titanium(IV) Complexes

A number of $Ti(acac)_2(phenoxy)_2$ complexes have been shown (62,126) to exist as the stereochemically nonrigid cis diastereomer using a combination of variable temperature proton nmr and dipole moment studies. Exchange of acetylacetonate and isopropyl methyl groups in a number of such complexes was studied using a TLS analysis of variable temperature proton nmr spectra. Such systems present another possible means of establishing a relationship between terminal group exchange and inversion of the molecular configuration.

Figures 32 and 33 illustrate the temperature dependence of the acetylacetonate and isopropyl methyl resonances of the $Ti(acac)_2(2\text{-}^iPrC_6H_4O)_2$ and $Ti(acac)_2(4\text{-}^iPrC_6H_4O)_2$ complexes, respectively, in dichloromethane solutions. A single acetylacetonate methyl resonance is observed at ambient temperature, which on cooling broadens and splits into two resonances of equal intensity, indicative of a cis structure in solution. Such behaviour is typical of all the $Ti(acac)_2(phenoxy)_2$ complexes

Figure 32.- Temperature dependence of the (a) acetylacetonate and (b) isopropyl methyl resonances in the proton nmr spectrum of the $Ti(acac)_2(2\text{-}^{i}PrC_6H_4O)_2$ complex in dichloromethane solution, 0.300 M.

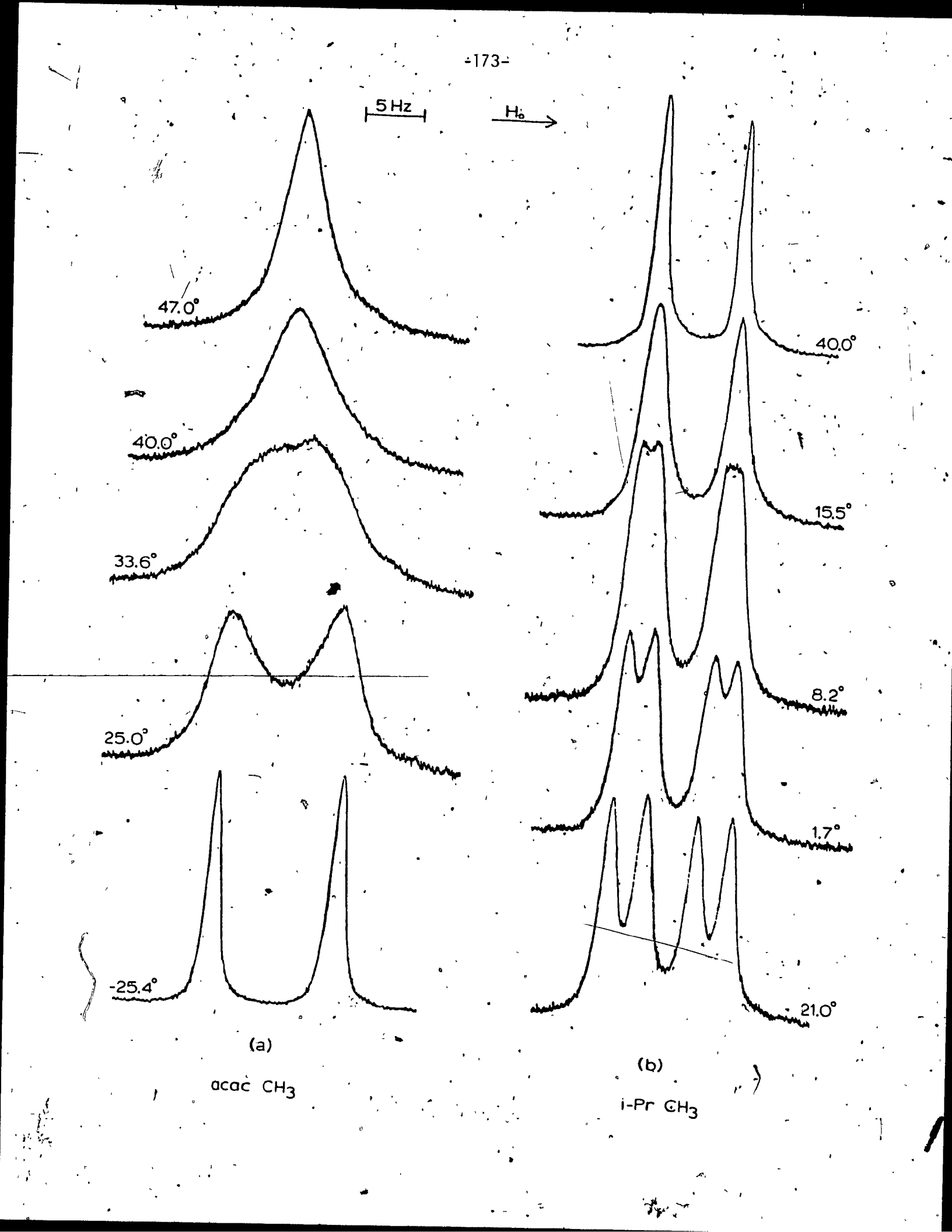
5 Hz
H_o
47.0°
40.0°
33.6°
25.0°
-25.4°
(a)
acac CH_3
40.0°
15.5°
8.2°
1.7°
21.0°
(b)
i-Pr CH_3

Figure 33.- Temperature dependence of the (a) acetylacetonate and (b) isopropyl methyl resonances in the proton nmr spectrum of the $Ti(acac)_2(4\text{-}^{i}PrC_6H_4O)_2$ complex in dichloromethane solution, 0.300 M.

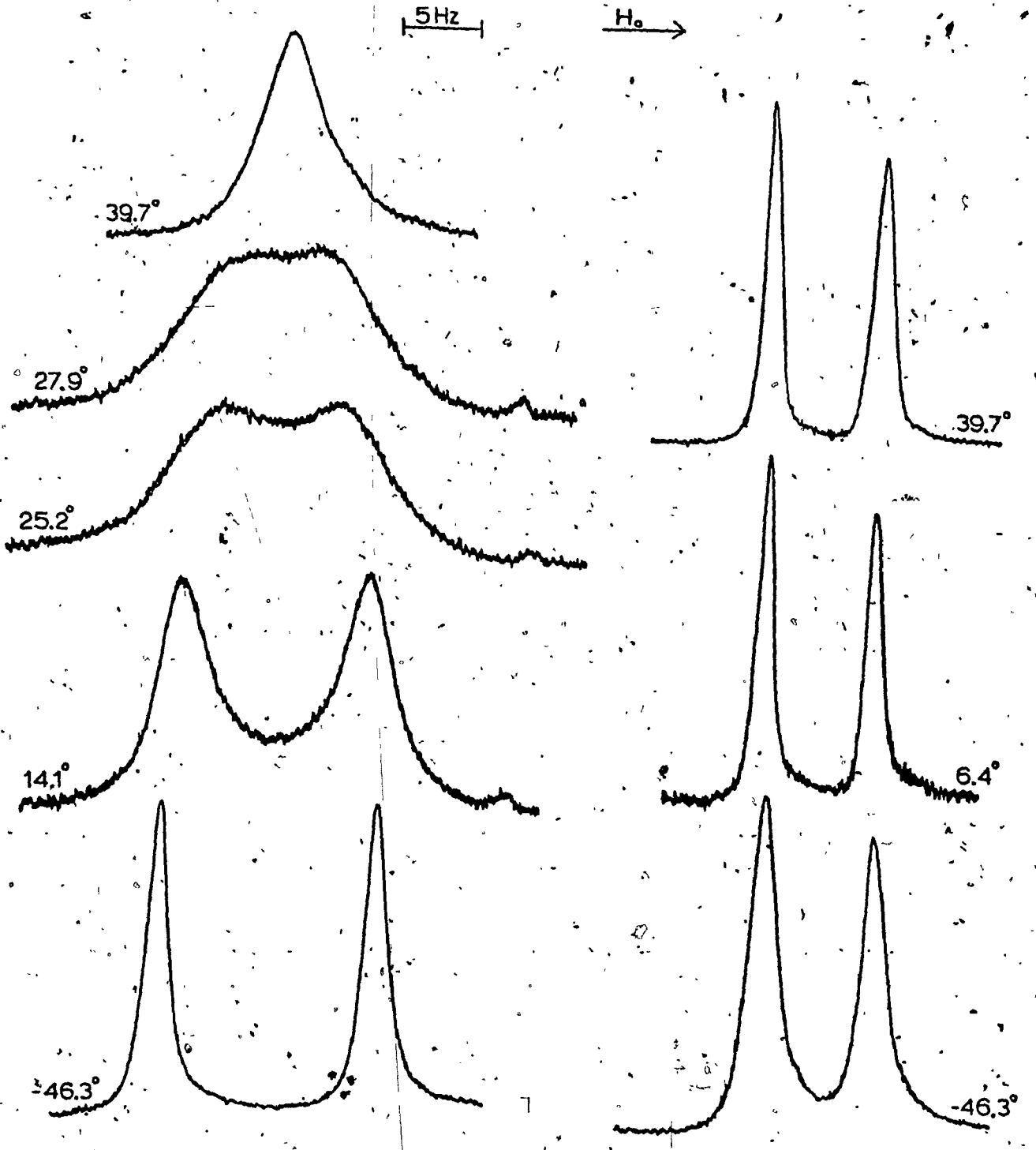
5Hz
H_o
39.7°
27.9°
25.2°
14.1°
-46.3°
39.7°
6.4°
-46.3°
(a)
acac CH_3
(b)
I-Pr CH_3

studied; only the coalescence temperatures differ. For the $Ti(acac)_2(2\text{-}^iPrC_6H_4O)_2$ complex, the isopropyl methyl resonance appears as a single doublet at room temperature. On cooling, this doublet broadens and eventually two doublets are observed. Similar behaviour occurs for the isopropyl methyl resonances of the $Ti(acac)_2(2,6\text{-}^iPr_2C_6H_3O)_2$ (see Figure 41) and $Ti(acac)_2Cl(2,6\text{-}^iPr_2C_6H_3O)$ (see Figure 48) complexes. However, as Figure 33(b) reveals, the isopropyl methyl resonance of the $Ti(acac)_2(4\text{-}^iPrC_6H_4O)_2$ complex fails to split into two doublets at low temperature. The $W_{1/2}$ values for the isopropyl methyl doublet change only from 1.09,1.07 Hz at 39.7° to 1.80,1.90 Hz at -46.3°. This reflects line broadening due to viscosity and solvation changes at low temperature.

A TLS analysis was performed on the exchange of terminal acetylacetonate methyl groups of the $Ti(acac)_2(phenoxy)_2$ [phenoxy = $2,6\text{-}Cl_2C_6H_3O$, $2\text{-}ClC_6H_4O$, $2\text{-}IC_6H_4O$, $4\text{-}ClC_6H_4O$, $4\text{-}^iPrC_6H_4O$, $2\text{-}^iPrC_6H_4O$, $2\text{-}(C_6H_5)C_6H_4O$, and $2,6\text{-}^iPr_2C_6H_3O$] complexes in dichloromethane solution and the $Ti(acac)_2(2,6\text{-}^iPr_2C_6H_3O)_2$ complex in m-dichlorobenzene solution. Tables XXV through XXXII list the lineshape parameters used to extract the mean lifetimes, τ, for these two-site exchange processes, except for the $Ti(acac)_2(2,6\text{-}Cl_2C_6H_3O)_2$ complex, discussed below. Mean lifetimes were obtained by comparing experimental lineshape parameters with those from theoretical spectra generated by the Gutowsky-Holm total lineshape equation (17), as described in Section II-C. The temperature dependence of $\delta\upsilon$ was measured in the slow exchange region and the straight-line portion extrapolated into the intermediate and fast exchange regions; the data are listed in Appendix B. For dichloromethane solutions, the temperature dependence of T_2 was corrected for by using the observed linewidth of the acetylacetonate methyl resonance of the cis-$Zr(acac)_2Cl_2$ complex to

Table XXV

Acetylacetonate Methyl PMR Lineshape Parameters[a] and Values of τ for $Ti(acac)_2(2\text{-}ClC_6H_4O)_2$[b]

	R			Linewidths, Hz						
				$W_{1/4}$		$W_{1/2}$		$W_{3/4}$		
Temp., [c] °C	LF	HF	$\delta\upsilon_e$, Hz	LF	HF	LF	HP	LF	HF	$\tau \times 10^2$, sec
-15.5	7.04	7.11	10.24	4.50	4.85	2.61	2.53	1.53	1.41	9.4
-11.0	4.37	4.31	9.97	6.09	6.88	3.18	3.35	2.02	1.87	7.0
-7.6	2.39	2.54	9.32	-	-	4.86	4.92	2.58	2.54	4.9
-3.2	1.54	1.64	8.02	-	-	-	-	3.83	3.64	3.6
0.8	1.16	1.23	6.53	-	-	-	-	-	-	2.9
3.5	-		-	14.57		11.26		8.50		2.4
7.3	-		-	12.20		8.56		5.14		1.8
11.4	-		-	9.33		5.45		3.18		1.3
16.9	-		-	8.02		4.58		2.65		1.1
26.8	-		-	3.54		2.09		1.23		0.50

[a] Symbols are defined in Table XXII; [b] 0.250 M in dichloromethane; [c] Calculated from the Van Geet equation for methanol.

Table XXVI

Acetylacetonate Methyl PMR Lineshape Parameters[a] and Values of τ for $Ti(acac)_2(2\text{-}IC_6H_4O)_2$[b]

	R			Linewidths, Hz						
				$W_{1/4}$		$W_{1/2}$		$W_{3/4}$		
Temp.,[c] °C	LF	HF	$\delta\upsilon_e$, Hz	LF	HF	LF	HF	LF	HF	$\tau \times 10^2$, sec
-13.4	-	-	15.35	2.91	3.01	1.78	1.79	1.05	1.09	13
-9.1	-	-	14.61	4.41	4.52	2.50	2.62	1.47	1.51	8.2
-2.7	5.95	5.89	14.29	6.61	6.92	3.66	3.68	2.06	2.11	5.5
0.2	3.82	3.98	13.94	-	-	4.66	4.64	2.56	2.43	4.4
4.6	2.46	2.54	13.04	-	-	6.21	6.43	3.29	3.42	3.5
7.5	1.58	1.67	11.63	-	-	-	-	4.84	4.89	2.7
11.1	1.22	1.23	9.22	-	-	-	-	-	-	2.2
12.0	1.06	1.06	6.92	-	-	-	-	-	-	1.9
16.1	-		-	16.49		11.80		7.97		1.4
19.1	-		-	13.14		8.35		4.84		1.0
25.2	-		-	8.93		5.15		3.09		0.75
30.0	-		-	5.54		3.20		1.88		0.48
34.8	-		-	4.11		2.35		1.38		0.35
38.1	-		-	4.10		2.41		1.34		0.36

[a]Symbols are defined in Table XXII; [b]0.250 M in dichloromethane; [c]Calculated from the Van Geet equation for methanol.

Table XXVII

Acetylacetonate Methyl PMR Lineshape Parameters[a] and Values of τ for $Ti(acac)_2(4\text{-}ClC_6H_4O)_2$[b]

	Linewidths, Hz									
	R			$W_{1/4}$		$W_{1/2}$		$W_{3/4}$		
Temp., [c] °C	LF	HF	$\delta\upsilon_e$, Hz	LF	HF	LF	HF	LF	HF	$\tau \times 10^2$, sec
-9.1	-	-	11.24	2.53	2.60	1.53	1.54	0.89	0.87	17
-2.7	-	-	11.09	3.16	3.21	1.81	1.88	1.09	1.08	13
0.2	7.64	7.62	10.79	4.15	4.30	2.40	2.49	1.39	1.42	9.0
4.6	5.05	5.01	10.61	5.48	5.60	2.85	2.93	1.61	1.69	7.3
7.5	3.37	3.37	10.19	-	-	3.71	3.82	2.07	2.10	5.6
11.1	2.14	2.11	9.48	-	-	5.58	5.71	2.73	2.80	4.3
12.0	1.25	1.30	7.52	-	-	-	-	-	-	3.0
15.2	1.30	1.30	7.66	-	-	-	-	-	-	3.0
16.1	1.18	1.19	6.86	-	-	-	-	-	-	2.8
16.8	1.05	1.09	5.09	-	-	-	-	-	-	2.5
18.9	-		-	13.99		10.47		7.60		2.0
19.1	-		-	14.58		11.12		8.34		2.1
20.8	-		-	13.93		10.38		7.22		2.0
25.2	-		-	12.04		7.97		4.98		1.6
30.0	-		-	6.73		3.86		2.23		0.90
34.8	-		-	5.26		3.08		1.75		0.72
38.1	-		-	5.23		3.02		1.77		0.73

[a]Symbols are defined in Table XXII; [b]0.300 M in dichloromethane; [c]Calculated from the Van Geet equation for methanol.

Table XXVIII

Acetylacetonate-Methyl PMR Lineshape Parameters[a] and Values of τ for $Ti(acac)_2(4\text{-}^{i}PrC_6H_4O)_2$[b]

	R			Linewidths, Hz						
				$W_{1/4}$		$W_{1/2}$		$W_{3/4}$		
Temp.,[c] °C	LF	HF	$\delta\upsilon_e$, Hz.	LF	HF	LF	HF	LF	HF	$\tau \times 10^2$, sec
6.4	9.28	9.17	12.02	4.30	4.29	2.43	2.41	1.38	1.41	8.9
8.5	6.85	6.65	11.84	4.98	4.98	2.72	2.78	1.63	1.64	7.5
12.3	4.56	4.49	11.48	6.74	6.88	3.45	3.43	1.99	2.02	5.9
14.1	3.44	3.37	11.33	-	-	4.07	4.13	2.25	2.28	5.1
17.5	2.63	2.52	10.87	-	-	5.13	5.07	2.67	2.65	4.3
20.2	2.00	1.93	10.31	-	-	-	-	3.34	3.35	3.7
20.9	1.56	1.54	9.36	-	-	-	-	4.17	4.31	3.1
23.8	1.39	1.31	8.71	-	-	-	-	5.37	5.34	2.9
25.2	1.15	1.10	6.92	-	-	-	-	-	-	2.4
26.8	1.06	1.03	5.17	-	-	-	-	-	-	2.2
27.9	1.04	1.01	4.31	-	-	-	-	-	-	2.1
30.0	-		-	14.95		10.69		7.49		1.7
32.0	-		-	12.86		8.56		5.20		1.3
37.2	-	-	-	9.87		6.18		3.46		1.1
39.7	-	-	-	8.07		4.72		2.72		0.91

[a]Symbols are defined in Table XXII; [b]0.300 M in dichloromethane; [c]Calculated from the Van Geet equation for methanol.

Table XXIX

Acetylacetonate Methyl PMR Lineshape Parameters[a] and Values of τ for $Ti(acac)_2(2\text{-}^{i}PrC_6H_4O)_2$[b]

	R			Linewidths, Hz						
				$W_{1/4}$		$W_{1/2}$		$W_{3/4}$		
Temp.,[c] °C	LF	HF	$\delta\upsilon_e$, Hz	LF	HF	LF	HF	LF	HF	$\tau \times 10^2$, sec
14.6	6.99	7.09	10.17	4.20	4.40	2.40	2.44	1.37	1.42	8.8
15.5	6.06	6.31	10.17	4.66	4.62	2.52	2.56	1.44	1.45	8.3
17.9	4.91	5.01	9.99	5.31	5.66	2.77	2.83	1.61	1.63	7.5
20.3	3.67	3.87	9.84	-	-	3.39	3.32	1.92	1.85	6.3
22.1	2.92	3.05	9.66	-	-	3.94	3.99	2.14	2.22	5.4
25.0	1.85	1.99	8.88			-	-	3.10	2.88	4.2
25.1	2.02	2.11	9.12	-		5.80	5.97	2.76	2.80	4.4
28.6	1.39	1.52	7.94	-	-	-	-	4.43	3.86	3.5
30.2	1.16	1.21	6.68	-	-	-	-	-	-	2.9
32.2	1.04	1.15	5.37	-	-	-	-	-	-	2.6
33.6	-		3.46	-	-	-	-	-	-	2.4
36.1	-		-	13.72		9.85		6.57		2.1
40.0	-		-	10.86		6.54		3.79		1.5
43.6	-		-	8.90		5.30		3.19		1.3
47.0	-		-	7.12		4.14		2.34		1.0

[a]Symbols are defined in Table XXII; [b]0.300 M in dichloromethane; [c]Calculated from the Van Geet equation for methanol.

Table XXX

Acetylacetonate Methyl PMR Lineshape Parameters[a] and Values of τ for $Ti(acac)_2(2\text{-}(C_6H_5)C_6H_4O)_2$[b]

	R			Linewidths, Hz						
				$W_{1/4}$		$W_{1/2}$		$W_{3/4}$		
Temp., [c] °C	LF	HF	$\delta\upsilon_e$, Hz	LF	HF	LF	HF	LF	HF	$\tau \times 10^2$, sec
20.5	3.69	3.69	10.05	-	-	3.36	3.21	1.85	1.84	6.3
22.9	2.48	2.47	9.50	-	-	4.68	4.28	2.45	2.28	5.0
24.3	1.92	1.91	9.09	-	-	-	-	2.94	2.74	4.3
27.3	1.33	1.36	7.78	-	-	-	-	-	-	3.3
29.4	1.12	1.12	6.33	-	-	-	-	-	-	2.8
30.2	-		-	14.72		11.65		9.34		2.5
32.6	-		-	13.69		10.32		7.52		2.2
36.2	-		-	10.98		7.44		4.63		1.6
37.4	-		-	9.58		6.19		3.72		1.4
41.5	-		-	6.85		4.00		2.36		1.0

[a] Symbols are defined in Table XXII; [b] 0.300 M in dichloromethane; [c] Calculated from the Van Geet equation for methanol.

Table XXXI

Acetylacetonate Methyl PMR Lineshape Parameters[a] and Values of τ for $Ti(acac)_2(2,6\text{-}^{i}Pr_2C_6H_3O)_2$[b]

	R			Linewidths, Hz						
				$W_{1/4}$		$W_{1/2}$		$W_{3/4}$		
Temp., [c] °C	LF	HF	$\delta\upsilon_e$, Hz	LF	HF	LF	HF	LF	HF	$\tau \times 10^2$, sec
13.8	12.76	12.67	9.42	3.02	3.01	1.77	1.75	1.05	1.05	13
16.1	8.47	8.36	9.41	3.67	3.61	2.02	2.02	1.17	1.16	11
22.7	4.33	4.51	9.22	5.92	5.43	2.78	2.86	1.58	1.62	7.6
25.2	4.29	4.33	9.22	6.00	5.55	2.89	2.81	1.66	1.60	7.5
28.6	1.84	1.99	8.32	-	-	-	-	2.84	2.63	4.5
29.5	1.63	1.60	7.86	-	-	-	-	3.23	3.38	4.2
33.3	1.35	1.38	7.17	-	-	-	-	-	-	3.7
35.2	1.11	1.11	5.64	-	-	-	-	-	-	3.0
37.9	-		-	13.80		11.02		8.70		2.9
40.6	-		-	11.08		7.48		4.79		1.9

[a]Symbols are defined in Table XXII; [b]0.300 M in dichloromethane; [c]Calculated from the Van Geet equation for methanol.

Table XXXII

Acetylacetonate Methyl PMR Lineshape Parameters[a] and Values of τ for $Ti(acac)_2(2,6\text{-}^{i}Pr_2C_6H_3O)_2$[b]

	R			Linewidths, Hz						
				$W_{1/4}$		$W_{1/2}$		$W_{3/4}$		
Temp., [c] °C	LF	HF	$\delta\upsilon_e$, Hz	LF	HF	LF	HF	LF	HF	$\tau \times 10^2$, sec
22.0	5.89	6.09	10.90	4.70	5.19	2.60	2.69	1.49	1.51	10
25.5	4.67	4.80	10.89	6.00	5.95	3.06	3.10	1.73	1.75	8.5
28.0	3.60	3.69	10.85	-	-	3.69	3.68	2.03	2.05	6.9
31.6	2.29	2.41	10.29	-	-	-	-	2.73	2.72	5.0
33.3	2.03	2.09	10.22	-	-	-	-	2.96	2.93	4.6
35.6	1.51	1.70	9.71	-	-	-	-	3.96	3.87	3.8
37.0	1.37	1.48	9.30	-	-	-	-	4.84	4.95	3.4
40.4	1.02	1.12	5.56	-	-	-	-	-	-	2.6
40.8	1.01	1.13	5.47	-	-	-	-	-	-	2.5
44.5	-		-	15.40		10.60		6.53		1.9
48.1	-		-	13.42		8.60		5.29		1.6
51.5	-		-	10.47		6.47		4.05		1.2
54.4	-		-	8.89		5.50		3.47		1.1
62.5	-		-	5.93		3.68		1.99		0.64

[a]Symbols are defined in Table XXII; [b]0.250 M in 1,3-dichlorobenzene; [c]Calculated from the Van Geet equations for ethanol and ethylene glycol:

determine the appropriate value of T_2 at each temperature. In the case of the m-dichlorobenzene solutions, the quinaldinate methyl resonance of the $Ti(quin)_2(2,6\text{-}^{i}Pr_2C_6H_3O)_2$ complex was employed as the T_2 reference.

For the $Ti(acac)_2(2,6\text{-}Cl_2C_6H_3O)_2$ complex, the slow exchange region could not be attained; this necessitated the use of a computer fitting of digitized nmr spectra, as described in Section II-C-2c. The cis-$Zr(acac)_2Cl_2$ complex was employed as a source of linewidths for the program input and these linewidths were held constant at each temperature. Below coalescence, the only fixed parameter employed was the linewidth; the program was allowed to search for the best combination of τ_A, τ_B, and $\delta\upsilon$ which produced the closest fit to the observed spectrum. For temperatures above coalescence, problems were encountered in obtaining reasonable computer-fittings when $\delta\upsilon$ was allowed to be a variable. To overcome this problem, the values of $\delta\upsilon$ obtained below coalescence were extrapolated into the intermediate exchange region. Values for $\delta\upsilon$ from this extrapolation were used as input data for temperatures above coalescence and remained fixed. The resulting mean lifetimes obtained through this procedure are listed in Table XXXIII.

The concentration dependence of the mean residence times for acetylacetonate methyl group exchange in $Ti(acac)_2(phenoxy)_2$ complexes, presented in Table XXXIV, demonstrates that the rate of exchange is independent of concentration and is a first-order process.

Arrhenius activation parameters were obtained in the usual fashion from the least-squares straight line plot of log k versus 1/T, where $k = 1/2\tau$ is the first-order rate constant for exchange. These plots are shown in Figures 34 through 38 for exchange of acetylacetonate methyl

Table XXXIII

Temperature Dependence of Mean Residence Times for Exchange of Acetylacetonate Methyl Groups in $Ti(acac)_2(2,6\text{-}Cl_2C_6H_3O)_2$ from Computer-fitted Spectra[a,b]

Temp, [c] °C	$1/T \times 10^3$	τ_A, sec	τ_B, sec	2τ, sec	$k (=1/2\tau)$, sec^{-1}	$\delta\upsilon_o$, Hz
-63.7	4.77	0.20	0.19	0.20	5.0	10.30
-61.1	4.72	0.16	0.15	0.16	6.3	10.39
-57.1	4.63	0.11	0.11	0.11	9.0	10.28
-51.5	4.51	0.059	0.058	0.058	17.2	10.73
-47.9	4.44	0.044	0.045	0.044	22.7	10.69
-42.6	4.34	0.026	0.030	0.028	35.7	10.23
-38.4	4.26	0.018	0.028	0.022	45.5	10.06[d]
-35.6	4.21	0.013	0.018	0.015	66.7	10.04[d]
-29.5	4.10	0.0099	0.013	0.011	90.9	9.98[d]

[a] 0.250 M in dichloromethane; [b] The τ_A, τ_B, and $\delta\upsilon_o$ parameters were allowed to vary in the computer-fitting procedure unless noted otherwise; [c] Calculated from the Van Geet equation for methanol; [d] Fixed parameter.

Table XXXIV

Concentration Dependence of Mean Residence Times for Acetylacetonate Methyl Group Exchange in $Ti(acac)_2(phenoxy)_2$ Complexes at Selected Temperatures

Phenoxy Ligand	Solvent	Temp., °C	Concentration, M	τ, sec
$2,6\text{-}Cl_2C_6H_3O$	CH_2Cl_2	-53.3	0.250	0.036[a]
			0.150	0.041
		-43.6	0.250	0.016[a]
			0.150	0.014
$2\text{-}ClC_6H_4O$	CH_2Cl_2	-0.8	0.250	0.032[a]
			0.150	0.035
		5.5	0.250	0.020[a]
			0.150	0.021
$2\text{-}IC_6H_4O$	CH_2Cl_2	8.0	0.300	0.024[a]
			0.150	0.025
		16.7	0.300	0.013[a]
			0.150	0.014
$4\text{-}ClC_6H_4O$	CH_2Cl_2	11.4	0.300	0.033[a]
			0.150	0.034
		22.2	0.300	0.015[a]
			0.150	0.016
$4\text{-}^iPrC_6H_4O$	CH_2Cl_2	6.4	0.300	0.089
			0.150	0.109
		8.5	0.300	0.075
			0.150	0.083
		20.2	0.300	0.037
			0.150	0.038
		23.8	0.300	0.029
			0.150	0.028
		32.0	0.300	0.013
			0.150	0.014

Table XXXIV (continued)

2-^{i}PrC$_6$H$_4$O	CH_2Cl_2	28.6	0.300	0.035
			0.150	0.033
		36.1	0.300	0.021
			0.150	0.019
2,6-^{i}Pr$_2$C$_6$H$_3$O	CH_2Cl_2	28.7	0.300	0.048[a]
			0.150	0.043
		40.0	0.300	0.023[a]
			0.150	0.021
2,6-^{i}Pr$_2$C$_6$H$_3$O	1,3-$C_6H_4Cl_2$	37.0	0.250	0.034
			0.150	0.034
		44.5	0.250	0.019
			0.150	0.020
		48.1	0.250	0.016
			0.150	0.017
2-(C_6H_5)C$_6$H$_4$O	CH_2Cl_2	20.5	0.300	0.063
			0.150	0.067
		24.3	0.300	0.043
			0.150	0.043
		30.2	0.300	0.025
			0.150	0.025
		36.2	0.300	0.016
			0.150	0.016

[a] Calculated from the activation parameters of Table XXXV at the indicated temperatures.

groups in $Ti(acac)_2(phenoxy)_2$ complexes.

Arrhenius and Eyring activation parameters for exchange of acetylacetonate methyl groups in $Ti(acac)_2(phenoxy)_2$ complexes are collected in Table XXXV. As usual, the error limites in these activation parameters reflect only the random scatter of the data points in the Arrhenius plots, and are estimated at the 95% confidence level.

A Total Lineshape analysis was performed on the isopropyl methyl group exchange in the $Ti(acac)_2(2\text{-}^iPrC_6H_4O)_2$, $Ti(acac)_2Cl(2,6\text{-}^iPr_2C_6H_3O)$, and $Ti(acac)_2(2,6\text{-}^iPr_2C_6H_3O)_2$ complexes in dichloromethane solution; the latter complex was also studied in m-dichlorobenzene solution. The analysis was performed on the most intense low field doublet of the isopropyl methyl quartet; either doublet may be used to extract kinetic data. For the $Ti(acac)_2Cl(2,6\text{-}^iPr_2C_6H_3O)$ complex, both doublets were used and the results averaged to determine mean residence times. Mean lifetimes were obtained by comparing experimental lineshape parameters (listed in Tables XXXVI through XXXIX) with theoretical spectra generated with the Gutowsky-Holm equation (17), as described in Section II-C. The temperature dependence of $\delta\upsilon$ was measured in the slow exchange region and the straight line portion extrapolated into the intermediate and fast exchange regions; the data are listed in Appendix B. For the $Ti(acac)_2(2,6\text{-}^iPr_2C_6H_3O)_2$ complex in m-dichlorobenzene and the $Ti(acac)_2Cl(2,6\text{-}^iPr_2C_6H_3O)$ complex in dichloromethane, values for $\delta\upsilon$ for both doublets were used in the determination of the temperature dependence of $\delta\upsilon$. For dichloromethane solutions, the acetylacetonate methyl resonance of <u>cis</u>-$Zr(acac)_2Cl_2$ was employed as the T_2 reference, while the quinaldinate methyl resonance of the $Ti(quin)_2(2,6\text{-}^iPr_2C_6H_3O)_2$ complex was used as the T_2 reference for m-dichlorobenzene solutions.

Table XXXV

Kinetic Data for Acetylacetonate Methyl Group Exchange in $Ti(acac)_2(phenoxy)_2$ Complexes

Phenoxy Ligand	Solvent	k_{298} (sec^{-1})	$\Delta H^{\neq}_{298}$ (kcal/mole)	$\Delta S^{\neq}_{298}$ (eu)	$\Delta G^{\neq}_{298}$ (kcal/mole)	E_a (kcal/mole)	log A
2,6-$Cl_2C_6H_3O$[a]	CH_2Cl_2	2.6×10^3	8.1 ± 0.5 [e]	-15.7 ± 2.1	12.80 ± 0.05	8.7 ± 0.5	9.79 ± 0.45
2-ClC_6H_4O[a]	CH_2Cl_2[c]	84	9.8 ± 0.6	-16.8 ± 2.2	14.82 ± 0.06	10.4 ± 0.6	9.56 ± 0.49
	CH_2Cl_2[d]	86	8.9 ± 0.6	-19.7 ± 2.0	14.80 ± 0.06	9.5 ± 0.6	8.93 ± 0.45
2-IC_6H_4O[b]	CH_2Cl_2	67	11.0 ± 0.6	-13.2 ± 2.0	14.96 ± 0.04	11.6 ± 0.6	10.33 ± 0.43
4-ClC_6H_4O[b]	CH_2Cl_2	34	11.2 ± 0.8	-13.7 ± 2.6	15.36 ± 0.04	11.9 ± 0.8	10.24 ± 0.58
4-$^iPrC_6H_4O$[b]	CH_2Cl_2	21	11.3 ± 0.6	-14.5 ± 2.2	15.66 ± 0.02	11.9 ± 0.6	10.05 ± 0.64
2-$^iPrC_6H_4O$[b]	CH_2Cl_2	12	11.9 ± 0.4	-13.7 ± 1.2	16.43 ± 0.01	12.5 ± 0.4	10.24 ± 0.26
2-$(C_6H_5)C_6H_4O$[b]	CH_2Cl_2	12	15.0 ± 0.4	-3.2 ± 1.4	15.97 ± 0.01	15.6 ± 0.4	12.53 ± 0.31
2,6-$^iPr_2C_6H_3O$	CH_2Cl_2[b]	8.1	11.8 ± 1.7	-15 ± 6	16.21 ± 0.05	12.4 ± 1.7	10.0 ± 1.2
	1,3-$C_6H_4Cl_2$[a]	5.9	13.2 ± 0.3	-10.6 ± 1.0	16.39 ± 0.02	13.8 ± 0.3	10.91 ± 0.22

[a] 0.250 M; [b] 0.300 M; [c] Van Geet temperatures; [d] Varian temperatures; [e] All errors are random errors estimated at the 95% confidence level.

Table XXXVI

Isopropyl Methyl PMR Lineshape Parameters[a] and Values of τ for $Ti(acac)_2(2\text{-}^iPrC_6H_4O)_2$[b]

	R			Linewidths, Hz						
				$W_{1/4}$		$W_{1/2}$		$W_{3/4}$		
Temp., [c] °C	LF	HF	$\delta\upsilon_e$, Hz	LF	HF	LF	HF	LF	HF	$\tau \times 10^2$, sec
-8.4	1.90	1.96	2.49	-	-	-	-	1.06	1.09	25
-1.0	1.50	1.54	2.13	-	-	-	-	1.16	1.21	20
1.7	1.28	1.30	1.95	-	-	-	-	-	-	18
3.8	1.16	1.17	1.74	-	-	-	-	-	-	18
4.9	1.13	1.15	1.65	-	-	-	-	-	-	17
7.3	1.04	1.05	1.28	-	-	-	-	-	-	15
8.2	1.03	1.03	1.14	-	-	-	-	-	-	14
12.1	-		-	4.18		2.79		1.94		13
12.6	-		-	4.04		2.75		1.91		13
14.6	-		-	3.67		2.42		1.57		13
15.5	-		-	3.55		2.25		1.39		11
17.9	-		-	3.19		1.99		1.26		11
19.9	-		-	2.86		1.78		1.08		10
20.3	-		-	2.83		1.71		1.04		10
22.9	-		-	2.51		1.55		0.93		9.4
24.8	-		-	2.35		1.47		0.87		9.1
25.0	-		-	2.40		1.44		0.86		9.2

[a] Symbols are defined in Table XXII; [b] 0.300 M in dichloromethane; [c] Calculated from the Van Geet equation for methanol.

Table XXXVII

Isopropyl Methyl PMR Lineshape Parameters[a] and Values of τ for $Ti(acac)_2(2,6\text{-}^iPr_2C_6H_3O)_2$[b]

	R			Linewidths, Hz						
				$W_{1/4}$		$W_{1/2}$		$W_{3/4}$		
Temp., [c] °C	LF	HF	$\delta\upsilon_e$, Hz	LF	HF	LF	HF	LF	HF	$\tau \times 10^2$, sec
3.0	3.81	3.76	4.86	-	-	1.71	1.80	0.95	1.05	15
7.7	2.39	2.27	4.44	-	-	2.22	2.32	1.17	1.23	12
13.8	1.49	1.55	3.54	-	-	-	-	1.79	1.86	9.3
16.1	1.21	1.31	3.06	-	-	-	-	-	-	8.6
22.4	1.04	1.06	1.83	-	-	-	-	-	-	7.5
22.7	-		-	-	-	4.78		3.26		6.8
25.2	-		-	-	-	4.31		2.84		6.5
28.6	-		-	5.03		2.84		1.71		5.2
29.5	-		-	4.23		2.33		1.42		4.6
33.3	-		-	3.35		2.05		1.21		4.6
35.2	-		-	2.72		1.55		0.91		3.7
40.6	-		-	2.09		1.18		0.67		3.3

[a] Symbols are defined in Table XXII; [b] 0.300 M in dichloromethane; [c] Calculated from the Van Geet equations for methanol and ethylene glycol.

Table XXXVIII

Isopropyl Methyl PMR Lineshape Parameters[a] and Values of τ for $Ti(acac)_2(2,6\text{-}^iPr_2C_6H_3O)_2$[b]

Temp., [c] °C	$\delta\upsilon_e$, [d] Hz	Linewidths, Hz						$\tau \times 10^2$, sec
		$W_{1/4}$		$W_{1/2}$		$W_{3/4}$		
		LFD[e]	HFD[f]	LFD	HFD	LFD	HFD	
16.7	2.30 ; 2.30	-	-	-	-	-	-	17
19.7	1.59 ; 1.56	-	-	-	-	-	-	13
25.5	-	-	-	3.66	3.51	2.30	2.23	12
28.0	-	-	-	2.94	2.99	1.75	1.79	10
31.6	-	4.19	4.13	2.31	2.29	1.37	1.32	9.3
37.0	-	3.08	3.08	1.77	1.75	0.98	1.01	8.1

[a] Symbols are defined in Table XXII; [b] 0.250 M in 1,3-dichlorobenzene; [c] Calculated from the Van Geet equations for methanol and ethylene glycol; [d] Separations for low- and high-field doublets, respectively; [e] Low field doublet; [f] High field doublet.

Table XXXIX

Isopropyl Methyl PMR Lineshape Parameters[a] and Values of τ for $Ti(acac)_2Cl(2,6\text{-}{}^{i}Pr_2C_6H_3O)$[b]

	R			Linewidths, Hz						
				$W_{1/4}$		$W_{1/2}$		$W_{3/4}$		
Temp.,[c] °C	LF	HF	$\delta\upsilon_e$, Hz[d]	LF	HF	LF	HF	LF	HF	$\tau \times 10^2$, sec
-18.7	1.50	1.47	2.69 ; 2.72	-	-	-	-	1.47	1.56	16
-17.4	1.49	1.41	2.66 ; 2.65	-	-	-	-	1.51	1.63	16
-14.9	1.36	1.27	2.50 ; 2.50	-	-	-	-	-	-	15
-11.7	1.17	1.10	2.05 ; 2.00	-	-	-	-	-	-	14
-7.6	1.03	1.03	1.37 ; 1.17	-	-	-	-	-	-	11
-3.0	-		-	-		3.63		2.48		11
-1.5	-		-	5.21		3.51		2.35		11
1.1	-		-	4.57		2.91		1.75		10
3.1	-		-	4.01		2.43		1.47		8.4
4.8	-		-	3.86		2.37		1.37		8.3
5.7	-		-	3.49		2.10		1.19		7.4
7.1	-		-	3.32		1.91		1.14		7.0
7.3	-		-	3.82		2.36		1.47		8.9
10.0	-		-	3.36		2.02		1.19		7.8
10.2	-		-	2.96		1.71		1.01		6.6
10.6	-		-	3.11		1.87		1.11		7.3
12.5	-		-	2.81		1.63		0.99		6.6

[a]Symbols are defined in Table XXII; [b]0.300 M in dichloromethane; [c]Calculated from the Van Geet equation for methanol; [d]Separations for low- and high-field doublets, respectively.

The concentration dependence of the mean residence times for isopropyl methyl group exchange, presented in Table XL, demonstrate that the rate of exchange is independent of concentration and is a first-order process.

Arrhenius activation parameters were obtained in the usual fashion from the least-squares straight line plots of log k versus 1/T, where $k = 1/2\tau$ is the first-order rate constant for isopropyl methyl group exchange. These plots are shown in Figures 36 through 39 for exchange of isopropyl methyl groups in bis(acetylacetonato)titanium(IV) complexes containing isopropyl-substituted phenoxy ligands. Arrhenius and Eyring activation parameters for exchange of isopropyl methyl groups in these complexes are collected in Table XLI. The error limits attached to these activation parameters reflect only the random scatter of the data points, estimated at the 95% confidence level, and do not contain any possible contributions from systematic errors (59,60).

Table XXXV also demonstrates that substantial errors are introduced in kinetic parameters when the Varian methanol "thermometer" is used to measure the sample temperatures. For the $Ti(acac)_2(2\text{-}ClC_6H_4O)_2$ complex, activation parameters were calculated utilizing temperatures calculated from Van Geet's equation (79) for methanol and the Varian methanol calibration curve. The latter results in decreased values for $\Delta H^{\neq}$, E_a, and log A, while $\Delta S^{\neq}$ becomes more negative; these differences are outside the error limits estimated at the 95% confidence level. Thus, serious systematic errors are introduced in the activation parameters through the use of temperatures derived from the Varian methanol chart. While other activation parameters change, the $\Delta G^{\neq}$ values are constant using these two temperature scales. This suggests that the $\Delta G^{\neq}$ parameter is insensitive to systematic errors, as the negative error in $\Delta H^{\neq}$ is offset by the error in $\Delta S^{\neq}$, resulting

Table XL

Concentration Dependence of Mean Residence Times for Isopropyl Methyl Group Exchange in Bis(acetylacetonato)titanium(IV) Complexes Containing Isopropyl-substituted Phenoxy Ligands

Complex	Solvent	Temp., °C	Concentration, M	τ, sec
$Ti(acac)_2(2\text{-}^iPrC_6H_4O)_2$	CH_2Cl_2	3.8	0.300	0.175
			0.150	0.179
		12.6	0.300	0.133
			0.150	0.128
$Ti(acac)_2(2,6\text{-}^iPr_2C_6H_3O)_2$	CH_2Cl_2	15.5	0.300	0.089[a]
			0.150	0.093
		23.4	0.300	0.064[a]
			0.150	0.064
$Ti(acac)_2(2,6\text{-}^iPr_2C_6H_3O)_2$	$1,3\text{-}C_6H_4Cl_2$	13.5	0.250	0.267
			0.150	0.281
		25.5	0.250	0.120
			0.150	0.117
		37.0	0.250	0.085
			0.150	0.078
$Ti(acac)_2Cl(2,6\text{-}^iPr_2C_6H_3O)$	CH_2Cl_2	-17.4	0.300	0.162
			0.150	0.161
		-1.5	0.300	0.113
			0.150	0.115
		1.1	0.300	0.100
			0.150	0.095
		10.6	0.300	0.073
			0.150	0.064

[a] Calculated from the activation parameters of Table XLI at the indicated temperatures.

Table XLI

Kinetic Data for Isopropyl Methyl Group Exchange in Bis(acetylacetonato)titanium(IV) Complexes Containing Isopropyl-substituted Phenoxy Ligands

Complex	Solvent	k_{298} (sec^{-1})	$\Delta H^{\neq}_{298}$ (kcal/mole)	$\Delta S^{\neq}_{298}$ (eu)	$\Delta G^{\neq}_{298}$ (kcal/mole)	E_a (kcal/mole)	log A
$Ti(acac)_2$-$(2\text{-}^{i}PrC_6H_4O)_2$	CH_2Cl_2 [a]	5.5	4.3 ± 0.2 [c]	-40.7 ± 0.8	16.43 ± 0.01	4.9 ± 0.2	4.32 ± 0.19
$Ti(acac)_2$-$(2,6\text{-}^{i}Pr_2C_6H_3O)_2$	CH_2Cl_2 [a]	8.3	6.5 ± 0.7	-32.6 ± 2.3	16.19 ± 0.03	7.1 ± 0.7	6.10 ± 0.50
$Ti(acac)_2$-$(2,6\text{-}^{i}Pr_2C_6H_3O)_2$	$1,3\text{-}C_6H_4Cl_2$ [b]	4.2	5.7 ± 1.7	-36.5 ± 5.7	16.60 ± 0.04	6.3 ± 1.7	5.3 ± 1.2
$Ti(acac)_2$-$Cl(2,6\text{-}^{i}Pr_2C_6H_3O)$	CH_2Cl_2 [a]	10	3.7 ± 0.6	-41.5 ± 2.2	16.08 ± 0.06	4.3 ± 0.6	4.16 ± 0.47

[a] 0.300 M; [b] 0.250 M; [c] All errors are random errors estimated at the 95% confidence level.

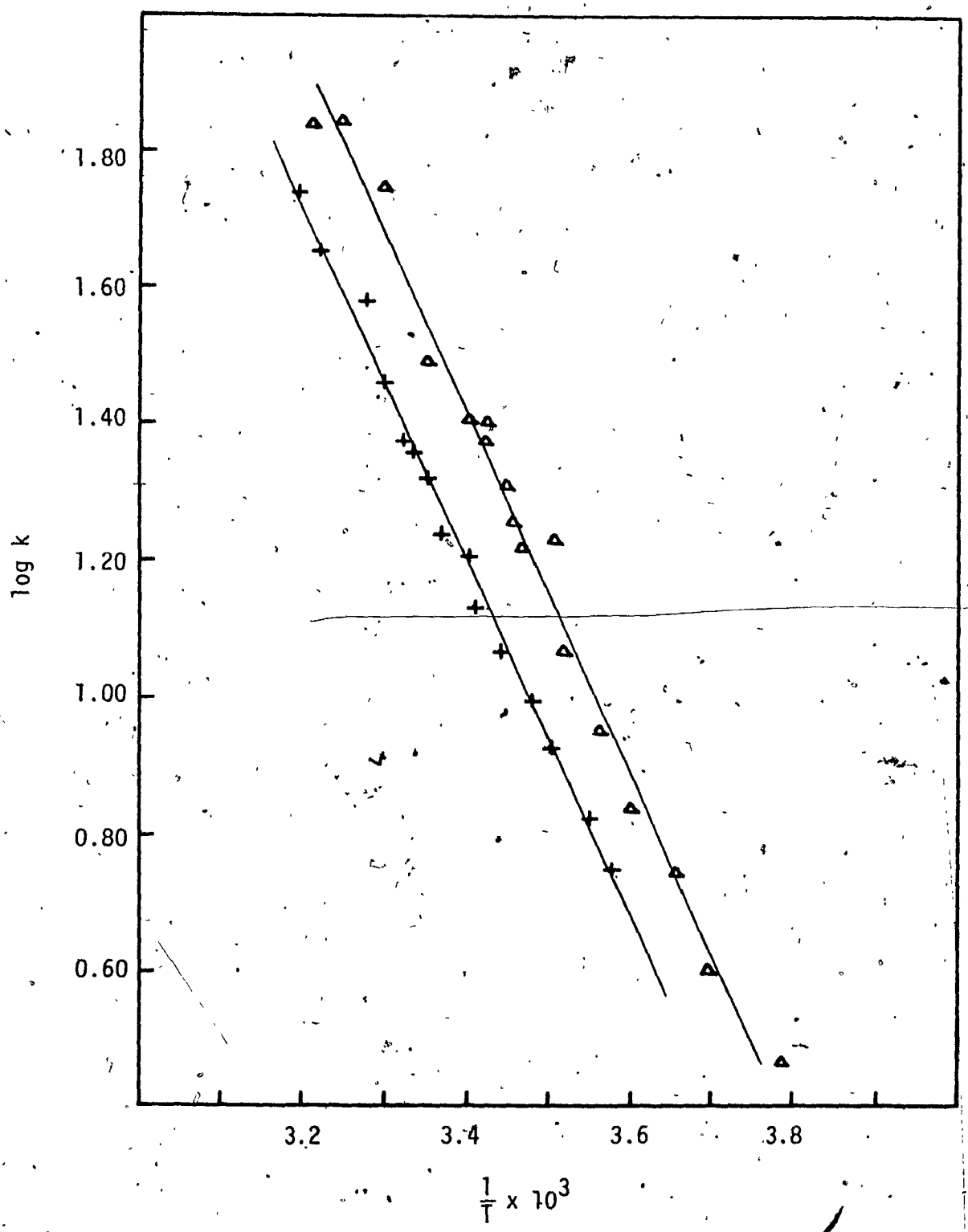

Figure 34.- Arrhenius (log k versus 1/T) least-squares plots for acetylacetonate methyl group exchange in the $Ti(acac)_2(4\text{-}ClC_6H_4O)_2$ (+) and $Ti(acac)_2(4\text{-}^iPrC_6H_4O)_2$ (Δ) complexes in dichloromethane solution.

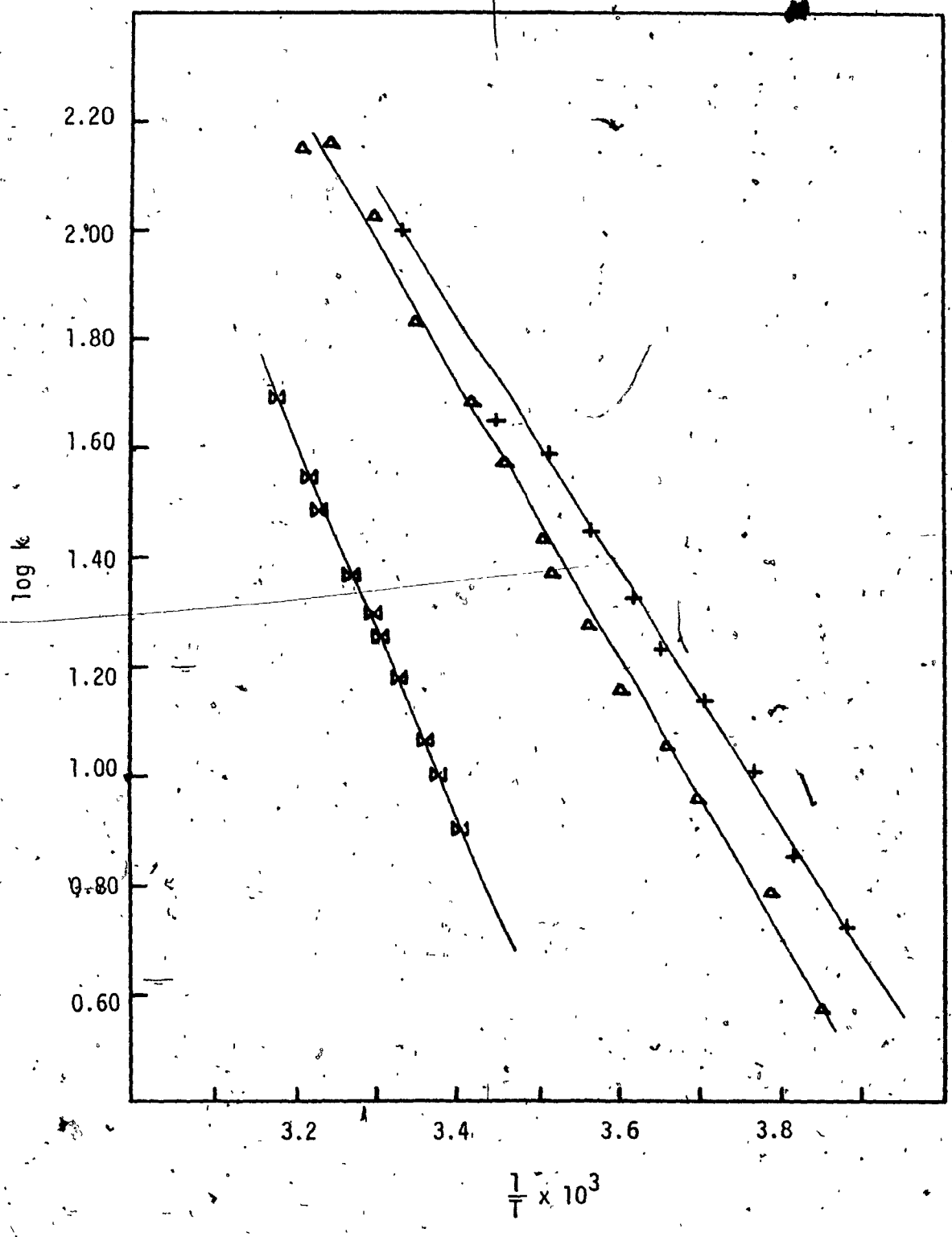

Figure 35.- Arrhenius (log k versus 1/T) least-squares plots for acetylacetonate methyl group exchange in the $Ti(acac)_2(2\text{-}(C_6H_5)C_6H_4O)_2$ (⋈), $Ti(acac)_2(2\text{-}IC_6H_4O)_2$ (Δ), and $Ti(acac)_2(2\text{-}ClC_6H_4O)_2$ (+) complexes in dichloromethane solution.

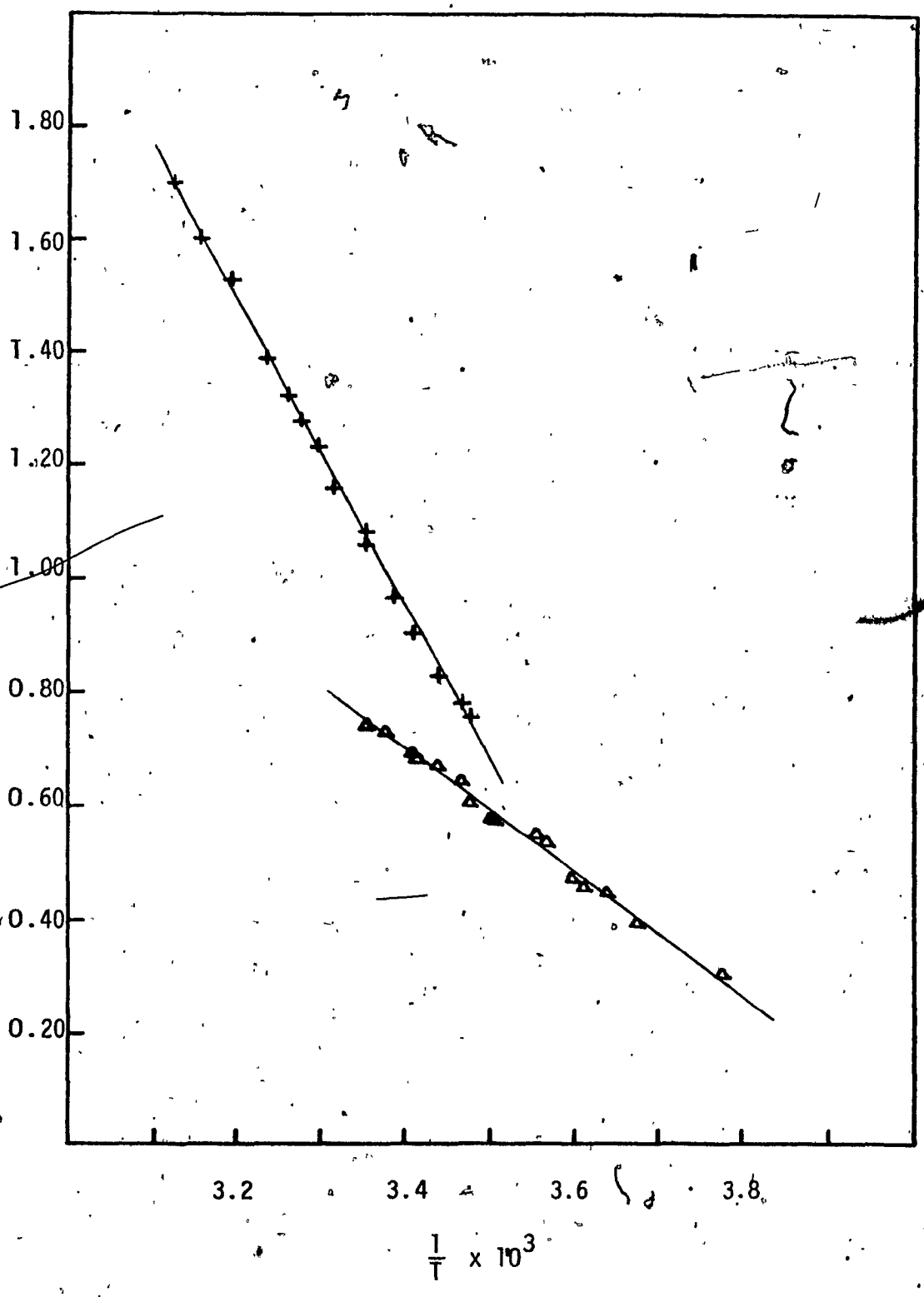

Figure 36.- Arrhenius (log k versus 1/T) least-squares plots for acetylacetonate methyl group (+) and isopropyl methyl group (Δ) exchange in the $Ti(acac)_2(2\text{-}^iPrC_6H_4O)_2$ complex in dichloromethane solution.

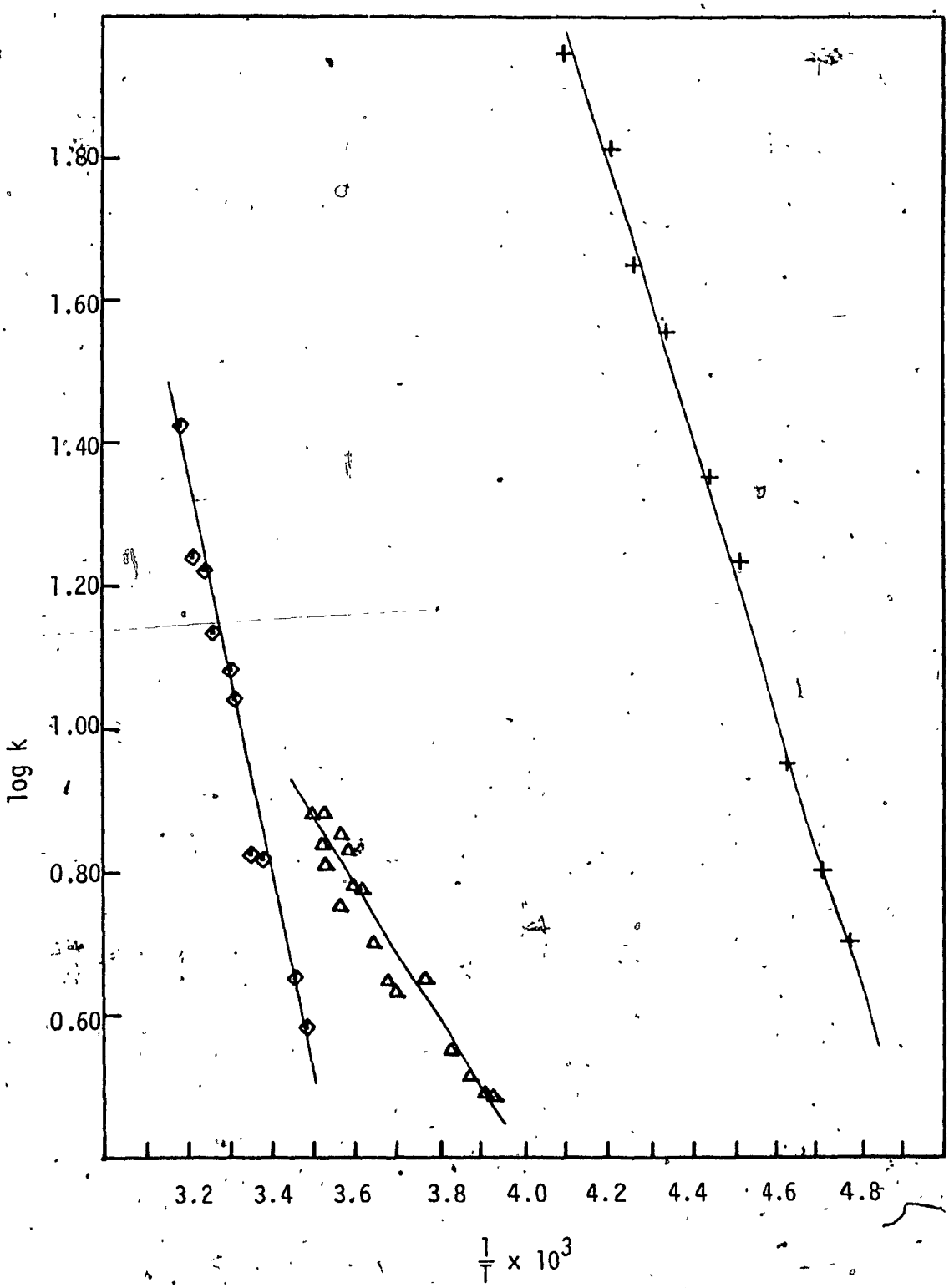

Figure 37.--Arrhenius (log k versus 1/T) least-squares plot for acetylacetonate methyl group exchange in the $Ti(acac)_2(2,6\text{-}Cl_2C_6H_3O)_2$ (+) and $Ti(atac)_2(2,6\text{-}^iPr_2C_6H_3O)_2$ (◇) complexes and isopropyl methyl group exchange in the $Ti(acac)_2Cl(2,6\text{-}^iPr_2C_6H_3O)$ complex (Δ), in dichloromethane solution.

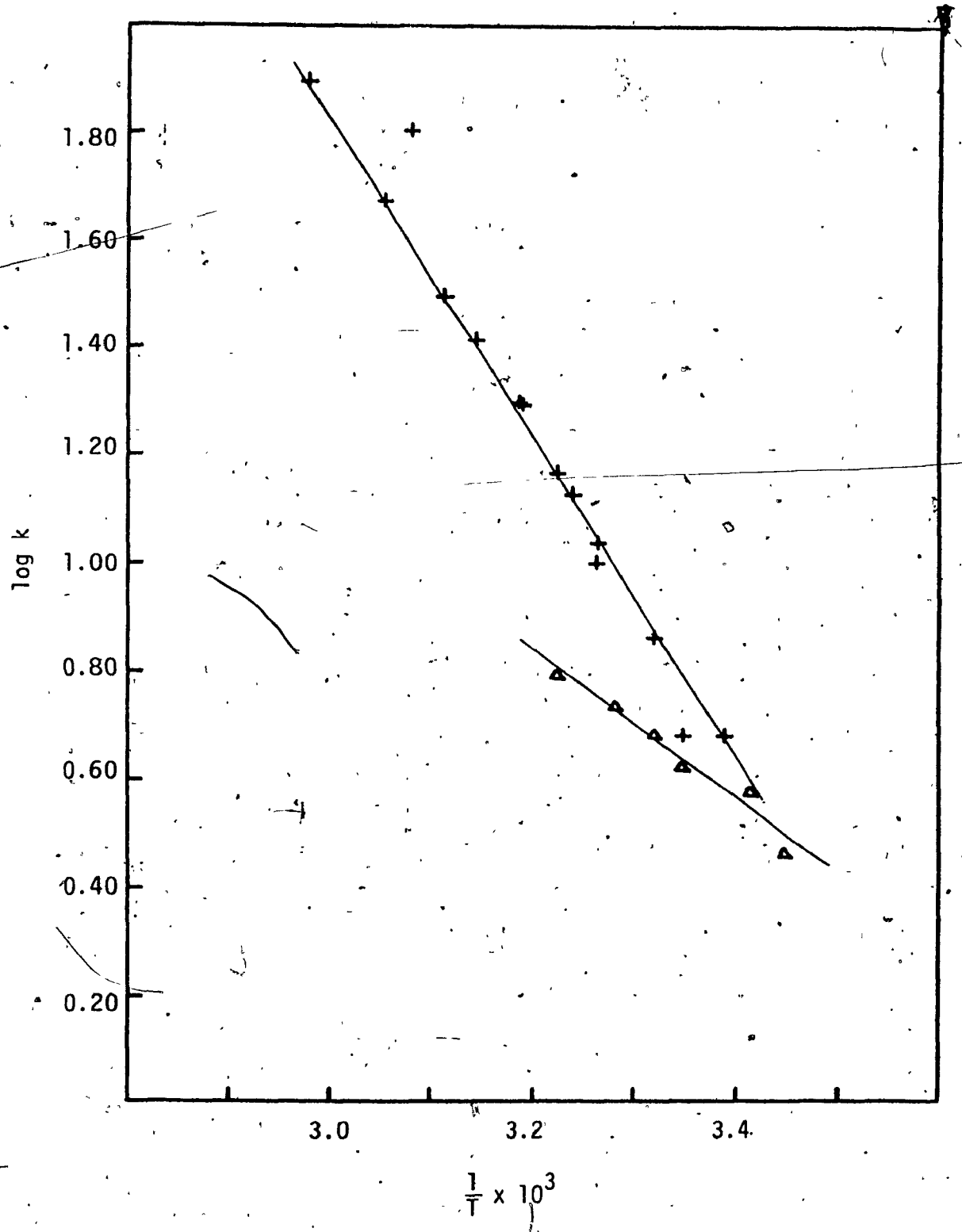

Figure 38.- Arrhenius (log k versus 1/T) least-squares plots for acetylacetonate methyl group (+) and isopropyl methyl group (Δ) exchange in the $Ti(acac)_2(2,6\text{-}^iPr_2C_6H_3O)_2$ complex in 1,3-dichlorobenzene solution.

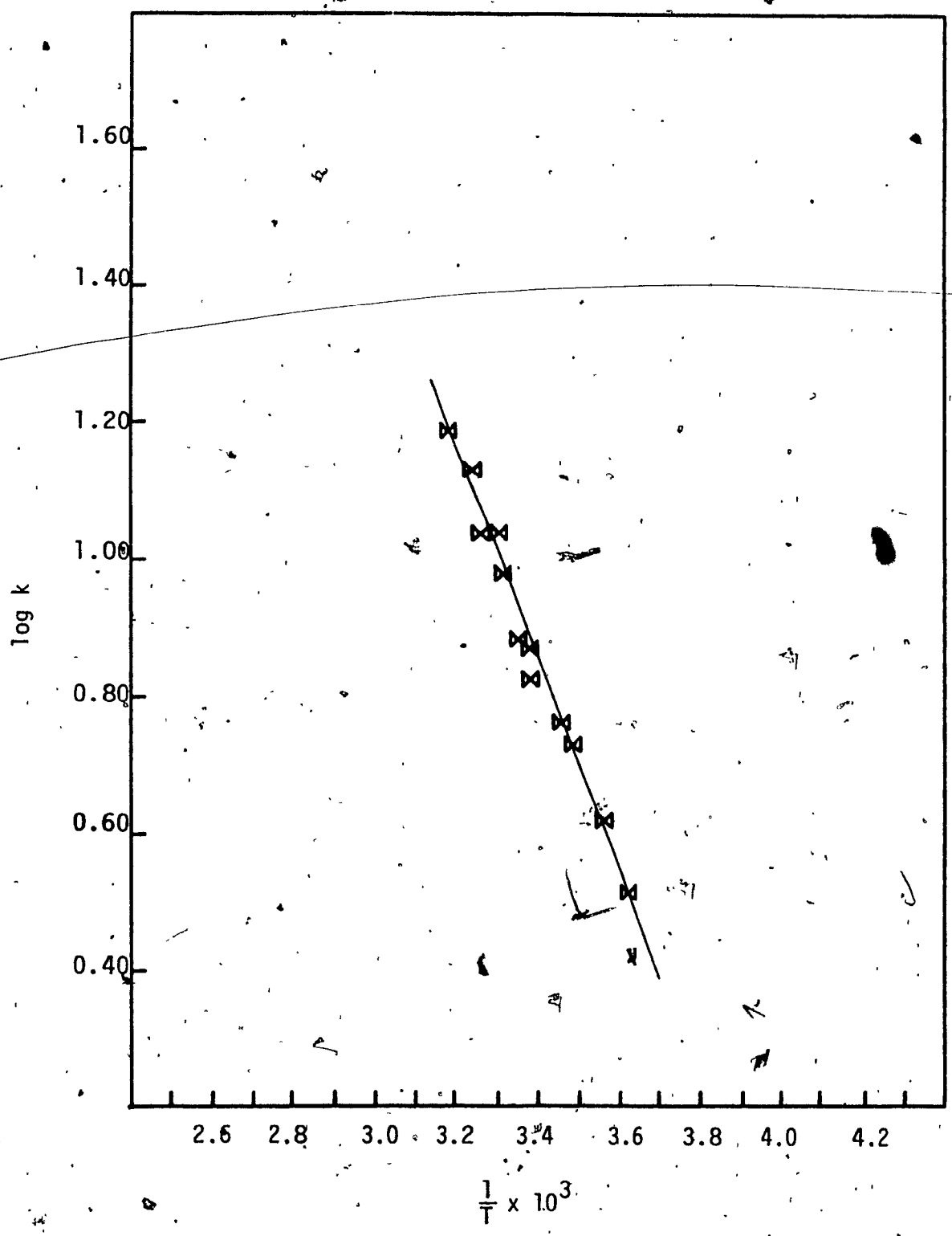

Figure 39.- Arrhenius (log k versus 1/T) least-squares plot for isopropyl methyl group exchange in the $Ti(acac)_2$-$(2,6\text{-}^{i}Pr_2C_6H_3O)_2$ complex in dichloromethane solution.

in no change in $\Delta G^{\neq}$ values.

It is interesting to compare kinetic data for exchange of acetylacetonate methyl groups in $Ti(acac)_2X_2$ [X = halide or pseudo-halide] (Table XXIV) and $Ti(acac)_2(phenoxy)_2$ complexes (Table XXXV). Excluding the $Ti(acac)_2(2,6\text{-}Cl_2C_6H_3O)_2$ complex, the phenoxy complexes are considerably less labile than their halide counterparts. For example, using the $\Delta H^{\neq}$ and $\Delta S^{\neq}$ values in Table XXIV for $Ti(acac)_2Cl_2$, $\Delta G^{\neq}$ may be calculated to be 12.6 kcal/mole, which is ca. 2 - 4 kcal/mole smaller than the corresponding values for the phenoxy complexes. In general, the k_{298} values are reduced by an order of one or two on progressing from halo to phenoxy complexes. This may be a result of electronic or steric effects and data for a wider range of X ligands are necessary before any definite trends can be determined.

Within the phenoxy series of complexes there appears to be some degree of relationship between the Lewis basicity of the phenoxide anion and the rate of rearrangement of its complex. The $2,6\text{-}Cl_2C_6H_3OH$ phenol is the most acidic phenol studied (least basic phenoxide) with a pKa of 7.00 (155); the $Ti(acac)_2(2,6\text{-}Cl_2C_6H_3O)_2$ complex is the most labile of the phenoxy complexes studied. Alkyl-substituted phenols generally possess pKa values in the 10 - 11 range (155) and their phenoxide anions are more basic than halogen-substituted analogues. The alkyl-substituted phenoxy complexes of Table XXXV appear to be less labile than $Ti(acac)_2(2,6\text{-}Cl_2C_6H_3O)_2$. In bonding to the titanium center, the most basic phenoxide anions are expected to possess the strongest Ti-O(phenoxide) bonds and result in a relative weakening of the trans Ti-O(acac) bonds. Should a bond rupture mechanism be operative, the rearrangement rate would be expected to increase as the basicity of the ohenoxide anion increases (pKa of the parent phenol increases). This trend is not observed, which tends to argue against a bond rupture mechanism. However, more data for a wider variety of phenols

are necessary to firmly establish such a relationship.

It must also be pointed out that the use of pKa values for aqueous solutions may not be valid in nonaqueous solvents. For example, 2-t-butylphenol is less acidic than phenol in aqueous solution but is more acidic than phenol in the gas phase (156). The solvent medium attenuates substituent effects in determining the acidities of phenols (156).

Before discussing the kinetic data for isopropyl methyl group exchange in $Ti(acac)_2$(isopropyl-substituted phenoxy)$_2$ complexes, it is necessary to establish the cause of the observed nonequivalence of isopropyl methyl groups and of the exchange process. Two possible sources need be considered: (i) the dissymmetry centered on the titanium renders the isopropyl methyl groups diastereotopic and exchange results from inversion of the molecular configuration, and (ii) hindered rotation about the Ti-O-C(phenoxide) moiety results in nonequivalent isopropyl methyl groups and rapid rotation at higher temperatures results in exchange of the nonequivalent groups.

In the $Ti(acac)_2(2,6\text{-}^{i}Pr_2C_6H_3O)_2$ complex, there are a total of four different isopropyl methyl groups in the event of no exchange processes of any kind. Sources (i) and (ii) would interconvert different pairs of isopropyl methyl groups and would result in a single doublet if both are operative or two doublets if only one is functioning. Thus the observed behaviour (Figure 41) of two doublets coalescing into one is consistent with either source (i) or (ii). However, source (ii) cannot cause isopropyl methyl group exchange in the $Ti(acac)_2(2\text{-}^{i}PrC_6H_4O)_2$ complex and only source (i) remains as a viable explanation for the behaviour of this complex (Figure 32). Comparison of kinetic data for isopropyl methyl group exchange in the $Ti(acac)_2(2,6\text{-}^{i}Pr_2C_6H_3O)_2$ and $Ti(acac)_2(2\text{-}^{i}PrC_6H_4O)_2$ complexes (Table XLI) suggests that the same process is operative for both

complexes. Thus the exchange process involving isopropyl methyl groups is identified as resulting from inversion of the molecular configuration at the titanium center.

Further support for this conclusion is forthcoming from the $Ti(acac)_2(O^iC_3H_7)_2$ complex. A single isopropyl methyl doublet is observed at room temperature, but on cooling, this resonance broadens and splits into two doublets (61,126). A hindered rotation process (source (ii)) is not possible for this complex as the isopropyl methyl groups remain diastereotopic in any rotational configuration and in the event of rapid rotation. Analagous behaviour is expected for the $Ti(acac)_2(4\text{-}^iPrC_6H_4O)_2$ complex, but as Figure 33 reveals, the isopropyl methyl groups, apparently, are not anisochronous. This may result from the greater distance of the diastereotopic probe from the center of dissymmetry and/or the isopropyl group being outside the region of magnetic anisotropy generated by the aromatic ring resulting in unresolvable chemical shift differences between the diastereotopic isopropyl methyl groups.

Table XLI summarizes kinetic data for exchange of isopropyl methyl groups in complexes containing isopropyl-substituted phenoxy ligands. It is interesting to compare k_{298} and $\Delta G^{\ddagger}$ values for acetylacetonate and isopropyl methyl group exchange for complexes in which both processes occur simultaneously (cf. Tables XXXV and XLI). The relative rates for isopropyl methyl (k_{inv}) and acetylacetonate methyl (k_{exch}) group exchange will depend on the mechanism (6,7); however, the free energies of activation would be expected to be similar. The $\Delta G^{\ddagger}$ values for both exchange processes are identical for the $Ti(acac)_2(2\text{-}^iPrC_6H_4O)_2$ complex and similar (differing by 0.39 and 0.31 kcal/mole in dichloromethane and m-dichlorobenzene, respectively) for the $Ti(acac)_2(2,6\text{-}^iPr_2C_6H_3O)_2$ complex. This suggests that a common physical pathway is responsible for exchange of acetylacetonate

and isopropyl methyl groups.

The ratio of rates of acetylacetonate methyl group exchange to isopropyl methyl group exchange, k_{exch}/k_{inv}, may provide some indication of mechanism. This ratio is 1.0, 1.4, and 2.1 for $Ti(acac)_2(2,6\text{-}^iPr_2C_6H_3O)_2$ in dichloromethane, $Ti(acac)_2(2,6\text{-}^iPr_2C_6H_3O)_2$ in m-dichlorobenzene, and $Ti(acac)_2(2\text{-}^iPrC_6H_4O)_2$ in dichloromethane, respectively.

Consulting Table IV, the changes in signal multiplicities for isopropyl-substituted phenoxy complexes of the type cis-$M(AA)_2X_2$ are consistent with either averaging set A_8 or the combination $(A_6 + A_7)$. A_8 predicts a k_{exch}/k_{inv} ratio of unity; $(A_6 + A_7)$ predicts a ratio of 1/2.

The observed ratio of unity for the $Ti(acac)_2(2,6\text{-}^iPr_2C_6H_3O)_2$ complex in dichloromethane solution allows the averaging set for this complex to be identified as A_8. In the nomenclature of Figure 4, this limits the rearrangement reactions to

$$\text{cis-}\Lambda_{23} \leftrightarrow \text{cis-}\Delta_{14}$$
$$\text{cis-}\Lambda_{24} \leftrightarrow \text{cis-}\Delta_{13}$$

and no others. Referring to Figures 12, 13, and 14, it is found that a bond rupture mechanism via TBP intermediates (axial and equatorial) does not provide a path for this rearrangement. Also, no TBP intermediate undergoing pseudorotation processes (cf. Section III-C-2b) generate these reactions (7). Figures 12 and 14 demonstrate that these reactions are easily accomodated by a twist mechanism and a bond rupture mechanism via SP-axial intermediates. No choice between these alternatives can be made; however, the $\Delta S^{\neq}$ values for exchange are quite negative (-33 and -15 for isopropyl and acac methyl group exchange, respectively) and negative entropies of activation have long been argued as supporting a twist mechanism (6,7). However, in the light of more recent results, $\Delta S^{\neq}$

values are unreliable indicators of mechanism (111).

The increase in the k_{exch}/k_{inv} ratio for the $Ti(acac)_2$-$(2,6\text{-}^{i}Pr_2C_6H_3O)_2$ complex on progressing from dichloromethane to m-dichlorobenzene solutions is enigmatic. As this change in ratio appears to be outside of experimental error (estimated at 10%), the most simple rationalization is that more than one physical process is occurring. This ratio implies that acac methyl groups are exchanged more rapidly than inversion occurs, a result which no single physical process accomodates. In addition to the motion suggested for this complex in dichloromethane, another process which exchanges acac methyl groups but does not result in inversion is also operative. A study of Figures 12, 13, and 14 indicates that only TBP-equatorial and SP-axial intermediates could possibly accomodate such a pathway.

The $Ti(acac)_2(2\text{-}^{i}PrC_6H_4O)_2$ complex possesses a larger, more puzzling value for the k_{exch}/k_{inv} ratio of 2.1. As no single physical pathway can generate such a large ratio, a mixture of rearrangement mechanisms is also indicated. Partrcipation of TBP-equatorial and SP-axial intermediates are indicated, since some component of the mixture of physical mechanisms must result in exchange without inversion.

The increased lability of $Ti(acac)_2X_2$ complexes observed on progressing from X = phenoxy to X = halogen, for acac methyl group exchange, (cf. Tables XXIV and XXXV) is also manifested in isopropyl group exchange in the $Ti(acac)_2Cl(2,6\text{-}^{i}Pr_2C_6H_3O)_2$ complex. Data in Table XLI indicate that this complex is more labile than the bis(isopropyl-substituted phenoxy) complexes. This complex is discussed further in Section III-C-2c.

Chemical shift data for the phenoxy complexes discussed in this section may be found in Appendix C.

(ii) A Comparison of Kinetic Parameters Derived from NMR Studies using Total Lineshape and Approximate Methods

The nuclear magnetic resonance technique has provided the chemist with a powerful tool to investigate the rate of exchange phenomena. For an uncoupled two-site exchange process Gutowsky and Holm (17) provided the most reliable line-shape function; however, application of this procedure generally required the use of computer facilities. Consequently, it was desirable to reduce the complicated equation to simpler ones by making some appropriate approximations, which may result in the introduction of serious systematic errors in kinetic data.

In the last decade, a study was reported (15) in which factors affecting the accuracy of high-resolution nmr determinations of chemical exchange rates were analyzed and discussed, including mathematical as well as experimental aspects. Numerical methods employing mathematical approximations commonly used to evaluate exchange rates from high-resolution spectra were shown to be subject to systematic error, and circumstances under which the error becomes appreciable were presented. Also activation parameters for internal rotation of N,N-dimethyltrichloroacetamide and N,N-dimethyl carbamyl chloride (157), and for the chair-chair isomerization of cyclohexane and of cyclohexane-d_{11} (158) have been compared as obtained from several types of proton magnetic measurements, viz., spin echo, high resolution methods involving total lineshape (TLS) and approximate calculations. These revealed that discrepancies resulted in using approximate equations in extracting kinetic data from nmr spectra. However, several studies (61,62,138,159) of configurational rearrangements in metal complexes in recent years still use the approximate methods in evaluating the nmr data, leading to some doubtful values for the activation parameters. In many cases, these values have been

used to argue for some particular rearrangement mechanism. In part to compare our TLS results of Section III-C-1-c(i) with Harrod and Taylor's (62) results from approximate methods, a study of the procedures and errors involved in the use of various approximate methods for the study of configurational rearrangements in a variety of six-coordinate metal chelates is presented in this section. These complexes were chosen on the basis of large to small chemical shift separations between the components of the uncoupled AB doublet.

The nuclear magnetic resonance technique provides means of accessing the mean lifetime, τ_i, of an absorbing nucleus at the site giving rise to the ith resonance absorption (13). Several methods (14,15,160) have been put forward to determine the quantity $1/\tau_i$, the first-order rate constant for transfer of the resonating nucleus out of the ith site, from the the experimental line-shape data. For the case of an uncoupled two-site exchange system, as is the case here, one such method involves calculating the over-all line shape as a function of τ.

The total lineshape method presents a reliable method for evaluating exchange rates from the nmr spectral data by matching the observed spectra with a series of calculated spectra in which the exchange rate is varied. In a system under investigation it is possible to assign values of $1/T_2$, ν, P_A, and P_B at each temperature, and thus to calculate a realistic line shape as a function of the exchange rate. The line-shape function is given (161) by suitable modifications of the Block phenomenological equations as developed by Gutowsky and Holm (17), but retaining terms involving the transverse relaxation times.

The general line-shape function is given in equation [11]

$$v = \frac{\left| P\left(1 + \tau\left(\frac{P_B}{T_{2A}} + \frac{P_A}{T_{2B}}\right)\right) + Q\left(R + \tau\left(\frac{1}{T_{2B}} - \frac{1}{T_{2A}}\right)\frac{\delta\omega}{2}\right)\right| \omega_1 M_o}{P^2 + R^2 + \tau^2\left(\frac{1}{T_{2B}} - \frac{1}{T_{2A}}\right)^2\left(\frac{\delta\omega}{2}\right)^2 + 2R\left(\frac{1}{T_{2B}} - \frac{1}{T_{2A}}\right)\frac{\delta\omega}{2}} \qquad [11]$$

where

$$P = \tau\left[\frac{1}{T_{2A}T_{2B}} - \Delta\omega^2 + \left(\frac{\Delta\omega}{2}\right)^2\right] + \frac{P_A}{T_{2A}} + \frac{P_B}{T_{2B}}$$

$$Q = \tau\left[\Delta\omega - \frac{\delta\omega}{2}(P_A - P_B)\right]$$

$$R = \Delta\omega\left[1 + \frac{\tau}{T_{2A}} + \frac{\tau}{T_{2B}}\right] + \frac{\delta\omega}{2}(P_A - P_B)$$

and

$$\tau = \frac{\tau_A\tau_B}{\tau_A + \tau_B} \qquad [12]$$

The notations used in these expressions have their usual denotations: v, the transverse component of the resultant magnetic moment perpendicular to the rotating field H_1, which is proportional to the absorption intensity; ω_1, the applied rotating radiofrequency field; $\Delta\omega$, the difference of the resonance frequencies (radians/sec) corresponding to the states A and B; τ_A and τ_B, the mean lifetimes for a stay on A and B sites; P_A and P_B, the fractional populations of A and B sites; T_2, the transverse relaxation times in the absence of exchange; M_o, the equilibrium value of the z component of the resultant magnetic moment.

Fortran programs have been written to compute a normalized lineshape function over the frequency range of interest, for a given set of input parameters. The modified version (88) of one particular program (89) requires as input parameters for each temperature a value of $\pi\delta\upsilon$ where $\delta\upsilon$

is the chemical shift separation (in Hz) in the absence of exchange between the two resonance components of the exchanging system, a value for the fractional population at sites A and B, viz., P_A and P_B, and a value for T_{2A} and T_{2B} [= $1/\pi$(linewidth)], the transverse relaxation times at sites A and B in the absence of exchange. For T_{2A} and T_{2B}, the full linewidth (in the absence of exchange) at one-half maximum amplitude can be obtained either from nmr spectra of complexes which resemble the system under study but in which no exchange occurs (54,59,87), (in cases where T_2's are temperature dependent), or from the linewidths of the resonances under conditions of very fast exchange or very slow exchange, or from the linewidths of the standard TMS reference, or from some other internal standard. $\delta\upsilon$ in the absence of exchange can be obtained from the very slow exchange limit or from a plot (87) of $\delta\upsilon$ vs. temperature in which the linear portion in the slow exchange region is extrapolated in the intermediate and fast exchange regions. Early investigators of restricted rotation in N,N-disubstituted amides often assumed that $\delta\upsilon$ remained constant throughout the exchange region. This assumption has resulted in serious systematic errors in the activation energy (15), since $\delta\upsilon$ often varies with temperature because of changes in the degree of molecular association (82).

Models chosen for an uncoupled two-site exchange process, although appropriate, can present some problems in applying them to the data for the exchanging system because line-shape equations derived from such models might still render the task sufficiently complex that a computer is required to extract the exchange rates. Thus it is useful to have equations relating some readily calculated parameters to those of the experimental spectrum. Even such equations might still require use of a computer, however. Therefore what is needed is to reduce these complicated equations to simpler ones by making some appropriate approximations. The accuracy of such approximations

depends upon the relative values of the exchange rates $1/2\tau$ (or $1/\tau_A$) as compared to values of the chemical shift separation, $\delta\upsilon$, and the natural (full) linewidth $1/\pi T_2^o$ in the absence of exchange. Neglect of such dependence may well lead to appreciable systematic errors in the kinetic data (15). In using approximate equations, the range of their validity should be known and tested numerically for the case under study. In addition, the validity of the equations should never be exceeded beyond their usefulness.

For an equally populated uncoupled two-site exchange problem, approximate equations result (15) if

$$1/\tau \text{ and } \delta\upsilon >> (1/\pi T_2'') \equiv W'' \qquad [13]$$

where

$$\frac{1}{T_2''} = \frac{1}{T_2^o} + \frac{1}{T_2'} \qquad [14]$$

and $1/T_2'$ represents contributions to W", the effective full linewidth in the absence of exchange, from magnetic field inhomogeneity, machine instability, and other such instrumental limitations. Conditions of equation [13] on the exchange rates can be met (15) for many systems by careful adjustment of the temperature and/or concentrations of the reactants; the chemical shift separation, however, is less adjustable, control being limited to solvent effects and increasing the magnetic field (15). For very small chemical shifts, the approximate equations may not be valid. In cases where they have failed, graphical methods have been employed to extract exchange rates (17,162,163).

Under conditions of slow exchange, where exchange rates are too slow to coalesce the AB doublet to a single resonance line, the experimentally observed resonance peak separation, $\delta\upsilon_e$ (in Hz), has been used (17) in the following approximation

$$\frac{1}{2\tau} = \frac{1}{\tau_A} = \frac{\pi}{\sqrt{2}} \left(\delta\upsilon_o^2 - \delta\upsilon_e^2 \right)^{\frac{1}{2}} \qquad [15]$$

where $\delta\upsilon_o$ is the peak separation in the absence of exchange. As has already been pointed out by Gutowsky and Holm (17), the major change in peak separation with exchange rate occurs over a rather narrow range, $0.45 \leq 2\tau\delta\upsilon_o \leq 2$; and $\delta\upsilon_e$ becomes decreasingly sensitive to rate for slower rates-that is, for $2\tau\delta\upsilon_o > 2$ (15). At very slow rates, the errors in determining $\delta\upsilon_e$ may well exceed the errors involved in using equation [15], in this case, both types of errors become comparable to the exchange rate itself (17,164) and the peak separation should then not be used under these conditions (15). It has also been shown (15) that the effect of T_2^o on the percent error for a particular pair of $\delta\upsilon$ and $1/2\tau$ values is inversely proportional to $\delta\upsilon$-that is, the percent error increases the smaller the values of $\delta\upsilon$. In a theoretical treatment to test the validity and to find the magnitude of errors, Allerhand and co-workers (15) contend that the error introduced in $1/2\tau$ values obtained from equation [15] does not exceed 10% in systems for which $2\tau\delta\upsilon \leq 5$. It should be pointed out, however, that in the theoretical calculations, instrumental broadening of the resonance lines was neglected. Inclusion of such broadening effects which are not negligible, especially when $\delta\upsilon_e$ are small, would yield a higher percent error in exchange rates. On the other hand, use of complete line-shape numerical methods will minimize errors in $1/2\tau$ because these generally include the instrumental broadening as a convolution function. Another possible source (15) of error in equation [15] is the narrow temperature range accessible for some systems so that systematic errors in the exchange rates and/or temperatures can produce quite large errors in the apparent enthalpy and entropy of activation.

The mean lifetime of nuclei at sites A and B has also been

related to the maximum to central minimum intensity ratio (164), R, as in

$$\pi\delta\upsilon_o = \frac{1}{\pi\sqrt{2}}\sqrt{R + (R^2 - R)^{1/2}} \qquad [16]$$

$$\text{for } \pi\sqrt{2}\tau\delta\upsilon_o > 1$$

which implies that the effect of overlap of the components of the AB doublet is negligible [$1/T_{2A} << \delta\upsilon >> 1/T_{2B}$]. Equation [16] also assumes that the fractional populations at the two sites are equal ($P_A = P_B$ and $\tau_A = \tau_B = 2\tau$), that RF saturation is negligible, and that "slow passage" conditions are maintained[≠] in the nmr experiment. An error analysis (15) of the Rogers-Woodbrey relationship indicates that it yields apparent rates larger than the "true" rates.

When the fractional populations on sites A and B are the same, $P_A = P_B$, and when equation [13] holds, the exchange rate at the coalescence temperature T_c is given (17) by

$$\frac{1}{2\tau} = \frac{\pi\delta\upsilon_o}{\sqrt{2}} \qquad [17]$$

Because of the narrow temperature range generally accessible below coalescence, it is desirable, in fact it is essential to extend this range so as to minimize the errors discussed above. To do so requires an analysis of the lineshape above the coalescence temperature T_c, where only a single resonance line is obtained. The most obvious parameter is the observed linewidths W^* of the resonance line at half-maximum amplitude

$$W^* = \frac{1}{\pi T_2^*} = \left(\frac{1}{\pi T_2}\right)_{exch} + \frac{1}{\pi T_2''} \qquad [18]$$

where $(1/\pi T_2)_{exch}$ is the exchange contribution to the linewidth. For the

≠It should be noted that these conditions apply to all equations derived and not just equation [16].

uncoupled two-site exchange model, Piette and Anderson (165) have derived the relationship

$$\frac{1}{2\tau} = \frac{1}{\tau_A} = \frac{2\pi P_A P_B (\delta\upsilon_o)^2}{(W^* - W'')} \qquad [19]$$

where W" has been defined by equations [13] and [14] as the effective linewidth in the absence of exchange. Equation [19] holds under conditions of very fast exchange- that is, when

$$\frac{1}{2\tau} >> \delta\upsilon_o \qquad [20]$$

Allerhand and co-workers (15) have questioned the validity of the Piette-Anderson equation. They have shown by computer line-shape calculations that equation [19] leads to large errors in the exchange rate unless the rate is sufficiently larger than the coalescence value such that equation [20] applies. In addition to this, they contend that for small $\delta\upsilon_o$ values, the contribution to W^* from exchange becomes so small that $(W^* - W'')$ approaches the experimental error in W^*, and the error in the exchange rate $1/2\tau$ becomes very large. This error is a systematic error (decreasing with increasing rate), and if equation [19] is used to extract exchange rates it generally leads (15) to (a) low rates, (b) too large $\Delta H^{\ddagger}$, and (c) to more positive values of $\Delta S^{\ddagger}$.

A more valid expression was derived (15) on condition that equation [13] holds. Expression [21] reduces to the Piette-Anderson (165) relationship [19] when the exchange rate is sufficiently fast that $W^*/\delta\upsilon_o << 1$ with P_A and $P_B = 0.5$ (15).

$$\frac{1}{2\tau} = \frac{\pi\delta\upsilon_o}{2}\left(\frac{\frac{W''}{\delta\upsilon_o} + \frac{W^*}{\delta\upsilon_o}\sqrt{1 + 2\left(\frac{W^*}{\delta\upsilon_o}\right)^2 - \left(\frac{W^*}{\delta\upsilon_o}\right)^4}}{\left(\frac{W^*}{\delta\upsilon_o}\right)^2 - \left(\frac{W''}{\delta\upsilon_o}\right)^2}\right) \qquad [21]$$

Furthermore, if the conditions of the exchanging system are such that the exchange contribution to the linewidth is much greater than W"- that is, if $W^* >> W''$, then equation [21] leads to expression [22] (15). This

$$\frac{1}{2\tau} = \frac{\pi\delta\upsilon_o}{2}\sqrt{\left(\frac{\delta\upsilon_o}{W^*}\right)^2 - \left(\frac{W^*}{\delta\upsilon_o}\right)^2 + 2} \qquad [22]$$

last expression has been shown to be valid at and above coalescence when equation [13] holds. It is also valid below coalescence (15) if W^* is more generally defined as the width of the spectrum at the point where it possesses an amplitude one-half of the central intensity (166). Notwithstanding this, if equation [13] holds, the linewidth W^* at the coalescence temperature is equal to the chemical shift $\delta\upsilon_o$ and in addition $W^* > \delta\upsilon_o$ below T_c and $W^* < \delta\upsilon_o$ above T_c (15). These results provide a means of estimating $\delta\upsilon_o$ without going to the very low temperatures where exchange is "frozen out".

In the region of very fast exchange, errors from the approximation to equations [19] and [21] have been shown to be comparable and negligible- but as the exchange rate decreases toward the rate at coalescence, the former expression yields very large negative errors while the latter is accurate up to $\delta\upsilon_o 2\tau \sim 1.0$ (15). As a general rule then (15), if the errors in using the approximate Piette-Anderson relationship [19] are to be kept to <5%, then it should be used only for rates for which $\delta\upsilon_o 2\tau \leq 0.2$. In addition, it was also demonstrated (15) that the approximate expression [22] yields errors of less than 5% in the range $1.0 > \delta\upsilon_o 2\tau \geq 0.04$; however, its range of applicability is strongly dependent on $\delta\upsilon_o$ and T_2^o (the transverse relaxation time in the absence of exchange), and, in fact, for small values of these two parameters its use is limited (15).

The Si(IV), Ge(IV), and Sn(IV) complexes used in this comparison of TLS and approximate methods have been prepared and characterized previously (167). The Ti(IV) complexes have been prepared previously (126) and characterized fully in this thesis. Variable temperature nmr spectra for the Ti(IV) complexes were obtained on a 60 MHz instrument using the procedures and precautions discussed in Section II-C. Spectra for the Si(IV), Ge(IV), and Sn(IV) complexes were processed similarly on a 100 MHz instrument (167). Care was taken to ensure that spectra were obtained under conditions of low-radiofrequency fields to avoid saturation, and under slow passage conditions (0.2 Hz/sec).

Lineshape parameters obtained from the nmr experiment for the complexes $Ti(acac)_2(2\text{-}IC_6H_4O)_2$, $Ti(acac)_2(4\text{-}ClC_6H_4O)_2$, $(C_6H_5)ClSi(acac)_2$, $(CH_3)ClSn(acac)_2$, $(C_6H_5)ClGe(acac)_2$, and $(C_6H_5)_2Sn(acac)_2$ are set out in Table XLII, in addition to exchange rates (expressed as $1/2\tau$) extracted from approximate equations [15], [16], [17], [19], [21], and [22] and from Total Lineshape (TLS) calculations. Figure 40 presents Arrhenius plots of $\log (1/2\tau)$ versus $1/T$, while in Tables XLIII - XLVIII activation parameters obtained from approximate and TLS calculations are compared. The bracketed activation parameters in Tables XLIII - XLVIII were obtained from corresponding $1/2\tau$ values using the largest observed chemical shift separation (for $\delta\upsilon_0$) as a constant value in the calculations. The lines in Figure 40 represent the linear least-squares-line fit to the TLS - calculated exchange rates. Error limits in Tables XLIII - XLVIII are given at one standard deviation.

(A) $Ti(acac)_2(2\text{-}IC_6H_4O)_2$ $\delta\upsilon_0 > 15$ Hz - Equations [15] and [16] yield exchange rates in the region below coalescence which are in fair agreement with those from the TLS method; the error is <10% in both cases. Agreement is satisfactory because the conditions that $0.45 \leq 2\tau\delta\upsilon_0 \leq 2$ and

Table XLII

Lineshape Parameters[a] and Comparison of Exchange Rates Derived from Approximate and Total Lineshape Methods

Temp., °C	W* (Hz)	W" (Hz)	$\delta\upsilon_e$ (Hz)	R	$\delta\upsilon_o$ (Hz)	$1/2\tau$ (sec^{-1}) Equation [15]	[16]	[17]	[19]	[21]	[22]	TLS
					$Ti(acac)_2(2\text{-}IC_6H_4O)_2$							
2.7	-	-	14.29	5.92	14.81	8.6	9.8	-	-	-	-	9.0
0.2	-	-	13.94	3.90	14.68	10	12	-	-	-	-	11
4.6	-	-	13.04	2.50	14.48	14	13	-	-	-	-	14
7.5	-	-	11.63	1.63	14.35	19	20	-	-	-	-	19
11.1	-	-	9.22	1.22	14.19	24	24	-	-	-	-	23
12.0	-	-	-	-	14.15	-	-	31	-	-	-	27
16.1	11.80	0.48	-	-	13.97	-	-	-	27	37	36	37
19.1	8.35	0.47	-	-	13.83	-	-	-	38	47	45	48
25.2	5.15	0.46	-	-	13.56	-	-	-	62	69	63	67
30.0	3.20	0.45	-	-	13.34	-	-	-	102	105	92	105
34.8	2.35	0.44	-	-	13.13	-	-	-	142	145	119	143
38.1	2.41	0.43	-	-	12.98	-	-	-	134	139	113	133
					$Ti(acac)_2(4\text{-}ClC_6H_4O)_2$							
0.2	-	-	10.79	7.63	11.08	5.6	6.4	-	-	-	-	5.5
4.6	-	-	10.61	5.03	11.00	6.5	7.9	-	-	-	-	6.9
7.5	-	-	10.19	3.37	10.95	8.9	9.8	-	-	-	-	8.9
11.1	-	-	9.48	2.13	10.88	12	13	-	-	-	-	12
12.0	-	-	7.52	1.28	10.86	17	18	-	-	-	-	17
15.2	-	-	7.66	1.30	10.80	17	17	-	-	-	-	16
16.1	-	-	6.86	1.18	10.79	19	19	-	-	-	-	18
16.8	-	-	5.09	1.07	10.77	21	21	-	-	-	-	20
18.9	10.47	0.47	-	-	10.73	-	-	-	18	25	24	25
19.1	11.12	0.47	-	-	10.73	-	-	-	17	24	23	23
20.8	10.38	0.47	-	-	10.70	-	-	-	18	25	24	25

Table XLII (continued)

25.2	7.97	0.46	-	-	10.62	-	-	-	24	31	30	31
30.0	3.86	0.45	-	-	10.53	-	-	-	51	57	50	55
34.8	3.08	0.44	-	-	10.44	-	-	-	65	70	60	69
38.1	3.02	0.43	-	-	10.38	-	-	-	65	70	60	69

$(C_6H_5)ClGe(acac)_2$

13.2	-	-	20.06	24.69	20.05	-	6	-	-	-	-	4.4
20.8	-	-	19.86	14.59	19.87	-	8	-	-	-	-	6.8
30.2	-	-	18.93	5.15	19.66	12	14	-	-	-	-	12
38.9	-	-	16.43	1.88	19.46	23	24	-	-	-	-	23
41.9	-	-	11.93	1.13	19.40	34	35	-	-	-	-	33
44.5	-	-	-	-	19.34	-	-	43	-	-	-	32
53.2	12.40	0.89	-	-	19.14	-	-	-	50	63	60	61
62.2	6.50	0.87	-	-	18.94	-	-	-	100	105	96	110

$(C_6H_5)_2Sn(acac)_2$

-56.8	-	-	6.11	3.35	6.36	-	5.7	-	-	-	-	2.5
-53.8	-	-	6.32	3.19	6.36	-	5.9	-	-	-	-	3.1
-51.7	-	-	6.31	2.97	6.36	-	6.1	-	-	-	-	3.2
-48.8	-	-	6.42	2.33	6.36	-	7.0	-	-	-	-	4.4
-48.4	-	-	6.40	2.01	6.36	-	7.6	-	-	-	-	4.8
-46.8	-	-	6.33	1.73	6.36	1.4	8.4	-	-	-	-	6.3
-45.0	-	-	6.30	1.80	6.36	1.9	8.2	-	-	-	-	6.1
-42.3	-	-	5.77	1.49	6.36	5.9	9.3	-	-	-	-	7.2
-38.6	-	-	4.90	1.14	6.36	9.0	11	-	-	-	-	8.6
-37.4	-	-	-	-	6.36	-	-	14	-	-	-	11
-35.1	7.70	1.12	-	-	6.36	-	-	-	9.7	12	11	13
-30.5	5.46	1.06	-	-	6.36	-	-	-	14	19	16	18
-24.8	3.82	0.99	-	-	6.36	-	-	-	22	27	21	26
-17.5	2.87	0.91	-	-	6.36	-	-	-	32	36	26	36

Table XLII (continued)

-9.5	2.18	0.85	-	-	6.36	-	-	-	48	52	32	51
-6.0	1.88	0.83	-	-	6.36	-	-	-	61	75	37	64
3.0	1.48	0.80	-	-	6.36	-	-	-	93	101	45	99

$(CH_3)ClSn(acac)_2$

-0.5	-	-	8.51	5.43	8.47	-	5.9	-	-	-	-	3.5
4.5	-	-	8.01	3.02	8.31	4.9	7.9	-	-	-	-	6.1
7.5	-	-	7.44	2.07	8.22	7.8	9.7	-	-	-	-	7.6
11.5	-	-	6.04	1.24	8.09	12	13	-	-	-	-	11
13.5	-	-	3.74	1.04	8.03	16	16	-	-	-	-	15
16.0	-	-	0	1.00	7.96	18	18	-	-	-	-	16
21.5	5.30	0.95	-	-	7.78	-	-	-	22	28	23	26
26.5	3.75	0.94	-	-	7.63	-	-	-	33	43	29	35
29.5	2.57	0.93	-	-	7.54	-	-	-	54	59	38	55

$(C_6H_5)ClSi(acac)_2$

-69.6	-	-	29.4	3.32	33.9	38	31	-	-	-	-	29
-64.9	-	-	27.3	2.14	33.9	45	39	-	-	-	-	36
-61.3	-	-	33.5	1.48	33.9	54	50	-	-	-	-	52
-54.7	-	-	-	-	33.9	-	-	75	-	-	-	81
-49.3	20.0	1.3	-	-	33.9	-	-	-	96	-	-	116

[a]Symbols are defined in Table XXII and text.

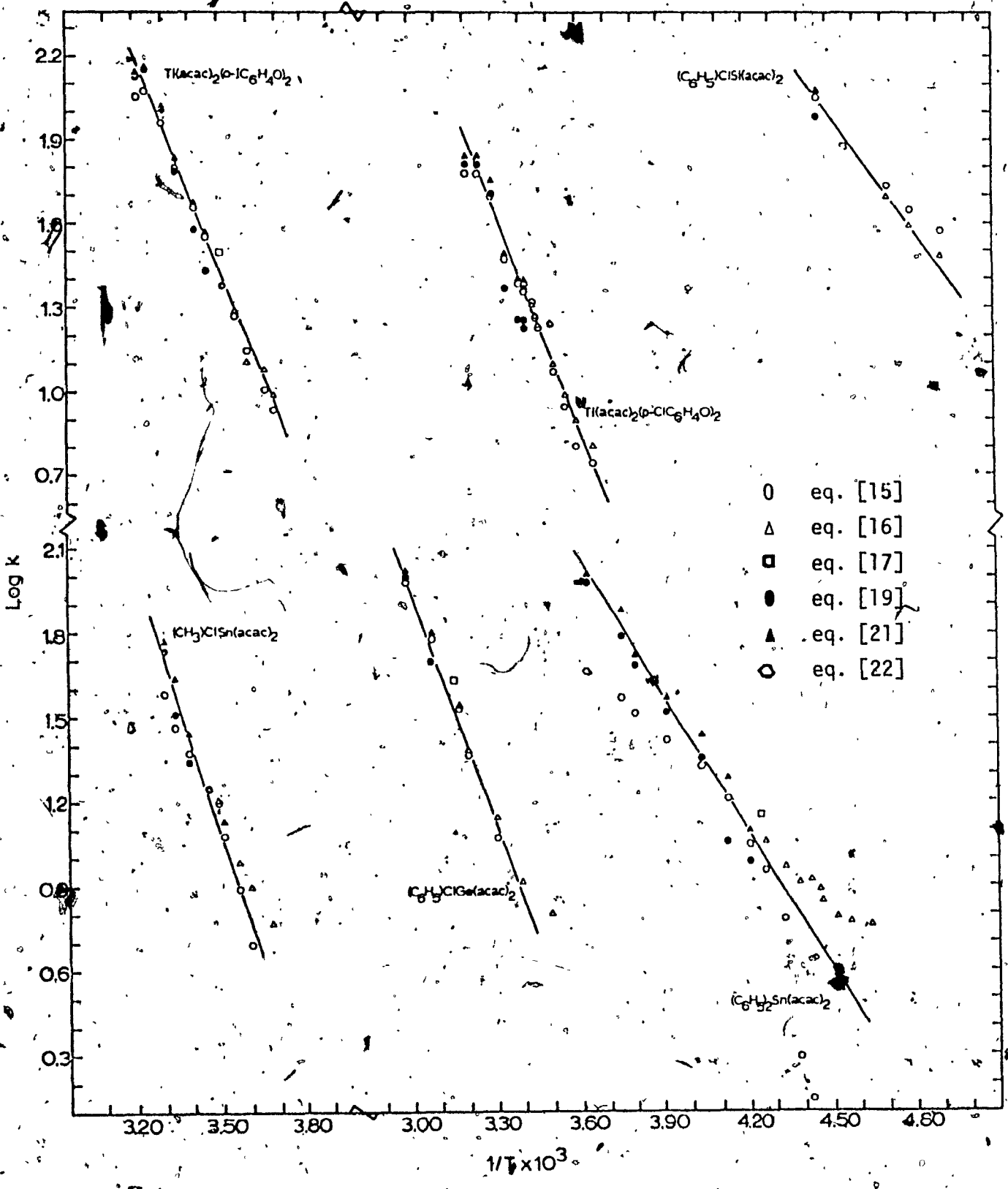

Figure 40.- Arrhenius (log k versus 1/T) plots for the complexes shown. Points represent exchange rates obtained from approximate equations; solid lines represent the Total Lineshape least-squares straight lines.

Table XLIII

Comparison of Activation Parameters for $Ti(acac)_2(2\text{-}IC_6H_4O)_2$

Equation	E_a (kcal/mole)	log A	$\Delta S^{\neq}$ (eu)	$\Delta H^{\neq}$ (kcal/mole)	$\Delta G^{\neq}$ (kcal/mole)	k_{298} (sec^{-1})
[15]	11.5 ± 0.6[a]	10.3 ± 0.4	-14 ± 2	10.9 ± 0.6	15.01 ± 0.04	61
	(3.5 ± 0.4)[b]	(4.2 ± 0.3)	(-41 ± 1)	(2.9 ± 0.4)	(15.26 ± 0.04)	(40)
[16]	9.8[c] ± 1.6	8.9 ± 1.2	-20[d] ± 6	9.2 ± 1.6	15.11 ± 0.12	52
	(10.4 ± 0.4)	(9.4 ± 0.3)	(-17 ± 1)	(9.8 ± 0.4)	(14.95 ± 0.03)	(68)
[19]	13.8 ± 1.2	11.9 ± 0.9	-6 ± 4	13.2 ± 1.2	15.02 ± 0.03	60
	(15.1 ± 1.2)	(13.0 ± 0.9)	(-1 ± 4)	(14.5 ± 1.2)	(14.75 ± 0.03)	(96)
[21]	11.6 ± 0.9	10.3 ± 0.7	-13 ± 3	11.0 ± 0.9	14.93 ± 0.02	70
	(13.0 ± 1.1)	(11.6 ± 0.8)	(-7 ± 4)	(12.5 ± 1.1)	(14.68 ± 0.03)	(107)
[22]	10.1 ± 0.9	9.2 ± 0.6	-19 ± 3	9.5 ± 0.9	14.99 ± 0.02	63
	(11.6 ± 0.9)	(10.5 ± 0.7)	(-12 ± 3)	(11.0 ± 0.9)	(14.73 ± 0.03)	(97)
All eqs[e]	11.6 ± 0.3	10.34 ± 0.22	-13 ± 1	11.0 ± 0.3	14.98 ± 0.02	65
TLS[f]	11.6 ± 0.3	10.33 ± 0.19	-13 ± 1	11.0 ± 0.3	14.95 ± 0.02	67 ± 5

[a]One standard deviation with variable $\delta\upsilon_0$ (see text); [b]Constant $\delta\upsilon_0$ (see text); [c]Lit., (62) value 8.1 ± 1.1 kcal/mole; [d]Lit., (62) value -25 eu; [e]Data points from all equations were used in the analysis; [f]Calculated from a Total Lineshape analysis.

Table XLIV

Comparison of Activation Parameters for $Ti(acac)_2(4\text{-}ClC_6H_4O)_2$

Equation	E_a (kcal/mole)	log A	$\Delta S^{\neq}$ (eu)	$\Delta H^{\neq}$ (kcal/mole)	$\Delta G^{\neq}$ (kcal/mole)	k_{298} (sec^{-1})
[15]	13.2 ± 1.3[a]	11.3 ± 1.0	-9 ± 5	12.6 ± 1.3	15.29 ± 0.07	38
	(5.7 ± 0.6)[b]	(5.7 ± 0.5)	(-35 ± 2)	(5.2 ± 0.6)	(15.46 ± 0.04)	(29)
[16]	11.4[c] ± 1.0	9.9 ± 0.8	-15[d] ± 4	10.8 ± 1.0	15.34 ± 0.06	35
	(11.7 ± 1.0)	(10.2 ± 0.8)	(-14 ± 4)	(11.1 ± 1.0)	(15.27 ± 0.06)	(39)
[19]	14.2 ± 1.5	11.8 ± 1.1	-6 ± 5	13.6 ± 1.5	15.48 ± 0.04	28
	(14.8 ± 1.5)	(12.4 ± 1.1)	(-4 ± 5)	(14.2 ± 1.5)	(15.39 ± 0.04)	(35)
[21]	11.3 ± 1.1	9.8 ± 0.8	-16 ± 4	10.7 ± 1.1	15.34 ± 0.03	35
	(11.8 ± 1.1)	(10.3 ± 0.8)	(-13 ± 4)	(11.2 ± 1.1)	(15.21 ± 0.03)	(44)
[22]	10.0 ± 1.0	8.9 ± 0.7	-20 ± 3	9.4 ± 1.0	15.38 ± 0.02	33
	(10.6 ± 1.0)	(9.4 ± 0.7)	(-18 ± 3)	(10.0 ± 1.0)	(15.24 ± 0.02)	(41)
All eqs[e]	11.3 ± 0.4	9.78 ± 0.30	-16 ± 1	10.7 ± 0.4	15.39 ± 0.02	32
TLS[f]	11.6 ± 0.4	10.2 ± 0.3	-14 ± 1	11.3 ± 0.4	15.36 ± 0.02	34 ± 3

[a]One standard deviation with variable $\delta\upsilon_o$ (see text); [b]Constant $\delta\upsilon_o$ (see text); [c]Lit., (62) value 6.7 ± 1.6 kcal/mole; [d]Lit., (62) value -31 eu; [e]Data points from all equations were used in the analysis; [f]Calculated from a Total Lineshape analysis.

Table XLV

Comparison of Activation Parameters for $(C_6H_5)ClSi(acac)_2$[a]

Equation	E_a (kcal/mole)	log A	$\Delta S^{\neq}$ (eu)	$\Delta H^{\neq}$ (kcal/mole)	$\Delta G^{\neq}$ (kcal/mole)	k_{298} (sec^{-1})
[15]	3.8 ± 0.5[b]	5.6 ± 0.5	-35 ± 2	3.2 ± 0.5	13.5 ± 0.2	732
[16]	5.0 ± 0.3	6.8 ± 0.3	-29 ± 2	4.4 ± 0.3	13.1 ± 0.1	1500
All eqs[c]	5.3 ± 0.4	7.2 ± 0.4	-27 ± 2	4.7 ± 0.4	12.9 ± 0.1	2107
TLS[d]	6.4 ± 0.3	8.3 ± 0.3	-22 ± 2	5.8 ± 0.3	12.5 ± 0.1	4207

[a]Constant $\delta\upsilon_o$ (see text); [b]One standard deviation; [c]Data points from all equations used in the analysis; [d]Calculated from a Total Lineshape analysis

Table XLVI

Comparison of Activation Parameters for $(CH_3)ClSn(acac)_2$

Equation	E_a (kcal/mole)	log A	$\Delta S^{\neq}$ (eu)	$\Delta H^{\neq}$ (kcal/mole)	$\Delta G^{\neq}$ (kcal/mole)	k_{298} (sec^{-1})
[15]	18.1 ± 1.4[a]	15.0 ± 1.1	8 ± 5	17.5 ± 1.4	15.13 ± 0.07	50
	(6.5 ± 0.7)[b]	(6.2 ± 0.6)	(-32 ± 3)	(5.9 ± 0.7)	(15.44 ± 0.05)	(30)
[16]	11.0 ± 0.5	9.5 ± 0.4	-17 ± 2	10.4 ± 0.5	15.39 ± 0.03	32
	(11.6 ± 0.5)	(10.1 ± 0.4)	(-14 ± 2)	(11.0 ± 0.5)	(15.24 ± 0.03)	(41)
[19]	19.5 ± 4.4	15.8 ± 3.2	12 ± 15	18.9 ± 4.4	15.41 ± 0.05	31
	(20.9 ± 4.5)	(17.0 ± 3.3)	(17 ± 15)	(20.3 ± 4.5)	(15.11 ± 0.05)	(51)
[21]	16.6 ± 0.5	13.8 ± 0.3	2 ± 2	16.0 ± 0.5	15.29 ± 0.01	38
	(18.1 ± 4.4)	(15.0 ± 3.2)	(8 ± 15)	(17.5 ± 4.4)	(15.04 ± 0.05)	(58)
[22]	10.5 ± 2.4	9.1 ± 1.7	-19 ± 8	9.9 ± 2.4	15.47 ± 0.03	28
	(12.6 ± 2.7)	(10.9 ± 1.9)	(-11 ± 9)	(12.6 ± 2.7)	(15.20 ± 0.03	(44)
All eqs[c]	12.3 ± 0.7	10.6 ± 0.5	-12 ± 2	11.7 ± 0.7	15.37 ± 0.03	33
TLS[d]	14.3 ± 0.4	12.1 ± 0.3	-5 ± 2	13.7 ± 0.4	15.34 ± 0.02	35 ± 3

[a]One standard deviation with variable $\delta\upsilon_0$ (see text); [b]Constant $\delta\upsilon_0$ (see text); [c]Data points from all equations were used in the analysis; [d]Calculated from a Total Lineshape analysis.

Table XLVII

Comparison of Activation Parameters for $(C_6H_5)ClGe(acac)_2$

Equation	E_a (kcal/mole)	log A	$\Delta S^{\neq}$ (eu)	$\Delta H^{\neq}$ (kcal/mole)	$\Delta G^{\neq}$ (kcal/mole)	k_{298} (sec^{-1})
[15]	16.6 ± 2.1[a] (4.8 ± 0.9)[b]	10.0 ± 1.5 (4.9 ± 0.7)	-1 ± 7 (-38 ± 3)	16.0 ± 2.1 (4.2 ± 0.9)	16.3 ± 0.9 (15.59 ± 0.03)	7 (23)
[16]	10.5 ± 1.1 (10.7 ± 1.1)	8.7 ± 0.8 (8.9 ± 0.8)	-21 ± 4 (-20 ± 4)	9.9 ± 1.1 (10.1 ± 1.1)	15.99 ± 0.04 (15.94 ± 0.04)	12 (13)
[19]	16.8 (17.4)	12.9 (13.4)	-1 (1)	16.2 (16.8)	16.6 (16.5)	4 (5)
[21]	12.3 (14.0)	10.0 (11.3)	-15 (-9)	11.7 (13.5)	16.05 (16.08)	11 (10)
[22]	11.4 (12.0)	9.4 (9.9)	-17 (-15)	10.8 (11.5)	16.01 (15.94)	11 (13)
All eqs[c]	11.5 ± 0.5	9.5 ± 0.3	-17 ± 3	10.9 ± 0.5	16.02 ± 0.07	11
TLS[d]	12.8 ± 0.5	10.3 ± 0.3	-13 ± 2	12.2 ± 0.5	16.12 ± 0.03	9 ± 1

[a]One standard deviation with variable $\delta\upsilon_0$ (see text); [b]Constant $\delta\upsilon_0$ (see text); [c]Data points from all equations were used in the analysis; [d]Calculated from a Total Lineshape analysis.

Table XLVIII

Comparison of Activation Parameters for $(C_6H_5)_2Sn(acac)_2$

Equation	E_a (kcal/mole)	log A	$\Delta S^{\neq}$ (eu)	$\Delta H^{\neq}$ (kcal/mole)	$\Delta G^{\neq}$ (kcal/mole)	k_{298} (sec^{-1})
[15]	26 ± 5[a]	24.9 ± 4.4	54 ± 20	25 ± 5	9.1 ± 1.4	1.3×10^6
[16]	4.0 ± 0.4	4.8 ± 0.4	-39 ± 2	3.4 ± 0.4	14.95 ± 0.12	67
[19]	7.6 ± 0.2	8.0 ± 0.2	-24 ± 1	7.0 ± 0.2	14.14 ± 0.04	266
[21]	7.0 ± 0.3	7.5 ± 0.3	-26 ± 1	6.4 ± 0.3	14.14 ± 0.06	265
[22]	4.5 ± 0.3	5.3 ± 0.3	-36 ± 1	3.9 ± 0.3	14.79 ± 0.06	88
TLS[b]	8.1 ± 0.1	8.5 ± 0.3	-22 ± 1	7.5 ± 0.3	13.95 ± 0.09	369 ± 58

[a]One standard deviation, $\delta\upsilon_0$ = 6.36 Hz; [b]Calculated from a Total Lineshape analysis.

$\pi\sqrt{2}\tau\delta\upsilon_0 \geq 1$ for equations [15] and [16], respectively, hold ($2\tau\delta\upsilon_0$ = 0.6 - 1.7; and $\pi\sqrt{2}\tau\delta\upsilon_0$ = 1.2-3.3). A much larger error is introduced when equation [17] is used to determine the exchange rate at the coalescence temperature. This is not surprising as $1/2\tau$ is a direct function of $\delta\upsilon_0$, which is often temperature dependent; thus, the particular value of $\delta\upsilon_0$ to be used in expression [17] is uncertain. The most general expression for exchange rates above the coalescence temperature, equation [21], results in exchange rates in good agreement with those obtained from the TLS calculation. This may be expected since the only condition that must be met for this expression is that equation [13] be satisfied. Expression [19] results in exchange rates which agree with TLS values only at temperatures well removed from the coalescence temperature. Large negative errors (i.e., lower rates) occur in $1/2\tau$ near coalescence since the conditions that $1/2\tau >> \delta\upsilon_0$ and $W^* << \delta\upsilon_0$ are no longer satisfied. An error of <5% (15) is expected when $\delta\upsilon_0 2\tau \leq 0.2$; in this case, taking $\delta\upsilon_0$ as 13.5 Hz, the exchange rate should be > 68 sec^{-1} if an error of <5% is desired. Rates obtained from equation [22] are in good agreement with TLS values near the coalescence region but begin to deviate markedly at temperatures significantly above coalescence. These negative errors (cf. Table XLII) arise from the relaxation of the condition $W^* >> W''$, since W^* approaches W" in the very fast exchange region. For example, at T = 16.1 ^oC, $W^* \sim 25W''$ while at T = 34.8 ^oC, $W^* \sim 6W''$.

Arrhenius plots for equations [15], [16], [19], [21], and [22] are shown in Figure 40 while activation parameters are collected in Table XLIII. Table XLIII also contains kinetic parameters resulting from $1/2\tau$ values obtained from the same equations in which $\delta\upsilon_0$ (= 17.09 Hz) was assumed to be temperature independent. Choice of the value to be used for the constant $\delta\upsilon_0$ calculations was made on the assumption that the largest value, either observed experimentally or observed at the lowest accessible temperature,

corresponded to $\delta\upsilon_d$. Activation parameters from equation [15] with a variable $\delta\upsilon_o$ agree well with TLS values. This is not unexpected since expression [15] was applied in the region in which peak separation is sensitive to changes in exchange rates. However, when a constant $\delta\upsilon_o$ value is used, a very large systematic error appears in the activation parameters as evidenced by the extremely low values for E_a, $\Delta H^{\neq}$, log A and thus large negative entropies of activation. Despite these discrepancies, the $\Delta G^{\neq}$ values remain essentially constant. Thus, it would appear that this latter parameter is insensitive to systematic errors. Equation [15], with constant $\delta\upsilon_o$, has been used by Fortman and Sievers (168) in their study of configurational rearrangement processes in mixed β-diketonate complexes of aluminum(III). Their kinetic data for $Al(acac)_2(hfac)$, (E_a = 2.7 kcal/mole and $\Delta S^{\neq}$ = -19 eu; chlorobenzene solution) have since been shown (153) to suffer from a large degree of systematic error (E_a = 18.4 kcal/mole and $\Delta S^{\neq}$ = 10 eu; dichloromethane solution) because of the neglect of the temperature dependence of $\delta\upsilon_o$. The difference in the activation parameters cannot be solely ascribed to different solvent effects (153). The remaining equations [16], [19], [21], and [22] all yield activation parameters which cluster about the TLS values; the largest differences appear to occur for equation [19] while the best agreement occurs for equation [21]. In all cases, except for expression [15], results using a constant $\delta\upsilon_o$ consistently yield larger values for E_a, $\Delta H^{\neq}$, and log A while $\Delta S^{\neq}$ values become more positive. In view of the large errors that may result from the paucity of data points, differences in the kinetic data are nearly equal to the error in using equation [15], and therefore are of doubtful significance. Inclusion of all $1/2\tau$ values obtained with a variable $\delta\upsilon_o$ in the linear-least-squares analysis results in activation parameters close to those from the TLS calculation. This is not unexpected since positive and negative deviations from the TLS values occur

in the different approximate equations; utilization of all equations tend to cancel these errors. The activation parameters from equation [16], with constant $\delta\upsilon_o$ (cf. Table XLIII), do not agree with those reported in the literature [E_a = 8.1 kcal/mole and $\Delta S^{\neq}$ = -25 eu] (62), though the same approximate method was employed. The discrepancy is probably the result of using different $\delta\upsilon_o$ values, and of not maintaining slow passage conditions (2 Hz/sec) in the nmr experiment (126).

(B) $Ti(acac)_2(4\text{-}ClC_6H_4O)_2$; $\delta\upsilon_o \geq 11$ Hz - Comparison of exchange rates calculated from the various approximate equations with the TLS values in Table XLII reveal the same general trend as in case (A). Below coalescence, expressions [15] and [16] are in general good agreement with TLS values, although results from equation [16] tend to be slightly larger. Conditions under which equations [15] and [16] apply are satisfied in this case, viz., $2\tau\delta\upsilon_o$ = 0.5-20, and $\pi\sqrt{2}\tau\delta\upsilon_o$ = 1.1-3.9, respectively. Trends similar to case (A) also are observed for exchange rates above coalescence using equations [19], [21], and [22]. Equation [19] results in large errors near the coalescence region and for an error of $\leq$5%, using a $\delta\upsilon_o$ of 10.5 Hz, $1/2\tau$ should be >58 sec^{-1}. The opposite effect is observed with equation [22]; large errors appear at very fast exchange rates as the condition $W^* >> W''$ relaxes. For example, at T = 18.9 °C, W^* = ca. 23 W" while at T = 38.1 °C, W^* = ca. 7W"; therefore serious errors begin to appear in $1/2\tau$ values at an exchange rate > 30 sec^{-1}.

The Arrhenius plot is presented in Figure 40 and activation parameters are summarized in Table XLIV. Results from equation [15], with a variable $\delta\upsilon_o$, are in reasonable agreement with TLS values; however, as in case (A), very large errors are introduced when equation [15] is used with a constant $\delta\upsilon_o$ value. The remaining approximate equations give activation parameters which tend to cluster around the TLS values. Equation [19] gives

slightly larger activation parameters while results from equation [22] are slightly smaller than those from the TLS method. Inclusion of exchange rates (variable $\delta\upsilon_0$) from all approximate equations results in activation parameters in close agreement with TLS-calculated data. Again the values E_a = 11.7 kcal/mole and $\Delta S^{\neq}$ = -14 eu obtained in using equation [16] (constant $\delta\upsilon_0$) are not in agreement with those (6.7 kcal/mole and -31 eu, respectively) reported earlier (62). This discrepancy cannot be solely ascribed to solvent effects (153) (CH_2Cl_2 versus $CHCl_3$), but probably arises because of the different values of $\delta\upsilon_0$ used, and the failure to maintain slow passage conditions (2 Hz/sec), necessary for equation [16] to be valid.

(C) $(C_6H_5)ClSi(acac)_2$; $\delta\upsilon_0$ > 34 Hz - Lineshape parameters for this complex are compiled in Table XLII along with exchange rates from approximate equations and TLS methods. To determine TLS values (167), $\delta\upsilon_0$ was treated as a constant. This was necessitated by the small accessible temperature range which can lead to uncertainty in the extent to which $\delta\upsilon_0$ varies with temperature. Use of equation [15] ($2\tau\delta\upsilon_0$ = 0.6-0.9) results in exchange rates that are numerically higher than TLS values; however, the percent error appears to decrease towards coalescence. Near coalescence, $\delta\upsilon_e$ becomes more sensitive to changes in rate. Equation [16] ($\pi/2\tau\delta\upsilon_0$ = 1.5) gives better agreement with TLS values than equation [15]. As was seen in cases (A) and (B), the use of equation [15] with constant $\delta\upsilon_0$ may lead to very large systematic errors. The error in using equation [16] with a constant $\delta\upsilon_0$ is much less than that for equation [15]. The reasonable agreement between $1/2\tau$ calculated from equation [17] and TLS procedures indicates that the use of $\delta\upsilon_0$ = 33.9 Hz is a close approximation to the actual $\delta\upsilon_0$ value. Above coalescence, only one data point is available. Equations [21] and [22] are in reasonable agreement with TLS values while equation [19] shows a large negative error, not unexpected since conditions under which the latter expression is valid break down at the

temperature of the experiment (cf. Table XLII). However, conditions for expressions [21] and [22] are met at this temperature and fair agreement with TLS values results.

Figure 40 contains Arrhenius plots for equations [15] and [16] and TLS calculations. As expected, equation [15] (with constant $\delta\upsilon_0$) results (cf. Table XLV) in low values for E_a, $\Delta H^{\neq}$, and log A (large negative $\Delta S^{\neq}$ values). Combination of data points from equations [15] and [16] yields an E_a about 1 kcal/mole and $\Delta S^{\neq}$ about 5 eu lower than the corresponding TLS-calculated values. Since only three data points are available for equations [15] and [16], discrepancies between their values and the TLS values are not statistically significant.

(D) $(CH_3)ClSn(acac)_2$; $\delta\upsilon_0 > 8.5$ Hz - Exchange rates (Table XLII) calculated from equation [15] ($2\tau\delta\upsilon_0 = 0.5\text{-}1.7$) agree fairly well with the TLS-calculated values. Deviations begin to appear when $1/2\tau$ = ca. 5, in the region in which $\delta\upsilon_e$ becomes less sensitive to changes in rates. Reasonable agreement exists between exchange rates calculated from equation [16] and from the TLS method, although deviations occur as temperatures become further removed from coalescence; this may reflect a relaxation of the condition that $\pi/2\tau\delta\upsilon_0 > 1$ and that effects of the neglect of overlap of the uncoupled AB doublet are ignored. Above coalescence, equation [21] yields values in some agreement with TLS values over the region from near coalescence to very fast exchange. As seen earlier, serious discrepancies from the use of equation [22] appear in the very fast exchange region while they appear in the results from equation [19] as coalescence is approached (see case (A) above).

Results (Table XLVI) from expression [15] (variable $\delta\upsilon_0$) are larger than TLS-calculated activation parameters; this may be due to the slightly lower values for the exchange rates (cf. Table XLII). When a

constant value of $\delta\upsilon_0$ (= 9.89 Hz) is used, serious errors result in the activation parameters derived from equation [15]. Parameters from expression [16] (constant $\delta\upsilon_0$) are slightly lower than those from the TLS method. Of the post-coalescence equations, expression [21] gives the best agreement with TLS values. Since equation [19] results in exchange rates smaller than TLS values, activation parameters from this equation are correspondingly larger. The opposite effect is observed for the exchange rates of equation [22]. A combination of data points from all equations results in activation parameters slightly lower than TLS values. As was observed in cases (A) and (B), except for equation [15], all approximate expressions show an increase in activation parameters on going from a variable to a constant $\delta\upsilon_0$.

(E) $(C_6H_5)ClGe(acac)_2$; $\delta\upsilon_0 \geq 20$ Hz - Lineshape parameters and exchange rates calculated from approximate equations and TLS procedures are presented in Table XLII. Exchange rates calculated from equation [15] ($2\tau\delta\upsilon_0$ = 0.6-1.7) agree well with TLS results while the agreement for $1/2\tau$ values for equation [16] deteriorate as the temperature decreases markedly below coalescence. Much larger errors result at the coalescence temperature when expression [17] is used. This is caused by the uncertainty concerning the appropriate value of $\delta\upsilon_0$, since the chemical shift separation is temperature dependent. Above coalescence, equation [21] gives the best agreement with TLS-calculated exchange rates. As observed previously, equation [19] results in larger negative errors near the coalescence region while equation [22] yields negative errors in the very fast exchange region.

Arrhenius plots are illustrated in Figure 40; activation parameters are listed in Table XLVII. Equation [15] (variable $\delta\upsilon_0$) results in larger values of activation parameters; however, the differences with the TLS-calculated values may not be significant because of error limits. Use of equation [15] with a constant $\delta\upsilon_0$ (= 21.64 Hz) results in serious

deviations in activation parameters. Expression [16] yields activation parameters in reasonable agreement with TLS values. Those determined from equations [19], [21], and [22] are not statistically significant as only two data points are available. Using data points from all approximate equations (variable $\delta\upsilon_0$) gives activation parameters in reasonable agreement with TLS values.

(F) $\underline{(C_6H_5)_2Sn(acac)_2;\ \delta\upsilon_0 \geq 6.4\ Hz}$ - Characteristic lineshape parameters for this complex are listed in Table XLII, along with exchange rates calculated from approximate equations and TLS procedures. In this case, $\delta\upsilon_0$ was observed (167) to be temperature independent. From inspection of Table XLII it is evident that equation [15] ($2\tau\delta\upsilon_0 = 0.7\text{-}4.6$) yields large negative errors in exchange rates, a result of the breakdown of the condition that $0.45 \leq 2\tau\delta\upsilon_0 \leq 2$. The positive error in using equation [16] results from the effect of overlap of the components of the uncoupled AB doublet. For this complex, $\delta\upsilon_0$ = ca. 6.4 Hz while $1/T_2$ = ca. 8 Hz; the requirement that $\delta\upsilon_0 >> 1/T_2$ is thus not satisfied. Rogers and Woodbrey (164) have devised a method for correcting the effect of overlap; unfortunately, computer calculations are necessary. Above coalescence, exchange rates from equation [21] give the best agreement with TLS values. Equation [19] is again seen to yield larger negative errors in exchange rates near coalescence while equation [22] results in larger negative errors in $1/2\tau$ in the fast exchange region.

In view of the large negative errors in exchange rates arising from the use of equation [15], it is not surprising to find large deviations in the activation parameters vis-a-vis the TLS ones (Table XLVIII). Activation parameters from expression [16] are lower than the TLS values. Figure 40 indicates that large deviations occur from the TLS least-squares straight line for rates derived from equation [16]. Expressions [19] and [21] give

reasonable agreement with TLS-calculated activation parameters. Equation [22] results in $\log(1/2\tau)$ values which deviate markedly from the linear-least-squares TLS line of Figure 40.

These results show that reasonable agreement exists, in some cases, between exchange rates calculated from approximate methods and the more rigorous total lineshape method. Where the Rogers-Woodbrey expression is used, deviations in E_a and $\Delta S^{\neq}$ of 0.5 - 3.3 kcal/mole and 1 - 12 eu (variable $\delta\upsilon_o$), respectively, lower than TLS values were found. On the other hand, the Piette-Anderson equation yields values of E_a and $\Delta S^{\neq}$ which can be as much as 2.2 - 5.2 kcal/mole and 7 - 17 eu (variable $\delta\upsilon_o$) larger than TLS values. However, when exchange rates from all the approximate expressions are used in the analysis, E_a and $\Delta S^{\neq}$ values differ from 0 - 2 kcal/mole and 2 - 7 eu, respectively. Larger deviations are found when using one constant value for the chemical shift separation in the absence of exchange (cf. results from equation [15] in Tables XLIII-XLVIII).

Comparisons performed above were done with TLS values as the "actual" values for the exchange process. Spin echo studies on these complexes may yet reveal different values for the activation parameters. For example, the value of 14.6 ± 0.6 kcal/mole obtained (157) for N,N-dimethyltrichloroacetamide by the spin echo method is not in good agreement with the value 9.9 ± 0.3 kcal/mole obtained previously (164) by the high-resolution intensity ratio method. Discrepancies also exist in E_a and $\Delta S^{\neq}$ values from spin echo and high-resolution methods for the chair-chair isomerization of cyclohexane-d_{11} (158).

(iii) Rearrangement Processes in Bis(2,6-diisopropylphenoxy)-bis(chelate)titanium(IV) Complexes

The $Ti(chelate)_2(2,6\text{-}^iPr_2C_6H_3O)_2$ [chelate = acac,ox,quin] complexes have been structurally characterized in the solid state (139). All members of this series adopt a distorted octahedral geometry with cis phenoxide ligands. The oxinate and quinaldinate groups coordinate with nitrogen atoms cis and oxygen atoms trans. This appears to be the favoured configuration for octahedral complexes containing two oxinate ligands. The cis(N),trans(O) arrangement of oxinate donor atoms has been found in $(CH_3)_2Sn(ox)_2$ (169), $Ti(ox)_2Cl_2$ (170), $Ti(ox)_2Cl(\eta^5\text{-}C_5H_5)$ (171), $Mo(ox)_2(O)_2$ (172), and $V(ox)_2(O)(O^iC_3H_7)$ (173). For a complex of the type $M(ox)_2X_2$, three diastereomers are possible assuming the X groups maintain their cis relationship. These isomers differ in the relative orientation of the oxinate donor atoms around the octahedral core and may be designated as cis(O),trans(N), cis(N),trans(O), and cis(O),trans(N). Only the cis(N),-trans(O) arrangement is observed for the 2,6-diisopropylphenoxy complexes. While the $Ti(ox)_2(2,6\text{-}^iPr_2C_6H_3O)_2$ complex provides no convenient means of establishing the configuration of the oxinate donor atoms in solution using nmr methods, the quinaldinate methyl groups in the $Ti(quin)_2(2,6\text{-}^iPr_2C_6H_3O)_2$ complex may provide such information. A solution of the quinaldinate complex in 1,3-dichlorobenzene displays a single quinaldinate methyl resonance. After heating for several hours at ca. 140° and cooling to room temperature, no change in the quinaldinate methyl resonance is observed. If isomerization to a different arrangement of donor atoms had occurred, a more complex quinaldinate methyl resonance would be expected. It is not likely that, if a mixture of diastereomers existed, their chemical shifts would be degenerate, given the highly anisotropic nature of the quinaldinate ligand. Although

the possibility cannot be eliminated, it is also unlikely that isomerization occurred on dissolution. On this basis, it is assumed that in solution, the $Ti(ox)_2(2,6\text{-}^iPr_2C_6H_3O)_2$ and $Ti(quin)_2(2,6\text{-}^iPr_2C_6H_3O)_2$ complexes exist as a single diastereomer possessing the cis(N),trans(O) configuration.

The temperature dependence of the acetylacetonate and isopropyl methyl resonances of the $Ti(acac)_2(2,6\text{-}^iPr_2C_6H_3O)_2$ complex in m-dichlorobenzene is shown in Figure 41. This behaviour is similar to that observed in dichloromethane but spanning a different temperature region. Figures 42 and 43 illustrate the temperature dependence of the isopropyl methyl resonances of the $Ti(quin)_2(2,6\text{-}^iPr_2C_6H_3O)_2$ and $Ti(ox)_2(2,6\text{-}^iPr_2C_6H_3O)_2$ complexes, respectively, in m-dichlorobenzene solution. The crossed lines in Figures 42 and 43 are due to spinning side bands or carbon-13 satellites of tetramethylsilane.

A TLS analysis of the rearrangements of the $Ti(acac)_2(2,6\text{-}^iPr_2C_6H_3O)_2$ complex in m-dichlorobenzene solution was carried out and the results have been presented in part (i) above. For the oxinate and quinaldinate complexes, a similar analysis was performed but with diminished accuracy as a result of the relative chemical shifts of the exchanging isopropyl methyl doublets. For the acac complex, the separation of the two doublets is small (ca. 6 Hz), which means that the simple coalescence of the low-field line from both doublets to the low-field part of the final, averaged doublet may be straightforwardly followed. With the ox and quin complexes, the huge chemical shift differences between the two doublets (ca. 20 - 40 Hz) necessitates the crossing and merging of the low field and high field components of the two doublets into a broad, featureless resonance, before re-sharpening to form a single time-averaged doublet. Thus only temperatures above and below this coalescence temperature could be used to extract mean lifetimes for isopropyl methyl group exchange.

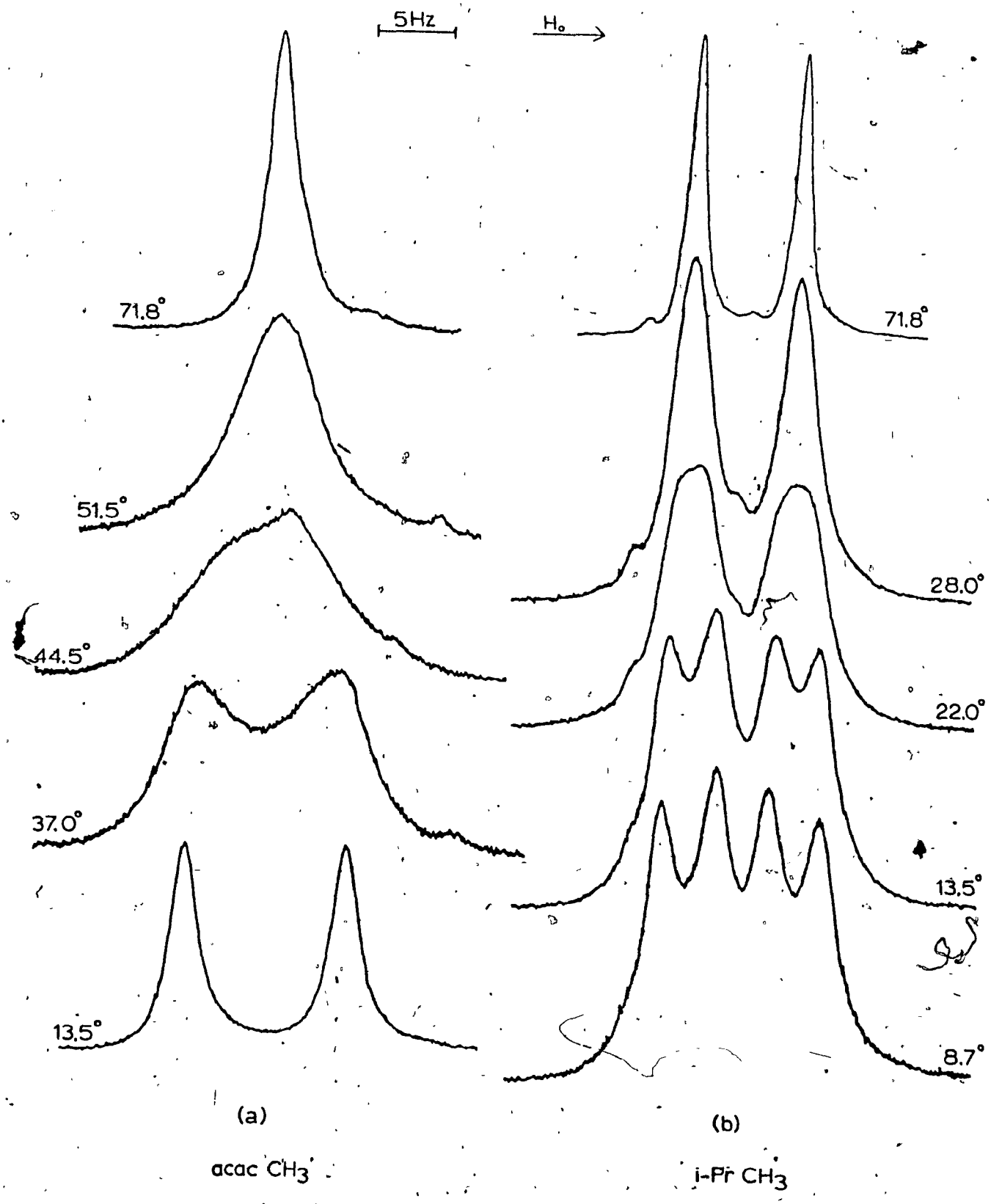

Figure 41. - Temperature dependence of the (a) acetylacetonate and (b) isopropyl methyl resonances of the $Ti(acac)_2(2,6\text{-}^{i}Pr_2C_6H_3O)_2$ complex in m-dichlorobenzene solution, 0.250M.

Figure 42.- Temperature dependence of the isopropyl methyl resonances of the $Ti(quin)_2(2,6\text{-}^{i}Pr_2C_6H_3O)_2$ complex in m-dichlorobenzene solution, 0.111M. Carbon-13 satellites or spinning side bands of TMS are labelled x.

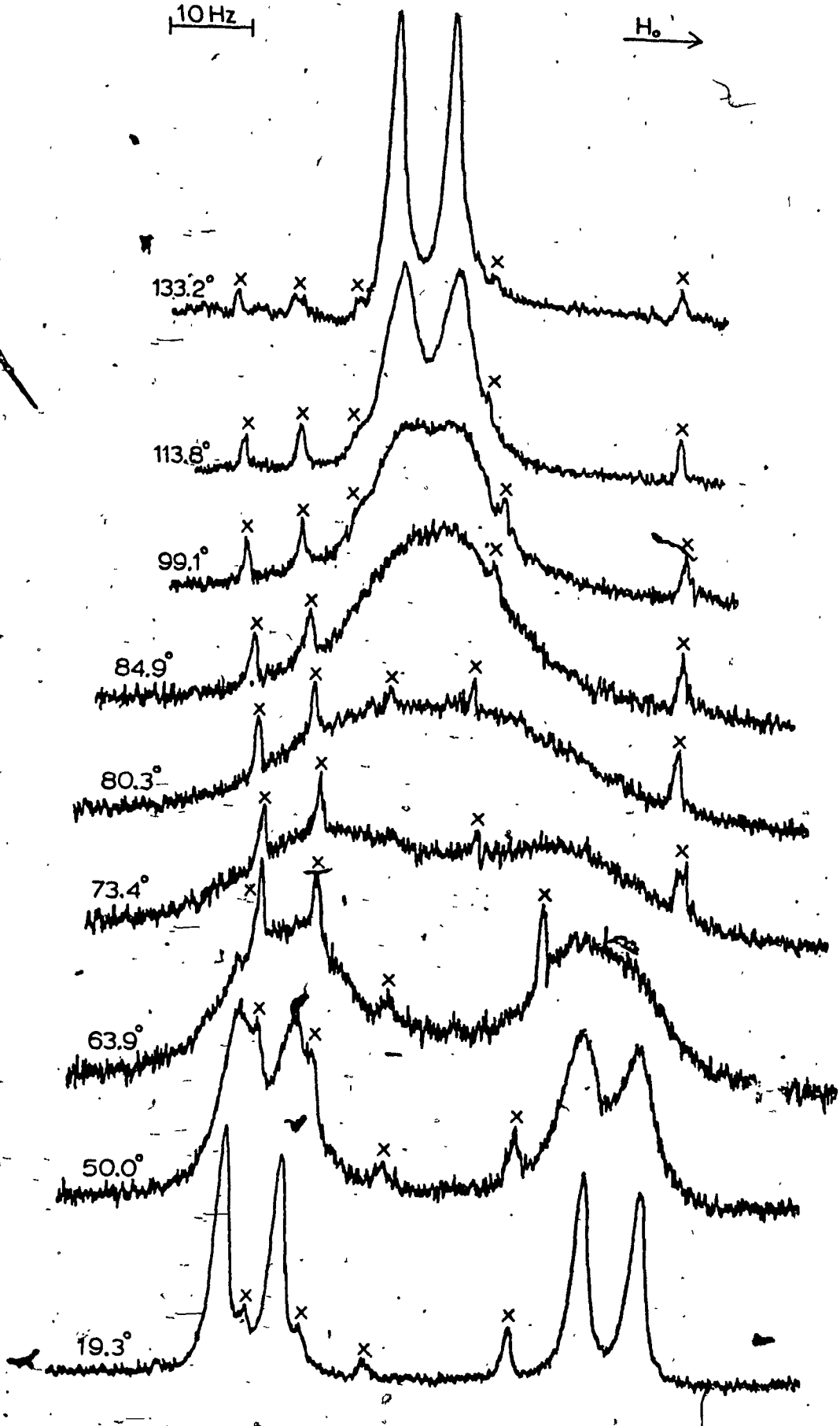
10 Hz
H_o
133.2°
113.8°
99.1°
84.9°
80.3°
73.4°
63.9°
50.0°
19.3°

Figure 43.- Temperature dependence of the isopropyl methyl resonances of the $Ti(ox)_2(2,6\text{-}^{i}Pr_2C_6H_3O)_2$ complex in m-dichlorobenzene solution, 0.145 M. Spinning side bands or carbon-13 satellites of TMS give rise to those lines labelled x. A constant sweep width was not maintained.

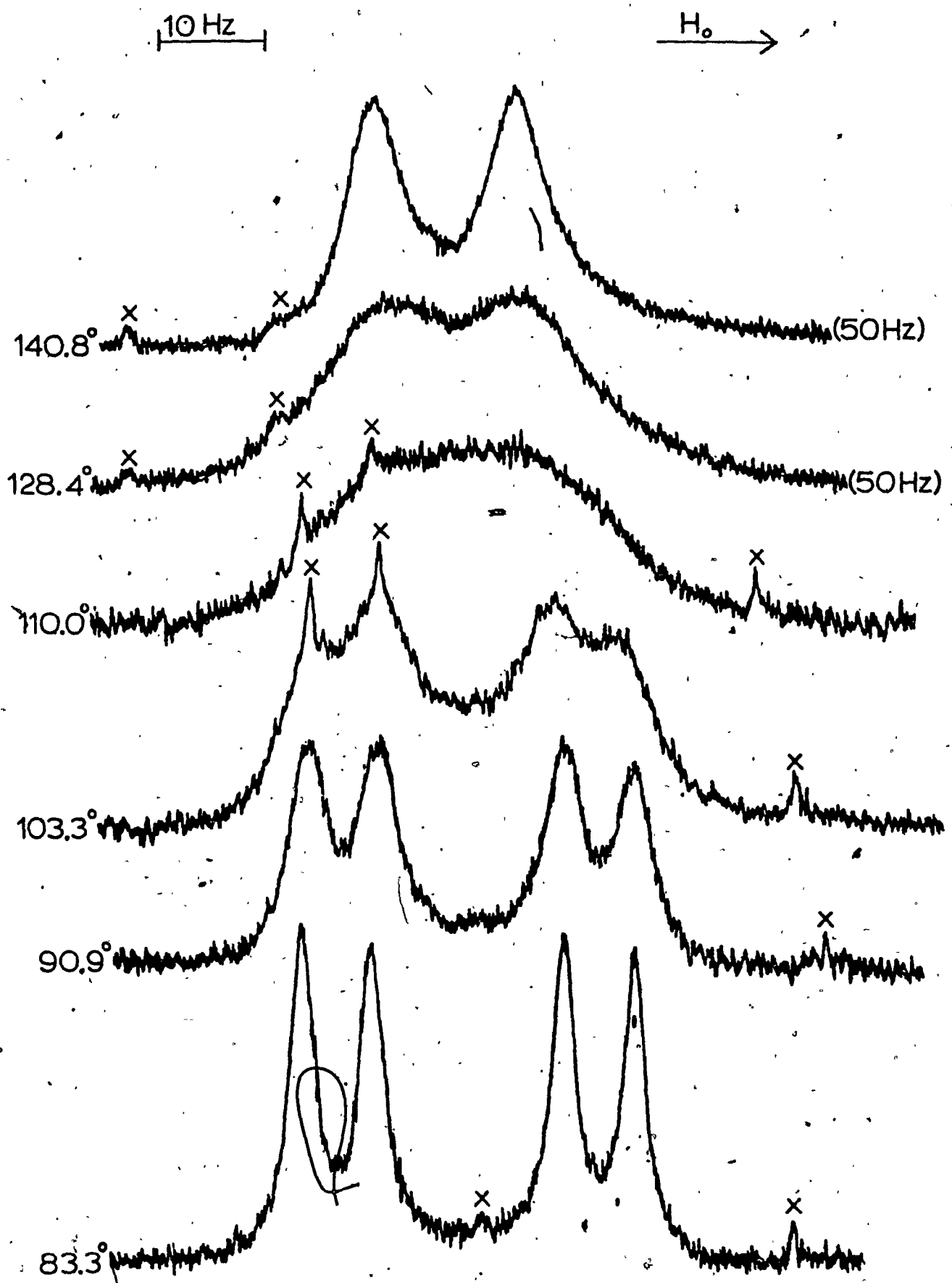
10 Hz
H_o
140.8°
(50Hz)
128.4°
(50Hz)
110.0°
103.3°
90.9°
83.3°

Tables IL and L list the characteristic lineshape parameters used to extract mean lifetimes, τ, for exchange of isopropyl methyl groups in the $Ti(quin)_2(2,6\text{-}^iPr_2C_6H_3O)_2$ and $Ti(ox)_2(2,6\text{-}^iPr_2C_6H_3O)_2$ complexes, respectively. Mean lifetimes were obtained by comparing experimental lineshape parameters with those from calculated spectra using the Gutowsky-Holm total lineshape equation (17), as described in Section II-C. The temperature dependence of $\delta\upsilon$ was measured and the straight line portion from the slow exchange region was extrapolated into the intermediate and fast exchange regions for lineshape calculations; these data are listed in Appendix B. Since the fast and slow exchange regions could not both be attained, the temperature dependence of T_2 was not known. In order to determine whether solvation and viscosity effects render T_2 temperature dependent, the quinaldinate methyl resonance was studied over the temperature range of ca. 40^o to ca. 160^o; the temperature dependence of $W_{1/2}$ for this resonance is listed in Table LI. Over this temperature range the average value of $W_{1/2}$ is 1.03 ± 0.05 Hz; this indicates that T_2 is independent of temperature (over this range) and the average value of 1.03 Hz was employed for a T_2 value in lineshape calculations. The concentration dependence of the mean residence times, presented in Table LII, demonstrates that the exchange of isopropyl methyl groups is independent of concentration and is a first-order process.

Arrhenius activation parameters were obtained in the usual fashion from the least-squares straight line plot of log k versus 1/T, shown in Figure 44, where $k = 1/2\tau$ is the first-order rate constant for isopropyl methyl group exchange. Arrhenius and Eyring activation parameters for exchange of isopropyl methyl groups in $Ti(chelate)_2(2,6\text{-}^iPr_2C_6H_3O)_2$ complexes [chelate = acac,ox,quin] are collected in Table LIII. The error limits attached to these activation parameters reflect only the random

Table IL

Isopropyl Methyl PMR Lineshape Parameters and Values of τ for $Ti(quin)_2(2,6\text{-}^{i}Pr_2C_6H_3O)_2$[b]

			Linewidths (Hz)						
	$\delta\upsilon_e$ (Hz)		$W_{1/4}$		$W_{1/2}$		$W_{3/4}$		
Temp., °C	LF	HF	LF	HF	LF	HF	LF	HF	$\tau \times 10^3$ (sec)
54.5	40.14[c] ; 40.22[d]		-	-	-	-	-	-	41
63.9	35.60		-	-	-	-	-	-	13
66.0	34.80		-	-	-	-	-	-	12
68.7	33.46		-	-	-	-	-	-	11
73.4	24.78		-	-	-	-	-	-	7.4
80.3	-		-		-		-		5.7
113.8	-		-		-		2.94		0.92
117.5	-		-		4.32		2.32		0.73
121.8	-		-		3.57		1.95		0.57
125.8	-		-		2.82		1.57		0.42
133.2	-		-		2.08		1.17		0.25

[a]Symbols are defined in Table XXII; [b]0.111 M in 1,3-dichlorobenzene; [c]Low-field doublet; [d]High-field doublet.

Table L

Isopropyl Methyl PMR Lineshape Parameters[a] and Values of τ for $Ti(ox)_2(2,6\text{-}^iPr_2C_6H_3O)_2$[b]

			Linewidths (Hz)						
	$\delta\upsilon_e$ (Hz)		$W_{1/4}$		$W_{1/2}$		$W_{3/4}$		
Temp., °C	LF	HF	LF	HF	LF	HF	LF	HF	$\tau \times 10^3$ (sec)
94.9	23.84[c] ; 23.79[d]		-	-	-	-	-	-	39
99.9	22.97 ; 22.23		-	-	-	-	-	-	26
103.3	21.65 ; 21.22		-	-	-	-	-	-	20
105.9	21.22 ; 20.64		-	-	-	-	-	-	19
108.2	20.59 ; 19.75		-	-	-	-	-	-	18
134.3	-			-		-		3.39	2.7
140.8	-			-		3.93		2.02	1.6
154.1	-			4.19		2.18		1.21	0.68

[a] Symbols are defined in Table XXII; [b] 0.145 M in 1,3-dichlorobenzene; [c] Low-field doublet; [d] High-field doublet.

Table LI

Temperature Dependence of the Linewidth at Half-Height of the Quinaldinate Methyl Resonance of the $Ti(quin)_2(2,6\text{-}^iPr_2C_6H_3O)_2$ Complex in *m*-dichlorobenzene Solution

Temp., °C	$W_{1/2}$ (Hz)[a]	Temp., °C	$W_{1/2}$ (Hz)[a]
27.9	1.40	84.9	1.04
33.3	1.34	85.2	0.97
41.0	1.16	99.1	0.99
50.0	1.26	105.3	0.97
54.5	1.12	113.8	1.00
59.0	1.11	121.8	1.05
63.9	1.10	125.8	1.00
73.4	1.01	133.2	1.09
80.3	0.91	158.2	1.05

Average $W_{1/2}$ (from 54.5° to 158.2°) = 1.03 ± 0.05 Hz

[a] Each value represents the average of five readings at the indicated temperature.

scatter of the data points, estimated at the 95% confidence level, and do not contain any possible contributions from systematic errors (59,60).

Kinetic data in Table LIII reveal that the rate of isopropyl methyl group exchange in $Ti(chelate)_2(2,6\text{-}^iPr_2C_6H_3O)_2$ complexes decreases in the order chelate = acac > quin > ox. However, large differences in the activation parameters between the acac and the quin and ox complexes suggest that a different physical process may be responsible for the rearrangement in the quin and ox complexes. For example, entropies of activation differ by 26.8 eu for the quin complex and 38.5 eu for the ox complex in comparison with the value for the acac complex. Equally dramatic differences exist in other activation parameters.

Table LII

Concentration Dependence of Mean Residence Times for Isopropyl Methyl Group Exchange in the $Ti(quin)_2(2,6\text{-}^iPr_2C_6H_3O)_2$ and $Ti(ox)_2(2,6\text{-}^iPr_2C_6H_3O)_2$ Complexes in m-dichlorobenzene Solution

Complex	Temp., °C	Concentration, M	τ, sec
$Ti(quin)_2(2,6\text{-}^iPr_2C_6H_3O)_2$	66.0	0.111	1.2×10^{-2}
		0.070	1.2×10^{-2}
	121.8	0.111	5.7×10^{-4}
		0.070	5.1×10^{-4}
$Ti(ox)_2(2,6\text{-}^iPr_2C_6H_3O)_2$	99.9	0.145	2.6×10^{-2}
		0.101	2.6×10^{-2}
	134.4	0.145	2.7×10^{-3}
		0.101	2.9×10^{-3}

Using the nomenclature defined in Figure 6 for a cis-$M(AB)_2X_2$ complex, the ox and quin complexes adopt the cis,cis,trans (R_1 = N; R_2 = O) geometry in the solid state (139), which appears to be maintained in solution (vide supra). Following the discussion in Section III-C-1-c(i), the exchange of isopropyl methyl groups is identified as resulting from inversion of the molecular configuration. Assuming the complexes retain the cis,cis,trans stereochemistry during the inversion, the sole reaction occurring in the ox and quin complexes appears to be

$$\text{cis,cis,trans-}\Delta(\Lambda) \leftrightarrow \text{cis,cis,trans-}\Lambda(\Delta) \qquad [23]$$

Inspection of Table XVI and Figure 21 reveals that a twist mechanism does accomodate the requirements of the rearrangement demanded by equation [23]. Similarly, Table XVIII and Figure 25 demonstrate that a bond rupture mechanism via a SP-axial intermediate formed and decaying to products through a primary process does not generate the rearrange-

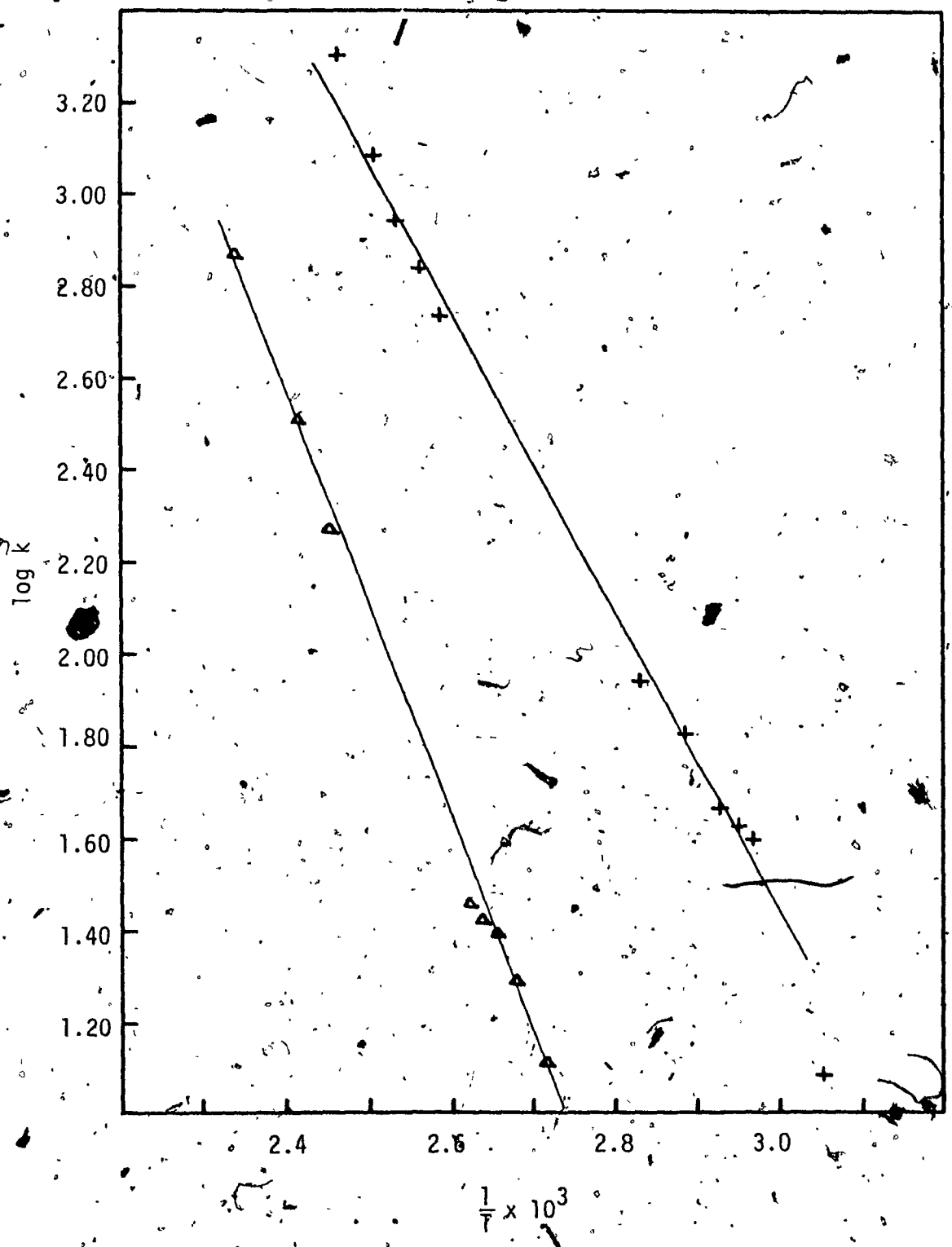

Figure 44. - Arrhenius (log k versus 1/T) least-squares plot for isopropyl methyl group exchange in the $Ti(ox)_2(2,6\text{-}^{i}Pr_2C_6H_3O)_2$ (Δ) and $Ti(quin)_2(2,6\text{-}^{i}Pr_2C_6H_3O)_2$ (+) complexes in m-dichlorobenzene solution.

Table LIII

Kinetic Data for Isopropyl Methyl Group Exchange in Ti(chelate)$_2$(2,6-diisopropylphenoxy)$_2$ Complexes[a]

Chelate	k_{298} (sec^{-1})	$\Delta H^{\neq}_{298}$ (kcal/mole)	$\Delta S^{\neq}_{298}$ (eu)	$\Delta G^{\neq}_{298}$ (kcal/mole)	E_a (kcal/mole)	log A
acac[b]	4.2	5.7 ± 1.7 [c]	-36.5 ± 5.7	16.60 ± 0.04	6.3 ± 1.7	5.3 ± 1.2
quin[d]	2.0	14.1 ± 0.8	-9.7 ± 2.2	17.1 ± 0.3	14.7 ± 0.8	11.10 ± 0.49
ox[e]	0.013	20.7 ± 1.3	2.2 ± 3.3	20.0 ± 0.3	21.2 ± 1.3	13.69 ± 0.72

[a]In m-dichlorobenzene solution; [b]0.250 M; [c]All errors are random errors estimated at the 95% confidence level; [d]0.111 M; [e]0.145 M.

ment required by reaction [23].

After consulting Table XVII and Figure 23 it is found that the stereochemistry of the rearrangement demanded by reaction [23] can only be generated *via* a bond rupture mechanism occurring through a single TBP-axial intermediate, labelled 5 in Table XVII and Figures 22 and 23, and which is illustrated below.

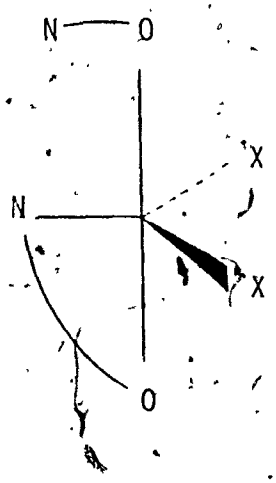

The sole intermediate capable of explaining reaction [23] for the $Ti(quin)_2(2,6\text{-}^iPr_2C_6H_3O)_2$ and $Ti(ox)_2(2,6\text{-}^iPr_2C_6H_3O)_2$ complexes arises from rupture of the Ti-N bond in the equatorial plane, *trans* to the X groups. From X-ray crystallographic structure determinations of these two complexes it was inferred that the Ti-N bond is weaker in the quin complex relative to the ox complex (139). If rupture of the Ti-N bond is the rate-determining step in the rearrangement, the quin complex should be more labile than the ox complex, as is observed.

Although the oxinate and quinaldinate ligands are not very flexible chelating ligands, from the structure of the proposed intermediate shown above, it is evident that the Ti-O-C(ox,quin) angle is sufficiently flexible to permit this end of the ligand to serve as a pivot. Reattachment of the nitrogen atom in the equatorial plane generates

the rearranged product.

From the discussion in Section III-C-1-c(i) concerning the $Ti(acac)_2(2,6\text{-}^iPr_2C_6H_3O)_2$ complex, a definite mechanism could not be established although available evidence favoured a twist mechanism. If a bond rupture mechanism is operative in the quin and ox complexes, this explains the large differences in activation parameters for isopropyl methyl group exchange in the $Ti(chelate)_2(2,6\text{-}^iPr_2C_6H_3O)_2$ series (cf. Table LIII). Entropies of activation are thought to be more positive for bond rupture mechanisms relative to twist mechanisms (6,7); however, caution must be exercised when employing $\Delta S^{\neq}$ as an indicator of mechanism (111).

The apparent Ti-N bond rupture mechanism for the quin and ox complexes is not suprising as this bond is expected to be the weakest of the core metal-ligand bonds from the relative electronegativities of nitrogen and oxygen. Although no thermochemical data for Ti-N and Ti-O bonds appear to have been reported, some data (174) for the analagous bonds with aluminum reveal the expected trend: Al-N and Al-O bond strengths are 71 and 107 kcal/mole, respectively (174).

This section has presented evidence for the operation of a bond rupture mechanism in the rearrangement of $Ti(quin)_2(2,6\text{-}^iPr_2C_6H_3O)_2$ and $Ti(ox)_2(2,6\text{-}^iPr_2C_6H_3O)_2$ complexes. Crucial to the arguments leading to this conclusion is the assumption that these complexes populate the cis(N), trans(O) isomer in solution and in the solid state and that no isomerization of this thermodynamically preferred arrangement occurs in solution. This allows the steric course of the rearrangement to be defined in detail.

Chemical shift data for the complexes reported in this section may be found in Appendix C.

2. The $M(AA)_2XY$ System

a. Introduction

A complex of the type $M(AA)_2XY$, where X and Y represent different monodentate ligands and AA represents a symmetrical bidentate ligand, may adopt configurations containing cis or trans X and Y groups, as illustrated in Figure 45. In the enantiomeric cis form all four terminal R groups of the bidentate ligand are symmetry nonequivalent. Should the bidentate ligand be a β-diketone, the -CH= or -CR= groups in the γ-position of the ring are also nonequivalent. Thus the cis isomer would reveal four R group resonances and two -CH= (or -CR=) resonances in the nmr spectrum while the trans diastereomer would reveal a single R group and -CH= (or -CR=) resonance. For reasons mentioned in Section III-C-1a, caution must be exercised in using this difference in signal multiplicities as a means of establishing configurations.

A paucity of data exists for this type of complex involving group IV elements. Probably the most thoroughly studied series of complexes are the $(\eta^5\text{-}C_5H_5)M(dik)_2X$ [M = Zr; dik = acac, dpm; X = Cl, Br; M = Hf, dik = acac, X = Cl] (175-176) complexes. The solid state structure of $(\eta^5\text{-}C_5H_5)\text{-}Zr(acac)_2Cl$ is known (177) and, although best visualized using a D_{2d} dodecahedral environment, solution behaviour for these complexes may be approximated by an octahedral formalism involving a single isomer of C_1 symmetry (175,176). This is only a formalism for the Zr(IV) and Hf(IV) complexes since analagous Ti(IV) derivatives exhibit two isomers of C_1 symmetry (178,179). For the Zr(IV) and Hf(IV) complexes, four acac (or dpm) methyl and two -CH= resonances are observed at room temperature. At elevated temperatures, a single methyl and -CH= resonance results from a rapid exchange process. Pinnavaia and co-workers (176) have reasoned

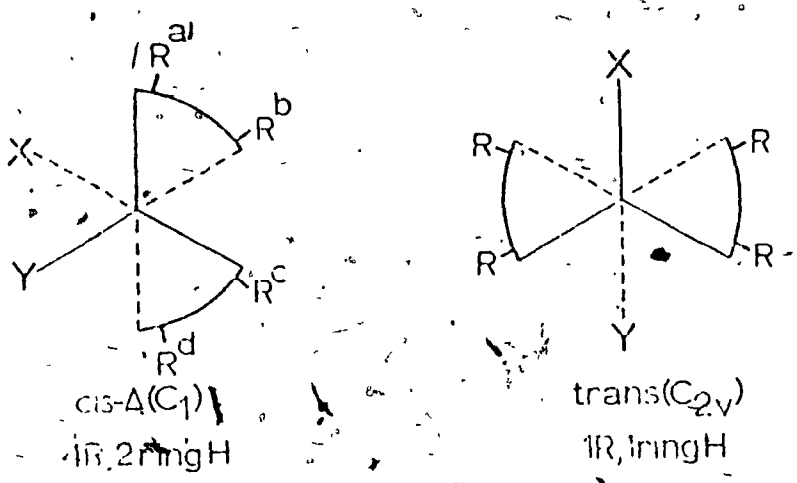

Figure 45.- Possible isomers for a $M(AA)_2XY$ complex. Letter superscripts label nonequivalent environments. Expected signal multiplicities are indicated below each diastereomer.

these rearrangements on the basis of twist mechanisms. Phenoxy derivatives of the type $(\eta^5\text{-}C_5H_5)M(acac)_2(OC_6H_5)$ [M = Zr,Hf] have been reported (180) and exhibit spectra analagous to the halo derivatives at room temperature; however, no mention of rearrangement processes occurring at higher temperatures appeared.

Another series of complexes that have received attention recently are of the type $RClM(acac)_2$ [M = Si,Ge,Sn; R = CH_3,C_6H_5], which have been shown to exist as the stereochemically nonrigid cis diastereomer (142,181,182). A detailed study (111,142) of the tin(IV) systems suggests that the rearrangement involves the operation of a twist mechanism.

Much less is known concerning titanium(IV) complexes of the type $Ti(dik)_2XY$. The $Ti(acac)_2F(OC_2H_5)$ complex has been generated by ligand exchange reactions and shown to adopt the cis geometry (58,71). A more

general method of preparing and isolating $Ti(acac)_2X(OR)$ complexes has appeared (70) and all of the complexes studied were found to exist as stereochemically nonrigid cis diastereomers.

This section reports the results of attempts to establish the operation of enantiomerization processes in complexes of the type $Ti(dik)_2Cl(OR)$ [dik = dibm, R = CH_3; dik = acac, R = i-C_3H_7, 2,6-$^iPr_2$-C_6H_3O], in which the diastereotopic probe is placed on the bidentate and monodentate ligands.

b. Diastereotopic Probe on the Bidentate Ligand

For a cis-$M(dibm)_2XY$ complex, eight isopropyl methyl spin doublets are expected as well as two -CH= resonances. The trans isomer should reveal a single isopropyl methyl doublet and -CH= resonance. Figure 46 illustrates the temperature dependence of the -CH= and isopropyl methyl resonances of the $Ti(dibm)_2Cl(OCH_3)$ complex in a dichloromethane solution. Below ca. -5^o, two -CH= resonances are observed. Above this temperature a single resonance is observed as a result of a rapid exchange process. The isopropyl methyl resonance is more revealing. At ambient temperature, a single doublet is observed. However, on cooling, this resonance broadens until a featureless resonance remains at ca. 10^o. Further cooling causes the appearance of two broad doublets by -10^o and eventually four doublets appear by -30^o. These observations indicate that the complex exists solely as the cis-diastereomer.

On the basis of previous assignments (142), the lowest-field isopropyl methyl doublet may be assigned to those groups in the equatorial plane trans to the chloro and methoxy groups. The four axial isopropyl methyl groups comprise the three less intense upfield spin doublets. Thus the isopropyl methyl resonance pattern at -30^o may be described as four

Figure 46.- Temperature dependence of the (a) ring proton (=CH=) and (b) isopropyl methyl resonances of the $Ti(dibm)_2Cl(OCH_3)$ complex in dichloromethane solution, 0.300 M.

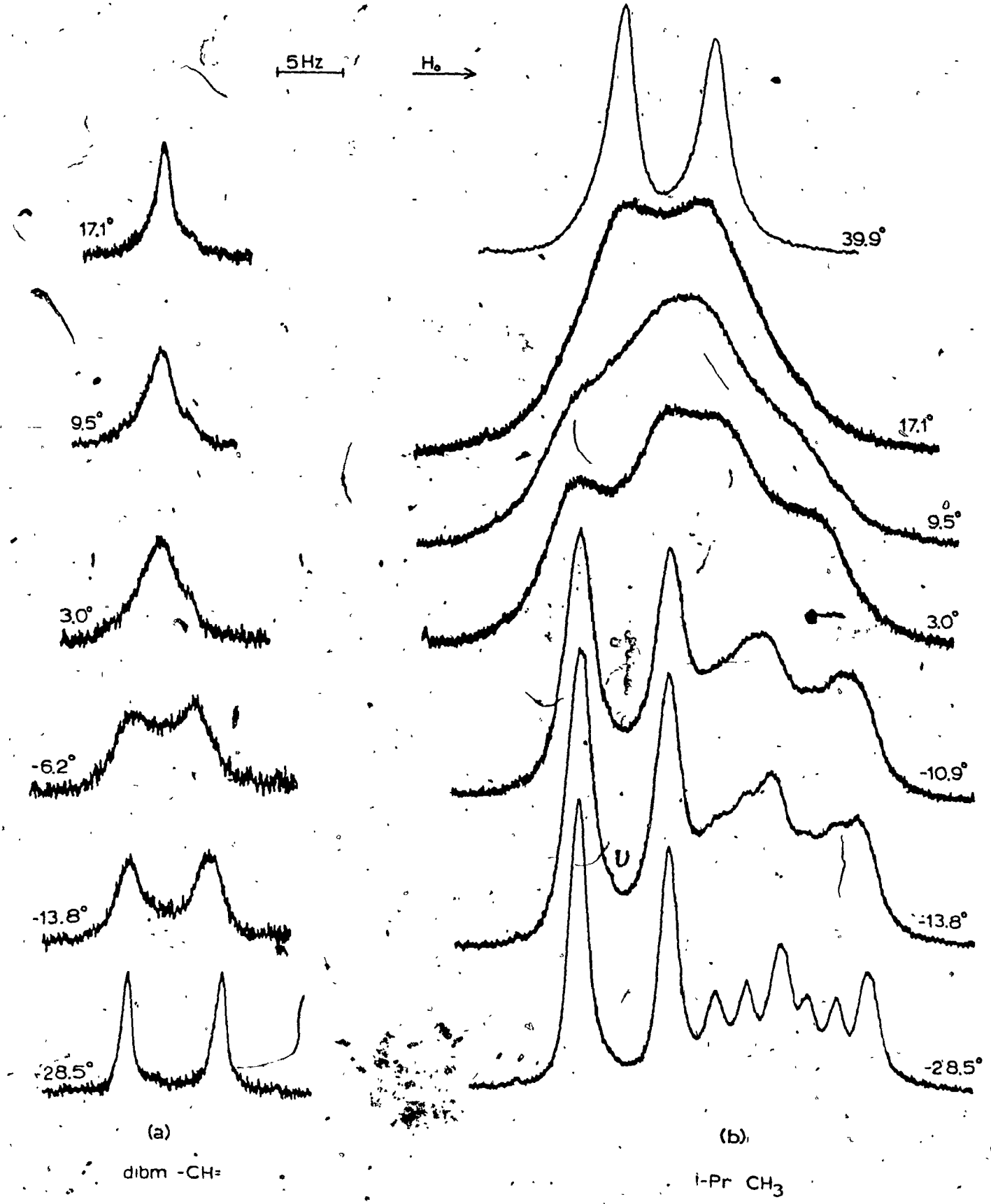
5 Hz
H_o
17.1°
9.5°
3.0°
-6.2°
-13.8°
-28.5°
(a)
dibm -CH=
39.9°
17.1°
9.5°
3.0°
-10.9°
-13.8°
-28.5°
(b)
i-Pr CH_3

spin doublets with relative areas of 4:1:1:2 which accounts for all eight isopropyl methyl groups in the cis-$Ti(dibm)_2Cl(OCH_3)$ complex. No change in this resonance pattern occurs on cooling to ca. -60^o, except for slight broadening of resonances due to solvation and viscosity effects.

No detailed lineshape analysis of the -CH= group exchange was attempted; however, an approximate rate constant may be calculated at the coalescence temperature for -CH= group exchange from the expression $k_{Tc} = \pi\delta\upsilon/\sqrt{2}$ (18), where $\delta\upsilon$ (in Hz) is the chemical shift separation of the two -CH= resonances in the slow exchange limit. For the cis-$Ti(dibm)_2Cl(OCH_3)$ complex, $\delta\upsilon$ is not constant in the slow exchange region; consequently, the observed value at the lowest measured temperature ($\delta\upsilon$ = 7.92 Hz at -60.4^o) was used. This yields a value of 17 sec^{-1} at the -CH= coalescence temperature of ca. 0^o. In order to compare the non-rigidity of this $Ti(dik)_2Cl(OR)$ complex with parent $Ti(dik)_2Cl_2$ and $Ti(dik)_2(OR)_2$ complexes, rate constants at 0^o were calculated from the accurate kinetic data for $Ti(acac)_2Cl_2$ (54) and the approximate data for $Ti(acac)_2(OCH_3)_2$ (61) for exchange of acetylacetonate methyl groups. These rate constants are ca. 117 sec^{-1} and 7.7 sec^{-1} for these complexes, respectively. The rate constant for -CH= group exchange in $Ti(dibm)_2Cl(OCH_3)$ is intermediate between these two extremes, suggesting that the substitution of an alkoxy group with a chloro group increases the lability, with the trend in labilities increasing in the order $Ti(dik)_2Cl_2 > Ti(dik)_2Cl(OR) > Ti(dik)_2(OR)_2$.

A permutational and mechanistic analysis of possible rearrangements within a cis-$M(AA')_2XY$ system was presented in Sections III-A-3c and III-A-4c, respectively. Consulting Table VI, which lists the expected changes in signal multiplicities for the various averaging sets,

one finds that no averaging set will predict the collapse of the diastereotopic terminal groups of the A-A ligand to a single doublet. The minimum number of doublets predicted is two; generated by averaging sets A_6' and A_{13}'. Using the same arguments as set out in Section III-C-1-b(i) for a similar problem with the $M(dibm)_2X_2$ complexes, the expected two isopropyl methyl doublets are assumed to have degenerate chemical shifts, and overlap of four isopropyl methyl doublets is considered improbable. In this case, the extra provision of nonequivalent -CH= groups allows a more definite exclusion of certain averaging sets. Since the isopropyl methyl resonances and -CH= resonances coalesce over the same temperature region, it is assumed that exchange of terminal groups and -CH= groups are intimately connected; i.e., they both originate from the same molecular motion.

Since -CH= groups are exchanged, the following averaging sets may be eliminated on the basis of Table VI: A_1', A_2', A_3', A_5', A_8', A_9', A_{10}', and A_{12}'. With the assumption that observation of a single isopropyl methyl doublet results from overlap of two doublets and since multiplicity changes of 4 → 1 are observed for a number of cis-$Ti(acac)_2Cl(OR)$ complexes (70), the A_4', A_7', A_{11}', and A_{14}' averaging sets may be eliminated. Only averaging sets A_6' and A_{13}' remain. The sole difference between these averaging sets is that A_6' does not cause enantiomerization while A_{13}' does. Since diastereotopic splitting is observed in the cis-$Ti(dibm)_2Cl(OCH_3)$ complex at low temperature, it is probable that the exchange process involves inversion of the molecular configuration. Thus only averaging set A_{13}' remains to explain the permutation of nonequivalent groups within the cis-$Ti(dibm)_2Cl(OCH_3)$ complex.

Attention is now focused on the most probable physical process which generates the unique set of permutations of nonequivalent

groups known as averaging set A'_{13}. An intramolecular mechanism is assumed. Details of the physical processes may be found in Section III-A-4c.

On consulting Table XV it is found that averaging set A'_{13} may be generated by twist motions about the $C_3(i')$ and $C_3(i''')$ axes of the octahedron. This process is illustrated in Figure 16.

Table XV also reveals that a bond rupture process proceeding via TBP-axial or -equatorial intermediates will not accomodate averaging set A'_{13}. This mechanism is illustrated in Figure 18 for rupture of bond a of Figure 5. However, the possibility exists that the TBP intermediate may rearrange intramolecularly to another TBP intermediate which may generate averaging set A'_{13} on reattachment of the dangling ligand. This rearrangement may occur via a pseudorotation process about each of the three metal-ligand bonds of the TBP intermediate (28). This mechanism is favoured for stereochemically nonrigid five-coordinate complexes (10). The pseudorotation process is illustrated in Figure 47 operating on the 5ℓ TBP-equatorial intermediate.

The pseudorotation analysis is summarized in Table LIV. All TBP intermediates formed after initial bond rupture are allowed to pseudorotate about all three metal-ligand equatorial pivots. TBP-axial intermediates yield only TBP-equatorial intermediates after pseudorotation and reattachment of the dangling ligand may generate averaging set A'_{13} in certain cases. Pseudorotation of TBP-equatorial intermediates generate a mixture of TBP-axial and -equatorial intermediates which can generate averaging set A'_{13} on reattachment of the dangling ligand to the metal ion.

However, due to the extensive ligand motion involved in the pseudorotation pathway, it does not present an attractive energetic pathway for configurational rearrangements in the cis-$Ti(dibm)_2Cl(OCH_3)$ complex.

Figure 47.- Illustration of the pseudorotation process in a five-coordinate TBP intermediate, 5ℓ, for a cis-$M(AA)_2XY$ system. (a) Labelling of rotation axes; (b) illustration of the pseudorotation process, [P], abouth the three axes of (a). Intermediates are defined in Figure 17.

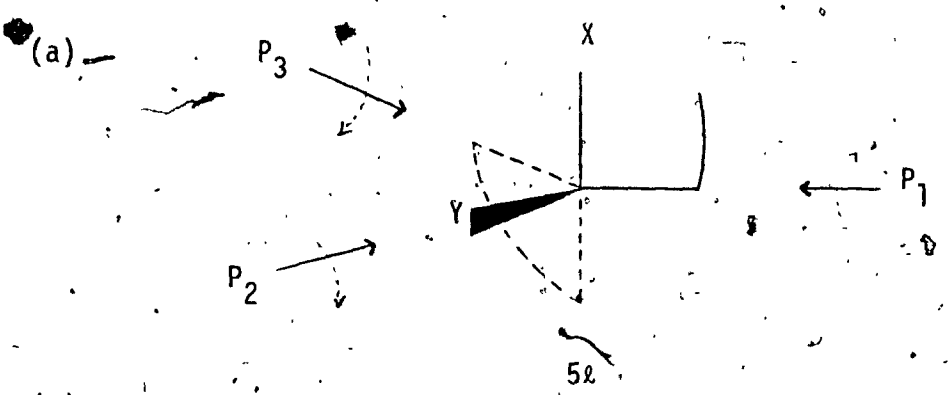

(b)

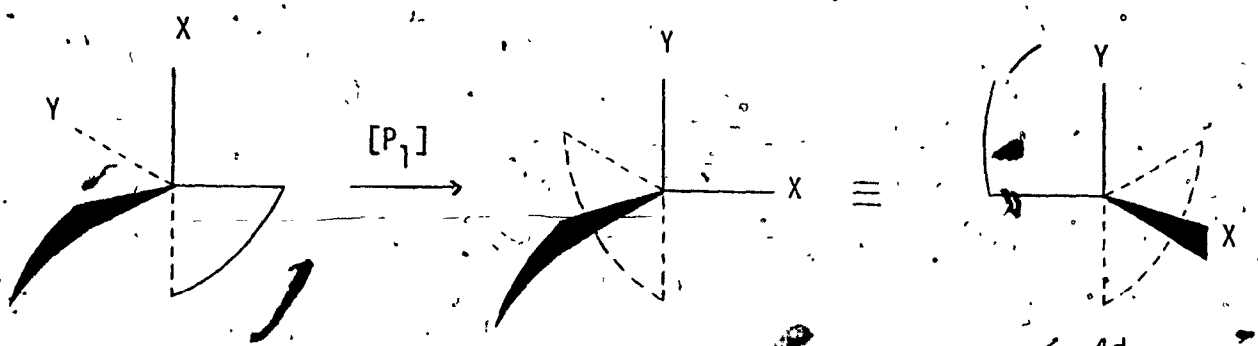

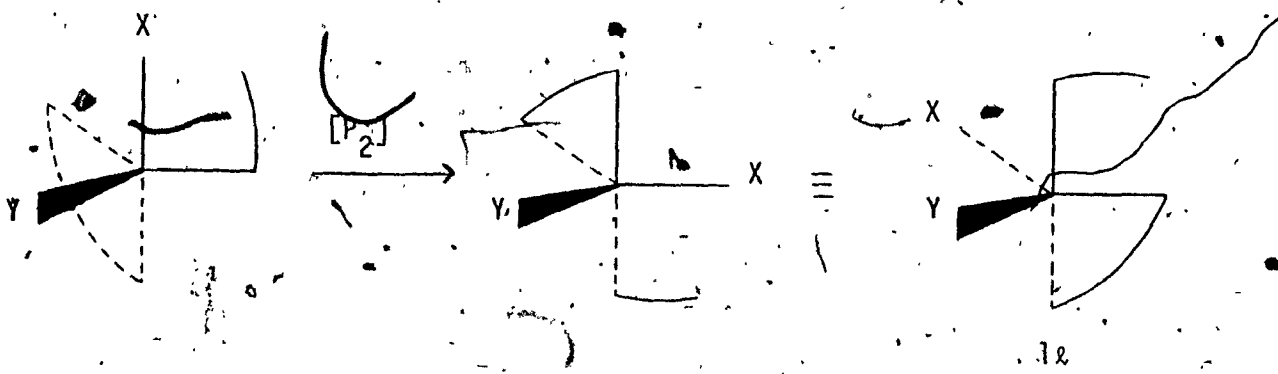

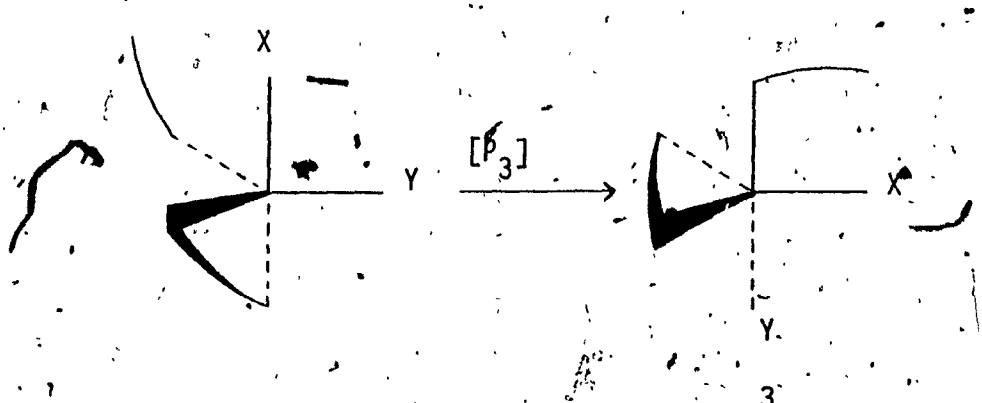

Table LIV

Intermediates and the Fate of the cis-Λ(Δ)(abcd;m) Permutamer of a cis-$M(AA)_2XY$ Complex after Pseudorotation of TBP Intermediates Resulting from Bond Rupture and Assignment of Averaging Sets[a]

Broken[b]	Intermediate[c]	Intermediate after Pseudorotation[c]	Product Permutamer	Averaging Set[d]
		(A) TBP-axial Intermediates		
a	1d (1ℓ)	5d (5ℓ)	c-Λ(Δ)(bacd;m)	A'_2
		4ℓ (4d)	c-Δ(Λ)(dcba;n)	A'_{11}
			c-Δ(Λ)(cdba;n)	A'_{13}
b	1ℓ (1d)	4d (4ℓ)	c-Λ(Δ)(abdc;m)	A'_3
		5ℓ (5d)	c-Δ(Λ)(dcba;n)	A'_{11}
			c-Δ(Λ)(dcab;n)	A'_{13}
c	3 (3)	5ℓ (5d)	c-Δ(Λ)(bacd;m)	A'_9
			c-Δ(Λ)(abcd;m)	A'_8
		5d (5ℓ)	c-Λ(Δ)(badc;m)	A'_5
			c-Λ(Δ)(abdc;m)	A'_3
d	2 (2)	4ℓ (4d)	c-Δ(Λ)(abdc;m)	A'_{10}
			c-Δ(Λ)(abcd;m)	A'_8
		4d (4ℓ)	c-Λ(Δ)(bacd;m)	A'_2
			c-Λ(Δ)(badc;m)	A'_5
		(B) TBP-equatorial Intermediates		
a	5d (5ℓ)	1d (1ℓ)	c-Δ(Λ)(dcba;n)	A'_{11}
		4ℓ (4d)	c-Δ(Λ)(dcab;n)	A'_{13}
			c-Δ(Λ)(cdab;n)	A'_{14}
		3 (3)	c-Δ(Λ)(badc;m)	A'_{12}
			c-Λ(Δ)(bacd;m)	A'_2

Table LIV (continued)

b	4d (4ℓ)	1ℓ (1d)	c-Δ(Λ)(dcba;n)	A'_{11}
		5ℓ (5d)	c-Λ(Δ)(cdba;n)	A'_6
			c-Λ(Δ)(cdab;n)	A'_7
		2 (2)	c-Δ(Λ)(badc;m)	A'_{12}
			c-Λ(Δ)(abdc;m)	A'_3
c	5d (5ℓ)	1d (1ℓ)	c-Λ(Δ)(bacd;m)	A'_2
			c-Δ(Λ)(cdba;n)	A'_{13}
		4ℓ (4d)	c-Δ(Λ)(dcab;n)	A'_{13}
			c-Δ(Λ)(cdab;n)	A'_{14}
		3 (3)	c-Δ(Λ)(abdc;m)	A'_{10}
d	4d (4ℓ)	1ℓ (1d)	c-Λ(Δ)(abdc;m)	A'_3
			c-Δ(Λ)(dcab;n)	A'_{13}
		5ℓ (5d)	c-Δ(Λ)(cdba;n)	A'_{13}
			c-Δ(Λ)(cdab;n)	A'_{14}
		2 (2)	c-Δ(Λ)(bacd;m)	A'_9

[a]Only products which differ from original c-Λ(Δ)(abcd;m) permutamer listed; [b]Defined in Figure 5; [c]Defined in Figure 17; [d]Defined in Table V.

From Table XV it can be seen that a bond rupture process occurring *via* SP-axial intermediates formed and decaying to products *via* the primary process will generate the A'_{13} averaging set. However, this result obtains only if the attack of the dangling end of the "monodentate" A-A ligand occurs at just one basal position. *A priori*, attack is not expected to be equally probable at all four positions since the basal plane is defined by dissimilar atoms (O_{acac}, O_{CH_3}, Cl). However, it is not expected that the attacking end be able to so effectively discriminate against certain ligand atoms in the basal plane so as to generate only averaging set A'_{13}. For this reason, a bond rupture process occurring through SP-axial intermediates is considered improbable.

Restricting the exchange process to a single physical pathway, the discussion above leads to the conclusion that rearrangement of the *cis*-$Ti(dibm)_2Cl(OCH_3)$ complex occurs *via* twist motions about the $C_3(i')$ and/or $C_3(i''')$ threefold rotation axes. Where direct permutational evidence has been unobtainable for rearrangements, mechanisms have generally been inferred from the magnitudes of frequency factors (or entropies of activation) and/or activation energies (6,7). Negative activation entropies (low frequency factors) have long been argued as support for a twist mechanism. Extending the conclusion for the *cis*-$Ti(dibm)_2Cl(OCH_3)$ complex to $Ti(dik)_2X_2$ [dik = acac,dpm; X = halide,alkoxy,phenoxy] complexes, which exchange terminal groups *via* a process with negative activation entropies (54,61,62, 114,126), necessitates that the latter complexes also rearrange *via* a twist mechanism. Thus the observed negative entropies of activation tend to support the twist mechanism; however, activation entropies are unreliable criteria for the assignment of mechanism (111).

As a final comment, the above conclusions are based on the assumption of a single averaging set existing for the $Ti(dibm)_2Cl(OCH_3)$

complex and a single physical process being responsible for the averaging set. Any linear combination of averaging sets (and hence physical processes) which effect -CH= and isopropyl methyl group exchange and $\Delta \leftrightarrow \Lambda$ interconversions cannot be precluded.

Chemical shift data for the $Ti(dibm)_2Cl(OCH_3)$ complex may be found in Appendix C.

c. Diastereotopic Probe on the Monodentate Ligand

In their report of the preparation and characterization of several cis-$Ti(acac)_2Cl(OR)$ complexes, Thompson and co-workers (70) reported that the acetylacetonate methyl resonance of $Ti(acac)_2Cl(O^iC_3H_7)$ split into three resonances at low temperature, but no information was given concerning the isopropyl methyl resonance.

The $Ti(acac)_2X(O^iC_3H_7)$ [X = Cl,Br] complexes were unexpected products from the reaction of the appropriate $Ti(acac)_2X_2$ complex and titanium(IV) isopropoxide and thus presented an opportunity to investigate enantiomerization processes in $Ti(acac)_2X(OR)$ complexes.

A 0.300 M solution of $Ti(acac)_2Cl(O^iC_3H_7)$ in dichloromethane revealed a single acetylacetonate methyl, ring proton, and isopropyl methyl doublet resonance at room temperature. By ca. -10^o the acetylacetonate methyl resonance appears as three peaks in a 1:1:2 ratio of intensities while the -CH= resonance appears as two equally intense absorptions. These results agree with those of Thompson and co-workers (70) and the identical behaviour is observed for the acetylacetonate methyl and ring proton resonances of the $Ti(acac)_2Br(O^iC_3H_7)$ complex, with the bromo complex possessing slightly larger chemical shift separations. However, the isopropyl methyl resonance for these $Ti(acac)_2X(O^iC_3H_7)$ [X = Cl,Br] complexes remains a sharp doublet down to ca. -63^o. The $W_{1/2}$ values

for the isopropyl methyl doublet of the $Ti(acac)_2Cl(O^iC_3H_7)$ complex vary only from 0.61 Hz at 39.6° to 1.49,1.57 Hz at -62.7°; the bromo complex has similar values of 0.62,0.65 Hz at 39.6° and 1.59,1.63 Hz at -62.7°. These changes in linewidths reflect changes in solvation and increased solvent viscosity at low temperatures.

The failure to detect optical inversion processes in these $Ti(acac)_2X(O^iC_3H_7)$ [X = Cl,Br] complexes is surprising in light of the observed (61,62,126) nonequivalence of isopropyl methyl groups in the $Ti(acac)_2(O^iC_3H_7)_2$ complex. Introduction of a halogen into the complex is expected to increase the lability (cf. previous section), but not to an extent so as to render inversion processes rapid even at -60°. It is probable that the diastereotopic isopropyl methyl groups in the mixed haloisopropoxy complexes exhibit chemical shift degeneracy.

Consulting Table VI with the observed changes in signal multiplicities of 4 → 1 for nondiastereotopic terminal groups on the A-A ligand and 2 → 1 for nondiastereotopic β-CH= groups leads to a choice of A'_6 or A'_{13} as the averaging set responsible for the rearrangement. Assuming optical inversion occurs during the rearrangement, A'_{13} remains as the only viable averaging set and arguments presented in the previous section suggest that A'_{13} correlates with a twist mechanism. Arguments suggestive of a twist mechanism are subject to the rearrangement occurring via a single physical pathway.

The reaction of 2,6-diisopropylphenol with the $Ti(acac)_2Cl(O^iC_3H_7)$ complex produced the $Ti(acac)_2Cl(2,6\text{-}^iPr_2C_6H_3O)$ complex. The temperature dependence of the isopropyl methyl and acetylacetonate methyl resonances for this complex are illustrated in Figure 48. A single isopropyl methyl doublet is observed at ambient temperature but below ca. -10° two doublets are observed. A TLS analysis of this exchange

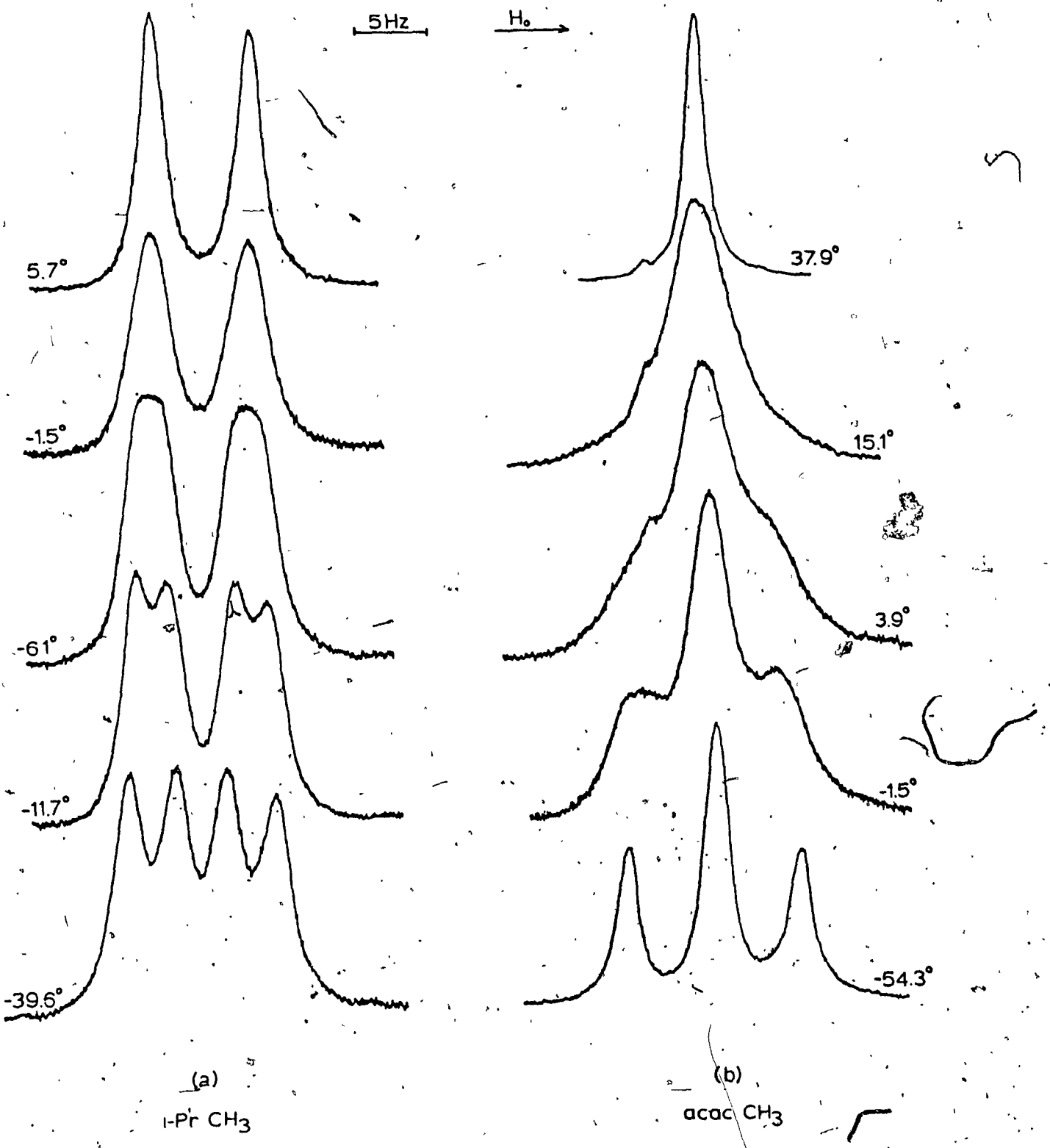

Figure 48.- Temperature dependence of the (a) isopropyl methyl and (b) acetylacetonate methyl resonances of the $Ti(acac)_2Cl(2,6\text{-}^{i}Pr_2\text{-}C_6H_3O)_2$ complex in dichloromethane solution.

process was performed and the results presented in Section III-C-1-c(i). A single acetylacetonate methyl resonance appears at room temperature but on cooling this resonance broadens and, by ca. -30^{o}, three sharp resonances are observed in 1:2:1 ratios of relative intensities. In contrast to the $Ti(acac)_2X(O^{i}C_3H_7)$ complexes, the 2,6-diisopropylphenoxy complex does not reveal two acetylacetonate ring proton (-CH=) resonances at low temperature. The $W_{1/2}$ values for the -CH= resonance of the $Ti(acac)_2Cl(2,6\text{-}^{i}Pr_2C_6H_3O)$ complex vary only from 0.52 Hz at 41.9^{o} to 1.55 Hz at -57.9^{o}, which presumably reflects solvation and viscosity changes at low temperature and the two nonequivalent -CH= groups probably possess identical chemical shifts.

No attempt was made to perform a TLS analysis of the exchange of acetylacetonate methyl groups as this presents a four-site exchange problem, which requires six first-order rate constants to completely describe the system. In addition, the relaxation times T_2 appear to be temperature dependent.

From the changes in signal multiplicities found for the $Ti(acac)_2Cl(2,6\text{-}^{i}Pr_2C_6H_3O)$ complex, and assuming that -CH= group exchange occurs, consulting Table VI identifies the averaging set responsible for the permutation of nuclei as, again, A'_{13}. Extending the arguments put foward in the previous section to this complex indicates that a twist mechanism is also operative in the $Ti(acac)_2Cl(2,6\text{-}^{i}Pr_2C_6H_3O)$ complex. Averaging set A'_{13} would predict a ratio of the rate of enantiomerization to the rate of terminal group exchange of unity. While the rate of optical inversion is known for this complex (cf. Section III-C-1-c(i)), unfortunately the rate of terminal group exchange is not known and an operational test for averaging set A'_{13} cannot be applied.

To summarize the results obtained for cis-$M(AA)_2XY$-type complexes, evidence supports the A'_{13} averaging set as being responsible for the observed changes in signal multiplicities for various combinations of diastereotopic and/or nondiastereotopic groups within the complexes. Assuming that a single physical process is responsible for the rearrangement, arguments outlined in Section III-C-2b suggest that the physical process involves twist motions about the $C_3(i')$ and/or $C_3(i'''')$ rotation axes of the octahedron.

Chemical shift data for the complexes discussed in this section may be found in Appendix C.

3. The $M(AB)_2X_2$ System

a. Introduction

Complexes of the type $M(AB)_2X_2$, where AB and X represent an unsymmetrical bidentate and monodentate ligands, respectively, may exist in a total of five possible diastereomeric forms, as shown in Figure 49. Nomenclature is defined in Section III-A-3d. Diastereomers possessing cis-X_2 groups are enantiomeric and the expected signal multiplicities are indicated below each diastereomer in Figure 49.

The most detailed study of $M(AB)_2X_2$-type complexes was performed on the $Ti(bzac)_2X_2$ [X = F,Cl,Br] complexes (55). These complexes were found to exist in the three diastereomeric forms possessing cis-X_2 groups. A rapid rearrangement process interconverted these three diastereomers (55). Similar observations were made for the $Sn(bzac)_2Cl_2$ complex (59, 60). In the case of the $Ge(dhd)_2Cl_2$ complex, all five isomers are observed (116); however, no information on possible exchange processes was presented.

This section reports the results of attempts to detect enantiomerization processes in complexes of the type $M(AB)_2X_2$ in which diastereotopic probes are present on the A-B and X ligands.

b. Diastereotopic Probe on the Bidentate Ligand

It is probable that $Ti(dik)_2X_2$ [dik = unsymmetrical β-diketonate; X = alkoxy,phenoxy] complexes will adopt the cis-X_2 geometries found for the $Ti(bzac)_2(halogen)_2$ complexes (55). Since the cis-X_2 diastereomers are enantiomeric, placement of a diastereotopic probe on the chelate ring presents the possibility of detecting enantiomerization processes occurring during the interconversions of the cis-X_2 isomers. This section presents the results of such experiments.

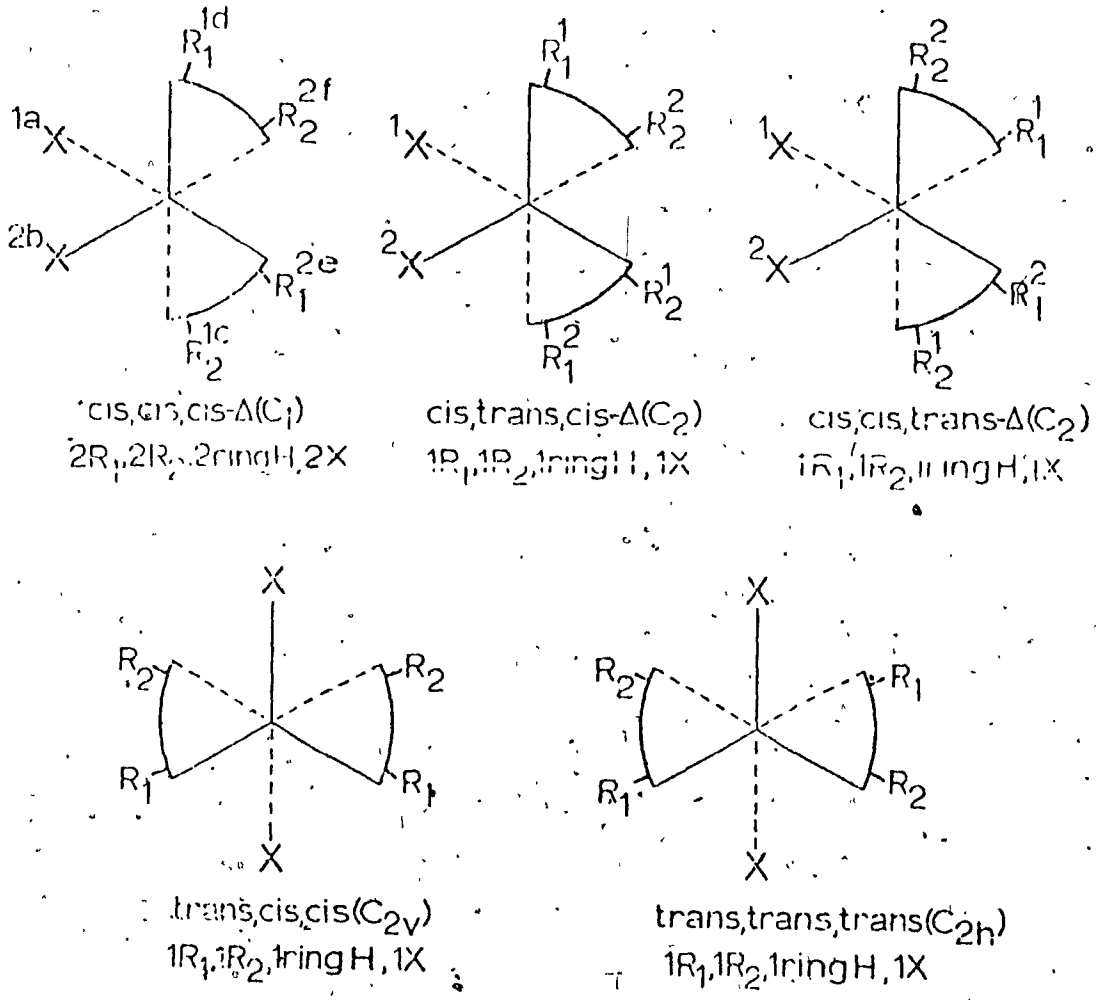

Figure 49.- Possible isomers for an $M(AB)_2X_2$ complex. Numerical superscripts label nonequivalent groups; letter superscripts label the different environments. Numerical subscripts label the different types of terminal groups on the A-B ligand. The stereochemistry is described by three cis or trans prefixes which denote the relative orientation of the X, R_1, and R_2 groups in that order.

Figure 50 shows the temperature dependence of the isopropyl methyl resonance of the $Ti(tibm)_2Cl_2$ complex in dichloromethane solution. At ambient temperature a single doublet is observed. On cooling the solution the doublet broadens into a broad, featureless resonance. Further cooling results in the emergence of three doublets in a 1:2:2 intensity ratio by ca. -55^0. At low temperature the ring proton (-CH=) resonance is broadened ($W_{1/2}$ values are approximately doubled on going from 25^0 to ca. -60^0) but no splitting is observed. The temperature dependence of the ^{19}F resonance was not investigated.

In order to determine whether the observed exchange of isopropyl methyl groups in the $Ti(tibm)_2Cl_2$ complex is a result of configurational rearrangement of the chelate rings or hindered rotation of the isopropyl moiety, the analagous derivative containing t-butyl groups was examined.

Figure 51 shows the temperature dependence of the ring proton (-CH=) and t-butyl methyl resonance of the $Ti(tdh)_2Cl_2$ complex. The t-butyl methyl resonance reveals a similar lineshape behaviour to that of the isopropyl methyl resonance of the $Ti(tibm)_2Cl_2$ complex. Considerable broadening of the t-butyl methyl resonance occurs on cooling with the emergence of a resonance at lower field, with relative intensities of 1:3. The ring proton resonance also undergoes exchange broadening and two resonances can be observed by ca. -50^0.

These results are in accord with the $Ti(tibm)_2Cl_2$ and $Ti(tdh)_2Cl_2$ complexes existing as a mixture of cis-X_2 diastereomers, based on the expected similarity with the $Ti(bzac)_2X_2$ [X = halogen] complexes. Although the $Ti(tdh)_2Cl_2$ spectra can be rationalized as a mixture of trans-X_2 isomers, the observed spectra for the $Ti(tibm)_2Cl_2$ complex necessitates the population of at least one cis-X_2 diastereomeric form, as the two

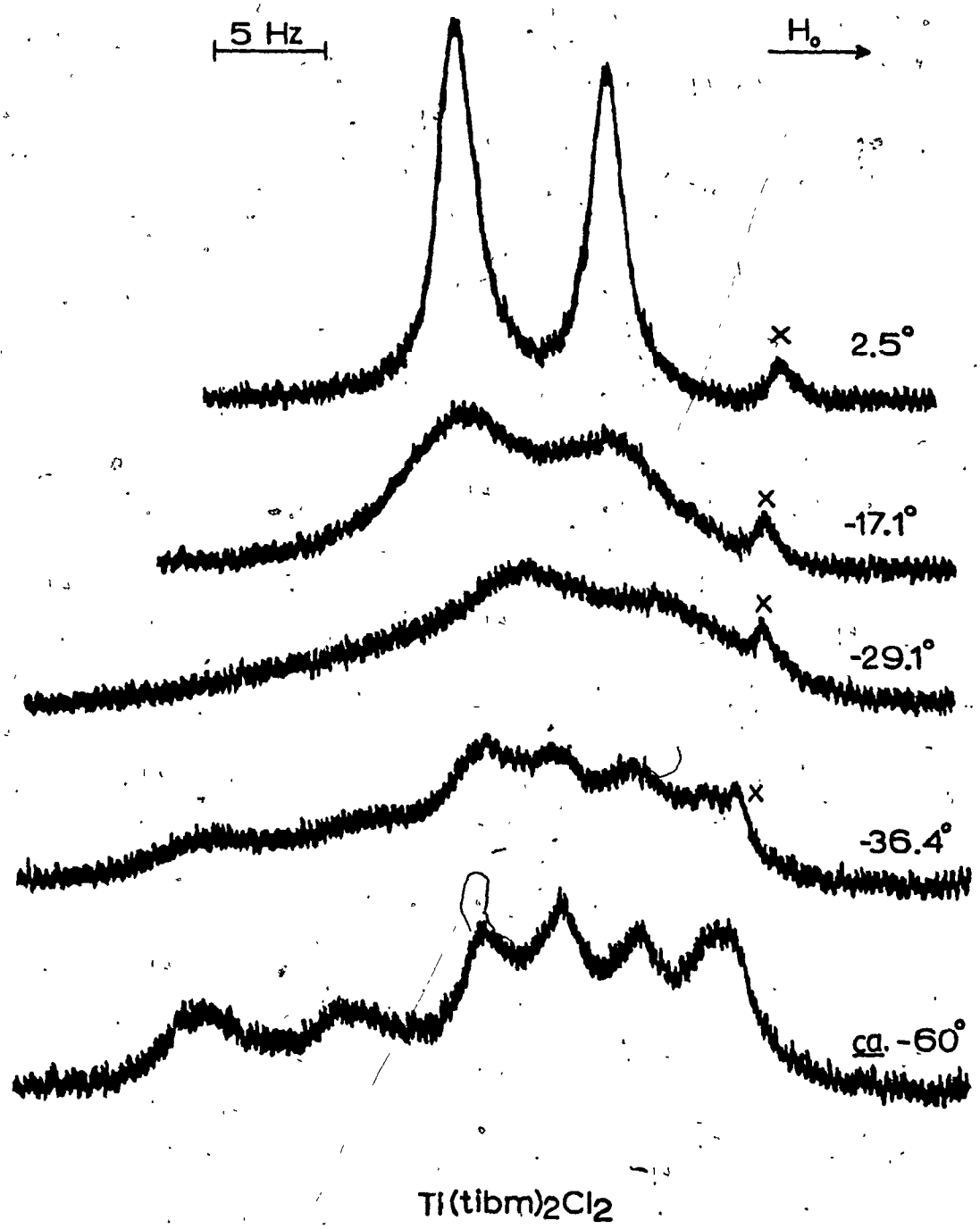

Figure 50.- Temperature dependence of the isopropyl methyl resonance of the $Ti(tibm)_2Cl_2$ complex in dichloromethane solution, 0.300 M. The resonance marked x arises from an impurity.

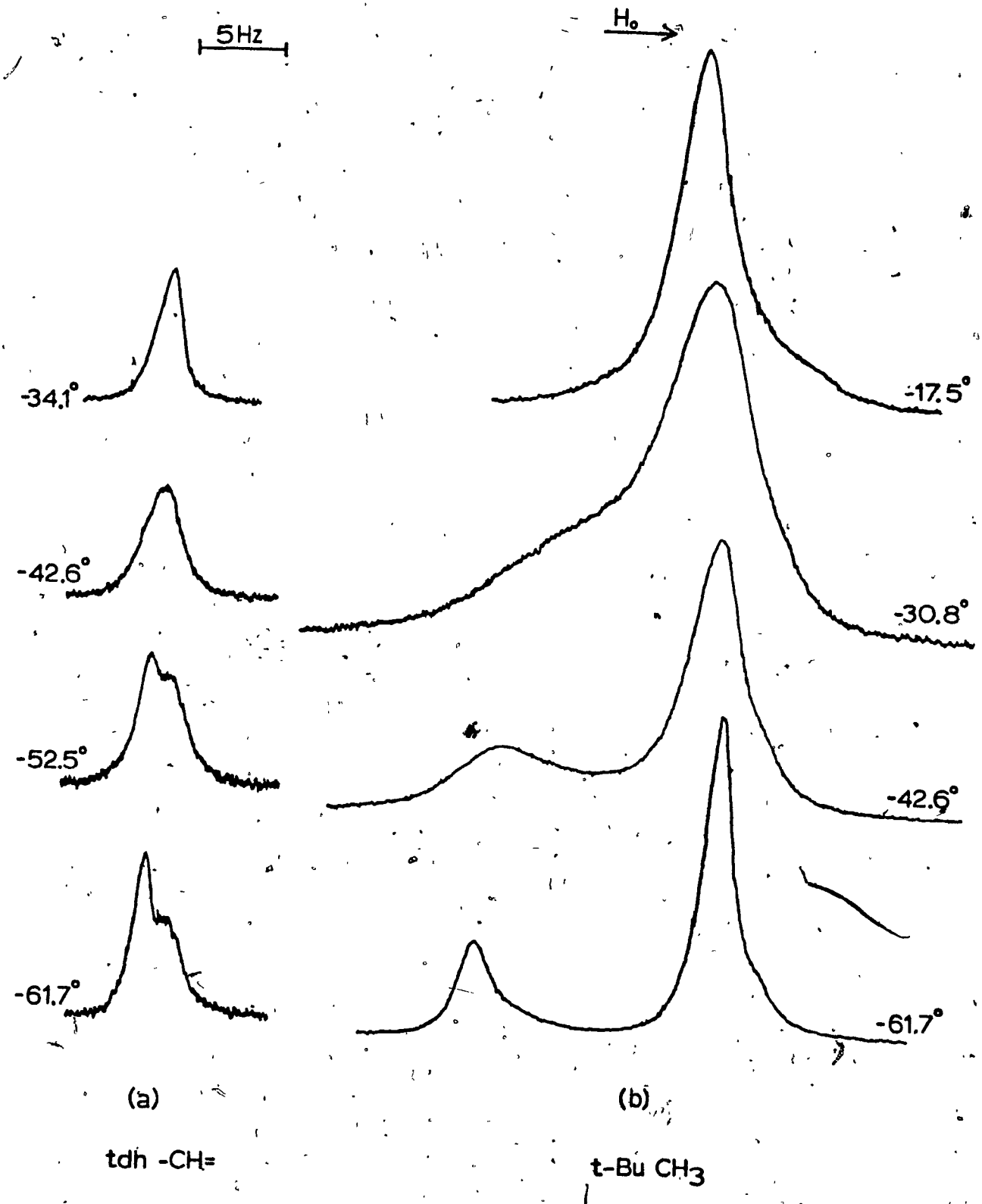

Figure 51.- Temperature dependence of the (a) tdh ring proton (-CH=) and (b) the t-butyl methyl resonance of the $Ti(tdh)_2Cl_2$ complex in dichloromethane solution, 0.300 M.

trans isomers would result in only two isopropyl methyl doublets. Since their related $Ti(dik)_2Cl_2$ [dik = acac,hfac,dibm,dpm] complexes (54,71,114) adopt the cis-Cl_2 configuration, the simplest rationalization for the $Ti(tibm)_2Cl_2$ and $Ti(tdm)_2Cl_2$ complexes is that they adopt all three cis-X_2 diastereomeric configurations. The isopropyl methyl pattern at ca. -60° for the $Ti(tibm)_2Cl_2$ complex thus appears to result from chemical shift differences between nonequivalent isopropyl groups rather than between the methyl groups of a particular isopropyl moiety. Enantiomerization must then either occur rapidly even at ca. -60° or the diastereotopic splitting of the isopropyl methyl groups is too small to be resolved.

The well documented (37) rate-accelerating influence of CF_3 groups led to the investigation of a system less labile than $Ti(tibm)_2Cl_2$. Figure 28(a) depicts the temperature dependence of the isopropyl methyl resonance of the $Sn(tibm)_2Cl_2$ complex in a 1,1,2,2-tetrachloroethane solution. In the fast exchange region (> ca. 80°) a single isopropyl methyl doublet is observed, which broadens into a single featureless resonance as the temperature is lowered. From this broad, featureless resonance fine structure begins to emerge as the temperature is lowered further until the complex pattern at 15° is observed. No further splitting is observed down to -2.2°, at which point viscosity broadening occurs and results in poorer resolution. Solvent interference prevents the reliable identification of the ring proton resonance in tetrachloroethane; a single -CH= resonance is found at room temperature in dichloromethane and deuteriochloroform solutions. The coupling of methyl groups with the isopropyl methine proton is complex; fine structure is visible near the slow- and fast-exchange regions.

The rate enhancement from the presence of CF_3 groups is evident from Figure 28 on comparing coalescence temperatures for the

$Sn(tibm)_2Cl_2$ and $Sn(dibm)_2Cl_2$ complexes. The former possesses a coalescence temperature ca. 25° lower than that for the $Sn(dibm)_2Cl_2$ complex.

The isopropyl methyl resonance pattern observed at 15° for the $Sn(tibm)_2Cl_2$ complex may be resolved into five partially overlapping doublets of unequal relative intensities. Assuming that this complex populates only the cis-X_2 diastereomers, then if terminal group exchange is slow and inversion fast, four doublets are expected. If terminal group exchange and inversion are both slow processes, eight doublets are expected. The observation of five doublets necessitates that terminal group exchange and inversion are slow at 15° in the $Sn(tibm)_2Cl_2$ complex.

Consulting Table X, which lists the expected changes in signal multiplicities for the various averaging sets for a cis-$M(AB)_2X_2$ system, one finds that no averaging set will predict the collapse of the diastereotopic terminal groups of the A-B ligand to a single doublet. It is reasonable to expect the collapse of the low temperature spectra (which already encompass groups with degenerate shifts) of the $Sn(tibm)_2Cl_2$ complex to a single doublet to be the result of an accidental shift degeneracy of the expected two doublets. Averaging sets A_1'' ($\equiv A_1'''$ in this case as Cl does not function as a nmr probe) predict that the number of doublets is a multiple of two and it is unlikely that four (or more) doublets would overlap in the fast exchange region. It is then necessary to distinguish between averaging sets A_4'' and A_9'' (which correspond to A_3''' and A_6''' of Table XII).

Table XIII reveals that, on the basis of changes in signal multiplicities, no distinctions between A_3''' and A_6''' can be made for any combination of diastereotopic and/or nondiastereotopic groups. Differences between A_3''' and A_6''' are such that the former does not cause enantiomerization while the latter does result in inversion.

Since slow inversion is detected for the $Sn(tibm)_2Cl_2$ complex, and following the arguments for analagous complexes in Sections III-C-1-b(i) and III-C-2b, it is probable that inversion does occur during the rearrangement, thus favouring averaging set A_6'''. Some additional evidence for the A_6''' averaging set is derived from its correlation with the A_{13}' averaging set suggested for the rearrangement of cis-$Ti(dibm)_2Cl(OCH_3)$ (cf. Section III-C-2b and Table XIV).

Consulting Tables XVI, XVII, and XVIII, with the equivalency $A_6''' \equiv A_9''$, one finds that this averaging set may be accomodated by a twist mechanism and a bond rupture mechanism via TBP-axial and SP-axial intermediates. The SP-axial pathway is less attractive as $A_6''' \equiv (A_9'')$ results only from selective attack of the dangling ligand in the basal plane; such discrimination is not expected a priori because of the difference in donor atoms (O and Cl) forming the basal plane. The twist mechanism about the $C_3(i')$ and/or $C_3(i''')$ axes of the octahedron and a bond rupture mechanism via TBP-axial intermediates are equally probable, and no choice between the two is possible on the basis of presently available evidence.

Some support for the twist mechanism derives from the correlation of averaging sets and physical processes for the cis-$Ti(dibm)_2Cl(OCH_3)$ and cis-$Sn(tibm)_2Cl_2$ complexes. This argument involves the tacit assumption that differences in metal ion and donor ligands do not impose different physical pathways for the rearrangement reactions.

The above discussion is based on the assumption that these $M(AB)_2X_2$ complexes adopt only the geometries possessing cis-X_2 groups and that the rearrangement process is the result of a single physical pathway.

In order to extend the complexity of the system as a means of

characterizing the rearrangement process in more detail, complexes in which the X group may function as an nmr probe were investigated. These complexes are discussed in the next section.

Chemical shift data for the complexes discussed in this section may be found in Appendix C.

c. Diastereotopic Probe on the Monodentate Ligand

Although $Ti(bzac)_2(alkoxy)_2$ complexes have been prepared (74), their stereochemistry was not investigated. This section reports the results of a study of the stereochemistry of and rearrangement processes in the $Ti(bzac)_2(O^iC_3H_7)_2$ and $Ti(bzac)_2(2,6\text{-}^iPr_2C_6H_3O)_2$ complexes. The latter complex is important for providing evidence that the $Ti(quin)_2(2,6\text{-}^iPr_2C_6H_3O)_2$ and $Ti(ox)_2(2,6\text{-}^iPr_2C_6H_3O)_2$ complexes exist as a single diastereomer in solution.

The temperature dependence of the various resonances of the $Ti(bzac)_2(O^iC_3H_7)_2$ complex are illustrated in Figures 52 and 53. Figure 52(a) shows that the benzoylacetonate methyl resonance is very broad at room temperature and on cooling splits into four resonances of equal intensity. The temperature dependence of the isopropyl methyl resonance is complex, as Figure 52(b) reveals. The -36.8^o isopropyl methyl pattern may be resolved into four partially overlapping doublets of equal intensity. Further cooling reveals no further splitting and the pattern is noticeably broadened at ca. -65^o, a result of viscosity broadening or a more complex unresolved pattern. The benzoylacetonate phenyl region of the proton nmr spectrum is also temperature dependent. Figure 53(a) shows that these phenyl groups appear as two broad lines at room temperature. On cooling to -36.8^o, fine structure caused by complicated coupling patterns of nonequivalent phenyl groups is observed. The resonance pattern

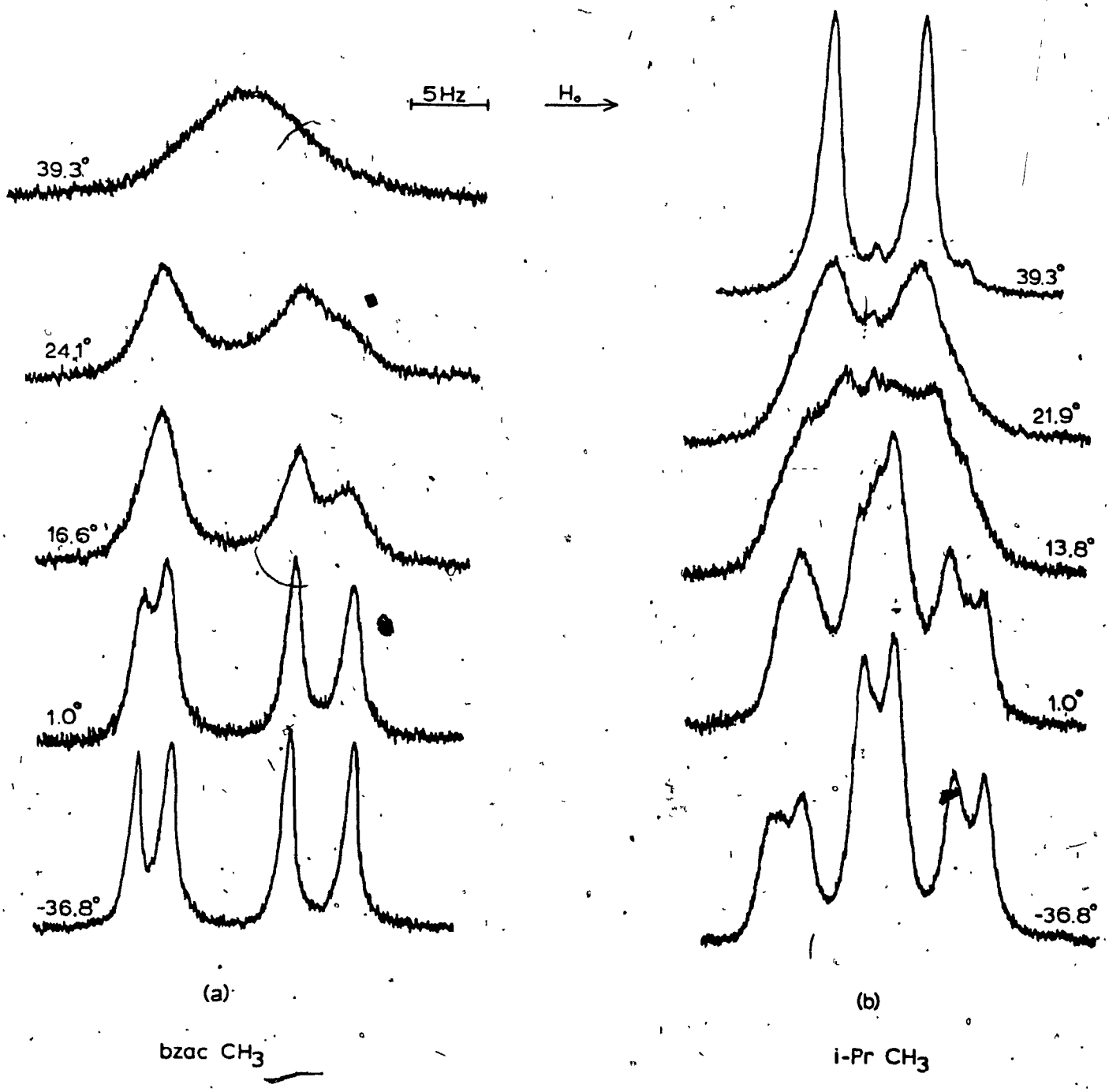

Figure 52.- Temperature dependence of the (a) benzoylacetonate methyl resonance and the (b) isopropyl methyl resonance of the $Ti(bzac)_2(O^iC_3H_7)_2$ complex in dichloroemthane solution.

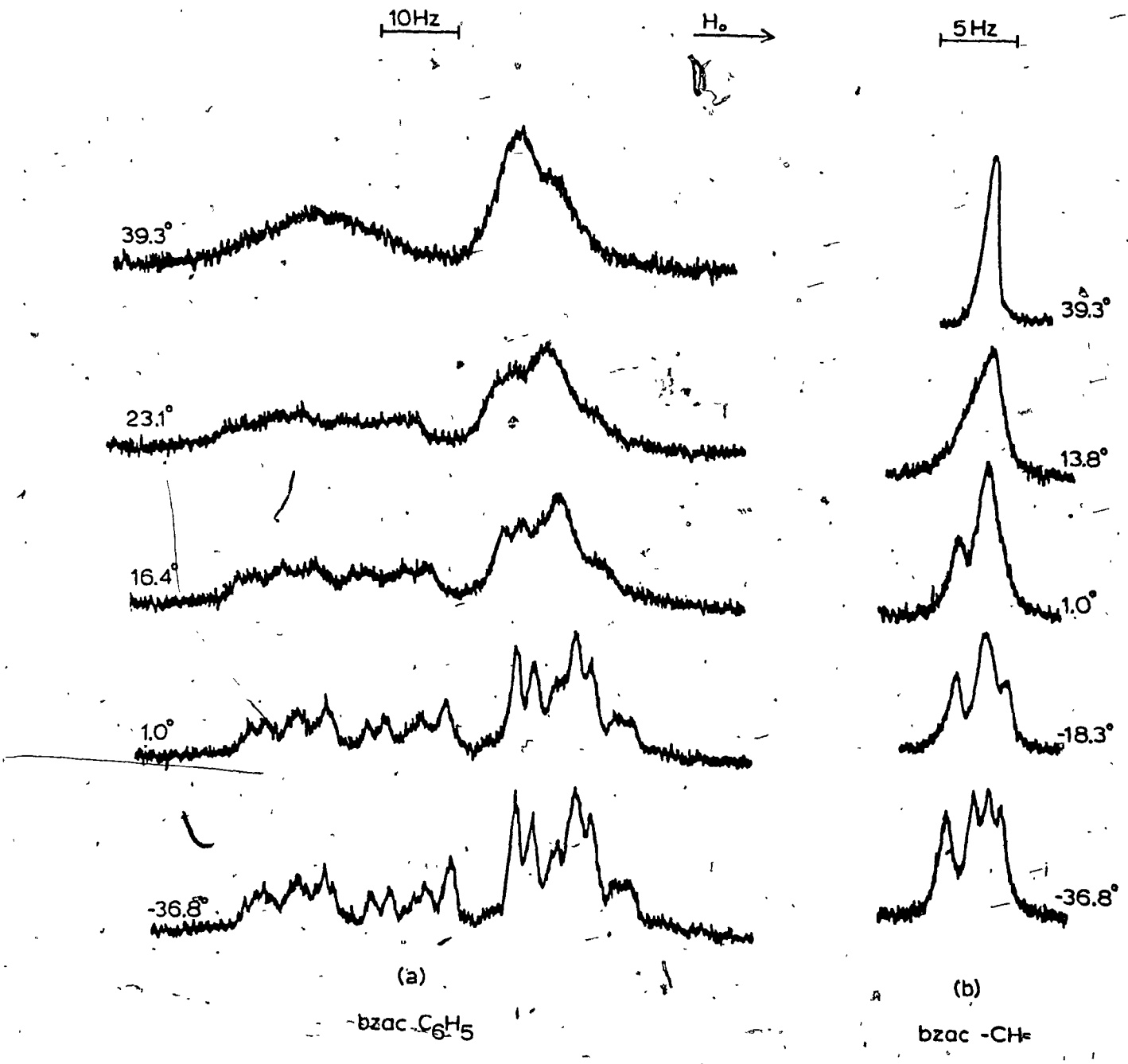

Figure 53.- Temperature dependence of the (a) benzoylacetonate phenyl resonance and the (b) benzoylacetonate ring proton (-CH=) resonance of the $Ti(bzac)_2(O^iC_3H_7)_2$ complex in dichloromethane solution.

at room temperature resembles the patterns observed for the phenyl region of the $Ti(bzac)_2X_2$ [X = F,Cl,Br] complexes at intermediate exchanges rates (55). It is expected that the resonances in Figure 53(a) would sharpen further and reveal fine structure again at the fast exchange limit. No experiments were conducted above room temperature. Figure 53(b) shows that the single benzoylacetonate ring proton (-CH=) resonance at room temperature broadens with decreasing temperature until four resonances, of almost equal intensity, are observed at -36.8^{o}. This represents the first $Ti(bzac)_2X_2$ complex for which more than one -CH= resonance is observed in the slow exchange region; the $Ti(bzac)_2X_2$ [X = F,Cl,Br] reveal a single -CH= resonance even at ca. -65^{o} (55), although considerably broadened.

Spectra for the $Ti(bzac)_2(2,6\text{-}^{i}Pr_2C_6H_3O)_2$ complex are similar to those for the isopropoxy complex. Figures 54 and 55 illustrate that the benzoylacetonate methyl, phenyl, and -CH= groups are involved in exchange processes, as well as the isopropyl methyl groups. Four bzac methyl resonances are observed at low temperature and, unlike the isopropoxy complex, possess unequal relative intensities: The isopropyl methyl pattern at -28.5^{o} [Figure 54(b)] may be resolved into three overlapping doublets with relative intensities of 1:2:1. No further splitting is observed at even lower temperatures. Figure 55(a) reveals that the temperature dependence of the benzoylacetonate phenyl region is similar to that for the isopropoxy complex. The bzac ring protons (-CH=) appear as a single resonance at ambient temperature, which broadens with decreasing temperature until three lines in a 1:2:1 intensity ratio are observed by -28.5^{o} [Figure 55(b)].

These observations may be rationalized, with analogy to the $Ti(bzac)_2(halogen)_2$ complexes (55), as resulting from a rapidly inter-

Figure 54.- Temperature dependence of the (a) benzoylacetonate methyl resonance and the (b) isopropyl methyl resonance of the $Ti(bzac)_2(2,6\text{-}^{i}Pr_2C_6H_3O)_2$ complex in dichloromethane solution.

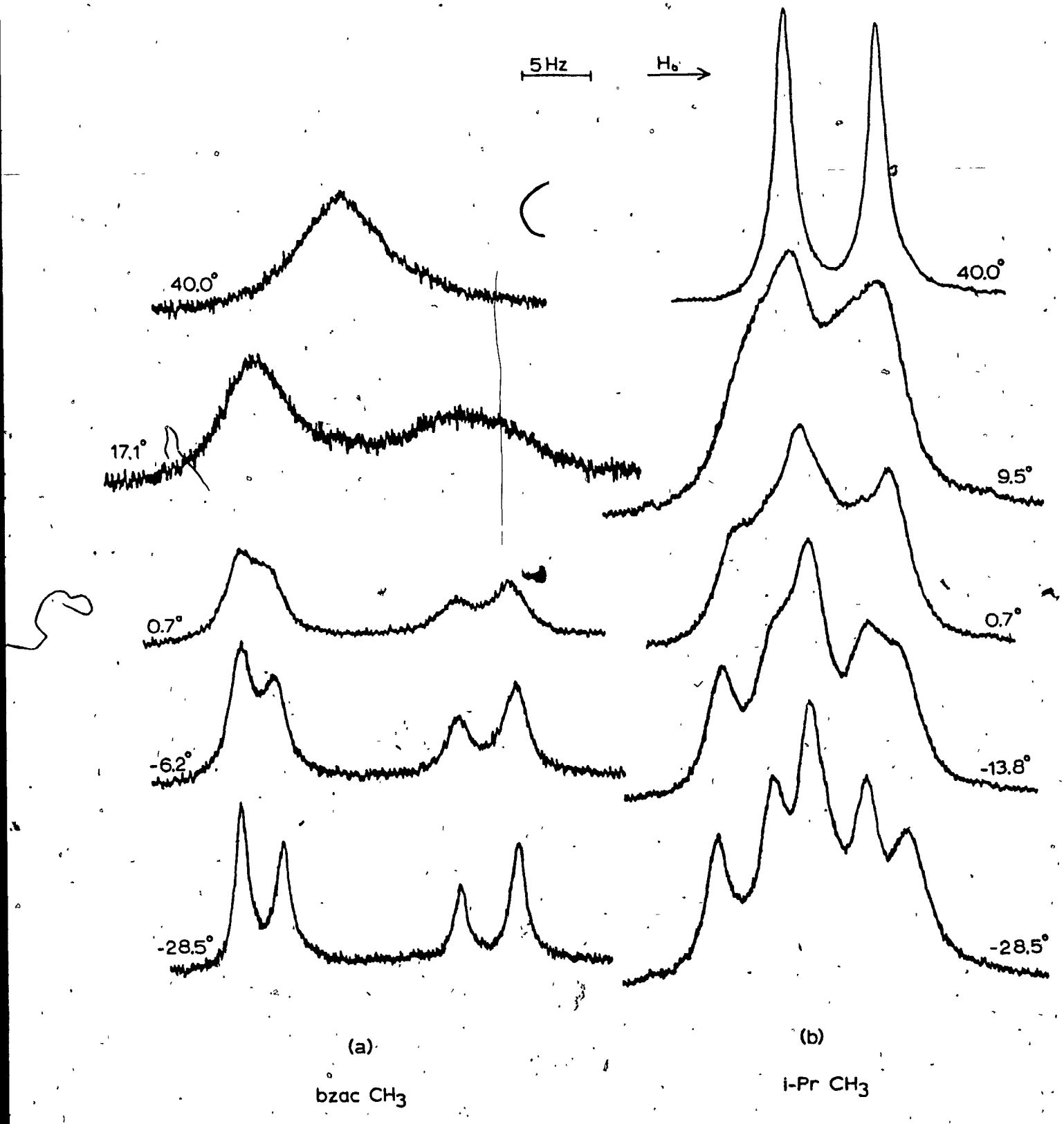
5 Hz
H_o
40.0°
17.1°
0.7°
-6.2°
-28.5°
40.0°
9.5°
0.7°
-13.8°
-28.5°
(a)
bzac CH_3
(b)
i-Pr CH_3

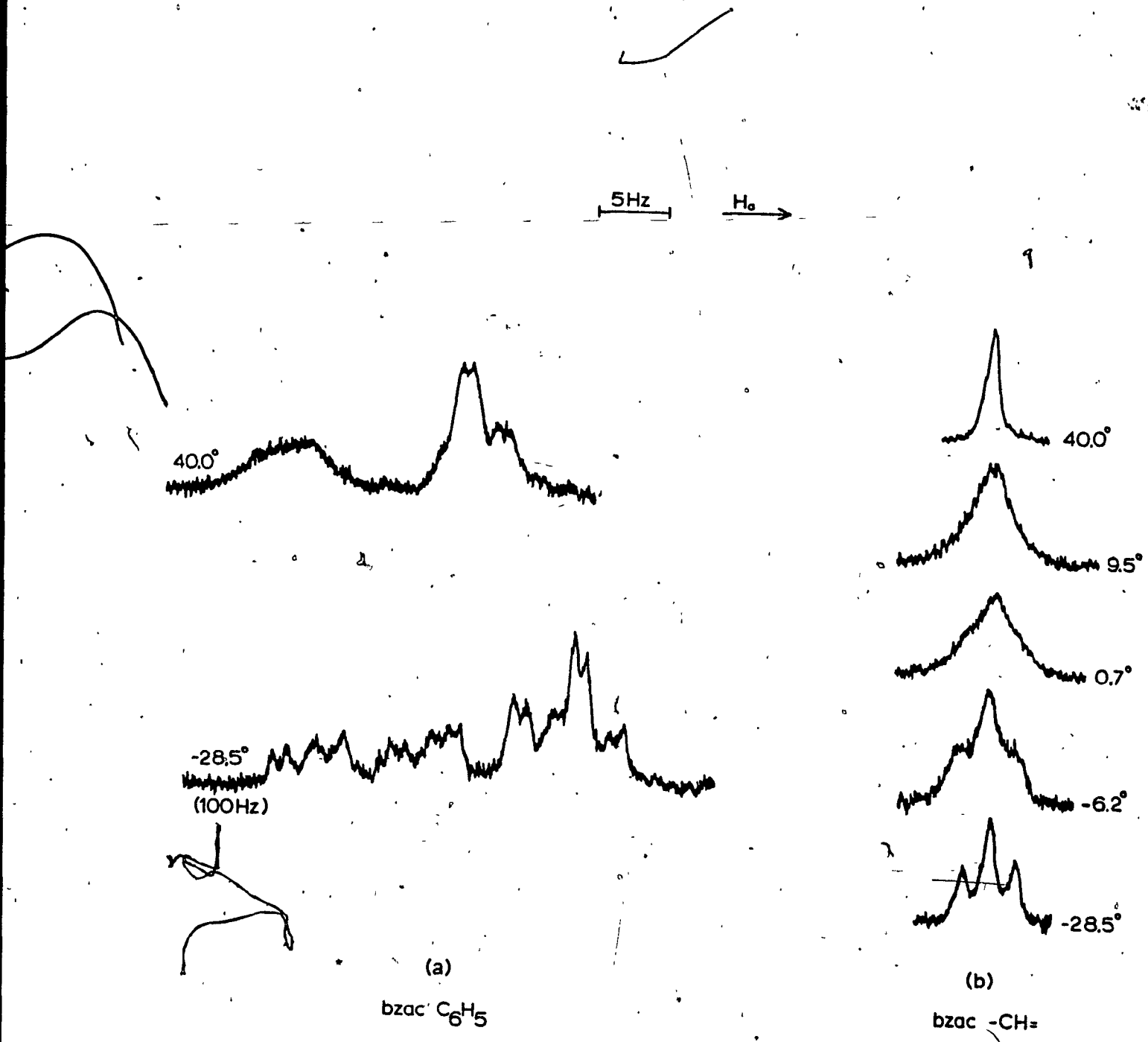

Figure 55.- Temperature dependence of the (a) benzoylacetonate phenyl resonance and the (b) benzoylacetonate ring proton (-CH=) resonance of the $Ti(bzac)_2(2,6\text{-}^{i}Pr_2C_6H_3O)_2$ complex in dichloromethane solution.

converting mixture of the three diastereomers possessing cis-X_2 groups (cf. Figure 49). Since $Ti(acac)_2(O^iC_3H_7)_2$ (61,62,126) and $Ti(acac)_2$-$(2,6\text{-}^iPr_2C_6H_3O)_2$ (62,126) adopt cis-X_2 geometries, it is reasonable to expect their bzac analogues to adopt similar configurations. With reference to Figure 49, a mixture of the cis-X_2 diastereomers will generate four bzac methyl, four bzac phenyl, four bzac -CH=, and four X (isopropyl methyl doublets) resonances in the absence of exchange processes. Spectra for the $Ti(bzac)_2(O^iC_3H_7)_2$ and $Ti(bzac)_2(2,6\text{-}^iPr_2C_6H_3O)_2$ complexes (Figures 52 through 55) are consistent with such a mixture occurring at low temperature. A rapid exchange process interconverts all nonequivalent groups amongst the three cis-X_2 diastereomers. From previous experience [Sections III-C-1 through III-C-3] it is expected that the diastereotopic splitting of isopropyl methyl groups will be relatively small. For the three cis-X_2 isomers, each of which is enantiomeric, a total of eight isopropyl methyl doublets are expected in the slow exchange limit. Four and three doublets may be resolved for the isopropoxy and diisopropylphenoxy complexes, respectively, and are probably a result of the gross molecular inequivalence of the X groups rather than from the dissymmetry centered on the titanium in each isomer. The isopropyl methyl patterns tend to broaden and are less resolved at temperatures below ca. -30^o. This probably results from the severe overlapping of the expected eight doublets at lower temperatures, as the smaller diastereotopic splittings require lower temperatures to be observed than the larger separations of environments resulting from overall symmetry nonequivalence.

The relative equilibrium concentrations of the three cis-X_2 isomers deserves some comment. If a statistical distribution of diastereomers obtains, the relative concentrations will be in the ratio cis,cis,cis: cis,trans,cis (or cis,cis,trans): cis,cis,trans (or cis,trans,cis) = 2:1:1

and four equally intense terminal group resonances are expected. The $Ti(bzac)_2F_2$ complex closely approaches a statistical distribution of diastereomers (55). The $Ti(bzac)_2(O^iC_3H_7)_2$ complex also exists as a near statistical mixture since the four bzac methyl resonances are of similar intensity. However, a distribution of intensities obtained for the $Ti(bzac)_2(2,6\text{-}^iPr_2C_6H_3O)_2$ complex indicates departures from a statistical mixture of diastereomers. It might be expected that the isomer possessing trans phenyl groups may experience some added steric strains with the more bulky 2,6-diisopropylphenoxy ligands than with isopropoxy ligands; thus the least intense resonance of Figure 54(a) may be assigned to this diastereomer. Since the cis,cis,cis isomer should generate two equally intense bzac methyl resonances, the two resonances of medium intensity in Figure 54(a) are assigned to this diastereomer. Finally, the resonance at lowest field may be assigned to the isomer containing trans bzac methyl groups. The relative concentrations are not known with sufficient accuracy to allow determination of isomerization enthalpies from the temperature dependence of the concentrations. However, enthalpies are expected to be small (74).

The observation of a mixture of cis-X_2 isomers for the $Ti(bzac)_2(2,6\text{-}^iPr_2C_6H_3O)_2$ complex supports the suggestion made in Section III-C-1-c(iii) that the $Ti(quin)_2(2,6\text{-}^iPr_2C_6H_3O)_2$ and $Ti(ox)_2(2,6\text{-}^iPr_2\text{-}C_6H_3O)_2$ complexes exist as a single diastereomer in solution possessing a cis(N),trans(O) arrangement of quin and ox donor atoms.

Assignment of an averaging set responsible for the rearrangement of the $Ti(bzac)_2(O^iC_3H_7)_2$ and $Ti(bzac)_2(2,6\text{-}^iPr_2C_6H_3O)_2$ complexes is difficult as both A_4'' and A_9'' of Table X predict identical changes in signal multiplicities. When X contains a diastereotopic isopropyl group,

no averaging set predicts a single isopropyl methyl doublet in the fast exchange region, and , as in Sections III-C-1-b(i), III-C-2b, and III-C-3b, it is assumed that the single doublet observed is a result of the chemical shift degeneracy of the expected two doublets; it is not probable that four (or more) doublets would possess degenerate chemical shifts. As was the case in the previous section, a distinction between averaging sets A_4'' and A_9'' is necessary; however, in this case, no information on whether the rearrangement occurs with or without enantiomerization is available as no diastereotopic splittings are observed for the isopropyl groups. Since the related $Ti(acac)_2(O^iC_3H_7)_2$ (61) and $Ti(acac)_2(2,6\text{-}^iPr_2C_6H_3O)_2$ [Section III-C-1-c(i)] complexes exhibit diastereotopic splitting for their isopropyl methyl resonances and hence indicative of inversion, it is probable that their benzoylacetonate analogues also undergo enantiomerization reactions. This would identify the averaging set as A_9''. A discussion of possible physical pathways that may generate this averaging set has been presented in the previous section. The identical assumptions and restrictions apply for the $Ti(bzac)_2(O^iC_3H_7)_2$ and $Ti(bzac)_2(2,6\text{-}^iPr_2C_6H_3O)_2$ complexes of this section.

Chemical shift data for the complexes reported in this section are tabulated in Appendix C.

4. Tris Chelate Systems

a. Cationic Tris(β-diketonato)metal(IV) Complexes

Complexes of the type $[M(dik)_3]^+X^-$ [M = Ti(IV),V(IV), Si(IV),Ge(IV)] are cationic octahedral systems (119,129-133) which are capable of being resolved into their enantiomeric forms. Only the $[Si(acac)_3]^+$ and $[Ge(acac)_3]^+$ complexes have been resolved (183-186) while cis and trans diastereomers have been detected for the $[Si(bzac)_3]^+$ cation (117). The Si(IV) and Ge(IV) systems are examples of "slow" complexes, with rearrangements occurring very slowly, if at all.

The $[Ti(dibm)_3]^+SbCl_6^-$ complex was prepared with the hope of detecting inversion processes and comparing the rate with the neutral $Ti(dibm)_2X_2$ species. For the $[Ti(dibm)_3]^+$ system, the only plausible rearrangement process is $\Delta \leftrightarrows \Lambda$ enantiomerization. In the slow exchange limit, the proton nmr spectrum of this species should reveal two isopropyl methyl doublets as a result of the dissymmetry at the metal center. At ambient temperature, a single isopropyl methyl doublet is observed, which broadens on cooling to ca. -70^0 (60 MHz instrument). At -80^0, on a 100 MHz instrument a broad doublet is observed. No splitting of this resonance was detected. Inversion processes must still be very rapid at these low temperatures. This was confirmed by preparing the $[Si(dibm)_3]^+$ and $[Ge(dibm)_3]^+$ complexes, which reveal two isopropyl methyl doublets at room temperature due to very slow enantiomerization. The increase in lability on going from the neutral to the charged titanium(IV) complex is interesting and is not expected if rearrangement occurs via bond rupture, since the Ti-O bonds should be stronger in the cationic complex.

On progressing from the neutral to cationic complexes of diisobutyrylmethane, a general downfield shift is observed in the proton

nmr spectra (cf. Appendix C for chemical shifts). Downfield shifts of 0.03, 0.15, and 0.27 ppm are observed for the isopropyl methyl, isopropyl methine proton, and -CH= ring protons, respectively, on going from $Ti(dibm)_2Cl_2$ to $[Ti(dibm)_3]^+$. Similar shifts have been observed (130) previously and have been ascribed to electric fields generated by the charge on the ion.

The loss of optical activity of the resolved $[Si(acac)_3]^+$ complex has been studied in protic solvents (183); the racemization process was found to be mainly due to solvolysis reactions. However, it has recently been found (185) that in carefully dehydrated organic solvents, the $[Si(acac)_3]^+$ complex undergoes a slow intramolecular racemization reaction with an enthalpy of activation at 50^o of 25.7 ± 0.2 kcal/mole and $k_{40}{}^o$ = 1.08×10^{-5} sec^{-1}. Similar behaviour occurs with the $[Ge(acac)_3]^+$ complex (186), with a $\Delta H^{\neq}$ of 24.3 ± 0.4 kcal/mole and $k_{40}{}^o = 7.97 \times 10^{-6}$ sec^{-1}. The small rate constants for racemization in these systems precludes observing the exchange of diastereotopic methyl groups in the nmr spectra of the $[Si(dibm)_3]^+$ and $[Ge(dibm)_3]^+$ complexes at readily accessible temperatures.

A potential use for these $[M(dibm)_3]X$ complexes is in the establishment of absolute configurations. The $(+)_D$-$[Si(acac)_3]ClO_4$ enantiomer has been assigned (184) the Λ configuration. If the $[Si(dibm)_3]^+$ cation could be resolved and the isopropyl methyl doublets in its pmr spectrum assigned to the appropriate absolute configurations, a potential secondary standard would be provided for the assignment of absolute configurations.

Chemical shift data are listed in Appendix C for complexes discussed in this section.

b. Titanium(IV) Complexes with Chelating Diols

Since there was a possibility that exchange processes in the isopropyl phenoxy complexes of Section III-C-1c might be a result of a hindered rotation process about the Ti-O-C bonds, complexes containing a rigid chelating diol were investigated. Hindered rotation processes would not be possible in such systems. Diols that were investigated were catechol and some of its isopropyl-substituted derivatives.

Diols reacted cleanly with $Ti(chel)_2(O^iC_3H_7)_2$ [chel = acac,bzac,quin] complexes to yield the corresponding $Ti(chel)_2(cat)$ complexes according to equation [10]. Two limiting structures can be considered for these complexes, illustrated by 7 and 8, which represent bonding extremes and oxidation states of II and IV, respectively, for titanium. Catechols are known to be oxidized by various metal ions to o-quinones (187-190). A structure such as the quinone-type adduct 7,

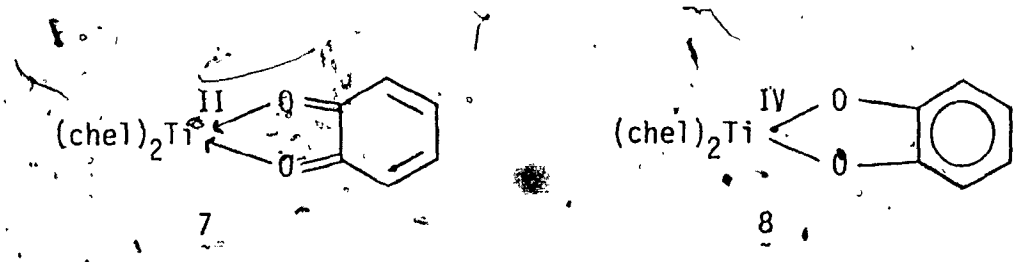

7 8

resulting from oxidation of the catechol is possible, but unlikely on the basis of infrared and proton nmr spectra. Infrared spectra of these complexes contain no O-H stretching bands and no C-O stretching vibrations above 1600 cm^{-1}. However, an adduct of titanium(IV) chloride with 9,10-phenanthrenequinone is known (191) and a reduction of the quinone C-O stretching frequency of ca. 100 cm^{-1} on complexation is reported. It appears that infrared spectra cannot conclusively support either structure 7 or 8.

Proton nmr spectra of the catechol ring protons revealed an AA'BB' pattern, unlike that expected for a 1,3-diolefinic unit as in 7. In conjunction with crystallographic studies on related systems (vide infra), these results suggest that structure 8 is the more proper representation for the bonding in these complexes.

The $Ti(acac)_2(cat)$ complex should reveal two acetylacetonate methyl resonances as the axial and equatorial terminal groups of the acac ligand are required to be nonequivalent. At room temperature, a single acac methyl resonance is observed. On cooling, the $W_{1/2}$ for this resonance increases to 1.20 Hz at -58.7° from 0.57 Hz at ambient temperature, a result which may be attributed to viscosity broadening. Similar results were obtained with the $Ti(acac)_2(3,6\text{-}^{i}Pr_2cat)$ complex, the acac methyl resonance broadening from a $W_{1/2}$ of 0.58 Hz at room temperature to only 1.72 Hz at -58.7°. A single isopropyl methyl doublet is observed for this complex, which broadens with decreasing temperature and possesses a $W_{1/2}$ of *ca.* 5 Hz at -58.7°. No splitting was observed.

A complex containing an unsymmetrical β-diketonate ligand, benzoylacetone, was also investigated. The $Ti(bzac)_2(cat)$ complex reveals a single bzac methyl and -CH= resonance at room temperature, indicating that if diastereomers exist, they are rapidly interconverting. No low temperature studies were performed on this complex following the lack of success with the acetylacetonate complex.

The $Ti(bzac)_2(3,6\text{-}^{i}Pr_2cat)$ complex revealed a single isopropyl methyl doublet, in conjunction with the same features of the $Ti(bzac)_2(cat)$ complex, at room temperature.

The $Ti(quin)_2(3,6\text{-}^{i}Pr_2cat)$ complex proved to be too insoluble in useful solvents and in addition was found to be prone to decomposition. Spectra of a dilute dichloromethane solution were obtained

until ca. 3°, at which time crystallization of the complex from solution occurred. A single quin methyl and isopropyl methyl doublet are observed at room temperature, with only slight broadening on cooling, part of which is probably due to the particulate matter in the solution.

Finally, an unsymmetrical catecholate ligand was employed. The $Ti(quin)_2(3,5\text{-}^{i}Pr_2cat)$ complex reveals two isopropyl methyl doublets at room temperature, consistent with structure 9, in which the molecular symmetry necessitates the gross nonequivalence of isopropyl groups. A single quin methyl resonance is observed. No low temperature studies were attempted on this complex owing to its general insolubility in useful nmr solvents.

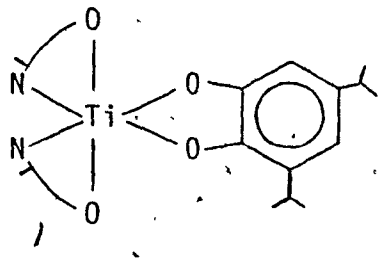

9

The dramatic increase in the rates of exchange processes in the $Ti(chel)_2(cat)$ complexes is enigmatic. It cannot simply be a result of chelation, since the neopentyl glycollate derivative $Ti(acac)_2(OCH_2CMe_2CH_2O)$ reveals nonequivalent acac methyl groups by ca. -42° in a CS_2 solution (61). Bonding effects would not be expected to cause such a difference in rates. For example, pKa_1 and pKa_2 for catechol are 9.1 and 13.2, respectively, compared to a pKa of 10.0 for phenol (155), and similar exchange rates are expected, since it was demonstrated in Section III-C-1-c(i) that rearrangement rates within $Ti(acac)_2(phenoxy)_2$ complexes increase as the pKa of

the phenol decreased. These considerations apply generally to σ-donor effects and the rigid, planar nature of the catecholate ligand may increase π-bonding effects considerably.

A potential cause for the rate increase may be found in the nature of the catecholate ligand. In several X-ray crystallographic structure determinations of complexes containing chelated catecholate ligands, the average O···O separation, or "bite", is ca. 2.5-2.6 Å (192-194). This separation in chelated acetylacetonate complexes is ca. 2.7-2.8 Å (195). Discussions in the literature (45-47) have focused on the ability of short "bite" ligands to force the geometrical disposition of ligating nuclei from the usual octahedral core towards a trigonal prismatic arrangement. Simple calculations reinforce this argument (46). Indeed, in the related tris(benzenedithiolato)zirconium(IV) dianion, the distortion towards trigonal prismatic coordination is greater (196) than simple interligand repulsion arguments predict (46).

Should the short "bite" of the catechol ligand in these $Ti(chel)_2(cat)$ complexes force the geometry of the complex away from octahedral towards a trigonal prism to a greater extent than in the corresponding $Ti(chel)_2(phenoxy)_2$ complexes, the rate of rearrangement should increase if a twist mechanism is involved.

More detailed studies of these titanium(IV) complexes are warranted. The tris(1,2-benzenediolato)titanium(IV) dianion has recently been reported (197); a structural investigation of this complex would be desirable.

Chemical shift data for complexes discussed in this section are tabulated in Appendix C.

D. Apparent Five-Coordinate Titanium(IV) Complexes

a. Introduction

A coordination number of five is extremely rare for titanium(IV) complexes (198). It does occur in $[TiCl_2(OR)_2]_2$ complexes where R = phenyl (199) and ethyl (200) and has recently been observed in the $[TiCl_2NSiMe_3]_n$ polymer (201). The square pyramidal $[TiOCl_4]^{2-}$ anion is the only known monomeric five-coordinate titanium(IV) complex (202). The propensity of titanium(IV) complexes to obtain an octahedral geometry by forming dimers with bridging ligands is well known (198).

Interest has developed in recent years concerning the nature of the apparent five-coordinate titanium(IV) complexes of the type $Ti(dik)X_3$ [X = halogen, alkoxy group]. Mehrotra and co-workers (64,65,203, 204) found that titanium tetrachloride and acetylacetone reacted in a 1:1 mole ratio to give a complex of the stoichiometry $Ti(acac)Cl_3$. They also found that the $Ti(dik)(OR)_3$ complexes, prepared from the diketone and the appropriate titanium(IV) alkoxide in a 1:1 mole ratio, underwent a disproportionation reaction according to equation [24]. Molecular weights were close to the monomeric formulation in cases of large R groups; less bulky R groups resulted in molecular weights significantly above that required for a monomer.

$$2\ Ti(dik)(OR)_3 \rightleftharpoons Ti(dik)_2(OR)_2 + Ti(OR)_4 \qquad [24]$$

Thompson and co-workers (56) prepared the $Ti(3\text{-}CH_3\text{-}acac)X_3$ [X = Cl,Br] complexes and found them to be monomeric nonelectrolytes in nitrobenzene. Complicated temperature dependent nmr spectra in nitrobenzene precluded the assignment of stereochemistry. The $Ti(3\text{-}CH_3\text{-}acac)_2Cl_2$ complex was found to react with an additional mole of titanium(IV)

chloride to form the identical $Ti(3\text{-}CH_3\text{-acac})Cl_3$ complex. A similar reaction occurs with the acetylacetonate complexes (67).

On the basis of nmr studies, Holloway and Sentek (67) proposed that apparently five-coordinate $Ti(dik)X_3$ complexes were weakly associated dimers of the well known four- and six-coordinate complexes TiX_4 and $Ti(dik)_2X_2$, according to equation [25].

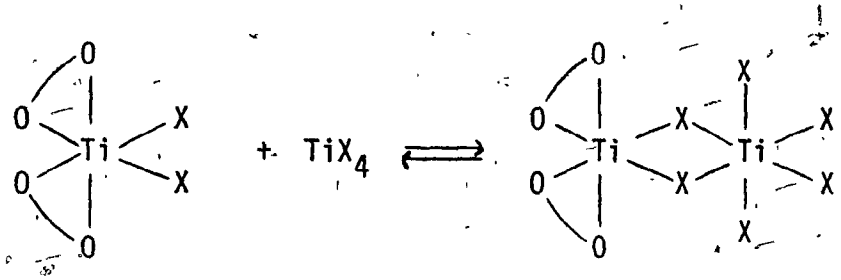

[25]

Subsequent studies on the $Ti(bzac)Cl_3$ species were interpreted by Thompson and co-workers (66) in terms of a five-coordinate structure participating in an equilibrium according to equation [24]. The proton nmr spectrum for the $Ti(bzac)Cl_3$ species revealed two bzac methyl resonances which were assigned to the $Ti(bzac)_2Cl_2$ and $Ti(bzac)Cl_3$ species and supported the equilibrium depicted in equation [24]. Coalescence of these two signals at high temperature indicated that the interconversion depicted by equation [24] is a facile and rapid process.

Recently, Alyea and Merrell (68) have presented evidence for five-coordinate titanium(IV) complexes of the type $Ti(chel)(OR)_3$, in which chel is a uninegative, bidentate ligand with an ethane backbone, e.g., $OCH_2CH_2N(CH_3)_2$. A different synthetic route was employed; the lithium salt of the bidentate ligand was reacted with the $Ti(OR)_3Cl$ species. Unfortunately, these products are liquids and thus not amenable to crystallographic studies to establish their structure.

A crystallographic investigation of the $Ti(acac)Cl_3$ complex

revealed (127) that this complex, in the solid state, exists as a centrosymmetric chlorine-bridged dimer in which each titanium atom is six-coordinate and carries a bidentate acetylacetonate ligand.

Solution behaviour of the $[Ti(acac)Cl_3]_2$ dimer may then be interpreted in terms of equation [25]; however, the appearance of an acac group on each titanium is enigmatic. The dimer may result from dimerization of two five-coordinate species *via* an associative process similar to equation [25].

b. Infrared Spectroscopic Studies

Preparation of apparent five-coordinate species *via* direct reaction of the octahedral $Ti(dik)_2X_2$ complex with one mole of TiY_4 proved to be the simplest and most convenient synthetic route, according to equation [26]. Reactions were conducted in dichloromethane solution

$$Ti(dik)_2X_2 + TiY_4 \underset{X = Y,\ X \neq Y}{\rightleftharpoons} 2\ Ti(dik)_2XY_2 \text{ or } [Ti(dik)XY_2]_2 \qquad [26]$$

by adding the TiY_4 reagent dropwise to a solution of the $Ti(dik)_2X_2$ complex. If necessary, small amounts of hexane were added to effect crystallization. Table LV summarizes the reactions attempted; this establishes the scope of the reaction and several of these products have been reported previously.

In general, products containing bromine were very unstable and extremely moisture sensitive; poor quality solid state infrared spectra were obtained. A reaction occurred between $Ti(acac)_2Cl_2$ and TiF_4 but no solid product could be isolated; only intractable oils formed. None of the complexes of Table LV were completely characterized. The present study merely constitutes some initial explorations on the nature of these

Table LV

$Ti(dik)_2X_2 + TiY_4 \rightleftharpoons$ "$Ti(dik)XY_2$" Reactions

dik	X	Y	Comments
acac	F	Cl	stable
acac	F	Br	unstable
acac	Cl	F	reaction occurred; could not isolate product
acac	Cl	Cl	stable
acac	Br	Br	unstable
acac	Cl	Br	unstable
acac	Br	Cl	unstable
dibm	F	Cl	stable
dibm	Cl	Cl	stable
dpm	F	Cl	stable
dpm	Cl	Cl	stable
dpm	Br	Br	unstable
bzac	F	Cl	stable
bzac	Cl	Cl	stable
acac	F	$O^iC_3H_7$	forms the corresponding $Ti(acac)_2X(O^iC_3H_7)$ complexes; cf. Section III-B-3
acac	Cl	$O^iC_3H_7$	
acac	Br	$O^iC_3H_7$	

complexes; consequently, detailed preparations are not reported. General synthetic techniques are described in Section II-A. The "$Ti(dik)XY_2$" species are very moisture sensitive.

Attention is focused on the mixed fluorine-chlorine complexes "$Ti(dik)FCl_2$". The parent $Ti(dik)_2F_2$ complexes exhibit an intense, broad absorption centered at ca. 620 cm^{-1} assigned to a terminal Ti-F stretching frequency (71,74). On reaction with $TiCl_4$ to form a five-coordinate species, the ν(Ti-F) band in the parent complex should shift to higher frequency (205). In the case where the Ti-F moiety forms

a bridging unit in a dimeric structure, the $\nu(Ti\text{-}F)_{ter}$ band should then disappear and be replaced with a $\nu(Ti\text{-}F)_{br}$ band at lower frequency. This provides a convenient spectroscopic test on the nature of these species.

Infrared spectra for the $Ti(acac)_2F_2$, "$Ti(acac)FCl_2$", $Ti(acac)_2Cl_2$, and "$Ti(acac)Cl_3$" complexes in the 1000 - 400 cm^{-1} region are shown in Figure 56. Band positions are listed in Table LVI. The spectrum of the $Ti(acac)_2F_2$ complex reveals two $\nu(Ti\text{-}F)_{ter}$ bands at 634 and 615 cm^{-1}, as reported previously (71). These bands are absent from the spectra of the "$Ti(acac)FCl_2$", $Ti(acac)_2Cl_2$, and "$Ti(acac)Cl_3$" complexes. No extra band(s) appear in the region of higher frequency that that can be correlated with a vibration of the parent $Ti(acac)_2F_2$ complex, as might be expected from the formation of a five-coordinate complex. Thus the Ti-F stretching frequency has been shifted to a lower frequency and must result from the formation of a dimeric unit with bridging fluorine groups.

Apparently there have been no reports of values for $\nu(Ti\text{-}F)_{br}$ in titanium(IV) complexes.

Monocyclopentadienyltitanium(III) halides, $(\eta^5\text{-}C_5H_5)TiX_2$, are at least dimeric and probably polymeric in the solid state (206). The X = F complex has only recently been reported (207) and a strong band at 470 cm^{-1} was assigned to the bridging Ti-F stretching frequency. As a crude guide, $\nu(Ti\text{-}F)_{br}$ should increase (205) as the oxidation state is changed to a titanium(IV) complex and $\nu(Ti\text{-}F)_{br}$ in the $[Ti(acac)FCl_2]_2$ complex should therefore be expected at ca. 500 cm^{-1}.

The solid state structures of the $Ti_2Cl_9^-$ and $Ti_2Cl_{10}^{2-}$ anions are known (208). The differences between $(Ti\text{-}Cl)_{br}$ and $(Ti\text{-}Cl)_{ter}$ bond distances in the above two anions are 0.28 Å and 0.20 - 0.24 Å, respect-

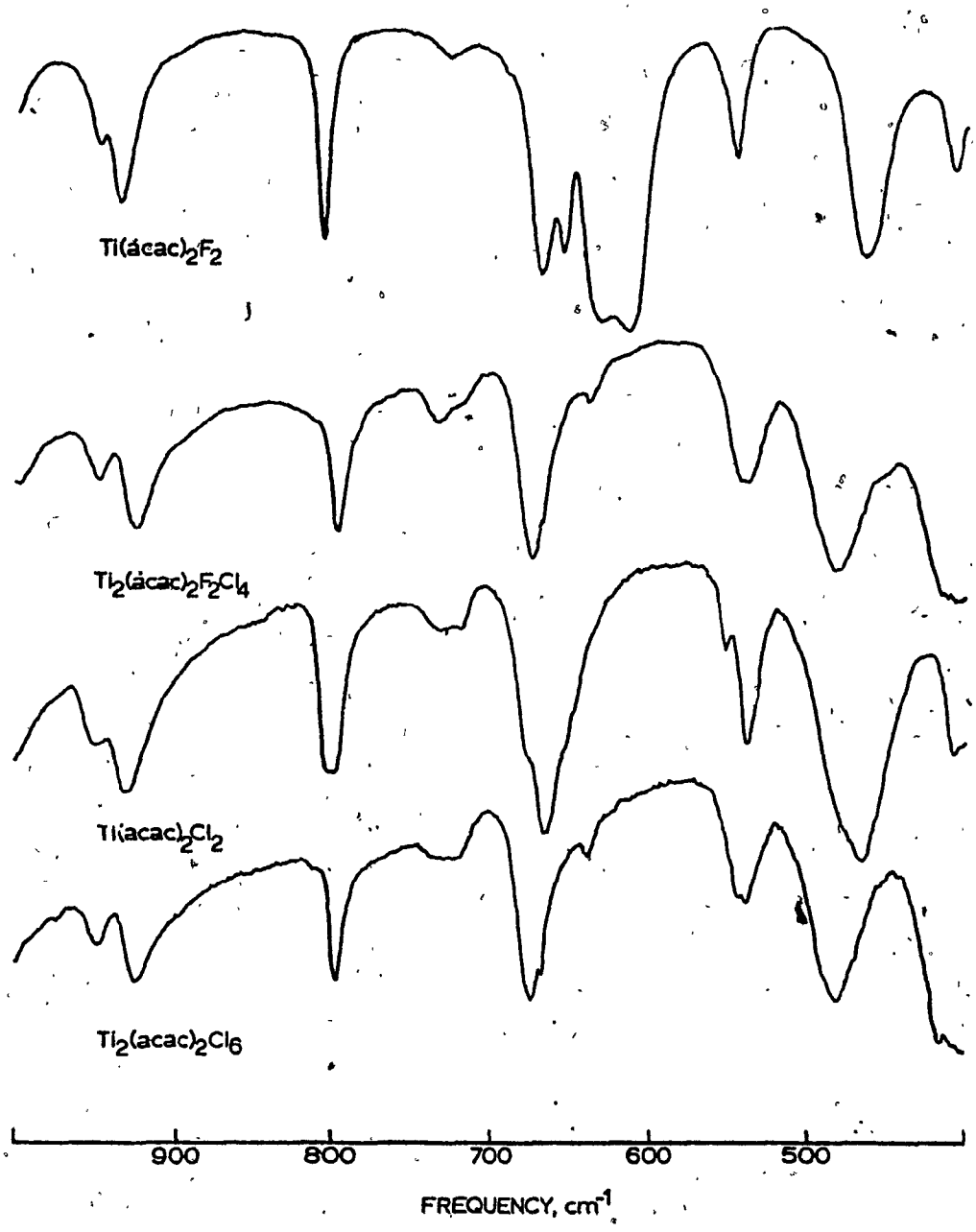

Figure 56.- Infrared spectra for solid $Ti(acac)_2F_2$, $[Ti(acac)FCl_2]_2$, $Ti(acac)_2Cl_2$, and $[Ti(acac)Cl_3]_2$ in nujol in the frequency range 1000 - 400 cm^{-1}.

Table LVI

Infrared Frequencies for Solid $Ti(acac)_2X_2$ and $[Ti(acac)X_3]_2$ Complexes in Nujol (Range 1000 - 400 cm^{-1})[a]

$Ti(acac)_2F_2$[b]	$[Ti(acac)FCl_2]_2$	$Ti(acac)_2Cl_2$[b]	$[Ti(acac)Cl_3]_2$
947 (m)	948 (m)	948 (m)	947 (m)
935 (ms)	926 (ms)	930 (ms)	924 (ms)
806 (ms)	799 (ms)	802 (ms)	798 (ms)
-	-	678 (sh)	-
669 (s)	676 (s)	666 (s)	675 (s)
-	641 (w)	652 (sh)	668 (sh)
-	-	-	640 (w)
634 (vs)	-	-	-
615 (vs)	-	-	-
556 (sh)	-	-	-
546 (m)	541 (m,br)	553 (m)	544 (m)
-	-	-	539 (m)
466 (s,br)	485 (s,br)	472 (s,br)	483 (s,br)
-	-	411 (m)	-

[a] Key: sh, shoulder; s, strong; v, very; br, broad; m, medium; w, weak. [b] Band positions agree with those reported by Lowry (71).

ively. From the assignment of $\nu(Ti\text{-}Cl)_{ter}$ and $\nu(Ti\text{-}Cl)_{br}$ for the $Ti_2Cl_9^-$ anion (209), one may calculate a range of ratios of $\nu(Ti\text{-}Cl)_{br}/\nu(Ti\text{-}Cl)_{ter}$ of 0.55 - 0.74. Since the $Ti_2Cl_{10}^{2-}$ anion, which bears greater structural resemblance to the $[Ti(acac)FCl_2]_2$ complex, has a slightly smaller difference in Ti-Cl bond lengths (208), the ratio $\nu(Ti\text{-}Cl)_{br}/\nu(Ti\text{-}Cl)_{ter}$ should increase slightly in this dianion. Extending this range of ratios found for the $Ti_2Cl_9^-$ spectra (cf. 0.55 - 0.74) to the $[Ti(acacFCl_2]_2$ complex, on the assumption of a similar ratio involving Ti-F bonds, leads to the prediction of the $\nu(Ti\text{-}F)_{br}$ band in the 340 - 460 cm^{-1} region.

Unfortunately, bands ascribable to terminal Ti-Cl stretching frequencies occur in the 400 cm^{-1} region for the $[Ti(acac)Cl_3]_2$ complex and the expected $\nu(Ti\text{-}F)_{br}$ band for the $[Ti(acacFCl_2]_2$ complex cannot be identified. However, the absence of a $\nu(Ti\text{-}F)_{ter}$ band in the infrared spectra of the $[Ti(acac)FCl_2]_2$ complex is strong evidence for a dimeric species involving fluorine bridges.

Similar observations were made on the same series of complexes in which the diketonate ligand was benzoylacetone. However, owing to the presence of the phenyl groups in the benzoylacetonate system, more bands are observed and the implications are less straightforward. The intense, broad band centered at ca. 609 cm^{-1} in the spectrum of the $Ti(bzac)_2F_2$ complex has been assigned to the $\nu(Ti\text{-}F)_{ter}$ vibration (74). The "$Ti(bzac)FCl_2$" complex possesses a band at 603 cm^{-1} but is considerable less intense than in the $Ti(bzac)_2F_2$ complex, suggesting that the fluorine atoms are in a bridging position. No band could be found that was not present in the $Ti(bzac)_2F_2$, $Ti(bzac)_2Cl_2$, or "$Ti(bzac)Cl_3$" spectra and thus no assignment of $\nu(Ti\text{-}F)_{br}$ can be made.

Spectra were also obtained for the $Ti(dik)_2F_2$ and $[Ti(dik)FCl_2]_2$ complexes [dik = dibm,dpm]. However, apparent overlap of ligand (or ν(Ti-O)) vibrations with ν(Ti-F) of the $Ti(dik)_2F_2$ complexes made it difficult to determine whether the $\nu(Ti\text{-}F)_{ter}$ band was diminished in intensity on forming the $[Ti(dik)FCl_2]_2$ complex. Some loss of intensity was noted so that it is likely that these complexes also possess fluorine bridges.

There are other spectroscopic techniques which may be applied to these systems. Large chemical shift differences have been observed between bridging and terminal fluorine nuclei (210); the ^{19}F nmr chemical shifts for the $[Ti(dik)FCl_2]_2$ complexes could provide evidence for the solution structure of these complexes.

The use of nuclear quadropole resonance (nqr) has been able to distinguish between bridging and terminal chloride groups in the $[(\eta^5\text{-}C_5H_5)TiCl_2(pyridine)]_2$ dimer (206). This technique may be applicable to these apparent five-coordinate titanium(IV) complexes.

Differentiation between a monomeric five-coordinate and dimeric structure for the "$Ti(acac)Cl_3$" species is difficult using chemical reactivity. The "$Ti(acac)Cl_3$" complex reacts with alcohols (70) to form the $Ti(acac)_2Cl_2$ complex and with an alcohol/pyridine mixture to give the $Ti(acac)_2Cl(OR)$ complex. The "$Ti(bzac)Cl_3$" complex reacts with pyridine to give the $Ti(bzac)(pyridine)Cl_3$ complex; however, this could result from the addition of pyridine to a coordinatively unsaturated five-coordinate species or from a bridge-cleaving reaction.

A number of reactions of the "$Ti(acac)Cl_3$" species with potential donor ligands were investigated. The very dark red titanium(IV) complex reacted with $P(C_6H_5)_3$, $As(C_6H_5)_3$, $Sb(C_6H_5)_3$, pyridine, $P(OC_6H_5)_3$, and acetonitrile in dichloromethane solution to give lighter red-colored

solutions. However, no solid products could be isolated from these reactions as evaporation of the solvent yielded viscous red liquids. The chemistry of these "Ti(dik)X_3". complexes has the potential of providing routes to a number of new titanium(IV) complexes.

IV. APPENDICES

A. Abbreviations for Bidentate Ligands

Table LVII

Nomenclature and Abbreviations for β-Diketonate Ligands

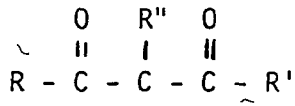

Abbreviation	Ligand	R	R"	R'
dik	any β-diketonate			
acac	acetylacetonate (2,4-pentanedionate)	CH_3	H	CH_3
dibm	diisobutyrylmethanate (2,6-dimethyl-3,5-heptanedionate)	$i\text{-}C_3H_7$	H	$i\text{-}C_3H_7$
dpm	dipivaloylmethanate (2,2,6,6-tetramethyl-3,5-heptanedionate)	$t\text{-}C_4H_9$	H	$t\text{-}C_4H_9$
tibm	1,1,1-trifluoro-5-methyl-2,4-hexanedionate	CF_3	H	$i\text{-}C_3H_7$
tdh	1,1,1-trifluoro-5,5-dimethyl-2,4-hexanedionate	CF_3	H	$t\text{-}C_4H_9$
3-^{i}Pr-acac	3-isopropylacetylacetonate (3-isopropyl-2,4-pentanedionate)	CH_3	$i\text{-}C_3H_7$	CH_3
bzac	benzoylacetonate (1-phenyl-1,3-butanedionate)	CH_3	H	C_6H_5
bzbz	dibenzoylmethanate (1,3-diphenyl-1,3-propanedionate)	C_6H_5	H	C_6H_5
tfac	trifluoroacetylacetonate (1,1,1-trifluoro-2,4-pentanedionate)	CF_3	H	CH_3

Table LVII (continued)

hfac	hexafluoroacetylacetonate (1,1,1,5,5,5-hexafluoro-2,4-pentanedionate)	CF_3	H	CF_3
bztf	benzoyltrifluoroacetonate (4,4,4-trifluoro-1-phenyl-1,3-butanedionate)	CF_3	H	C_6H_5
thtf	thenoyltrifluoroacetonate (4,4,4-trifluoro-1-(2-thienyl)-1,3-butanedionate)	CF_3	H	C_4H_3S
dhd	2,2-dimethyl-3,5-hexanedionate	CH_3	H	$t\text{-}C_4H_9$
$3\text{-}CH_3\text{-}acac$	3-methylacetylacetonate (3-methyl-2,4-pentanedionate)	CH_3	CH_3	CH_3

Table LVIII

Abbreviations for Other Bidentate Ligands

Abbreviation	Ligand
α-C_3H_5T	α-isopropenyltropolonate
α-C_3H_7T	α-isopropyltropolonate
R_1,R_2-dtc	N,N-R_1R_2-dithiocarbamate ($R_1=R_2$; $R_1\neq R_2$; R_1,R_2=alkyl, aryl)
tfd	perfluoromethyldithiolene
mnt	maleonitriledithiolene
ox	oxinate (8-quinolinolate)
quin	quinaldinate (2-methyl-8-quinolinolate)
cat	catecholate (1,2-benzenediolate)
3,6-$^{i}Pr_2$cat	3,6-diisopropylcatecholate (3,6-diisopropyl-1,2-benzenediolate)
3,5-$^{i}Pr_2$cat	3,5-diisopropylcatecholate (3,5-diisopropyl-1,2-benzenediolate)
dmm	dimethylmalonate
tmm	N,N,N',N'-tetramethylmalonamide

B. Temperature Dependence of Experimental Chemical Shift Separations, $\delta\upsilon_e$, for Exchange of Nonequivalent Groups in Titanium(IV) Complexes

Table LIX

Temperature Dependence of $\delta\upsilon_e$ for Exchange of Terminal Methyl Groups in the $Ti(3\text{-}^{i}Pr\text{-}acac)_2Cl_2$ Complex[a]

Temp., °C	$\delta\upsilon_e$ (Hz)[b]	Temp., °C	$\delta\upsilon_e$ (Hz)[b]
-38.9	2.94	-52.2	7.82
-40.0	4.64	-54.7	7.92
-42.6	6.33	-59.5	8.06
-46.2	7.22	-62.2	8.08
-49.8	7.65	-69.6[c]	8.14

[a]In dichloromethane solution; [b]Experimental values at the indicated temperature; [c]A constant value of $\delta\upsilon_o$ = 8.09 Hz used for lineshape calculations.

Table LX

Temperature Dependence of $\delta\upsilon_e$ for Exchange of Acetylacetonate Methyl Groups in the $Ti(acac)_2(2\text{-}ClC_6H_4O)_2$ Complex[a]

Temp., °C	$\delta\upsilon_e$ (Hz)[b]	Temp., °C	$\delta\upsilon_e$ (Hz)[b]
0.8	6.53	-29.5	10.64[c]
-3.2	8.02	-38.4	10.72[c]
-7.6	9.32	-42.6	10.75[c]
-11.0	9.97	-51.5	10.82[c]
-15.5	10.24	-61.1	11.04[c]
-23.0	10.53[c]	-68.6	10.94[c]

[a]In dichloromethane solution; [b]Experimental values at the indicated temperature; [c]These data points were fitted to the linear least-squares relationship $\delta\upsilon_e = 10.326 - 0.010\ T(^{o}C)$.

Table LXI

Temperature Dependence of $\delta\upsilon_e$ for Exchange of Acetylacetonate Methyl Groups in the $Ti(acac)_2(2\text{-}IC_6H_4O)_2$ Complex[a]

Temp., °C	$\delta\upsilon_e$ (Hz)[b]	Temp., °C	$\delta\upsilon_e$ (Hz)[b]
12.0	6.92	-9.1	14.61
11.1	9.22	-13.4	15.35[c]
7.5	11.63	-21.9	15.63[c]
4.6	13.04	-29.7	16.02[c]
0.2	13.94	-42.5	16.55[c]
-2.7	14.29	-52.1	17.09[c]

[a]In dichloromethane solution; [b]Experimental values at the indicated temperatures; [c]These data points were fitted to the linear least-squares relationship $\delta\upsilon_e = 14.692 - 0.050\ T(^oC)$.

Table LXII

Temperature Dependence of $\delta\upsilon_e$ for Exchange of Acet[redacted]te Methyl Groups in the $Ti(acac)_2(4\text{-}ClC_6H_4O)_2$ Comple[redacted]

Temp., °C	$\delta\upsilon_e$ (Hz)[b]	Temp., °C	$\delta\upsilon_e$ (Hz)[b]
16.8	5.09	-2.7	11.09[c]
16.1	6.86	-9.1	11.24[c]
15.2	7.66	-13.4	11.32[c]
11.1	9.48	-21.9	11.50[c]
7.5	10.19	-29.7	11.79[c]
4.6	10.61	-42.5	11.83[c]
0.2	10.79	-52.1	12.00[c]

[a]In dichloromethane solution; [b]Experimental values at the indicated temperature; [c]These data points were fitted to the linear least-squares relationship $\delta\upsilon_e = 11.085 - 0.019\ T(^oC)$.

Table LXIII

Temperature Dependence of $\delta\upsilon_e$ for Exchange of Acetylacetonate Methyl Groups in the $Ti(acac)_2(4\text{-}^iPrC_6H_4O)_2$ Complex[a]

Temp., °C	$\delta\upsilon_e$ (Hz)[b]	Temp., °C	$\delta\upsilon_e$ (Hz)[b]
27.9	4.31	8.5	11.84
26.8	5.17	6.4	12.02
25.2	6.92	-0.5	12.31[c]
23.8	8.71	-7.1	12.50[c]
20.9	9.36	-13.9	12.57[c]
17.5	10.87	-21.8	12.73[c]
20.2	10.31	-33.9	12.96[c]
14.1	11.33	-46.3	13.21[c]
12.3	11.48		

[a]In dichloromethane solution; [b]Experimental values at the indicated temperature; [c]These data points were fitted to the linear least-squares relationship $\delta\upsilon_e = 12.321 - 0.019\ T(^oC)$.

Table LXIV

Temperature Dependence of $\delta\upsilon_e$ for Exchange of Acetylacetonate Methyl Groups in the $Ti(acac)_2(2\text{-}^iPrC_6H_4O)_2$ Complex[a]

Temp., °C	$\delta\upsilon_e$ (Hz)[b]	Temp., °C	$\delta\upsilon_e$ (Hz)[b]
33.6	3.46	17.9	9.99
32.2	5.37	15.5	10.17
30.2	6.68	14.6	10.17
28.6	7.94	8.2	10.29
25.1	9.12	-1.0	10.31[c]
25.0	8.88	-17.4	10.20
22.1	9.66	-25.4	10.12
20.3	9.84	-39.7	9.90

[a]In dichloromethane solution; [b]Experimental values at the indicated temperature; [c]A constant value of $\delta\upsilon_o = 10.31$ Hz used for lineshape calculations.

Table LXV

Temperature Dependence of $\delta\upsilon_e$ for Exchange of Acetylacetonate Methyl Groups in the $Ti(acac)_2(2\text{-}(C_6H_5)C_6H_4O)_2$ Complex[a]

Temp., °C	$\delta\upsilon_e$ (Hz)[b]	Temp., °C	$\delta\upsilon_e$ (Hz)[b]
29.4	6.33	3.9	10.85
27.3	7.78	-6.2	11.07[c]
24.3	9.09	-14.2	11.27[c]
22.9	9.50	-17.7	11.33[c]
20.5	10.05	-24.9	11.38[c]
14.1	10.42	-25.7	11.54[c]
7.7	10.62	-28.9	11.60[c]

[a]In dichloromethane solution; [b]Experimental values at the indicated temperature; [c]These data points were fitted to the linear least-squares relationship $\delta\upsilon_e = 10.942 - 0.022\ T(^oC)$.

Table LXVI

Temperature Dependence of $\delta\upsilon_e$ for Exchange of Acetylacetonate Methyl Groups in the $Ti(acac)_2(2,6\text{-}^iPr_2C_6H_3O)_2$ Complex[a]

Temp., °C	$\delta\upsilon_e$ (Hz)[b]	Temp., °C	$\delta\upsilon_e$ (Hz)[b]
35.2	5.64	16.1	9.41
33.3	7.17	13.8	9.42
29.5	7.86	7.7	9.49[c]
28.6	8.32	3.0	9.38
25.2	9.22	-3.6	9.33
22.7	9.22		

[a]In dichloromethane solution; [b]Experimental values at the indicated temperature; [c]A constant value of $\delta\upsilon_o$ = 9.49 Hz used for lineshape calculations.

Table LXVII

Temperature Dependence of $\delta\upsilon_e$ for Exchange of Acetylacetonate Methyl Groups in the $Ti(acac)_2(2,6\text{-}^iPr_2C_6H_3O)_2$ Complex[a]

Temp., °C	$\delta\upsilon_e$ (Hz)[b]	Temp., °C	$\delta\upsilon_e$ (Hz)[b]
40.8	5.47	28.0	10.85
40.4	5.56	25.5	10.89
37.0	9.30	22.0	10.90[c]
35.6	9.71	13.5	10.78
33.3	10.22	9.6	10.77
31.6	10.29	-15.3	9.55

[a]In m-dichlorobenzene solution; [b]Experimental values at the indicated temperature; [c]A constant value of $\delta\upsilon_o$ = 10.90 Hz used for lineshape calculations.

Table LXVIII

Temperature Dependence of $\delta\upsilon_e$ for Exchange of Isopropyl Methyl Groups in the $Ti(acac)_2(2\text{-}^iPrC_6H_4O)_2$ Complex[a]

Temp., °C	$\delta\upsilon_e$ (Hz)[b]	Temp., °C	$\delta\upsilon_e$ (Hz)[b]
8.2	1.14[c]	-12.2	2.63[d]
7.3	1.28	-17.4	2.83[d]
4.9	1.65	-21.0	2.82[d]
3.8	1.74	-25.4	2.95[d]
1.7	1.95	-32.8	3.09[d]
-1.0	2.13	-39.7	3.29[d]
-8.4	2.49[d]		

[a]In dichloromethane solution; [b]Experimental values at the indicated temperature; [c]Separations listed for the low field doublet only; [d]These data points were fitted to the linear least-squares relationship

$$\delta\upsilon_e = 2.332 - 0.024\ T(^oC).$$

Table LXIX

Temperature Dependence of $\delta\upsilon_e$ for Exchange of Isopropyl Methyl Groups in the $Ti(acac)_2(2,6\text{-}^iPr_2C_6H_3O)_2$ Complex[a]

Temp., °C	$\delta\upsilon_e$ (Hz)[b]	Temp., °C	$\delta\upsilon_e$ (Hz)[b]
22.4	1.83[c]	3.0	4.86[d]
16.1	3.06	-3.6	5.33[d]
13.8	3.54	-12.8	5.91[d]
7.7	4.44	-27.6	6.72[d]

[a]In dichloromethane solution; [b]Experimental values at the indicated temperature; [c]Separations listed for the low field doublet only; [d]These data points were fitted to the linear least-squares relationship

$$\delta\upsilon_e = 5.086 - 0.060\ T(^oC).$$

Table LXX

Temperature Dependence of $\delta\upsilon_e$ for Exchange of Isopropyl Methyl Groups in the $Ti(acac)_2(2,6\text{-}^iPr_2C_6H_3O)_2$ Complex[a]

Temp., °C	$\delta\upsilon_e$ (Hz)[b]	Temp., °C	$\delta\upsilon_e$ (Hz)[b]
19.7	1.59[c] ; 1.56[d]	1.3	3.99 ; 3.83[e]
16.7	2.30 ; 2.30	-4.8	4.30 ; 4.29[e]
13.5	2.82 ; 2.86	-9.5	4.52 ; 4.59[e]
9.6	3.34 ; 3.32[e]	-15.3	4.96 ; 5.05[e]
8.7	3.39 ; 3.38[e]	-19.6	5.20 ; 5.15[e]
5.6	3.62 ; 3.60[e]		

[a]In m-dichlorobenzene solution; [b]Experimental values at the indicated temperature; [c]Low field doublet; [d]High field doublet; [e]These data points were fitted to the linear least-squares relationship

$$\delta\upsilon_e = 3.964 - 0.064\ T(^oC).$$

Table LXXI

Temperature Dependence of $\delta\upsilon_e$ for Exchange of Isopropyl Methyl Groups in the $Ti(acac)_2Cl(2,6\text{-}^iPr_2C_6H_3O)$ Complex[a]

Temp., °C	$\delta\upsilon_e$ (Hz)[b]	Temp., °C	$\delta\upsilon_e$ (Hz)[b]
-7.6	1.37[c] ; 1.17[d]	-25.3	2.95 ; 2.90[e]
-11.7	2.05 ; 2.00	-33.3	3.11 ; 3.09[e]
-14.9	2.50 ; 2.50	-39.6	3.23 ; 3.22[e]
-17.4	2.66 ; 2.65	-48.7	3.41 ; 3.36[e]
-18.7	2.69 ; 2.72		

[a]In dichloromethane solution; [b]Experimental values at the indicated temperature; [c]Low field doublet; [d]High field doublet; [e]These data points were fitted to the linear least-squares relationship

$$\delta\upsilon_e = 2.437 - 0.020\ T(^oC)$$

Table LXXII

Temperature Dependence of $\delta\upsilon_e$ for Exchange of Isopropyl Methyl Groups in the $Ti(ox)_2(2,6\text{-}^iPr_2C_6H_3O)_2$ Complex[a]

Temp., °C	$\delta\upsilon_e$ (Hz)[b]	Temp., °C	$\delta\upsilon_e$ (Hz)[b]
108.2	20.59[c]; 19.75	83.3	24.95 ; 25.05[e]
105.9	21.22 ; 20.64	79.0	25.07 ; 25.11[e]
103.3	21.65 ; 21.22	70.7	25.40 ; 25.34[e]
99.9	22.97 ; 22.23	62.4	25.67 ; 25.65[e]
94.9	23.84 ; 23.79	53.6	25.94 ; 25.91[e]
90.9	24.29 ; 24.30	39.7	26.39 ; 26.38[e]
87.1	24.72 ; 24.62		

[a]In m-dichlorobenzene solution; [b]Experimental values at the indicated temperature; [c]Low field doublet; [d]High field doublet; [e]These data points were fitted to the linear least-squares relationship

$$\delta\upsilon_e = 27.654 - 0.032\ T(^oC)$$

Table LXXIII

Temperature Dependence of $\delta\upsilon_e$ for Exchange of Isopropyl Methyl Groups in the $Ti(quin)_2(2,6\text{-}^iPr_2C_6H_3O)_2$ Complex[a]

Temp., °C	$\delta\upsilon_e$ (Hz)[b]	Temp., °C	$\delta\upsilon_e$ (Hz)[b]
73.4	24.78	45.3	41.19 ; 41.20[e]
68.7	33.46	41.0	41.17 ; 41.54[e]
66.0	34.80	33.3	41.82 ; 41.80[e]
63.9	35.60	27.9	42.06 ; 42.14[e]
54.5	40.14[c]; 40.22[d]	19.3	42.68 ; 42.68[e]
50.0	40.64 ; 40.70		

[a]In m-dichlorobenzene solution; [b]Experimental values at the indicated temperature; [c]Low field doublet; [d]High field doublet; [e]These data points were fitted to the linear least-squares relationship

$$\delta\upsilon_e = 43.746 - 0.058\ T(^oC).$$

Table LXXIV

Chemical Shift Data[a] for Complexes Containing i-Propyl or t-Butyl Groups on the Bidentate Ligand

Complex	Solvent	isopropyl(J, Hz) or t-butyl CH_3	-CH=	Other
$Ti(dibm)_2F_2$	CH_2Cl_2	-1.10 (6.8)	-5.83	i-Pr CH: -2.53
	C_6H_6	-0.95 (6.8)	-5.52	i-Pr CH: -2.23
$Ti(dibm)_2Cl_2$	CH_2Cl_2	-1.13 (6.7)	-5.94	i-Pr CH: -2.59
	C_6H_6	-0.96 (6.7)	-5.60	i-Pr CH: -2.25
$Ti(dibm)_2Br_2$	CH_2Cl_2	-1.14 (6.9)	-5.96	i-Pr CH: -2.59
	C_6H_6	-0.98 (6.6)	-5.62	i-Pr CH: -2.24
$Sn(dibm)_2Cl_2$	$C_2H_2Cl_4$	-1.21(7.1),-1.09(6.6), -1.05(6.6)	-5.72[b]	i-Pr CH: -2.48
$Ge(dibm)_2Cl_2$	$C_2H_2Cl_4$	-1.29(6.7),-1.10(6.8), -1.04(6.7)	-5.76[b]	i-Pr CH: -2.47
$Ti(3\text{-}^{i}Pr\text{-}acac)_2Cl_2$	CH_2Cl_2	-1.31 (7.1)	-	i-Pr CH: -3.11 ter. CH_3: -2.24
$Ti(dibm)_2Cl(OCH_3)$	CH_2Cl_2	-1.10 (6.8)	-5.77	i-Pr CH: -2.53 O-CH_3: -4.45
$[Ti(dibm)_3]SbCl_6$	CH_2Cl_2	-1.16 (6.9)	-6.21	i-Pr CH: -2.74
$[Si(dibm)_3]Cl$	CH_2Cl_2	-1.18(6.8),-1.05(6.7)	-5.86	i-Pr CH: -2.66
$[Ge(dibm)_3]SbCl_6$	CH_2Cl_2	-1.17(6.7),-1.03(6.5)	-5.83	i-Pr CH: -2.61

Table LXXIV (continued)

$Ti(tibm)_2Cl_2$	CH_2Cl_2	-1.16 (6.8)	-6.36	i-Pr CH: -2.72
$Sn(tibm)_2Cl_2$	$C_2H_2Cl_4$	-1.31(7.1),-1.28(7.0) -1.18(6.2),-1.14(6.8)[d]	-6.07[c]	i-Pr CH: -2.65
$Ti(dpm)_2F_2$	CH_2Cl_2	-1.15	-6.11	-
$Ti(dpm)_2Cl_2$	CH_2Cl_2	-1.17	-6.19	-
$Ti(dpm)_2Br_2$	CH_2Cl_2	-1.18	-6.21	-
$Ti(tdh)_2Cl_2$	CH_2Cl_2	-1.24	-6.51	-

[a]ppm (±0.01) relative to internal TMS (1% by volume); concentrations are ca. 0.25 M; temperature is ~39°. [b]In CH_2Cl_2. [c]In CCl_4. [d]Temperature is -2.2°.

Table LXXV

Chemical Shift Data for $Ti(chel)_2(phenoxy)_2$ Complexes

Chelate	Phenoxy	Solvent	acac or quin CH_3	-CH=	Other
acac	C_6H_5O	CH_2Cl_2	-2.01	-5.76	-
acac	2-ClC_6H_4O	C_6H_6	-1.63	-5.24	-
acac	2-ClC_6H_4O	CH_2Cl_2	-2.03	-5.84	-
acac	2,6-$Cl_2C_6H_4O$	CH_2Cl_2	-1.99	-5.75	-
acac	4-ClC_6H_4O	CH_2Cl_2	-2.00	-5.75	-
		C_6H_6	-1.60	-5.22	-
acac	2-IC_6H_4O	CH_2Cl_2	-2.03	-5.78	-
		C_6H_6	-1.67	-5.26	-
acac	2-$(C_6H_5)C_6H_4O$	CH_2Cl_2	-1.78	-5.41	-
		C_6H_6	-1.50	-5.04	-
acac	4-$(OCH_2C_6H_5)$-C_6H_4O	CH_2Cl_2	-1.97	-5.66	-
		C_6H_6	-1.69	-5.33	
acac	2-$^i PrC_6H_4O$	CH_2Cl_2	-1.98	-5.65	i-Pr CH_3: -1.16(6.8) i-Pr CH: -3.43
		C_6H_6	-1.67	-5.25	i-Pr CH_3: -1.31(7.0) i-Pr CH: -3.78

Table LXXV (continued)

acac	2,6-$^{i}Pr_2C_6H_3O$	CH_2Cl_2	-2.03	-5.78	i-Pr CH_3: -1.11(7.2) i-Pr CH: -3.86
		C_6H_6	-1.70	-5.22	i-Pr CH_3: -1.25(6.9) i-Pr CH: -4.04
acac	4-$^{i}PrC_6H_4O$	CH_2Cl_2	-1.97	-5.65	i-Pr CH_3: -1.19(6.9) i-Pr CH: -2.81
		C_6H_6	-1.69	-5.34	i-Pr CH_3: -1.15(7.0) i-Pr CH: -2.76
quin	2,6-$^{i}Pr_2C_6H_3O$	m-$C_6H_4Cl_2$	-3.15	-	i-Pr CH_3: -1.24(6.8) -0.57(6.8) i-Pr CH: -3.88
ox	2,6-$^{i}Pr_2C_6H_3O$	m-$C_6H_4Cl_2$	-	-	i-Pr CH_3: -1.23(6.8) -0.70(6.8) i-Pr CH: -3.95

[a] Ppm (±0.01) relative to internal TMS (1% by volume); concentrations are ca. 0.25 M for acac complexes and ca. 0.15 M for ox and quin complexes; temperature is ~39°.

Table LXXVI

Chemical Shift Data[a] for $Ti(acac)_2X(OR)$ and $Ti(bzac)_2(OR)_2$ Complexes

Complex	Solvent	acac or bzac CH_3	-CH=	Other
$Ti(acac)_2Cl(O^iC_3H_7)_2$	CH_2Cl_2	-2.04	-5.76	i-Pr CH_3: -1.31(6.7) i-Pr CH: -3.92
$Ti(acac)_2Br(O^iC_3H_7)$	CH_2Cl_2	-2.03	-5.77	i-Pr CH_3: -1.34(6.8) i-Pr CH: -3.98
$Ti(acac)_2Cl(2,6\text{-}^iPr_2\text{-}C_6H_3O)$	CH_2Cl_2	-2.06	-5.81	i-Pr CH_3: -1.21(6.8) i-Pr CH: -3.92
$Ti(bzac)_2(O^iC_3H_7)_2$	CH_2Cl_2	-2.14	-6.27	i-Pr CH_3: -1.21(6.3) i-Pr CH: -4.88
$Ti(bzac)_2(2,6\text{-}^iPr_2\text{-}C_6H_3O$	CH_2Cl_2	-2.20	-6.36	i-Pr CH_3: -1.68(6.8) i-Pr CH: -3.96

[a] Ppm (±0.01) relative to internal TMS (1% by volume); concentrations are 0.300 M; temperature is ~39°.

Table LXXVII

Chemical Shift Data[a] for Complexes Containing the Catechol Ligand

Complex	Solvent	acac, bzac, or quin CH_3	-CH=	cat-H	Other
$Ti(acac)_2(cat)$	CH_2Cl_2	-2.16	-5.93	-6.40	-
	C_6H_6	-1.63	-5.28	-	-
$Ti(acac)_2(3,6\text{-}^iPr_2cat)$	CH_2Cl_2	-2.14	-5.85	-6.45	i-Pr CH_3: -1.07(7.0)
	C_6H_6	-1.66	-5.32	-6.65	i-Pr CH_3: -1.25(7.0)
$Ti(bzac)_2(cat)$	CH_2Cl_2	-2.32	-6.58	-6.40	- -
$Ti(bzac)_2(3,6\text{-}^iPr_2cat)$	CH_2Cl_2	-2.29	-6.51	-6.46	i-Pr CH_3: -1.08(6.9) i-Pr CH: -2.79
$Ti(quin)_2(3,6\text{-}^iPr_2cat)$	CH_2Cl_2	-3.28	-	-6.47	i-Pr CH_3: -1.08(6.9) i-Pr CH: -2.80
$Ti(quin)_2(3,5\text{-}^iPr_2cat)$	CH_2Cl_2[b]	-3.30	-	-	i-Pr CH_3: -1.11(6.9) -1.14(6.7)

[a] Ppm(0.01) relative to internal TMS (1% by volume); concentrations are ca. 0.25 M unless otherwise noted; temperature is ca. 39°. [b] Saturated solution at room temperature.

V. REFERENCES

(1). E. L. Muetterties, Accounts Chem. Res., 3, 266 (1970).

(2). E. L. Muetterties, MTP Int. Rev. Sci., Ser. One, 9, 77 (1972).

(3). E. L. Eliel, J. Chem. Ed., 48, 163 (1971).

(4). E. L. Muetterties, J. Amer. Chem. Soc., 90, 5097 (1968).

(5). F. A. Cotton, Accounts Chem. Res., 1, 257 (1968).

(6). J. J. Fortman and R. E. Sievers, Coord. Chem. Rev., 6, 331 (1971).

(7). N. Serpone and D. G. Bickley, Progr. Inorg. Chem., 17, 391 (1972).

(8). E. L. Muetterties, Inorg. Chem., 4, 769 (1965).

(9). K. Vrieze and P. W. N. M. Van Leeuwen, Progr. Inorg. Chem., 14, 1 (1970).

(10). J. R. Shapley and J. A. Osborn, Accounts Chem. Res., 6, 305 (1973).

(11). K. Mislow and M. Raban, Topics in Stereochem., 1, 1 (1967).

(12). H. Kessler, Angew. Chem., Int. Ed. Engl., 9, 219 (1970).

(13). J. A. Pople, W. G. Schneider, and H. J. Bernstein, "High-Resolution Nuclear Magnetic Resonance", McGraw-Hill Book Co., Inc., New York, N. Y., 1959, Chapter 10.

(14). C. S. Johnson, Advan. Mag. Resonance, 1, 33 (1965).

(15). A. Allerhand, H. S. Gutowsky, J. Jonas, and R. A. Meinzer, J. Amer. Chem. Soc., 88, 3185 (1966).

(16). G. Binsch, Topics in Stereochem., 3, 97 (1968).

(17). H. S. Gutowsky and C. H. Holm, J. Chem. Phys., 25, 1228 (1956).

(18). J. P. Jesson in "Transition Metal Hydrides", E. L. Muetterties, Ed., Vol. 1, M. Dekker, Inc., New York, N. Y., 1971, Chapter 3.

(19). P. Meakin, E. L. Muetterties, and J. P. Jesson, J. Amer. Chem. Soc., 95, 75 (1973).

(20). R. K. Pomeroy and W. A. G. Graham, J. Amer. Chem. Soc., 94, 274 (1972).

(21). J. G. Gordon, II, and R. H. Holm, J. Amer. Chem. Soc., 92, 5319 (1970).

(22). R. C. Fay, A. Y. Girgis, and U. Klabunde, J. Amer. Chem. Soc., 92, 7056 (1970).

(23). A. Y. Girgis and R. C. Fay, J. Amer. Chem. Soc., 92, 7061 (1970).

(24). C. S. Springer, Jr., R. E. Sievers, and B. Feibush, Inorg. Chem., 10, 1242 (1971).

(25). S. S. Eaton and R. H. Holm, J. Amer. Chem. Soc., 93, 4913 (1971).

(26). S. S. Eaton, J. R. Hutchison, R. H. Holm, and E. L. Muetterties, J. Amer. Chem. Soc., 94, 6411 (1972).

(27). L. H. Pignolet and R. H. Holm, J. Amer. Chem. Soc., 92, 1791 (1970).

(28). L. H. Pignolet, R. A. Lewis, and R. H. Holm, J. Amer. Chem. Soc., 93, 360 (1971).

(29). L. H. Pignolet, R. A. Lewis, and R. H. Holm, Inorg. Chem., 11, 99 (1972).

(30). D. J. Duffy and L. H. Pignolet, Inorg. Chem., 11, 2843 (1972).

(31). L. H. Pignolet, D. J. Duffy, and L. Que, Jr., J. Amer. Chem. Soc., 95, 295 (1973).

(32). M. C. Palazzotto, D. J. Duffy, B. L. Edgar, L. Que, Jr., and L. H. Pignolet, J. Amer. Chem. Soc., 95, 4537 (1973).

(33). L. Que, Jr., and L. H. Pignolet, Inorg. Chem., 13, 351 (1974).

(34). B. Jurado and C. S. Springer, Jr., Chem. Commun., 85 (1971).

(35). J. R. Hutchison, J. G. Gordon, II, and R. H. Holm, Inorg. Chem., 10, 1004 (1971).

(36). E. L. Muetterties and C. W. Alegranti, J. Amer. Chem. Soc., 91, 4420 (1969).

(37). S. S. Eaton, G. R. Eaton, R. H. Holm, and E. L. Muetterties, J. Amer. Chem. Soc., 95, 1116 (1973).

(38). A. Werner, Ber., 45 3061 (1912).

(39). E. L. Muetterties, Rec. Chem. Progr., 31, 51 (1970).

(40). P. Ray and N. K. Dutt, J. Indian Chem. Soc., 20, 81 (1943).

(41). C. S. Springer, Jr., and R. E. Sievers, Inorg. Chem., 6, 852 (1967).

(42). J. C. Bailar, J. Inorg. Nucl. Chem., 8, 165 (1958).

(43). J. S. Wood, Progr. Inorg. Chem., 16, 227 (1972).

(44). R. Eisenberg, Progr. Inorg. Chem., 12, 295 (1970).

(45). E. I. Stiefel and G. F. Brown, Inorg. Chem., 11, 434 (1972).

(46). D. L. Kepert, Inorg. Chem., 11, 1561 (1972).

(47). E. L. Muetterties and L. J. Guggenberger, J. Amer. Chem. Soc., 94, 5665 (1972).

(48). M. C. Palazzotto and L. H. Pignolet, J. C. S., Chem. Commun., 6 (1972).

(49). R. H. Holm, Accounts Chem. Res., 2, 307 (1969).

(50). R. A. D. Wentworth, Coord. Chem. Rev., 9, 171 (1972-73).

(51). E. Larsen, G. N. LaMar, B. E. Wagner, J. E. Parks, and R. H. Holm, Inorg. Chem., 11, 2652 (1972).

(52). T. J. Pinnavaia and R. C. Fay, Inorg. Chem., 7, 502 (1968).

(53). T. J. Pinnavaia and R. C. Fay, Inorg. Chem., 7, 508 (1968).

(54). R. C. Fay and R. N. Lowry, Inorg. Chem., 6, 1512 (1967).

(55). N. Serpone and R. C. Fay, Inorg. Chem., 6, 1835 (1967).

(56). D. W. Thompson, W. A. Somers, and M. O. Workman, Inorg. Chem., 9, 1252 (1970).

(57). R. C. Fay and R. N. Lowry, Inorg. Chem., 9, 2048 (1970).

(58). R. C. Fay and R. N. Lowry, Inorg. Chem., 13, 1309 (1974).

(59). R. W. Jones, Jr., and R. C. Fay, Inorg. Chem., 12, 2599 (1973).

(60). R. W. Jones, Jr., Ph. D. Thesis, Cornell University, 1971.

(61). D. C. Bradley and C. E. Holloway, J. Chem. Soc. (A), 282 (1969).

(62). J. F. Harrod and K. Taylor, Chem. Commun., 696 (1971).

(63). D. C. Bradley, personal communication.

(64). D. M. Puri, K. C. Pande, and R. C. Mehrotra, J. Less-Common Metals, 4, 393 (1962).

(65). D. M. Puri, K. C. Pande, and R. C. Mehrotra, J. Less-Common Metals, 4. 481 (1962).

(66). D. W. Thompson, R. W. Rosser, and P. B. Barrett, Inorg. Nucl. Chem. Letters, 7, 931 (1971).

(67). C. E. Holloway and A. E. Sentek, Can. J. Chem., 49, 519 (1971).

(68). E. C. Alyea and P. H. Merrell, Inorg. Nucl. Chem. Letters, 9, 69 (1973).

(69). T. J. Pinnavaia and R. C. Fay, Inorg. Syn., 12, 88 (1970).

(70). D. W. Thompson, W. R. C. Munsey, and T. V. Harris, Inorg. Chem., 12, 2190 (1973).

(71). R. N. Lowry, Ph. D. Thesis, Cornell University, 1969.

(72). A. L. Allred and D. W. Thompson, Inorg. Chem., 7, 1196 (1968).

(73). K. R. Taylor, Ph. D. Thesis, McGill University, 1973.

(74). N. Serpone, Ph. D. Thesis, Cornell University, 1968.

(75). G. H. Dahl and P. H. Block, Inorg. Chem., 5, 1394 (1966).

(76). P. J. Paulsen and W. D. Cooke, Anal. Chem., 35, 1560 (1963).

(77). R. Ishayek, M. Sc. Thesis, Sir George Williams University, 1973.

(78). G. V. D. Tiers, "NMR Summary", Minnesota Mining and Manufacturing Co., St. Paul, Minn., January 15, 1962.

(79). A. L. Van Geet, Anal. Chem., 40, 2227 (1968); 42, 679 (1970).

(80). R. C. Neuman and V. Jonas, J. Amer. Chem. Soc., 90, 1970 (1968).

(81). O. Yamamoto and M. Yanagisawa, Anal. Chem., 42, 1463 (1970).

(82). R. R. Shoup, E. D. Becker, and M. L. McNeel, J. Phys. Chem., 76, 71 (1972).

(83). G. C. Levy and J. D. Cargioli, J. Mag. Resonance, 6, 143 (1972).

(84). J. Jonas, A. Allerhand, and H. S. Gutowsky, J. Chem. Phys., 42, 3396 (1965).

(85). L. W. Reeves and R. N. Shaw, Can. J. Chem., 48, 3641 (1970).

(86). D. C. Bradley and P. Thornton in "Comprehensive Inorganic Chemistry", Pergamon Press Ltd., Vol. 3, p. 468, 1973.

(87). T. J. Pinnavaia, J. M. Sebeson, II, and D. A. Case, Inorg. Chem., 8, 644 (1969).

(88). We thank Professor R. C. Fay for providing the modified version of Brown's (89) program.

(89). T. L. Brown and J. A. Ladd, Department of Chemistry, University of Illinois, Urbana, Illinois.

(90). For a description of this program see A. Granata, M. Sc. Thesis, Sir George Williams University, 1972. We thank Professor L. D. Colebrook for a copy of this program.

(91). L. M. Jackman and F. A. Cotton, Eds.,"Dynamic Nuclear Magnetic Resonance Spectroscopy", Academic Press, New York, N. Y., 1975.

(92). E. L. Muetterties,"Stereochemistry", Cornell University Press, Ithaca, N. Y., 1974.

(93). M. Gielen and N. Van Laytem, Bull. Soc. Chim. Belges, 79, 679 (1970).

(94). P. Meakin, E. L. Muetterties, F. N. Tebbe, and J. P. Jesson, J. Amer. Chem. Soc., 93, 4701 (1971).

(95). W. G. Klemperer, J. Chem. Phys., 56, 5478 (1972).

(96). W. G. Klemperer, Inorg. Chem., 11, 2668 (1972).

(97). W. G. Klemperer, J. Amer. Chem. Soc., 94, 6940 (1972).

(98). W. G. Klemperer, J. Amer. Chem. Soc., 95, 2105 (1973).

(99). J. I. Musher, Inorg. Chem., 11, 2335 (1972).

(100). J. I. Musher, J. Chem. Ed., 51, 94 (1974).

(101). J. I. Musher and W. C. Agosta, J. Amer. Chem. Soc., 96, 1320 (1974).

(102). A. T. Balaban, Rev. Roumaine Chim., 18, 841 (1973).

(103). W. Hasselbarth and E. Ruch, Theoret. Chim. Acta, 29, 259 (1973).

(104). S. S. Eaton and G. R. Eaton, J. Amer. Chem. Soc., 95, 1825 (1973).

(105). H. C. Longuet-Higgins, Mol. Phys., 6, 445 (1963).

(106). R. D. Adams and F. A. Cotton, J. Amer. Chem. Soc., 95, 6589 (1973).

(107). I. Ugi, D. Marquarding, H. Klusacek, G. Gokel, and P. Gillespie, Angew. Chem., Internat. Ed. Engl., 9, 703 (1970).

(108). E. L. Muetterties, J. Amer. Chem. Soc., 91, 1636 (1969).

(109). W. G. Klemperer, J. Amer. Chem. Soc., 94, 8360 (1972).

(110). I. Ugi, D. Marquarding, H. Klusacek, P. Gillespie, and F. Ramirez, Accounts Chem. Res., 4, 288 (1971).

(111). D. G. Bickley and N. Serpone, Inorg. Chem., 13, 2908 (1974).

(112). F. Basolo and R. G. Pearson,"Mechanisms of Inorganic Reactions", Second Ed., J. Wiley and Sons, New York, N. Y., 1967.

(113). L. H. Pignolet and G. N. LaMar in "Chemical Applications of NMR in in Paramagnetic Molecules", G. N. LaMar, W. D. Horrocks, Jr., and R. H. Holm, Eds., Academic Press, New York, N. Y., Chapter 8, 1973.

(114). A. F. Lindmark and R. C. Fay, Inorg. Chem., 14, 282 (1975).

(115). D. W. Thompson, Inorg. Chem., 8, 2015 (1969).

(116). T. J. Pinnavaia, L. J. Matienzo, and Y. A. Peters, Inorg. Chem., 9, 993 (1970).

(117). J. A. S. Smith and E. J. Wilkens, J. Chem. Soc. (A), 1749 (1966).

(118). R. B. Von Dreele and R. C. Fay, J. Amer. Chem. Soc., 94, 7935 (1972).

(119). R. B. Von Dreele, Ph. D. Thesis, Cornell University, 1971.

(120). G. Doyle, Inorg. Chem., 10, 2348 (1971).

(121). K. Nakamoto,"Infrared Spectra of Inorganic and Coordination Compounds", Second Ed., J. Wiley and Sons, New York, N. Y., 1970, p. 247-256.

(122). B. Bock, K. Flatau, H. Junge, M. Kuhr, and H. Musso, Angew. Chem., Internat. Ed. Engl., 10, 225 (1971).

(123). A. Yamamoto and S. Kambara, J. Amer. Chem. Soc., 79, 4344 (1957).

(124). D. C. Bradley and C. E. Holloway, Chem. Commun., 284 (1965).

(125). D. C. Bradley, Progr. Inorg. Chem., 2, 303 (1960).

(126). K. R. Taylor, Ph. D. Thesis, McGill University, 1973.

(127). N. Serpone, P. H. Bird, D. G. Bickley, and D. W. Thompson, Chem. Commun., 217 (1972).

(128). T. V. Harris, R. A. Coleman, R. B. Dickson, and D. W. Thompson, J. Organometal. Chem., 69, C27 (1974).

(129). M. Cox, J. Lewis, and R. S. Nyholm, J. Chem. Soc., 6113 (1964).

(130). R. C. Fay and N. Serpone, J. Amer. Chem. Soc., 90, 5701 (1968).

(131). W. K. Ong and R. H. Prince, J. Inorg. Nucl. Chem., 27, 1037 (1965).

(132). R. West, J. Amer. Chem. Soc., 80, 3246 (1958).

(133). R. F. Riley, R. West, and R. Barbarin, Inorg. Syn., 7, 30 (1963).

(134). A. Deluzarche and M. Brini, Bull. Soc. Chim. France, 3, 537 (1961).

(135). K. Andra, J. Organometal. Chem., 11, 567 (1968).

(136). J. L. Martin and J. Takats, Inorg. Chem., 14, 73 (1975).

(137). N. Serpone and R. C. Fay, Inorg. Chem., 8, 2379 (1969).

(138). H. Weingarten. M. G. Miles, and N. K. Edelman, Inorg. Chem., 7. 879 (1968).

(139). P. H. Bird, A. R. Fraser, and C. F. Lau, Inorg. Chem., 12, 1322 (1973).

(140). E. O Schlemper, unpublished results quoted in ref. (144).

(141). N. Serpone and K. A. Hersh, Inorg. Nucl. Chem. Letters, 7, 115 (1971)..

(142). N. Serpone and K. A. Hersh, Inorg. Chem., 13, 2901 (1974).

(143). B. W. Fitzsimmons, N. J. Seeley, AND A. W. Smith, J. Chem. Soc.(A), 143 (1969).

(144). G. A. Miller and E. O. Schlemper, Inorg. Chem., 12, 677 (1973).

(145). V. B. Ramos and R. S. Tobias, Spectrochim. Acta, 29A, 953 (1973).

(146). R. M. Pike, Coord. Chem. Rev., 2, 163 (1967).

(147). V. Doron and W. Durham, Inorg. Nucl. Chem. Letters, 6, 285 (1970).

(148). V. Doron, W. Durham, and D. Frazier, Inorg. Nucl. Chem Letters, 7, 91 (1971).

(149). N. K. Wilson and J. B. Stothers, Topics in Stereochem., 8, 1 (1974).

(150). L. H. Pignolet, personal communication.

(151). A. Mannschreck and L. Ernst, Tetrahedron Lett., 5939 (1968).

(152). M. Pickering, B. Jurardo, and C. S. Springer, Jr., submitted to J. Amer. Chem. Soc.

(153). D. A. Case and T. J. Pinnavaia, Inorg. Chem., 10, 482 (1971).

(154). M. C. Baird, J. Organometal. Chem., 64, 289 (1974).

(155). G. Kortum, W. Vogel, and K. Andrussow, "Dissociation Constants of Organic Acids in Aqueous Solutions", IUPAC, Butterworths, 1961.

(156). R. T. McIver, Jr., and J. H. Silvers, J. Amer. Chem. Soc., 95, 8462 (1973).

(157). A. Allerhand and H. S. Gutowsky, J. Chem. Phys., 41, 2115 (1964).

(158). A. Allerhand, F. Chen, and H. S. Gutowsky, J. Chem. Phys., 42, 3040 (1965).

(159). Y. Kawasaki and T. Tanaka, Inorg. Nucl. Chem. Letters, 3, 13 (1967).

(160). L. W. Reeves, Advan. Phys. Org. Chem., 3, 187 (1965).

(161). K. C. Williams and T. L. Brown, J. Amer. Chem. Soc., 88, 4134 4134 (1966).

(162). E. Greenwald, A. Loewenstein, and S. Meiboom, J. Chem. Phys., 27, 630 (1957).

(163). A. Loewenstein and S. Meiboom, J. Chem. Phys., 27, 1067 (1957).

(164). M. T. Rogers and J. C. Woodbrey, J. Phys. Chem., 66, 540 (1962).

(165). L. H. Piette and W. A. Anderson, J. Chem. Phys., 30, 899 (1959).

(166). M. Takeda and E. D. Stejskal, J. Amer. Chem. Soc., 82, 25 (1960).

(167). K. A. Hersh, M. Sc. Thesis, Concordia University, 1975.

(168). J. J. Fortman and R. E. Sievers, Inorg. Chem., 6, 2022 (1967).

(169). E. O. Schlemper, Inorg. Chem., 6, 2012 (1967).

(170). B. F. Studd and A. G. Swallow, J. Chem. Soc. (A), 1961 (1968).

(171). J. D. Matthews, N. Singer, and A. G. Swallow, J. Chem. Soc. (A), 2545 (1970).

(172). L. O. Atovmyan and Yu. A. Sokolova, Chem. Commun., 649 (1969).

(173). W. R. Scheidt, Inorg. Chem., 12, 1758 (1973).

(174). "Handbook of Chemistry and Physics", 52nd Ed., Chemical Rubber Co., Cleveland, Ohio, 1972, p. F-177.

(175). T. J. Pinnavaia and A. L. Lott, II, Inorg. Chem., 10, 1338 (1971).

(176). T. J. Pinnavaia, J. J. Howe, and R. E. Teets, Inorg. Chem., 13, 1074 (1974).

(177). J. J. Stezowski and H. A. Eick, J. Amer. Chem. Soc., 91, 2890 (1969).

(178). M. Elder, J. G. Evans, and W. A. G. Graham, J. Amer. Chem. Soc., 91, 1245 (1969).

(179). M. J. Frazer and W. E. Newton, Inorg. Chem., 10, 2137 (1971).

(180). E. M. Brainina, L. A. Fedorov, and M. Kh. Minacheva, Dokl. Akad. Nauk U.S.S.R., Engl. Ed., 196, 120 (1971).

(181). N. Serpone and K. A. Hersh, J. Organometal. Chem., 84, 177 (1975).

(182). N. Serpone and K. A. Hersh, Can. J. Chem., 53, 448 (1975).

(183). S. K. Dhar, V. Doron, and S. Kirschner, J. Amer. Chem. Soc., 80, 753 (1958).

(184). E. Larsen, S. F. Mason, and G. H. Searle, Acta Chem. Scand., 20, 191 (1966).

(185). T. Inoue and K. Saito, Bull. Chem. Soc. Japan, 46, 2417 (1973).

(186). A. Nagasawa and K. Saito, Bull. Chem. Soc. Japan, 47, 131 (1974).

(187). C. A. Tyson and A. E. Martell, J. Amer. Chem. Soc., 94, 939 (1972).

(188). E. Mentasti and E. Pelizzetti, J. C. S. Dalton, 2605 (1973).

(189). E. Mentasti, E. Pelizzetti, and G. Saini, J. C. S. Dalton, 2609 (1973).

(190). E. Pelizzatti, E. Mentasti, and G. Saini, Gazz. Chim. Ital., 104, 1015 (1974).

(191). C. Floriani, R. Henzi, and F. Calderazzo, J. C. S. Dalton, 2640 (1972).

(192). J. J. Flynn and F. P. Boer, J. Amer. Chem. Soc., 91, 5756 (1969).

(193). H. R. Allcock and E. C. Bissell, J. Amer. Chem. Soc., 95, 3154 (1973).

(194). C. G. Pierpont and H. H. Downs, Inorg. Chem., 14, 343 (1975).

(195). J. P. Fackler, Jr., and A. Avdeef, Inorg. Chem., 13, 1864 (1974).

(196). M. J. Bennett, M. Cowie, J. L. Martin, and J. Takats, J. Amer. Chem. Soc., 95, 7504 (1973).

(197). J. L. Martin and J. Takats, Can. J. Chem., 53, 572 (1975).

(198). R. J. H. Clark,"The Chemistry of Titanium and Vanadium", Elseveir Publ. Co., Amsterdam, The Netherlands, 1968.

(199). K. Watenpaugh and C. N. Caughlan, Inorg. Chem., 5, 1782 (1966).

(200). H. Hoppe and W. Haase, Acta Cryst., B24, 281 (1968).

(201). N. W. Alcock, M. Pierce-Butler, and G. R. Willey, J. C. S. Chem. Commun., 627 (1974).

(202). A. Feltz, Z. Chem., 7, 158 (1967).

(203). D. M. Puri and R. C. Mehrotra, J. Less-Common Metals, 3, 247 (1961).

(204). D. M. Puri and R. C. Mehrotra, J. Less-Common Metals, 3, 253 (1961).

(205). J. R. Ferraro,"Low-Frequency Vibrations of Inorganic and Coordination Compounds", Plenum Press, New York, N. Y., 1971, Chapter 6.

(206). R. S. P. Coutts and P. C. Wailes, J. Organometal. Chem., 84, 47 (1975).

(207). R. S. P. Coutts, P. C. Wailes, and R. L. Martin, J. Organometal. Chem., 47, 375 (1973).

(208). T. J. Kistenmacher and G. J. Stucky, Inorg. Chem., 10, 122 (1971).

(209). R. J. H. Clark and M. A. Coles, J. C. S. Dalton, 2454 (1972).

(210). P. A. W. Dean, Can. J. Chem., 51, 4024 (1973).